14th Congress of the World Federation of Nuclear Medicine and Biology

WFNMB

Cartagena de Indias
Colombia

2026

13–16 February

Book of Abstracts

Organized by

WORLD FEDERATION OF NUCLEAR MEDICINE AND BIOLOGY

ACMNIM
ASOCIACIÓN COLOMBIANA DE MEDICINA NUCLEAR E IMÁGENES MOLECULARES

alasbimn
Asociación Latinoamericana de Sociedades de Biología y Medicina Nuclear

In cooperation with

IAEA

Index

General Information

General Information for Oral Presentations

- Please download and use the official template when preparing your presentation.
- The full schedule of oral communications is available on the Congress website: WFNMB 2026 Scientific Program.
- At the beginning of this email, you will find complete **details of your participation, including session, date, time, room, and your assigned presentation slot.**
- The assigned **'Paper Reference'** code identifies the type and number of your presentation (O01: Oral presentation 01).
- **Each oral presentation has a total duration of 7 minutes**: 5 minutes for the presentation and 2 minutes for questions and answers. We kindly ask you to adhere strictly to the allotted time to ensure the smooth progression of the session.
- **All presentations must be delivered exclusively in English.**
- All rooms will be equipped with standard audiovisual facilities, including a projector, sound system, microphones, and a computer for displaying presentations. **The use of personal laptops is not allowed.**

Instructions for Submitting Presentations

- **Presenters must bring their presentation on a USB flash drive** and submit it to the Speaker Room (Room 101) with sufficient advance time. The room will be available during Congress hours from February 13 to 16. On February 12, presentations can also be submitted starting at 3:00 PM.
- All presentations must be submitted in **PDF format**. **No animations, videos, or transitions** are allowed.
- The number of slides should be appropriate for a **5-minute presentation.**

General Information

General Information about E-Posters

- Your poster **must be submitted in digital format (E-Poster).**
- Please **read the instructions** below carefully before creating your E-Poster.
- To **upload your E-Poster**, please access the platform and follow the steps provided. The process is simple and intuitive: E-Poster Submission Portal.
- The **deadline** for submitting your E-Poster is **Friday, January 9, 2026.**
- All E-Posters will be displayed on interactive screens in the **"Claustro de las Ánimas" hallway**, where the commercial exhibition takes place.
- There will be **no in-person poster presentations**. However, during the coffee breaks and lunch times, which will serve as poster walks, it will be a great opportunity to be near the screens and interact with other attendees interested in the E-Posters.

Instructions for Preparing Your E-Poster

- Before you begin, please download and use the official template, which contains the required dimensions and format.
- The E-Poster must consist of **one single vertical slide** (vertical format) and must be saved as a **PDF file**. Maximum: **1 slide.**
- Please **include your contact details and email address** so that interested attendees can easily reach you with any questions or further information they may need.
- You are free to design your E-Poster as you consider appropriate, but we recommend the following guidelines:

    1. Use fonts such as **Arial, Tahoma, or Verdana**.
    2. Choose a **white or light background** with high-contrast text colors.
    3. Insert all images **directly into the slide**; please avoid external links.
    4. **Animations and effects are not allowed.**

List of Oral Presentations

O01 Diagnostic performance of 18F-choline PET/CT correlated with MRI in brain tumor recurrence: experience from an oncology hospital in Ecuador
Dr. Christian Toalongo Moreno[1,2], Dr. Abel Llaguno Buzetta[1,2], Dr. Rodney Vaca Montenegro[2]
[1]SOLCA Oncology Hospital, Guayaquil, Ecuador, [2]Indoamérica Technological University, Quito, Ecuador

O02 Diagnostic value of cisternoscintigraphy and CT cystenography in the detection of CSF leaks in patients with intracranial hypotension
Dr. Sebastián Rojas Lara[1]
[1]Fundación Universitaria Sanitas, BOGOTÁ, D.C., Colombia

O03 Beyond clinical assessment: The value of combined metabolic and dopaminergic mapping with PET/CT for the differential diagnosis of parkinsonian syndromes
Dr. Abigail Arriaga Contreras[1], Dr. Rodrigo Hernández Ramírez[1], Dr. Juan Pablo Chávez Torres[1], Dr. Miguel Angel Corza Ayala[1], Dr. Francisco Jesús Solano Caballero[1], Dr. Oscar Enrique Lucio Baez[1], Dra. Blanca Estela López Graciano[1]
[1]Instituto Nacional de Ciencias Médicas y Nutrición Salvador Zubirán, Ciudad De México, Mexico

O04 Semiquantitative difference in the uptake of the pineal gland of [18F] fluorodopamine in patients with Parkinson's disease versus atypical parkinsonism
Dr. Kinari Ortega[1], Dr. Manlio Gerardo Gama[1], Dr. Gustavo Vázquez[1], Dr. Miguel Ángel Olarte Casas[1]
[1]National Autonomous University of Mexico, CDMX, Mexico

O05 In vitro biological evaluation of a 99mTc tricarbonyl complex derived from Erlotinib for molecular imaging in triple negative breast cancer
Dr. María Emilia Tejería Pérez[1], Romina Rossi[1], Ana María Rey Ríos[1]
[1]Área Radioquímica/ Facultad de Química, Montevideo, Uruguay

O06 Results from a First-In-Human Phase I Trial of [68Ga]Ga-OncoCAIX in ccRCC: Safety, Dosimetry, Pharmacokinetics and Preliminary Diagnostic Performance
Dr. Fabrizia Gelardi[1], Prof Martina Sollini[1,2], Dr Cristiano Pini[2], Rita Petrelli[1], Alessia Tudda[1], Prof Paola Anna Erba[3,4], Jacqueline Mock[5], Samuele Cazzamalli[5], Dario Neri[5], Prof Arturo Chiti[1,2]
[1]IRCCS San Raffaele Hospital, Milano, Italy, [2]Vita-Salute San Raffaele University, Milano, Italy, [3]School of Medicine and Surgery, University of Milano-Bicocca, Milano, Italy, [4]Nuclear Medicine Unit, ASST Papa Giovanni XXIII Hospital, Bergamo, Italy, [5]Philochem AG, Otelfingen, Switzerland

O07 Ampelomins radiolabelled with Tc-99m and F-18: Synthesis and functionalization of tracers for imaging infectious processes

Quim. Carolina Brindisi[1,2], Dr. Javier Giglio[2,3], **Dra. Mariella Adriana Terán Gretter**[2], Dra. Margarita Brovetto[1]
[1]Química Orgánica (DQO) - Universidad de la República, Montevideo, Uruguay, [2]Área Area Radioquímica (DEC) - Universidad de la República, Montevideo, Uruguay, [3]Centro Uruguayo de Imagenología Molecular (CUDIM), Montevideo, Uruguay

O08 Radiosensitization of Theranostics for Pancreatic Ductal Adenocarcinoma

Dr. Moralba Dominguez Garcia[1], Alexa Michel[1], Mohamed Hussien[1], Amy Morrison[2], Dr. Jason S. Lewis[1]
[1]Memorial Sloan Kettering Cancer Center, New York, United States, [2]King's College London, London, United Kingdom

O09 Validation of an Alternative Analytical Technique for Determining the Radiochemical Purity of 99mTc-HMDP

Mr. Eliecer Cantillo[1], Mr. Renzo Guardo[1], Mr. Juan Balanta[1], Ms. Viviana Montoya[1], Mr. Giovani Naranjo[1]
[1]Hospital Universitario Fundación Valle Del Lili, Cali, Colombia

O10 R1 from 18F-PR04.MZ as a proxy for cerebral blood flow in degenerative parkinsonisms: comparison with 15O-H2O PET/CT

Dr. Andres Damian[1,2], Dr. Ignacio Amorin[3], Dr. Vasko Kramer[4], Dr. Juan R. Higgie[3], TRI. Ismael Cordero[1,2], Dr. Luis Gutierrez[2], Dr. Eduardo Savio[1], Dra. Thalia Arias[2], Dr. Omar Alonso[1,2], Dr. Rodolfo Ferrando[1,2]
[1]Centro Uruguayo De Imagenología Molecular - Cudim, Montevideo, Uruguay, [2]Unidad Académica de Medicina Nuclear e Imagenología Molecular, Hospital de Clínicas, Universidad de la República, Montevideo, Uruguay, [3]Instituto de Neurología, Hospital de Clínicas, Universidad de la República, Montevideo, Uruguay, [4]Nuclear Medicine and PET/CT Center PositronMed, PositronPharma SA. , Santiago, Chile

O11 Evaluation of cortical amyloid burden and tau deposition in cognitively normal and preclinical Alzheimer's disease through positron emission tomography

Mr. Phelipi Nunes Schuck[1], Dr Ana Maria Marques da Silva[1,2]
[1]Faculdade de Medicina FMUSP, Universidade de Sao Paulo, São Paulo, Brazil, [2]Medical Imaging & Data Analytics (MEDIIMA), Porto Alegre, Brazil

O12 Influence of EEG Discharges During FDG-PET Cerebral Metabolism Assessment in Patients with Pharmacoresistant Epilepsy

Dr. Valentino Mendez[1], Dr Andrés Damian[1,2,3], LIC Maria Pages[3], Dra Mariana Legnani[3], Dr Andrés Bertinat[3], Dra Patricia Braga[3], Dr Omar Alonso[1,2], Dr Rodolfo Ferrando[1,2,3]
[1]Unidad Académica de Medicina Nuclear e Imagenología Molecular, Hospital de Clínicas, Universidad de la República, Montevideo, Uruguay, [2] Centro Uruguayo de Imagenología Molecular (CUDIM), Montevideo, Uruguay, [3]Programa de Cirugía de Epilepsia del Hospital de Clínicas, Montevideo, Uruguay

O13 Evaluation of a murine model of metastatic castration resistant prostate cancer for combination radioligand therapy and immunotherapy

Dr. Cindy Rodriguez[1], Alexa Michel[1], Moralba Dominguez Garcia[1], Angelique Loor[1], Yana Reshetnyak[2], Jason S. Lewis[1]
[1]Molecular Pharmacology Program Memorial Sloan Kettering Cancer Center, New York, United States, [2]Department of Physics University of Rhode Island, Kingston, United States

O14 Optimizing Pretargeted Radiotheranostics: From PET to Therapy

Mr. Mike Cornejo[1,2,3], Zachary V. Samuels[1,2,3], Gina Dehlavi[1,2,4], Lukas Carter[5], Emilia Strugala[1], Brian M. Zeglis[1,2,4,6]
[1]Department of Chemistry, Hunter College, The City University of New York, New York, United States, [2]Ph.D. Program in Chemistry, Graduate Center of the City of New York, New York, United States, [3]Department of Radiology, Memorial Sloan Kettering Cancer Center, New York, United States, [4]Ph.D. Program in Biochemistry, Graduate Center of the City University of New York, New York, United States, [5]Department of Medical Physics, Memorial Sloan Kettering Cancer Center, New York, United States, [6]Department of Radiology, Weill Cornell Medical College, New York, United States

O15 Design and Astatination of Radioligands for the Pretargeted Delivery of Astatine-211

Mr. Mike Cornejo[1,2,3], Cindy Rodriguez[2], Zachary Samuels[1,2,3], Yutian Feng[5], Michael R. Zalutsky[5], Brian M. Zeglis[1,2,3,4]
[1]Department of Chemistry, Hunter College, The City University of New York, New York, United States, [2]Department of Radiology, Memorial Sloan Kettering Cancer Center, New York, United States, [3]PhD. Program in Chemistry, Graduate Center of the City University of New York, New York, United States, [4]Department of Radiology, Weill Cornell Medical College, New York, United States, [5]Department of Radiology, Duke University Medical Center, Durham, United States

O16 Combining deep learning and kinetic modeling for cerebral PET parametric imaging with reduced-time dynamic acquisitions

Lic. Santiago Burgos[1], Dr. Arturo Avendaño[1,2], Dr. Miguel Ávila[1,2]
[1]Unidad Radiofarmacia-Ciclotrón, División de Investigación, Facultad de Medicina, Universidad Nacional Autónoma de México, Ciudad De México, México, [2]Centro de Investigación sobre el Envejecimiento, CINVESTAV Sede Sur, Ciudad de México, México

O17 High throughput scanning with a vertical and compact Walk-Through flat panel PET

Prof. Stefaan Vandenberghe[1], dr Jens Maebe[1], Msc Maya Abi Akl[1], Ir. Boris Vervenne[1], Msc Rabia Aziz[1], Ir. Thibault D'Hulster[1], Ir. Florence Marie Muller[1,3], Prof Dr Nadia Withofs[2], Prof Dr Christian Vanhove[1]
[1]MEDISIP, Ghent University, Gent, Belgium, [2]CHU Liege, Liege, Belgium, [3]PET instrumentation group, University Pennsylvania, Philadelphia, USA

O18 Internal Dosimetry Calculation for PET/CT with ^{18}F-PSMA-1007 Using OpenDose Software

Prof. Kelly Sandoval Sandoval[1], Prof. M. José Abarzua[1], Prof. Jose Ceballos[1]
[1]Fundación Arturo Lopez Perez, Santiago, Chile

O19 Quantitative Evaluation of Scatter Correction Strategies in Long Axial Field-of-View PET/CT

Dr. Mohammadreza Teimoorisichani[1], Dr. Inki Hong[1]
[1]Siemens Medical Solutions USA Inc., Knoxville, United States

O20 A Quantitative CT-less Reconstruction Workflow for Long-axial Field-of-view PET Scanners with Enhanced Scaling

Dr. Mohammadreza Teimoorisichani[1], Dr. Josh Schaefferkoetter[1], Dr. Hasan Sari[2,3]
[1]Siemens Medical Solutions USA Inc., Knoxville, United States, [2]Department of Nuclear Medicine, Inselspital, Bern University Hospital, Bern, Switzerland, [3]Siemens Healthineers International AG, Zurich, Switzerland

O21 High-Precision PET/CT: Optimization and Quality strategies led by the Nuclear Medicine Technologist

Sra. Andrea Milena Bautista Beltran[1]
[1]Clínica De Marly, Bogotá Dc, Colombia

O22 Brain MRI-guided PET Reconstruction in a New PET/MRI System with <200ps TOF resolution

Dr. Jorge Cabello[1], Dr Karen Kettless[2], Dr Patrick Lehmann[2,3], Dr Anders Rodell[2], Dr Joshua Schaefferkoetter[1], Dr Ian Law[4], Prof Flemmin Littrup Andersen[4,5], Dr Thomas Lund Andersen[4,5], Dr Paul Schleyer[1]
[1]Siemens Medical Solutions USA, Knoxville, United States, [2]Siemens Healthcare A/S, Ballerup, Denmark, [3]Research & Clinical Translation, Magnetic Resonance, Siemens Healthineers AG, Erlangen, Germany, [4]Department of Clinical Physiology and Nuclear Medicine, Copenhagen University Hospital—Rigshospitalet, Copenhagen, Denmark, [5]Department of Clinical Medicine, University of Copenhagen, Copenhagen, Denmark

O23 Colombian Guide for the support of Radiological Events in Nuclear Medicine and Radiopharmacy

Mrs. Lorena Sandoval Castillo[1,2], Mrs. Eliana Franco[1,3], Mrs. Angela Londoño[1,4], Mrs. Stephany Calderón[1,5], Mrs. Erika Xiomara Cely[1,6], Mrs. Patricia Rico[1,7], Mrs. Nathalia Nuñez[1,7], Mr. Harley J. Orjuela B.[1,8], Mrs. Claudia Blanco[1,9], Mr. Omar Patiño[1,10]
[1]Asociación Colombiana De Física Médica- ACOFIMED, Bogotá, Colombia, [2]Clínica del Country, Bogotá, Colombia, [3]Hospital Universitario Mayor Méderi, Bogotá, Colombia, [4]Medicina nuclear, Clínica de Occidente, Cali, Colombia, [5]Medicina Nuclear S.A., Valledupar, Colombia, [6]Servicio de medicina nuclear, Clínica Internacional de alta tecnología -Clinaltec, Ibagué, Colombia, [7]Grupo de Física Médica, Fundación Valle de Lili, Cali, Colombia, [8]Área de Física Médica, Hospital Serena del Mar, Cartagena de Indias, Colombia, [9]Servicio Geológico Colombiano, Bogotá, Colombia, [10]Física Médica Hospitalaria, Hospital Universitario de Caldas, Manizales, Colombia

O24 Comparison of Patlak imaging with SUV imaging in metastatic uveal melanoma patients with a long axial field-of-view (LAFOV) PET/CT

Dr. Leyun Pan[1], Prof. Dr. Christos Sachpekidis[1], Prof. Dr. Antonia Dimitrakopoulou-Strauss[1]
[1]German Cancer Research Center, Heidelberg, Germany

O25 Clinical validation of deep learning denoising for low-count PET/CT: preserving SUV accuracy and image quality

Dr. Mauro Namías[1], **PhD Yamila Rotstein Habarnau**[1], Dr Nicolás Bustos[1], Dr Paola Corona[1], Dr Christian González[1], Dr Sonia Traverso[1], Dr Federico Matorra[1], BSc Francisco Funes[2], BSc Juan Martín Giraut[1], PhD Laura Pelegrina[2], Dr Gabriel Bruno[1]
[1]Fundación Centro Diagnóstico Nuclear, Buenos Aires, Argentina, [2]Comisión Nacional de Energía Atómica, Buenos Aires, Argentina

O26 Rapid scan assessment with non-quantitative FastPET: Generalizability to different tracers and count levels

Naveen Murthy[1], Dr. Yifan Zheng[1], Dr. Vladimir Panin[1], Dr. Deepak Bharkhada[1], Dr. Paul Schleyer[1]
[1]Siemens Medical Solutions, USA, Inc., Knoxville, United States

O27 Deep learning-based dose estimation for radionuclide therapy: a feasibility study

Dr. Yamila Rotsein Habarnau[1], Dr. Mauro Namías[1]
[1]Fundación Centro Diagnóstico Nuclear, Ciudad Autónoma de Buenos Aires, Argentina

O28 Assessment of the impact of gastrointestinal motion on PET quantification due to mismatched CT

Dr. Giordana Salvi De Souza[1], Maria Giulia Toro[1], Samaneh Mostafapour[1], Johannes H. van Snick[1], Adrienne H. Brouwers[1], Charalampos Tsoumpas[1]
[1]Nuclear Medicine and Molecular Imaging, University of Groningen, University Medical Center Groningen, Groningen, The Netherlands

O29 Optimization of pet/ct acquisition parameters for pregnant patients: phantom study with reduced dose and preserved image quality

Mr. Yann Cras[1], MD. Mariagiulia Longo[1], MD. Camilo Garcia[1], Pr. Désirée Deandreis[1], MD. Theophraste Henry[1]
[1]Gustave Roussy, Villejuif, France

O30 Implementation of Innovative Toilet Filtration Systems for Radionuclide Therapy Effluents: First Latin American Clinical Experience

MSc Eduardo Antonio Gonzalez Villa[1], MSc Cristhoper Camacho Herrera[2], Dr. Dany Mena Cortes[1,2], Bart Boots[3], Mattijs Maris[3], **Lic. Yesenia Saldierna Martinez**
[1]Oncologia San José, Hermosillo, Mexico, [2]Nuclear Medicine World, Ciudad de Mexico, Mexico, [3]Zereau, Netherlands

O31 Cocaine-dependent patients with depressive symptoms and suicide risk studied with brain perfusion SPECT and systemic inflammatory markers

Dr. Teresa Massardo[1], Dr. Juan Carlos Quintana[2], Dr. Carlos Ibáñez[1], Dr. Jonathan Veliz[1], Dr. Rodrigo Jaimovich[2], Dr. Claudia S Saez[2], Dr. Jaime Pereira[2], Dr. Francisco Javier Gomez[1], Dr. Isabel Berrocal[3], Dr. Rene Fernandez[1]
[1]hospital Clínico Universidad de Chile, Santiago, Chile, [2]Hospital Clínico Pontificia Universidad Catolica de Chile, Santiago, Chile, [3]hospital San Juan de Costa Rica, San Jose, Costa Rica

O32 Radiosynoviorthesis with Erbium-169 Following Surgery for Ankle Pigmented villonodular synovitis: A Rare Disease Series with more than 5 Year Follow-Up

Prof. Ioannis Iakovou[1], MD Evanthia Giannoula[1], MD Paraskevi Exadaktylou[1], MD Efthalia Gatzouli[1], MD Panos Charalambous[1], MD Kyriaki Papadopoulou[1], MD Agni Tsangaridi[1], Prof Argyrios Doumas[1], Prof Christos Sachpekidis[2]
[1]Aristotle University of Thessaloniki, Thessaloniki, Greece, [2]German Cancer Research Center, Heidelberg, Germany

O33 Deep-learning-based positron range correction (PRC) for Rb-82 cardiac PET

Dr. Yifan Zheng[1], Nerea Encina-Baranda[2], **Dr. Jorge Cabello**, Maurizio Conti[1], Joaquin López Herraiz[2]
[1]Siemens Medical Solutions USA, Inc., Knoxville, United States, [2]Nuclear Physics Group and IPARCOS, University Complutense of Madrid (IdISSC), Madrid, Spain

O34 Analysis of the Prognostic Value of Myocardial Perfusion Imaging – SPECT/CT Stratified by the AHA/ASCN 2021 Risk Algorithm

Dr. Sebastián Rojas Lara[1]
[1]Fundación Universitaria Sanitas, BOGOTÁ, D.C., Colombia

O35 Towards a new classification of therapeutic response in IgG4-related disease: A cluster approach based on 18F-FDG PET/CT

Dr. Miguel Angel Corza Ayala[1], Dr Rodrigo Hernandez Ramírez[1], Dr Joel Vargas Ahumada[1], Dr Eduardo Martín Nares[1], Dra Gabriela Aurora Hernández Molina[1], Dr Juan Pablo Chávez Torres[1]
[1]Instituto Nacional De Ciencias Médicas Y Nutrición Salvador Zubirán, Mexico CIty, Mexico

O36 [99mTc]Tc-iFAP SPECT/CT as a new radiotracer for the evaluation of lesions in IgG4-related disease: Comparison with 18F-FDG PET/CT

Dr. Miguel Angel Corza Ayala[1], Dr. Rodrigo Hernández Ramírez[1], Dr. Joel Eduardo Vargas Ahumada[1], Dr. Eduardo Marín Nares[1], Dra. Gabriela Aurora Hernández[1], Dr. Juan Pablo Chávez Torres[1], Dra Myrna Luna Gutierrez[2], Dr. Sevastián Salvador Medina Ornelas[1], Dr. Daniel Carrillo Vázquez[1], Dra. Abigail Arriaga Contreras[1]
[1]Instituto Nacional de Ciencias Médicas y Nutrición Salvador Zubirán, Mexico CIty, Mexico, [2]Instituto Nacional de Investigaciónes Nucleares, Mexico CIty, Mexico CIty

O37 Nitrate-enhanced technetium-99m-sestamibi single photon emission tomography for myocardial viability assessment: eleven-year single center experience

Dr. Eduardo Lischinsky[1], Dr. Mauricio Basantes[1], Dr. Manuel Román[1], Dr. Gerardo Dos Santos[1], PhD MD Omar Alonso[1]
[1]CMNIM, Hospital de Clínicas “Dr. Manuel Quintela” - Universidad de la República, Montevideo, Uruguay

O38 Myocardial perfusion patterns and ventricular function in patients with chagas disease, analysis at a regional reference center in eastern Colombia

Dr. Marvin Holman Anderson Achicanoy Botina[1], Ivan Camilo Ospina Florez[1], Jose Fernando Silva Llanos[1], Cesar Augusto Garcia Quintanilla[1,2], Lizeth Catherine Rodriguez Corredor[3]
[1]Nuclear Medicine Postgraduate Program - Universidad Autónoma De Bucaramanga (UNAB), Bucaramanga, Colombia, [2]SPECT Medicina Nuclear S.A.S., Bucaramanga, Colombia, [3]Faculty of Health Sciences - Universidad Autónoma De Bucaramanga (UNAB), Bucaramanga, Colombia

O39 Assessment of CCR2-Related Inflammatory Activity in Abdominal Aortic Aneurysms with 99mTc-HYNIC-CCR2-L and SPECT/CT

Dr. Jorge Rodríguez[1], Dr Javier Anaya Ayala, Dr Joel Eduardo Vargas Ahumada, Dr Rodrigo Hernandez Ramirez, Dr Felipe de Jesús Rodríguez Hernández
[1]Instituto Nacional de Ciencias Médicas y Nutrición, Mexico City, Mexico

O40 SPECT/CT with [99mTc]Tc-UBI 29-41 in challenging-to-diagnose infections: clinical concordance and impact on redefining the initial diagnosis

Dr. Hernando Andres Benavides Jimenez[1], Dr Luz Kelly Anzola Fuentes[3], Dr Viviana Andrea Daza Betancourt[1], Dr Cristian Camilo Vargas Lopez[1], Dr Sebastian Rojas Lara[1], Dr Sergio Moreno Lopez[4], Dr Carlos Alvarez Moreno[2]
[1]Fundacion Universitaria Sanitas, Bogota, Colombia, [2]Clinica Reina Sofia, Bogota, Colombia, [3]Clinica Universitaria Colombia, Bogota, Colombia, [4]Universidad Nacional de Colombia, Bogota, Colombia

O41 Splenic uptake in dipyridamole stress and rest tc-99m mibi spect: a potential vasodilatory marker

Dr. Paula Aristov[1], Dr. Andrés Damián[1], Dr. Rodolfo Ferrando[1], Dr. Omar Alonso[1], Dr. Federico Ferrando[1], Técnico Aldo Sanchez[1], Técnico Pablo Bracesco[1]
[1]Servicio Medicina Nuclear, Hospital De Clinicas, Montevideo, Uruguay

O42 Cannabidiol prevents age-related cognitive decline and neuroinflammation, and enhances brain metabolism in a Down syndrome animal model

Dr. Lidia Spelta[1], Chiara Righini[1], Jean Brizola[1], Dr. Carlos Buchpiguel[1], Dr. José Alexandre Crippa[2], Dr. Daniele de Paula Faria[1]
[1]Laboratory of Nuclear Medicina, Faculty of Medicine, University of São Paulo (USP), São Paulo, Brazil, [2]Department of Neurosciences and Behavior, Faculty of Medicine from Ribeirão Preto, University of São Paulo (USP), Ribeirão Preto, Brazil

O43 Quantitative 99mTc-PYP SPECT/CT in ATTR-CA: head-to-head MBR, LV/bone and SUVmax with near-perfect discrimination

Mr. Luciano Santos[1], Mrs. Agustina Pérez[1,2], Mr. Pablo Roman[1,2], Mrs. Karina Bayardo[2], Mr. Federico Ferrando[1,2], Mr. Rodolfo Ferrando[1,2]
[1]Consultorio De Medicina Nuclear Ffp., Montevideo, Uruguay, [2]Centro de Medicina Nuclear e Imagenología Molecular del Hospital de Clínicas, Universidad de la República, Montevideo, Uruguay., Montevideo, Uruguay

O44 Myocardial perfusion imaging: When is not just supine, not just prone

Dr. Romina Lorena Romero[1], Dr. Karina Quintero[2], Dr. María del Carmen Alak[1], Dr. César Mendez[1], Lic. Hernan Policella[1], Lic. Antonio Casares[1], Lic. Macarena Montaño[1]
[1]Hospital Británico De Buenos Aires, Buenos Aires, Argentina, [2]Hospital de Pediatría Dr. Juan P. Garrahan, Buenos Aires, Argentina

O45 Standardized Formulation of a Business Case for a PET-CT Nuclear Medicine Service in Colombia

Dr. Saule Karanauskas[1], Ingeniera Lenys Roncancio[1], Dr. María Martínez[1]
[1]Medicina Nuclear Diagnostica, Villavicencio, Colombia

O46 [177Lu]Lu-DOTA-ATWLPPR/(D-Lys6-LHRH) peptide heterodimer as a potential theragnostic agent for prostate and breast cancer

Dr. Ximena Camacho[1], MSc. Carolina Perroni[1], Dr. Mirel Cabrera[1], Dr. Lucía Alfaya[1], Dr. Marcos Tassano[1], MSc. Ana Laura Reyes[2], Tech. Andrea Paolino[2], Dr. Eduardo Savio[2], Dr. Juan Pablo Gambini[1,2], Dr. Pablo Cabral[1]
[1]Universidad de la República, Montevideo, Uruguay, [2]Centro Uruguayo de Imagenología Molecular, Montevideo, Uruguay

O47 Targeted ROR1 protein degradation combined with PET imaging reveals the role of ROR1 in overcomes EGFR Resistance in NSCLC

Mr. Bo Mei[1], Prof Zhi Yang[1], Prof Lei Xia[1]
[1]Peking University Cancer Hosiptal, Beijing, China

O48 Preclinical evaluation of ^{212}Pb-labeled CXCR4 peptides for targeted alpha therapy in colorectal carcinomatosis

Mr. Richard Whiteside[1], Nasrin Abbasi-Gharibkandi[1], Fabio Gallazzi[1], Jessica Newton-Northup[1], Meltem Ocak[1], David Bauer[1]
[1]The University of Missouri, Columbia, United States

O49 Intraoperative Sentinel Lymph Node Mapping with Dual Modality (Radioisotopic/Optical) Using 99mTc-ICG Nanocolloid: Improved Precision and Overcoming Clinical Limitations

Mrs. Carolina Furtado Prieto[1,2], Ms. Bettina Martinucci[1], Ms. Mirel Cabrera[2], Ms. Ximena Camacho[2], Mr. Marcos Tassano[2], Mr. Omar Alonso[1], Mr. Gustavo Burroso[3], Mr. Pablo Duarte[3], Mr. Alarico Rodríguez[3], Mr. Pablo Cabral[2], Mr. Juan Pablo Gambini[1,3]
[1]UA Medicina Nuclear e Imagenología Molecular, Hospital de Clínicas Dr. Manuel Quintela, Facultad de Medicina, UdelaR, Montevideo, Uruguay, [2]Centro de Investigaciones Nucleares, Facultad de Ciencias, UdelaR, Montevideo, Uruguay, [3]Centro Uruguayo de Imegenología Molecular, Montevideo, Uruguay

O50 Intraoperative near-infrared lymphatic mapping in thyroid cancer using intrathyroidal indocyanine green

Mrs. Carolina Furtado Prieto[1,2], Ms Bettina Martinucci[1], Ms Carolina Guarneri[3], Mr Ulises Parada[3], Mr Pablo Duarte[4], Mr Omar Alonso[1], Mr Gustavo Burroso[4], Mr Alarico Rodríguez[4], Mr Pablo Cabral[2], Mr Juan Pablo Gambini[1,4]
[1]UA Medicina Nuclear e Imagenología Molecular, Centro de Investigaciones Nucleares - Universidad de la República, Montevideo, Uruguay, [2]Centro de Investigaciones Nucleares, Facultad de Ciencias, UdelaR, Montevideo, Uruguay, [3]Unidad Académica Clínica Quirúrgica A, Hospital de Clínicas Dr. Manuel Quintela, Facultad de Medicina, UdelaR, Montevideo, Uruguay, [4]Centro Uruguayo de Imagenología Molecular, Montevideo, Uruguay

O51 Diagnostic Accuracy of Robotic Arm assisted Real time PET-CT guided Biopsy of Abdomino-pelvic lesions including Retroperitoneal lesions

Dr. Arun Ravi John[1], Dr Jeenu Varghese[1], Dr Srivallabh Dande[1], Dr TVSVGK Tilak[1]
[1]Command Hospital Air Force, Bengaluru, India

O52 Bridging Vision and Practice: The Journey to Implementing a Theranostics Centre at the University Health Network in Toronto, Canada

Dr. Luke Brzozowski[1]
[1]University Health Network, Toronto, Canada

O53 Real-world efficacy: first prospective study in Argentina of the effectiveness and safety of 177Lu-DOTATATE in GEP-NET

Dr. Silvina Racioppi[1], Dr. Eduardo Cardozo[2], Lic. Mariano Portillo[1], **Lic. Mariano Portillo**[1], Dr. Martina Musumeci[1], Lic. Marcos Mussio[1], Dr. Federico Esteso[2], Dr. Juan Manuel OConnor[2]
[1]Servicio de Medicina Nuclear, Instituto Alexander Fleming, Buenos Aires, Argentina, [2]Servicio de Oncología Clinica, Instituto Alexander Fleming, Buenos Aires, Argentina

O54 Intraoperative metabolic assessment (PET-CT) of surgical margins in breast cancer: a novel challenge in oncologic surgery

Dr. John Orozco Cortés[1], Dr. Jorge Sabater Sancho[2], Dr. Elvira Buch Villa[3], Dr. Ernesto Muñoz Sornosa[3], Dr. Vicente López Flor[3], Dr. Tomas Mut Dolera[3], Dr. LíLíria Térradezas[3], Dr. Octavio Burgués Gaisón Burgués Gaisón[3], Dr. MMarcos AdrianzenVargas[3], Dr. RafRafael Díazpósito[4]
[1]Hospital Universitario Dr. Peset, Valencia, Spain, [2]Consorcio Hospitalario Provincial de Castellón, Castellon, Spain, [3]Hospital Clínico Universitario de Valencia, Valencian, Spain, [4]Hospital Universitario y Politecnico la Fe, Valencia, Spain

O55 Freehand-SPECT augmented reality navigation compared with planar scintigraphy for sentinel lymph node biopsy in breast cancer

Dr. John Orozco Cortés[1], Dr. Franco Jose Cavagna Matti[1], Dr. Angela Esteban Hurtado[2], Dr Georgina Bonino[1], Dr PPedro AbreuSanchez[1], Dr. Jose Rafael Infante de la Torre[1], Dr Fabrizio Montenegro Muñoz[1], Dr. Laura Casas Calabuig[1], Dr. Maria Dolores Reyes Ojeda[1], Dr Elisa Veronica Caballero Calabuig[1]
[1]Hospital Universitario Dr. Peset, Valencia, Spain, [2]Centre Medic Alomar, Barcelona, Spain

O56 First experience with molecular surgery in pancreatic and hepatic cancer using PET radiopharmaceuticals

Dr. John Orozco Cortés[1], Dr. Jorge Sabater Sancho[2], Dr. Luis Sabater Ortí[3], Dr. Antonio Stacey Solis[3], Dr. Elena Muñoz Forner[3], Dr. Maria del Puig Cozar Santiago[3], Dr. Marina Garces Albir[3], Dr. Carolina Castillorias[3], Dr Maria Carmen Redal Peña[3], Dr. Rafael Díaz Expósito[4]
[1]Hospital Universitario Dr. Peset, Valencia, Spain, [2]Consorcio Hospital Provincial de Castellon, Castellon, Spain, [3]Hospital Clinico Universitario de Valencia, Valencia, Spain, [4]Hospital Universitario y Politecnico la Fe, Valencia, Spain

O57 Impact of fixed suv thresholds on lesion segmentation in psma pet/ct: methodological implications for recip response assessment to lu177-psma-617 therapy

Mr. Yann Cras[1], MD. Khalil Trabelsi[1], MD. Adam Bekkhoucha[1], MD. Tarek Kamoun[1], MD. Mehdi Borsali[1], Pr. Désirée Deandreis[1], DR. Camilo Garcia[1]
[1]Gustave Roussy, Villejuif, France

O58 Limitations of applying the hänscheid single-time-point method to 177lu-psma-617 organ dosimetry: toward psma-specific simplified protocols

Mr. Yann Cras[1], MD. Khalil Trabelsi[1], MD. Adam Bekkhoucha[1], MD. Tarek Kamoun[1], MD. Mehdi Borsali[1], Pr. Désirée Deandreis[1], MD. Camilo Garcia[1]
[1]Gustave Roussy, Villejuif, France

O59 Selection of Patients for Lutetium-177 DOTATATE Therapy Using Tc-99m HYNIC-TOC Scintigraphy: Preliminary Experience in a Peruvian Center

Dr. Shirley Alarcon[1], Dr. Estuardo Paredes
[1]Clinica Ricardo Palma, Lima, Perú

O60 Biochemical Variability in the Response to [177Lu]Lu-iPSMA in Heavily Pretreated Patients: Real-World Experience

Dr. Edgar Hernandez[1], Dr. Francisco Osvaldo García Pérez[1], Dra. Irma Soldevilla Gallardo[2], Dra. Quetzali Gabriela Pitalua Cortés[3], Dra. Sofía Denisse Gonzalez Rueda[1]
[1]INCan, Cdmx, México, [2]ABC, CDMX, México, [3]Medica Sur, CDMX, México

O61 Role of 18F-PSMA-(Pylclari) and 68Ga-PSMA-11 PET-CT in the staging of high-risk prostate cancer

Javier Jesus Robles Barba[1], Juan José Martín Marcuartu[1], **Dr. Carlos Andrés Tapias Mesa**[1], Jorge Luis Díaz Moreno[1], Andrea Bagan Trejo[1], Marta Zamorano Rivas[1], David Durany Lara[2], María Pane Foix[3], Jose Francisco Suarez Novo[4], Montserrat Cortes Romera[1]
[1]Servicio de Medicina Nuclear / PET (IDI). Hospital Universitario de Bellvitge, L'Hospitalet de Llobregat, Spain, [2]Servicio de Radiología. Hospital Universitario de Bellvitge, L'Hospitalet de Llobregat, Spain, [3]Servicio de Anatomía Patológica. Hospital Universitario de Bellvitge, L'Hospitalet de Llobregat, Spain, [4]Servicio de Urología. Hospital Universitario de Bellvitge, L'Hospitalet de Llobregat, Spain

O62 99mTc-HYNIC-iPSMA SPECT/CT in Prostate Cancer: A Real-World Data Multicentric Study in 457 Mexican Patients

Dr. Joel Vargas Ahumada[1], Dr. Luis Vargas Rodriguez[1], Dr. Sergio López Buenrostro[2], Dr. Paola Vallejo Armenta[1], Dr. Ana L. Calderón Ávila[3], Dr. Eleazar Ignacio Álvarez[4], Dr. Fabrio A. Sinisterra Solis[1]
[1]Imagenologia Diagnóstica, Xalapa, México, [2]Unidad de Patología Clínica, Guadalajara, México, [3]Centro Médico Nacional Siglo XXI, Ciudad de México, México, [4]Hospital Almater, Mexicali, México

O63 Prospective head-to-head comparison of 18F-PSMA -1007 and 18F-DCFPyl PET/CT for primary skeletal staging in high-risk prostate cancer

Dr. Marko Seppänen[1], Simona Malaspina[1], Ekaterina Saukko[2], Tommi Noponen[3], Jukka Kemppainen[1], Mikael Anttinen[4], Suvi Hartikainen[5], Janne Salonen[6], Peter Boström[4], Otto Ettala[4]
[1]Turku PET Centre, University of Turku, Turku University Hospital, Turku, Finland, [2]Department of Radiology, Turku University Hospital and University of Turku, Turku, Finland, [3]Department of Clinical Physiology, Nuclear Medicine, Turku PET Centre and Medical Physics, Turku University Hospital, Turku, Finland, [4]Department of Urology, University of Turku and Turku University Hospital, Turku, Finland, [5]Department of Clinical Physiology and Nuclear Medicine, Kuopio University Hospital, Kuopio, Finland, [6]Department of Nuclear Medicine, University of Helsinki and Helsinki University hospital, Helsinki, Finland

O64 Validation of PET/CT with 18F-NOTA-Oc and 18F-FDG for obtaining the "NETPET score" as a prognostic biomarker in neuroendocrine neoplasms

Dr. Francisco Jesus Solano Caballero[1], Dr. Rodrigo Hernández Ramírez[1], Dr. Juan Pablo Chávez Torres[1], Dra. Natalia Ramírez Pedraza[1], Dra. Ailan Hitandhui Barrientos Priego[1], Dr. Miguel Angel Corza Ayala[1], Dra. Abigail Arriaga Contreras[1]
[1]Instituto Nacional De Ciencias Médicas Y Nutrición Salvador Zubirán, Tlalpan, Mexico

O65 [99mTc]Tc-HYNIC-PEG4-ATWLPPR/Tricine peptide as a potential diagnostic agent for prostate cancer: In vitro evaluation

Mrs. Carolina Perroni Zanoniani[1], Dr Ximena Camacho[1], Dr Mirel Cabrera[1], Dr Lucía Alfaya[1], Dr Marcos Tassano[1], Dr Juan Pablo Gambini[3], Dr Pablo Cabral[1]
[1]Departamento de Radiofarmacia, Centro de Investigaciones Nucleares, Facultad de Ciencias, Universidad de la República, Montevideo, Uruguay, [2]Centro Uruguayo de Imagenología Molecular, Montevideo, Uruguay, [3]Centro de Medicina Nuclear e Imagenología Molecular Hospital de Clínicas, Facultad de Medicina, Universidad de la República, Montevideo, Uruguay, Montevideo, Uruguay

O66 Results from a Prospective Phase I Clinical Trial on [68Ga]Ga-OncoACP3 in Prostate Cancer: Safety, Dosimetry, Pharmacokinetics and Diagnostic Performance

Dr. Cristiano Pini[1], Dr. Fabrizia Gelardi[1], Prof. Martina Sollini[1,2], Dr. Anna Piai[3], Dr. Rita Petrelli[2], Prof. Paola Anna Erba[4,5], Dr. Jacqueline Mock[6], Dr. Samuele Cazzamalli[6], Dr. Dario Neri[6], Prof. Arturo Chiti[1,2]
[1]Vita-salute San Raffaele University, Milan, Italy, [2]Department of Nuclear Medicine, IRCCS Ospedale San Raffaele, Milan, Italy, [3]Medical Physics Department, IRCCS Ospedale San Raffaele, Milan, Italy, [4]School of Medicine and Surgery, University of Milano-Bicocca, Milan, Italy, [5]Nuclear Medicine Unit, ASST Papa Giovanni XXIII Hospital, Bergamo, Italy, [6]Philochem AG, Otelfingen, Switzerland

O67 Prostate Tumor Volume by 68Ga-PSMA PET/CT as a Predictor of Lymph Node Metastases in High-Risk Prostate Cancer

Dr. Angie Paola Llanos Cuellar[1], Ana Milena Gualdrón-Naranjo[1], Liliana Patricia Torres-Agredo[2], Humberto Varela-Ramirez[2], Alejandra Gomez-Marting[1], Helen Johanna Mejia-Efeer[1], Milton Yesid Gomez-Buitrago[1], Marco Antonio Parra-Pérez[1]
[1]Fundación Universitaria Sanitas, Bogotá, Colombia, [2]Instituto Nacional de Cancerología, Bogotá, Colombia

O68 Usefulness of Fluoride PET CT 18F-Alf Nota on suspicion of well-differentiated neuroendocrine tumors (NETs)

Dr. Francisco Gomez[1], Dr. Alejandro Rojas[1], Dr. Juan Dupouy[1], Dr. Teresa Massardo[1], Dr. Jose Tomas Donoso[1], Dr. Paloma Peña[1], Dr. Evelyn Ortiz[1], Dr. Francisco Tortorolo[1], Dr. Rocio Hidalgo[1], Ms. Sofia Rivas[1]
[1]Hospital Clinico Universidad De Chile, Santiago, Chile

O69 [18F]SiTATE in neuroendocrine neoplasia (NEN): first Latin America experience in prostate, lung and colon NEN patients

Dr. Emiliano Michel Sánchez[1], Dr. Vikas Prasad[2], MSc Eduardo Antonio González Villa[1], BSc. Francisco Rafael Peres Anaya[1], Dr. Danny Roberto Mena Cortes[1]
[1]Oncologia San Jose, HERMOSILLO, Mexico, [2]Mallinckrodt Institute of Radiology, St. Louis, US

O70 Clinical Impact Of 18F-PSMA-1007 PET/CT In the Evaluation of Prostate Cancer Patients: Analysis Of 511 Patients in Different Clinical Scenarios

Dr. Gerardo Dos Santos[1,2], Dra. Agustina Banchero[1], Dra. Marta Iraetha[1], Dr. Mauriel Díaz[1], Dr. César Ferreira[2], Dr. Eduardo Lischinky[2], Technician Ismael Cordero[1], Dr. Omar Alonso[1,2]
[1]Uruguayan Center of Molecular Imaging (CUDIM), Montevideo, Uruguay, [2]Nuclear Medicine and Molecular Imaging Center, Clinical Hospital “Dr. Manuel Quintela” University of Uruguay, Montevideo, Uruguay

O71 Magnitude of change in radiotherapy planning in biochemical recurrence of prostate cancer. From theoretical planned to definitive treatment post-PET-TC PSMA

Dr. Pedro Jose Plaza Lopez[1,2], Dr Francesco Amorelli[3], Dr Juan Sebastian Blanco[1], Dra Eliana Carrillo[1], Dra Natali Augusto[4], Dra Palmira Foro[2,3]
[1]Hospital del Mar. Nuclear Medicine Department, Barcelona, Spain, [2]Universitat Pompeu Fabra, Barcelona, España, [3]Hospital del Mar. Radiation Oncology Department, Barcelona, España, [4]Hospital Josep Trueta. Clinical Analysis Department, Girona, España

O72 Biochemical Response Following PSMA-1007 Metabolic Imaging-Guided Radiotherapy in Patients with Biochemical Recurrence of Prostate Cancer After Radical Prostatectomy

Dr. Pedro Jose Plaza Lopez[1,2], Dr Fracesco Amorelli[3], Dr Juan Sebastian Blanco[1], Dra Raquel Valhondo[1], Dra Cristina Soldevilla[1], Dra Patricia Stefanelli[1], Dra Palmira Foro[2,3]
[1]Hospital del Mar. Nuclear Medicine Department, Barcelona, Spain, [2]Universitat Pompeu Fabra, Barcelona, España, [3]Hospital del Mar. Radiation Oncology Department, Barcelona, España

O73 Comparison of 18F-PSMA-1007 and 18F-DCFPyL PET-CT in prostate cancer patients with occult biochemical recurrence with low PSA values

Dr. Pedro Jose Plaza Lopez[1], Dr Francesco Amorelli[3], Dr Juan Sebastian Blanco[1], Dra Eliana Carrillo[1], Dra Raquel Valhondo[1], Sr Guillermo García Álvaro[1], Dra Palmira Foro[2,3]
[1]Hospital del Mar. Nuclear Medicine Department, Barcelona, Spain, [2]Universitat Pompeu Fabra, Barcelona, España, [3]Hospital del Mar. Radiation Oncology Department, Barcelona, España

O74 Non-informative [18F]FDG PET/CT studies and rescheduling times as quality indicators in a Latin American reference center

Mr. Ismael Cordero[1], Mr. Martin Sabatella[1], Mr. Javier Giglio[1], Mr. Omar Alonso[1], Mr. Gustavo Burroso[1], Mr. Juan Pablo Gambini[1]
[1]Uruguayan Center of Molecular Imaging (CUDIM), Montevideo, Uruguay

O75 Synergy in sight: fusing PSMA PET/CT and mpMRI parameters to enhance prostate cancer risk stratification

Dr. Eva Lorena Valadez Montero[1], Dr. Bethsabel Rodríguez Encinas, MD. Irma Soldevilla Gallardo
[1]CENTRO MEDICO ABC, Mexico City, Mexico

O76 KANBAN: Implementation of Software for Patient Traceability in Radioiodine Treatments at the Arturo López Pérez Foundation

Prof. Cristina Gutiérrez Correa[1], Prof Dennys Cuevas Gómez[1], Prof Fernando Navarro[1], Prof Sergio Veliz[1], Prof. Ruben Olave[1], Prof. Miguel Rojas[1], Prof. Luis Madariaga[1], Dra. M. Josefina Jofre[1]
[1]Fundación Arturo Lopez Perez, Santiago, Chile

O77 Serum-stimulated thyroglobulin levels before radioactive iodine therapy as a predictive biomarker of disease-negative whole-body scan in differentiated thyroid cancer

Dr. Andres Gamboa[1], Dr. Liset Sanchez[1,2], Dr. Mabel Gomez[1], Dr. Wendy Gallegos[1], Dr. Cesar García[1,2], Dr. Tatiana Morales[1], Dr. Lizeth Rodriguez[1]
[1]Universidad Autónoma de Bucaramanga - UNAB, Bucaramanga, Colombia, [2]SPECT S.A.S, Bucaramanga, Colombia

O78 Positron emission tomography/computed tomography radiomics score predicts metabolically active disease and reflects glycolysis-related protein expression in aggressive B-cell lymphomas

Mr. Farid Cury Neto[1,2], Mr. Gabriel de Prince Garcia[2], MSc. Patrik da Silva Vital[1], Dr. Murilo Bonatelli[1], Mr. José Augusto Santanna Otteiro[3], MD., MSc. Flávia Fazzo Barbin[4], MD., MSc. Eduardo Caetano Albino da Silva[4], Dr. Marcelo Wilson Berbone Furlan Alves[5], MD., Dr. Wilson Eduardo Furlan Matos Alves[2,3], Dr. Céline Pinheiro[1,2]
[1]Molecular Oncology Research Center, Barretos Cancer Hospital, Barretos, Brazil, [2]Barretos School of Health Sciences Dr. Paulo Prata, Barretos, Brazil, [3]Department of Nuclear Medicine, Barretos Cancer Hospital, Barretos, Brazil, [4]Department of Pathology, Barretos Cancer Hospital, Barretos, Brazil, [5]Aeronautical Technology Institute, São José dos Campos, Brazil

O79 Head-to-head intrapatient qualitative comparison of 68Ga-FAPI-04 versus 18F-FDG PET/CT in various oncological pathologies

Dr. Eduardo Lischinsky[1], Javier Giglio[2], Eduardo Savio[2], Ismael Cordero[1,2], Dr. Omar Alonso[1,2], Dr. Gustavo Burroso[2], Dr. Alarico Rodriguez[2], Dr. Juan Pablo Gambini[1,2]
[1]CMNIM, Hospital De Clínicas "Dr. Manuel Quintela" - Universidad De La República, Montevideo, Uruguay, [2]Centro Uruguayo de Imagenología Molecular (CUDIM), Montevideo, Uruguay

O80 Comparison of 99mTc-MAA SPECT/CT and CECT with CBCT for Tumor Perfused Liver Volume Segmentation Prior to 90Y Radioembolization

Dr. Leticia Portillo[1], Dr. Rodrigo Hernández Ramírez[1], Dr. Miguel Angel Corza Ayala[1], Dr. Juan Pablo Chávez Torres[1]
[1]Instituto Nacional de Ciencias Médicas y Nutrición Salvador Zubirán, Mexico, Mexico

O81 SPECTRA trial: Study of PD-L1 expression and molecular hybrid imaging in triple negative breast cancer: Response prediction and assessement

Dr. Sofía Denisse González Rueda[1,2], Dr. José Antonio García Gordillo[1], Dr. Carlos Arturo González Núñez[1], Dr. Sergio Israel Aguilar Villanueva[1], Dr. Francisco Osvaldo García Pérez[1], Dr. Juan Enrique Bargalló Rocha[1,4], Dr. Paula Anel Cabrera Galeana[1], Dr. Guillermina Ferro Flores[3], Dr. Quetzali Gabriela Pitalúa Cortés[1,2], Dr. Irma Soldevilla Gallardo[1,4]
[1]National Cancer Institute of Mexico, Tlalpan, Mexico, [2]Medica Sur, Tlalpan, Mexico, [3]National Institute of Nuclear Research, Toluca, Mexico, [4]ABC Medical Center, Álvaro Obregón, México

O82 Associated factors with positive [18F]FDG-PET/CT for distant metastasis in breast cancer

Dr. Ada Katerine Franco-ardila[1], Iván Fabricio Vega-González[1,2], Noiver Arbey Graciano-Vera[3], Katerine Montoya-Lezcano[4], Sonia Luz Gómez-Garcés[1], Lina María López-Vélez[2], Indira Díaz-Contreras[1]
[1]Universidad Autónoma De Bucaramanga - Unab, Bucaramanga, Colombia, [2]Clínica Las Américas AUNA, Medellín, Colombia, [3]Instituto de cancerología Las Américas AUNA, Medellín, Colombia, [4]Fundación IDEAS AUNA, Medellín, Colombia

O83 Development and Evaluation of a Novel Dual-Targeted ^{68}Ga-FAPI-TTP PET Probe for Enhanced Tumor Imaging

Mrs. Yi-fei Pei[1], Mrs. Xiao-Yi Guo[1], prof Hua Zhu[1], prof Zhi Yang[1]
[1]State Key Laboratory of Holistic Integrative Management of Gastrointestinal Cancers, Beijing Key Laboratory of Carcinogenesis and Translational Research, NMPA Key Laboratory for Research and Evaluation of Radiopharmaceuticals (National Medical Products Administration), Department of Nuclear Medicine, Peking University Cancer Hospital & Institute, Beijing 100142, China, Beijing, China

O84 Real-life applicability of Fluorocholine PET/CT in primary hyperparathyroidism

Dr. Ivan Vega[1], **Dr. Monica Vidal**[2], Dra. Stefania Cruz[3], Dr. Antonio Rivera[4], Dr. Alejandro Delgado[2], Dra. Indira Diaz[5], Dra. Clara Arango[2], Dra. Carolina Prieto[2], Dr. Carlos Builes[2]
[1]Clínica Las Américas-AUNA, Medellín, Colombia, [2]Hospital Pablo Tobón Uribe, Medellín, Colombia, [3]Universidad Pontificia Bolivariana, Medellín, Colombia, [4]Universidad de Antioquia, Medellín, Colombia, [5]Unidad Gammanuclear , Armenia, Colombia

O85 Patient-specific factors in radioactive Iodine (I-131) clearance in Differentiated Thyroid Cancer (DTC) treatment

Mr George Thiveos[1], Mr Theofanis Petropoulos[1], Mr John Papantoniou[1], Mrs Agelliki Kokkini-Paschou[1], Mrs Garyfallia Livitsanou[1], Dr Evangelia Skoura[1], Dr Ioannis Datseris[1], **Dr. Ioannis Koutsikos**[1]
[1]Henry Dunant Hospital Center, Athens, Greece

O86 Bayesian survival modeling in multiple myeloma: prognostic PET/CT value with missing data imputation, preliminary results

Dr. Eliana Andrea González Artunduaga, Estadistico PhD Nelson Cruz, MD Hematologo Kenny Galvez
[1]Medico Nuclear IDIME, Bogotá, Colombia

O87 From Variability to Equity: An Eight-Year Retrospective Analysis of I-131 Therapeutic Practices in a Nuclear Medicine Service

Lic. Mariano Portillo[1], Dr. Martina Musumeci[1], Lic Marcos Mussio[1], Tec Delfina Eugeni[1], Dr Luciana Arburua[1], Tec Ariel Arispe[1], Dr. Silvina Racioppi[1]
[1]Servicio de Medicina Nuclear, Instituto Alexander Fleming, Buenos Aires, Argentina

O88 Immunosuppressive molecular mechanisms potentially supporting development and progression of haematological malignancies triggered by abnormal or accidental exposure to nuclear irradiation

Dr Inna Yasinska[1], **Dr. Vadim Sumbayev**[1]
[1]University Of Kent, Chatham Maritime, United Kingdom

O89 SPECT-CT in Primary Hyperparathyroidism: The Intermediate Localization Method

Dr. Carlos Collaud[1], Dra. Veronica Santana[1], Dra. Sandra Sunagua[1], Dra. Irene Arma[1], Dra. Isabel Hume[1], Dra Constanza Cianciarelli[1], Dra. Maria Chacon[1], Dra. Nadia Pabstleben[1], Dra. Ana Mollerach[1], Dra. AAna Mollerach
[1]Hospital Italiano De Buenos Aires, Buenos Aires, Argentina

O90 Multiparametric Radiomic Analysis Based on 18F-FDG PET, MRI and Biopsy for Predicting Pathological Complete Response to Breast Cancer Neoadjuvant Chemotherapy

Mr. MARCO GUARIN[1], Ms. Carolina Tinetti[2], Mr. Mauro Namías[2]
[1]Instituto Nacional De Cancerología, Bogotá, Colombia, [2]Fundación Centro Diagnóstico Nuclear, Buenos Aires, Argentina

List of E-Posters

P001 Myocardial perfusion in patients with suspected coronary artery disease: association with troponin T levels in three centers in Bogotá

Dr. Maria Camila Bedoya Gonzalez[1], Dr. Andrea Carolina Suarez Echavez[1], Dr. Mauricio Andrés Hinojosa Vidal[1], Dr. Alejandro Cortés Polanía[1], Dr. Humberto Varela Ramírez[1]
[1]Fundacion Universitaria De Ciencias De La Salud, Bogotá d.c., Colombia, [2]Fundacion Universitaria Sanitas, Bogotá d.c., Colombia, [3]Clinicas colsanitas, Bogotá d.c., Colombia

P002 Agreement of left ventricular ejection fraction by echocardiography and SPECT in patients with chest pain and suspected ischemia

Dr. Angie Cabrera Rojas[1], Dr. César García Quintanilla[2], Dr. Javier Rodríguez Prada[3], Dr. Adriana Reyes González[4]
[1]Universidad Autónoma de Bucaramanga, Floridablanca, Colombia, [2]SPECT Medicina Nuclear SAS, Floridablanca, Colombia, [3]Unidad de Investigación y Educación, Instituto del Corazón de Bucaramanga, Floridablanca, Colombia, [4]Universidad Autónoma de Bucaramanga, Floridablanca, Colombia

P003 Correlation between Chagas myocartiopathy and heart failure with sudden death over a 10-year period

Lic. Elizabeth Huanca[1], Doctor Raúl Araujo, licenciado Marcelo Torrez, Licenciada Patricia Bernal, Ingeniero Alfredo Zambrana, Doctora Greta Vargas, Doctor Daniel Salinas
[1]Universidad San Francisco Xavier De Chuquisaca, Sucre, Bolivia

P004 Experience at a university hospital with positron emission tomography using fluorine-18-labeled glucose metabolism in inflammatory/infectious cardiovascular processes

Dr. Teresa Massardo[1], Dr. Juan Dupouy[1], Dr. Alejandro Rojas, Dr. José Tomás Donoso, Dr. Diego Palma, Dr. Daniel Saavedra, Dr. Francisco Javier Gomez[1], Dr. Rocio Hidalgo[1], Dr. WWilfredo Navarrete, Dr. Axel Aranguiz[1], Dr. Daniel Schneider Dr Marcelo Llancaqueo[1]
[1]Hospital Clinico Universidad De Chile, Santiago/Chile, Chile, [2]hospital San Juan De Dios, Santiago/Chile, Chile

P005 18F-FDG PET/CT for the Detection and Reclassification of Infective Endocarditis in Corrected Congenital Heart Disease

Mrs. Sonia Simona Traverso, MD Roxana Campisi, MD Jessica Herrero, MD Christian Gonzalez, MD Calderon Laura, MD Paola Corona, MD Nicolas Bustos, MD Florencia Arabolaza, MD Gabriel Bruno
[1]Nuclear Diagnostic Center (FCDN), CABA, Argentina

P006 Is Cardiac Amyloidosis an Underdiagnosed Disease? Defining Frequency in Colombia

Dr. Monica Vidal[1], Dr. Alejandro Delgado[1], Dr. Juan Luis Londoño[2], Dr. Nilson Lopez[1]
[1]Hospital Pablo Tobón Uribe, Medellín, Colombia, [2]Hospital San Vicente Fundación, Medellín, Colombia

P007 Diagnostic Value of Dual-Time-Point 18F-Fluorocholine PET/CT in Hyperparathyroidism: A Latin American Retrospective Cohort

Dr. Melissa Alvarez[1], Dr. Rosita Nohemy Dorado Castillo[1], Dr. Diana Carolina Quijano Galvis[1], Dr. Luz Maritza Pabon Castilla[1], Jefe de enfermería John Jairo Torres Gallego[1], o Jefe de enfermería Beatriz Elena Guzman Narvaez[1], TECNICO Juliana Maria Venegas Sanchez[1], TECNICO Jessenia Jimenez Moreno[1], TECNICO Javier Andrés Garces Giraldo[1], TECNICO Jenner Pulido Pasaje[1]
[1]Fundación Valle Del Lili, Cali, Colombia

P008 Stimulated Pre-Ablative Thyroglobulin: Can It Be Used as a Parameter to Avoid Ablation?

Dr. Irene Arma[1], Ana Maria Mollerach[1], Isabel Hume[1], Constanza Cianciarelli[1], Maria Jose Chacon[1], Ana Wayngarten[1], Fabiana Russo Picasso[1], Nadia Pabstleben[1], Florencia Zalarrayan[1], Carlos Collaud[1]
[1]Hospital Italiano De Buenos Aires, CABA, Argentina

P009 Primary Cultures and FISH analysis in Mesenchymal Cells from Osteomalacia-Inducing Tumors (TIO)

Dra. Patricia Gargallo[1], **Dr. Maria Jose Bastianello**[1], Lic Diego Biscochea[1], Dr Roxana Chirico[1], Grupo Argentino de TIO Grupo Argentino de TIO[2], Tech Brenda Konowalik[1]
[1]CEMIC University Hospital, Buenos Aires, Argentina, [2]Grupo Argentino de TIO, CABA, Argentina

P010 Diagnostic utility of 11C-methionine PET/CT in primary hyperparathyroidism: national experience in Uruguay

Dr. Eduardo Lischinsky[1], Dr. Omar Alonso[1,2], Ismael Cordero[1,2], Eduardo Savio[1,2], Javier Giglio[2], Dr. Juan Pablo Gambini[1,2]
[1]CMNIM, Hospital De Clínicas "Dr. Manuel Quintela" - Universidad De La República, Montevideo, Uruguay, [2]Centro Uruguayo de Imagenología Molecular (CUDIM), Montevideo, Uruguay

P011 Synergistic role of 99mTc-MIBI radioguided surgery and ICG fluorescence in primary and secondary hyperparathyroidism: experience in three cases

Dr. Bettina Martinucci[1], Carolina Furtado[1,2], Mirel Cabrera[2], Ximena Camacho[2], Marcos Tassano[2], Omar Alonso[1], Pablo Duarte[3], Alarico Rodriguez[3], Pablo Cabral[2], Juan Pablo Gambini[2,3]
[1]UA Medicina Nuclear e Imagenología Molecular, Hospital de Clínicas Dr. Manuel Quintela, Facultad de Medicina, UdelaR, Montevideo, Uruguay, [2]Centro de Investigciones Nucleares, Facultad de Ciencias, Universidad de la Republica, Montevideo, Uruguay, [3]Centro Uruguayo de Imagenología Molecular, Montevideo, Uruguay

P012 Beyond the neck: utilizing 18-f-choline pet/ct to uncover the source of primary hyperparathyroidism

Dr. Alejandra Gabriela Salgado[1], Dr Laura Felipe[1], Dr Antonella Kovic[1], Dr Maria del Carmen Alak[1]
[1]Imat, Buenos Aires, Argentina

P013 Role of PET/CT in the follow-up of large vessel vasculitis-an experience in a single center

Dr. Irene Arma[1], Dr Isabel Hume[1], Dr Ana Mollerach[1], Dr Constanza Cianciarelli[1], Dr Nadia Pabstleben[1], Dr Maria Jose Chacon[1], Dr Ana Wayngarten[1], Dr Sandra Sunagua[1], University Technologist Mayra Borges[1], Dr Carlos Collaud[1]
[1]Hospital Italiano De Buenos Aires, Caba, Argentina

P014 Diagnostic Value of 18F-FDG PET/CT in Large-Vessel Vasculitis: A Retrospective Study from a Moroccan Cohort

Dr. Yasmine Lasry[1], Dr. Mahdi Ahmed Hassan, Dr. Abir Bakraoui Samlali, Dr. Achraf Msoune, Dr. Ali Benlemlih, Dr. Halima Batani, Dr. Hafsa Bensimimou, Dr. Zakaria Ouassfrar, Pr. Amal Guensi
[1]Ibn Rochd University Hospital, Casablanca, Morocco

P015 The value of FDG PET- CT imaging in the management of patients with bone sarcoma and soft tissue sarcoma

Dr. Rawnak Afrin[1], Dr. Shaila Sharmin[1], Dr. Afroza Akhter[1], Dr. Mohana Hossain[1], Prof. Shankar Biswas[1], Dr. Sadia Hossain[1], Dr. Farhana Rahman[1]
[1]Bangladesh Atomic Energy Commission, Dhaka, Bangladesh

P016 Role of Bone Scintigraphy in Evaluating Painful Knee Arthroplasty: Outcomes from a Single-Centre Cohort

Dr. Jigisha Amin[1], Mr Shreyas Satish[2], Dr Adeel Syed[1], Dr Arman Parsai[1], Dr Nagesh Nagabhusan[1], Dr Tahir Hussain[1], Dr Ewa Nowosinska[1], Dr Manuela Vadrucci[1], Dr Idris Badreddine[1], Dr Mohan Krishnamurthy[1], **Dr. Hosahalli K Mohan**
[1]Department of Nuclear Medicine, Barts Health NHS Trust, London, United Kingdom, [2]Department of Bioengineering, Imperial College London, London, United Kingdom

P017 Role of Bone Scintigraphy in Evaluating Painful Hip Arthroplasty: Outcomes from a Single-Centre Cohort

Mr Shreyas Satish[1], Dr. Jigisha Amin[2], Dr Adeel Syed[2], Dr Arman Parsai[2], Dr Nagesh Nagabhusan[2], Dr Tahir Hussain[2], Dr Ewa Nowosinska[2], Dr Manuela Vadrucci[2], Dr Idris Badreddine[2], Dr Mohan Krishnamurthy[2], **Dr. Hosahalli K Mohan**
[1]Department of Bioengineering, Imperial College London, London, United Kingdom, [2]Department of Nuclear Medicine, Barts Health NHS Trust, London, United Kingdom

P018 Comparative Imaging in Painful Joint Arthroplasty: Bone Scintigraphy versus X-ray imaging

Dr. Hosahalli K Mohan, Mr Shreyas Satish[1], Dr. Jigisha Amin[2], Dr Adeel Syed[2], Dr Arman Parsai[2], Dr Nagesh Nagabhusan[2], Dr Tahir Hussain[2], Dr Ewa Nowosinska[2], Dr Manuela Vadrucci[2], Dr Idris Badreddine[2], Dr Mohan Krishnamurthy[2]
[1]Department of Bioengineering, Imperial College London, London, United Kingdom, [2]Department of Nuclear Medicine, Barts Health NHS Trust, London, United Kingdom

P019 Value of dual fluorine-18-L-dopa and fluorine-18-fluorodeoxyglucose positron emission tomography in parkinsonism

Dr. Gerson Castillo[1], Miguel Olarte[1], Ana Piana[1], Juan Chavez[1]
[1]Unidad PET/CT, Facultad de Medicina, Universidad Nacional Autónoma de México, Ciudad de Mexico, Mexico

P020 PISCOM: Advanced Multimodal Functional Neuroimaging Integration of PET and SPECT for Presurgical Epileptogenic Zone Localization

Dr. Katherine Quintero[1], Arnau Farré-Melero[1], Nerea Gutiérrez[2], Sandra Rama[3], Carles Siscar[4], Erick García-Hernández[1], Aida Niñerola[1,2,5], Andrés Perissinotti[1,5], Xavier Setoain[1,2,5]
[1]Hospital Clinic Barcelona, Barcelona, Spain, [2]Universitat de Barcelona, Barcelona, Spain, [3]Hospital Universitario de Salamanca, Barcelona, Spain, [4]Hospital Universitari Doctor Peset de Valencia, Valencia, Spain, [5]Biomedical Research Networking Center of Bioengineering, Biomaterials and Nanomedicine (CIBER-BBN), ISCIII., Barcelona, Spain

P021 Artificial intelligence as an assistant in the interpretation of 18F-FDG PET/CT in lymphomas according to the Deauville and Lugano criteria

Dr. Luis Colmenter[1], Lic Juan Lubo[2], Dr José Calderón[2]
[1]Gamanuclear, Cali, Colombia, [2]Medicina Nuclear SA, Valledupar, Colombia

P022 Experience of the National Cancer Institute of Colombia with Lutetium-177 PSMA Therapy in Patients with Metastatic Castration-Resistant Prostate Cancer

Dr. Viviana Andrea Daza Betancourt[1], Dr. Daniel Felipe Galindo Cortes[1], Dr. Hernándo Andrés Benavides Jiménez[1], Dr. Camila Andrea Potal de Motta[1], Dr. Alejandro Jiménez Baraya[1], Dr. María Alejandra Gómez Marting[1], Dr. Marylin Acuña Hernández[2], Dr. Adriana Quiteria Buitrago Gómez[2]
[1]Fundación Universitaria Sanitas, Bogotá, Colombia, [2]Instituto Nacional de Cáncer, Bogotá, Colombia

P023 Standardization of tumor burden in lymphomas with PET/CT: integration of volumetric metrics Deauville and Lugano criteria to optimize clinical decision-making

Señor. Juan Lubo Marin[1], Dr. Luis Colmenter[2,4,6], Dr. José Calderón[1], Dr Sinay Arevalo[3,5]
[1]Medicina Nuclear S. A., Valledupar, Colombia, [2]Gamanuclear, Valle del Cauca, Colombia, [3]Medicina Nuclear Los Nogales, Bogotá, Colombia, [4]PETCIMAGENES, Quito, Ecuador, [5]Universidad del Rosario, Bogotá, Colombia, [6]Grupo Conceptualizando, Cali, Colombia

P024 Clinical experience in oncologic PET/CT: radiomics-based quantification to complement clinical interpretation and standardize tumor burden assessment

Señor. Juan Lubo Marin[1], Dr. Luis Colmenter[2], Dr. José Calderón[1]
[1]Medicina Nuclear S. A., Valledupar, Colombia, [2]Gamanuclear, Cali, Colombia

P025 Implementation of PET/CT 2.0 Reports: From Descriptive to Quantitative in Personalized Oncologic Practice

Señor. Juan Lubo Marin[1], Dr. Luis Colmenter[2], Dr. José Calderón[1]
[1]Medicina Nuclear S. A., Valledupar, Colombia, [2]Gamanuclear, Cali, Colombia

P026 Metabolic activity in primary tumor and metastatic lesions of breast cancer according to molecular subtype: preliminary analysis with pet/ct
Dr. Sofía Velázquez[1], Dra. Yazmín Sánchez[1], Dr. Miguel Olarte[1]
[1]Facultad De Medicina Unam, Coyoacan, Mexico

P027 18F-PSMA PET/CT in Prostate Cancer: Initial Experience and Theranostic Roadmap from Bangladesh
Dr. Afroza Akhter[1], Dr. Shaila Sharmin[1], Dr. Rawnak Afrin[1], Dr. Farhana Rahman[1], Dr. Sadia Hossain[1], Prof. Shankar Biswas[1]
[1]Institute of Nuclear Medicine and Allied Sciences, INMAS Dhaka, Bangladesh Atomic Energy Commission, Dhaka, Bangladesh

P028 99mTc-Labeled LHRH Analog versus Trastuzumab: Comparative Targeted Preclinical Imaging of Human Breast Cancer Models via LHRH/HER2 Receptors
Dr. Lucia Alfaya[1], Dr Ximena Camacho[1], Dr Mirel Cabrera[1], Dr María Fernanda García[1], Msc Ana Laura Reyes[2], TRI Andrea Paolino[2], Dr Eduardo Savio[2], Dr Juan Pablo Gambini[2,3], Dr Pablo Cabral[1]
[1]Departamento de Radiofarmacia, Centro de Investigaciones Nucleares, Facultad de Ciencias, Universidad de la República, Montevideo, Uruguay, [2]Centro Uruguayo de Imagenología Molecular, CUDIM, Montevideo, Uruguay, [3]Centro de Medicina Nuclear e Imagenología Molecular, Hospital de Clínicas, Facultad de Medicina, Universidad de la República, Montevideo, Uruguay

P029 Staging positron emission tomography in multiple myeloma: extramedullary disease as a predictor of adverse outcomes, cohort 2014–2023
Dr. Melissa Alvarez[1], Dr. Rosita Nohemy Dorado Castillo[1], Dr. Joaquin Donaldo Rosales[1], Dr. Ana María Aguilar González[2], Dr. Juliana Hernández Bolívar[1], Dr. Juan David Marín Escobar[1], Dr. Kevin Bueno Espitia[1], Dr. Diana Carolina Quijano Galvis[1], Dr. Luz Maritza Pabón Castilla[1], Dr. Lina María Góez Mogollón[1]
[1]Fundacion Valle Del Lili, Cali, Colombia, [2]Hospital Universitario Del Valle, Cali, Colombia

P030 Treatment with 177Lu-PSMA radioligand: tumor volume and PSA behavior and their relationship with overall survival
Dr. Matias Cimin[1], Dra. Roxana Chirico[1], Dra, Nathalie Abreu[1], Lic German Pitarch[1], Lic Brenda Konowalik[1], Dr. Alejandro Valda[1], **Dr. Maria Jose Bastianello**[1]
[1]CEMIC University Hospital, Buenos Aires, Argentina

P031 Correlation between PSA levels, SUVmax and total tumor volume (TTV) in evaluation response therapy using 18F-PSMA-PET/CT in prostate cancer (PC)
Dr. Indira Eliana Díaz Contreras[1], Dr. Ada Franco Ardila[2], Dr. Iván Vega González[3]
[1]Gamanuclear LTDA, Armenia, Colombia, [2]Universidad Autónoma de Bucaramanga, Bucaramanga, Colombia, [3]Clínica Las Américas AUNA, Medellín, Colombia

P032 Long axial field of view (LAFOV) PET-CT scanners in oncology
Prof. Antonia Dimitrakopoulou-Strauss[1], Dr Leyun Pan[1], Prof. Christos Sachpekidis[1]
[1]German Cancer Research Center, Heidelberg, Germany

P033 Bronchopulmonary neuroendocrine tumors: characterization with [18F]OC and [18F]FDG PET/CT

Dr. Abril Ariadna Flores Perez[1], Dr. Claudia Contreras-Rivera[1], Dr. Ana Lucia Calderón-Ávila[1], Dr. Miguel Ángel Olarte-Casas[1]
[1]Pet/ct Unam, Mexico City, Mexico

P034 Sacral insufficiency fracture after radioteraphy treatment for cervical cancer: detection and characterization by 18F-FDG-PET/CT: 12 years of experience

Dr. Maximiliano Francabandiera[1], Dra. Paola Corona[1], Dra. Florencia Arabolaza[1], Dr. Federico Matorra[1], Dr. Nicolás Bustos[1], Dra. Berenice Fiamingo[1], Dr. Christian González[1], Dra. Sonia Traverso[1], Dr. Gabriel Bruno[1]
[1]Centro Diagnostico Nuclear, Caba, Argentina

P035 Unspecific mesenteric uptake on 18F-PET/CT in post-treatment lymphoma: a "don't touch" pitfall

Dr. Maximiliano Francabandiera[1], Dra. Paola Corona[1], Dr. Christian González[1], Dra. Florencia Arabolaza[1], Dr. Nicolás Bustos[1], Dra. Berenice Fiamingo[1], Dra. Sonia Traverso[1], Dr. Gabriel Bruno[1]
[1]Fundacion Centro Diagnostico Nuclear, Caba, Argentina

P036 Clinical Significance of Sentinel Lymph Node Scintigraphy in Breast Cancer Patients Attended by the Brazilian Public Health Service

Mrs. Stephanie Freitas[1], Ms. Ana Julya Fernandes[2], Dr. Sandra Sanches[1,2], Dr. Talita Santos[2], Dr. Priscila Santana[2], Dr Luciene Mota[2]
[1]Hospital das Clinicas da Universidade Federal De Minas Gerais, Belo Horizonte, Brazil, [2]Faculdade de Medicina da Universidade Federal de Minas Gerais, Belo Horizonte, Brazil

P037 Disease-Free Survival in Thyroid Cancer Patients with Extrathyroidal Extension as the Sole Risk Factor

Dr. Helen Johana Mejía Efeer[1], **Dr. María Alejandra Gómez Marting**[1], Dr. Adriana Quiteria Buitrago Gómez[2], Dr. Edward Díaz Rodríguez[2], Dr. Diana Cuéllar[2], Dr. Humberto Varela Ramírez[1], Dr. Viviana Andrea Daza Betancourt[1], Dr. Angie Paola Llanos Cuellar[1], Dr. Ana Milena Guadrón Naranjo[1], Dr. Hernando Andrés Benavides Jiménez[1]
[1]Fundación Universitaria Sanitas, Bogotá, D.C., Colombia, [2]Instituto Nacional de Cancerología, Bogotá, D.C., Colombia

P038 Local experience with post-surgical hepatic remnant assessment using hepatobiliary SPECT scintigraphy

Dr. Alejandro Rojas[1], **Dr. Francisco Gomez**[1], Dr. Carlos Mandiola[1], Dr. Jaime Castillo[1], Dr. Juan Dupouy[1], Dr. Jose Tomas Donoso[1], Dr. Rocio Hidalgo[1], Dr. Byron Riedel[1], Dr. Francisco Tortorolo[1], Ms. Catalina Serrano[1], Dr. Teresa Massardo[1]
[1]Hospital Clinico Universidad De Chile, Santiago, Chile

P039 Intraoperative ICG Fluorescence for Perfusion Assessment in Digestive Tract Surgery

Dr. Bettina Martinucci[1], Carolina Furtado[1,2], Mirel Cabrera[2], Ximena Camacho[2], Marcos Tassano[2], Omar Alonso[1], Gustavo Burroso[3], Pablo Duarte[3], Pablo Cabral[2], Juan Pablo Gambini[2,3]
[1]UA Medicina Nuclear e Imagenología Molecular, Hospital de Clínicas Dr. Manuel Quintela, Facultad de Medicina, UdelaR, Montevideo, Uruguay, [2]Centeo de Investigaciones Nucleares, UdelaR, Montevideo, Uruguay, [3]Centro Uruguayo de Imagenología Molecular, Montevideo, Uruguay

P040 Utility of 18F-FDG PET/CT in the characterization of solitary pulmonary nodule

Dr. Rosita Aracely Mendoza Santa Cruz[1], Dr. Daniel Santos Orihuela[1], Dr. Benjamin Gamarra Mujica[1]
[1]Guillermo Almenara Irigoyen National Hospital, LIMA, Perú

P041 Preliminary analysis of clinical and radiomic correlations in castration-resistant prostate cancer using consecutive [18F]PSMA-PET

Dr. Claudia Paola Pedraza García[1], Dr Miguel Ángel Olarte Casas[1], Dra Ana Karina Miranda Playas[1], Dra Oliva Granados Rangel[1], Dr Gustavo Rafael Govea Torres[2], Dr Arturo Avendaño Estrada[3,4]
[1]Unidad PET/CT, Facultad de Medicina, Universidad Nacional Autónoma de México (UNAM), , Ciudad De México, México, [2]Departamento de Fisiología, Universidad Autónoma de Nuevo León, Monterrey, México, [3]Unidad Radiofarmacia-Ciclotrón, División de Investigación, Facultad de Medicina, Universidad Nacional Autónoma de México, Ciudad De México, México, [4]Centro de Investigación sobre el Envejecimiento, Centro de Investigación y de Estudios Avanzados Sede Sur, México., Ciudad de México, México

P042 Prognostic value of baseline 18F-FDG PET/CT metabolic parameters in breast cancer and their association with histologic features and disease-free survival

Dr. Bethsabel Rodriguez Encinas[1], MD Eva Lorena Valadez Montero[1], MD Irma Soldevilla Gallardo[1]
[1]The American British Cowdray Medical Center, Mexico City, Mexico

P043 Diagnostic Value of Quantitative Parameters of Intraprostatic Uptake of F18-PSMA-1007 in the Risk Classification of Prostate Cancer

Profe. Juan Carlos Rojas Montenegro[1], Dr. Sebastián Ayala Zapata[2], Prof. Miguel Angel Olarte Casas[3]
[1]Universidad Del Valle - Facultad de Salud - Medicina Nuclear, Cali, Colombia, [2]Hospital Universitario del Valle - Facultad de Salud - Medicina Interna, Cali, Colombia, [3]Universidad Autonoma de Mexico - Facultad de Medicina - Unidad de PET/CT, Ciudad de Mexico, Mexico

P044 Clinical impact of somatostatin analogue PET/CT on therapeutic decision-making in neuroendocrine tumors

Dr. Florencia Savio[1], Dr. Ivan Lyra, Dra Dahiana Amarillo, Dr. Diego Ferreira, Dra. Florencia Gentini, Dr Mathías Jeldrés, Dra. Cecilia Castillo, Dr. Gabriel Krygier, Ing. Rafael Alonso, Dra Marisa Fazzino, Dr Eduardo Savio, Dr Alarico Rodríguez, Dr Gustavo Burroso, Dr Nicolás Niell, Dr Juan Pablo Gambini
[1]Unidad Académica de Medicina Nuclear e Imagenología Molecular, Hospital de Clínicas "Dr. Manuel Quintela", Facultad de Medicina Udelar, MONTEVIDEO, Uruguay, [2]Unidad Académica de Oncología Clínica, Hospital de Clínicas "Dr. Manuel Quintela", Facultad de Medicina Udelar, Montevideo, Uruguay, [3]Servicio de Oncología Clínica, Asistencial Médica Maldonado, Maldonado, Uruguay, [4]Servicio de Oncología Clínica, Médica Uruguaya, Montevideo, Uruguay, [5]Servicio de Oncología Clínica, Hospital Británico, Montevideo, Uruguay, [6]Unidad Académica de Métodos Cuantitativos, Facultad de Medicina Udelar, Montevideo, Uruguay, [7]Centro Uruguayo de Imagenología Molecular, Montevideo, Uruguay

P045 Clinical impact of 99mTc-hynic-toc spect/ct in neuroendocrine tumors: experience from an oncology hospital in Ecuador

Dr. Christian Toalongo Moreno[1,2], Dra. Karina Zurita Vivero[2], Dr. Paul Villalba Meneses[2]
[1]SOLCA Oncology Hospital, Guayaquil, Ecuador, [2]Indoamérica Technological University, Quito, Ecuador

P046 Male Breast Cancer and F-18 FDG PET/CT, Preliminary Results

Prof. Funda Üstün[1], Mrs Büşra Özdemir Günay[2], Mr Aygün Aslan[3]
[1]Trakya University Medical Faculty, Edirne, Turkey, [2]Giresun Training and Research Hospital, Giresun, Turkey, [3]Rize Training and Research Hospital, Rize, Turkey

P047 Combined predictive value of quantitative PET/CT and multiparametric MRI parameters for risk stratification in prostate cancer: a preliminary analysis

MD Eva Lorena Valadez Montero[1], MD Bethsabel Rodriguez Encinas[1]
[1]Centro Medico ABC, Mexico City, Mexico

P048 Role of Meckel's Scan for Gastrointestinal Bleeding and/or Anemia: Experience in Nuclear Medicine, Hospital San Juan de Dios, Chile

Dr. Sebastián León[1], Dra. Gilda Donoso[1,2], Dra. Gabriela Mundaca[2]
[1]Universidad De Chile, Santiago, Chile, [2]Hospital San Juan de Dios, Santiago, Chile

P049 Reproducibility of Volumetric Parameters in [^{18}F]-PSMA-1007 PET/CT: A Comparison Between Two Analysis Platforms

Mrs. Nathaly Barbosa[1], Dr Daniel Felipe Galindo Cortés[2], MSc Adriana Carolina Aya-Porto[1], Dr Clarena Zuluaga[1], Dr Carlos Granados[1]
[1]Centro De Tratamiento e Investigación Sobre Cáncer, Bogota, Colombia, [2]Fundación Universitaria Sanitas, Bogota, Colombia

P050 Baseline [^{18}F]PSMA-1007 PET Uptake Predicts Lesion Absorbed Dose During ^{177}Lu-PSMA-I&T Therapy

Mrs. Nathaly Barbosa[1], Dr Clarena Zuluaga[1], Dr Carlos Granados[1]
[1]Centro De Tratamiento E Investigación Sobre Cáncer, Bogota, Colombia

P051 Protocol optimization for myocardial perfusion studies, based on image quality parameters

Señora. Juana Cárdenas Rojas[1], Señora. Andrea Abril Fajardo[1], Señor. Agustín Daza Moreno[2], Señora. Sara Rámirez Aguirre[2], Señora. Claudia Gutierrez Villamil[3]
[1]Universidad Nacional De Colombia, Bogotá, Colombia, [2]Fundación Santa Fe, Bogotá, Colombia, [3]Fundación Cardioinfantil, Bogotá, Colombia

P052 Real-Time Computational Framework for Standardizing Bed Speed Acquisition in PET/CT Imaging Using NECR-Based Predictive Metrics

Lic. Yesenia Saldierna Martinez[1], Dra. Rocio Hernandez Alvarez[1], MSc Cristhoper Camacho Herrera[1,2]
[1]Hospital Angeles Centro Sur, Queretaro, Mexico, [2]Nuclear Medicine World, Ciudad de Mexico, Mexico

P053 Analysis of the diversity and volume of PET CT procedures in prostate cancer patients performed at CUDIM Montevideo-Uruguay: statistical survey

Dr. Gerardo Dos Santos[1,2], Dra. Agustina Banchero[1], Dr. César Ferreira[2], Dr. Eduardo Lischinsky[2], Technologist Ismael Cordero[1], Dr. Omar Alonso[1,2]
[1]Uruguayan Center of Molecular Imaging (CUDIM), Montevideo, Uruguay, [2]Nuclear Medicine and Molecular Imaging Center, Clinical Hospital "Dr. Manuel Quintela", University of Uruguay, Montevideo, Uruguay

P054 "Redefining the Nursing Role in Nuclear Medicine: Furosemide-Assisted Preparation to Optimize Pelvic Imaging in Genitourinary Cancer"

Lic. Yesenia Saldierna Martinez[1], Dra Rocio Hernandez Alvarez[1], MSc Cristhoper Camacho Herrera[1,2]
[1]Hospital Angeles Centro Sur, Queretaro, Mexico, [2]Nuclear Medicine World, Ciudad de Mexico, Mexico

P055 Retreatment with 177Lu-DOTATATE in Patients with Neuroendocrine Tumors: Experience at an Oncology Center

Dr. Hernando Andres Benavides Jimenez[1], Dr Edward Andres Diaz Rodriguez[2], Dra Viviana Andrea Daza Betancourt[1]
[1]Fundacion Universitaria Sanitas, Bogotá, Colombia, [2]Instituto Nacional de Cancerología , Bogota, Colombia

P056 Transarterial radioembolization with Y-90 and Ho-166 in patients with portal vein thrombosis

Dr. Sandor Czibor[1,2], Boglarka Toth[3,4], Dr. Domonkos Nadasdy-Horvath[1], Dr. David Korda[4], Gabriella Taba[5], Dr. Andras Bibok[4], Dr. Denes Horvathy[4]
[1]Department of Nuclear Medicine, Medical Imaging Centre, Semmelweis University, Budapest, Hungary, [2]Pozitron Medical Diagnostics Ltd., Budapest, Hungary, [3]Faculty of Medicine, Semmelweis University, Budapest, Hungary, [4]Department of Interventional Radiology, Semmelweis University, Budapest, Hungary, [5]Radiation Protection Service, Semmelweis University, Budapest, Hungary

P057 Correlation between PSA kinetic parameters and progression-free and overall survival in a cohort of patients treated with 177LuPSMA in Colombia

Dr. Daniel Felipe Galindo-Cortes[1], Dr. Viviana Andrea Daza-Betancourt[1], Dr. Sofia Albornoz-Gutiérrez[1], Dr Valeria Andrea Villanueva Bueno[1], Dr Marylin Acuña-Hernández[2], Dr Adriana Quiteria Buitrago-Gómez[2]
[1]Fundación Universitaria Sanitas, Bogotá, Colombia, [2]Instituto Nacional de Cancerología, Bogotá, Colombia

P058 Discordant biochemical and radiological responses to Lu177-PSMA therapy in real-world mCRPC patients

Dr. Oscar Herrera Fomperosa[1], Dra. Irma Soldevilla Gallardo[1]
[1]Centro Medico Abc, Álvaro Obregon, Mexico

P059 Impact of pharmacogenomics on the management of patients with metastatic castrate-resistant prostate cancer requiring radionuclide therapy

Dr. Nihaad Jacobs[1], Ms Nosipho Mabizela[1], Dr Raisa Wessels[1,2], Prof Collet Dandara[1], Dr Khanyisile Hlongwa[1], Dr Stuart More[1]
[1]University of Cape Town, Cape Town, South Africa, [2]National Health Laboratory Service, Cape Town, South Africa

P060 Implementation of comprehensive geriatric assessment in older adults with differentiated thyroid cancer who require in-hospital radioiodine therapy

Dr. M. Josefina Jofre Manieu[1], Dr. Rocio Quilodrán[1]
[1]Fundacion Arturo Lopez Perez, Santiago, Chile

P061 Predictive factors of progression in neuroendocrine tumors and paragangliomas treated with lutetium-177-DOTATATE therapy

Dr. Oscar Lucio[1], Dr. Miguel Corza[1]
[1]Instituto Nacional De Ciencias Médicas Y Nutrición Salvador Zubirán, Mexico City, Mexico

P062 The role of SPECT/CT imaging after radionuclide therapy in metastatic castration-resistant prostate cancer

Mrs. Lisa MacFarlane[1,2]
[1]Peter MacCallum Cancer Centre, Melbourne, Australia, [2]Sir Peter MacCallum Department of Oncology, The University of Melbourne, Melbourne, Australia

P063 Exponential growth of lutetium-177 therapies at a leading cancer center in Latin America

Lic. Mariano Portillo[1], Dr. Martina Musumeci[1], Lic. Marcos Mussio[1], Tec. Luis Genovese[1], Tec. Delfina Eugeni[1], Tec. Ariel Arispe[1], Dr. Luciana Arburua[1], Dr. Silvina Racioppi[1]
[1]Servicio de Medicina Nuclear, Instituto Alexander Fleming, Buenos Aires, Argentina

P064 Low Risk, Lasting Vigilance: Recurrence Patterns in Papillary Thyroid Microcarcinoma

Dr. Shaila Sharmin[1], Dr. Afroza Akhter[1], Dr. Mohana Hossain[1], Dr. Rahima Perveen[1], Dr. Rawnak Afrin[1], Dr. Tanima Biswas[1], Dr. Sadia Hossain[1], Dr. Sabrina Islam[1], Dr. Farhana Rahman[1], Dr. Tanvirul Hasan[1], Dr. Shankar Biswas[1]
[1]Institute Of Nuclear Medicine & Allied Sciences, INMAS, Dhaka, Bangladesh, Atomic energy commission, Dhaka, Bangladesh

P065 Cost-utility analysis of [177Lu]PSMA therapy compared to Cabazitaxel in patients with mCRPC from the perspective of the Colombian Health System

Dr. Marylin Acuña Hernandez[1], Dr Sebastián Camilo Venegas Osorio[2], Magister Aurelio Mejía Mejía[2]
[1]Instituto Nacional De Cancerología - Universidad De Antioquia, Bogota, Colombia, [2]Universidad De Antioquia, Medellin, Colombia

P066 Cost-utility of therapy with 177Lu-DOTAPEPTIDE: Systematic review of the literature

Dr. Marylin Acuña Hernandez[1], Dr. Paula Alejandra Mendez Mercado[2], Dr. Olga Liset Sanchez Orduz[3]
[1]Instituto Nacional De Cancerología - Universidad De Antioquia, Bogota, Colombia, [2]Los Cobos Medical Center, Bogota, Colombia, [3]SPECT Medicina Nuclear SAS, Bucaramanga, Colombia

P067 Cost-utility of therapy with 177Lu-PSMA: Systematic review of the literature

Dr. Marylin Acuña Hernandez[1], Dr. Paula Alejandra Mendez Mercado[2], Dr. Olga Liset Sanchez Orduz[3]
[1]Instituto Nacional De Cancerología - Universidad De Antioquia, Bogota, Colombia, [2]Los Cobos Medical Center, Bogota, Colombia, [3]SPECT Medicina Nuclear SAS, Bucaramanga, Colombia

P068 Current situation and challenges of nuclear medicine In Perú

Dr. Shirley Alarcon[1]
[1]Clinica Ricardo Palma, Lima, Perú

P069 Public/public-private synergy in the creation of the Nuclear Medicine Service in Uruguay

Lic. Andreína Blanco[2], Dr. Alarico Rodriguez[1], Dr. Gustavo Burroso[1], Dr. Pablo Duarte[1], Dr. Carlos Heugerot[2], Dr. Pablo Cabral[2], Prof. Juan Gambini[1]
[1]Cudim, Montevideo, Uruguay, [2]DNSFFAA, Uruguay

P070 The current state of the PET Imaging Site Qualification Program for amyloid PET scans conducted in Japan

Dr. Hirofumi Fujii[1,2], Dr. Yasuhiko Ikari[3], Dr. Keisuke Tsuda[4], Mr. Kazuaki Mori[5], Dr. Ukihide Tateishi[6], Dr. Kenji Hirata[7], Dr. Hiromitsu Daisaki[8], Dr. Makoto Hosono[9], Dr. Hiroshi Ito[10], Dr. Michio Senda[3]
[1]Japan Radioisotope Association, Tokyo, Japan, [2]National Cancer Center, Kashiwa, Japan, [3]Kobe City Medical Center General Hospital, Kobe, Japan, [4]Juntendo University, Tokyo, Japan, [5]Toranomon Hospital, Tokyo, Japan, [6]Institute of Science Tokyo, Tokyo, Japan, [7]Hokkaido University, Sappro, Japan, [8]Gunma Prefectural College of Health Sciences, Maebashi, Japan, [9]Kindai University, Osakasayama, Japan, [10]Fukushima Medical University, Fukushima, Japan

P071 Implementation of the IAEA QUANUM Program to Achieve GMP Certification at CUDIM Radiopharmacy

Dr. Javier Giglio[1], Dra. Ingrid Kreimerman[1], Chemistry Maia Zeni[1], Dra. Ana Rey[2], Dr. Alarico Rodríguez[1], Dr. Gustavo Burroso[1], Dr. Eduardo Savio[1]
[1]Departamento de Radiofarmacia, Centro Uruguayo de Imagenología Molecular (Cudim), Montevideo, Uruguay, [2]Área de Radioquimica, Facultad de Química, UdelaR, Montevideo, Uruguay

P072 Ejection fraction obtained manually during the rotary internship at the Institute of Nuclear Medicine of the San Francisco Xavier University

Lic. Elizabeth Huanca[1], Lic. Marcelo Torrez, Doctora Lidya Quevedo, Lic. Mery Orosco, Lic. Katherine Romero
[1]Universidad San Francisco Xavier De Chuquisaca, Sucre, Bolivia

P073 Research work practice program of radiopharmacy with an integrative approach to the 5th level of the career pharmacy at USFX

Lic. Elizabeth Huanca[1], Licenciada Rita Vasquez
[1]Universidad San Francisco Xavier De Chuquisaca, Sucre, Bolivia

P074 Project Management Applied to the Implementation of a Nuclear Medicine Service in Bogotá, Colombia: Experience and Proposal for Standardization

Dr. Maria Martinez[1], Ingenieria Lenys Roncancio, Fisica medica Lorena Sandoval
[1]Clinica Del Country, Bogota, Colombia

P075 Radiological Safety: Estimating Radiation Exposure for Non-Occupationally Exposed Healthcare Personnel in Nuclear Medicine Procedures

Mrs. Lorena Sandoval Castillo[1], Mrs. Sandra Barrera[1], Mrs. Nidya Zambrano[1], Mr. Carlos Quiroga[1], Mr. Gerardo Cortés[1]
[1]Clínica Del Country, Bogotá, Colombia

P076 Reducing Extremity Radiation Exposure in Dynamic PET/CT Studies in Clinica del Country

Mrs. Lorena Sandoval Castillo[1], Mrs. Viviana Andrade[1], Mrs. Claudia Piñeros[1], Mr. Carlos Quiroga[1], Mr. Gerardo Cortés[1]
[1]Clínica Del Country, Bogotá, Colombia

P077 Role of PET/MRI in localizing the epileptogenic focus in drug-resistant epilepsy

Dr. Genesis Rodriguez Ugalde[1], Dra. Lady Sanchez Gomez., Dr. Andres Bello Murguia, Dr. Jose Antonio Serna Macias, Dr. Jorge Schalch De León.
[1]Hospital Privado, Ciudad de México, México

O01
Diagnostic performance of 18F-choline PET/CT correlated with MRI in brain tumor recurrence: experience from an oncology hospital in Ecuador

Dr. Christian Toalongo Moreno[1,2], Dr. Abel Llaguno Buzetta[1,2], Dr. Rodney Vaca Montenegro[2]
[1]SOLCA Oncology Hospital, Guayaquil, Ecuador, [2]Indoamérica Technological University, Quito, Ecuador

Oral Presentations 1: Neurology, Radiopharmacy and Chemistry, Arsenal Room, February 13, 2026, 14:00 - 16:00

Background / Aims: Differentiating tumor recurrence from treatment-related changes, such as radionecrosis, remains a challenge in neuro-oncology. Magnetic resonance imaging (MRI) is the standard follow-up method, although its specificity is limited by overlapping findings. Positron emission tomography/computed tomography (PET/CT) with 18F-fluorodeoxyglucose has been used, but its application in the brain is restricted due to cortical uptake. PET/CT with 18F-choline, owing to higher tumor-to-background contrast, emerges as a complementary diagnostic tool. The aim of this study was to evaluate the diagnostic performance of 18F-choline PET/CT correlated with MRI in patients with suspected brain tumor recurrence treated at an oncology hospital in Guayaquil, Ecuador.
Methods: A retrospective observational study was conducted at SOLCA Oncology Hospital in Guayaquil, Ecuador, including 38 patients aged 9–75 years (17 women and 21 men) between 2023 and 2025. Diagnoses included astrocytomas (n=17), glioblastomas (n=10), medulloblastomas (n=5), brain metastases (n=4), and ependymomas (n=2). All patients underwent 18F-choline PET/CT due to clinical or radiological suspicion of recurrence. Findings were compared with MRI (diffusion, perfusion, spectroscopy, and contrast) and, when available, histological confirmation. Sensitivity, specificity, and predictive values were calculated.
Results: 18F-choline PET/CT showed focal uptake with SUVmax values between 2.0 and 8.4 in 19 cases suspected of recurrence. Overall, 21 of the 38 patients (55.3%) had recurrence confirmed histologically or radiologically. Sensitivity was 90.4% and specificity 85.7%, with a positive predictive value of 91% and a negative predictive value of 84%. In 19 patients (50%), PET/CT findings modified therapeutic management, avoiding unnecessary invasive procedures or guiding targeted therapies.
Conclusions: 18F-choline PET/CT demonstrated high diagnostic performance in differentiating tumor recurrence from radionecrosis, overcoming MRI limitations. This experience in Ecuador, conducted at an oncology hospital in Guayaquil, highlights its clinical relevance and supports the incorporation of this technique as a decision-making aid and tool to optimize therapeutic management in neuro-oncology.

Conflict of Interest
None declared

Graphic

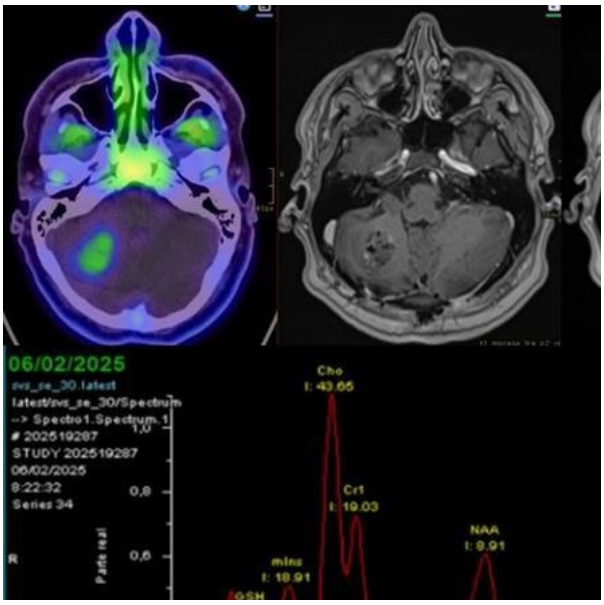

Table

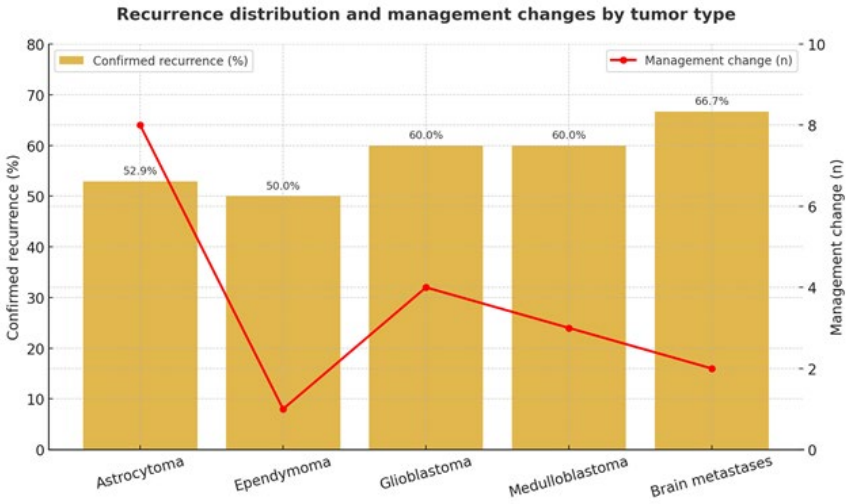

O02

Diagnostic value of cisternoscintigraphy and CT cystenography in the detection of CSF leaks in patients with intracranial hypotension

Dr. Sebastián Rojas Lara[1]
[1]Fundación Universitaria Sanitas, BOGOTÁ, D.C., Colombia

Oral Presentations 1: Neurology, Radiopharmacy and Chemistry, Arsenal Room, February 13, 2026, 14:00 - 16:00

Background: Spontaneous intracranial hypotension (SIH) is an underdiagnosed condition characterized by orthostatic headache caused by cerebrospinal fluid (CSF) leakage. Diagnosis is challenging due to nonspecific symptoms and limitations of conventional imaging techniques such as magnetic resonance imaging (MRI). In this context, cisternoscintigraphy and computed tomography (CT) cisternography have emerged as complementary tools for detecting CSF leaks.
Objectives: To evaluate the diagnostic value of cisternoscintigraphy and CT cisternography in detecting CSF leaks in patients with SIH treated at Colsanitas Clinics between 2019 and 2025.
Methods: An analytical, observational study was conducted with a retrospective, cross-sectional cohort design. Patients with clinically or radiologically suspected SHI underwent cisternoscintigraphy or CT cisternography. The gold standard was clinical outcome assessed between 6 and 60 months after the study, and outcomes were evaluated by chart review. Diagnostic performance was assessed by calculating sensitivity, specificity, positive predictive value (PPV), negative predictive value (NPV), and overall accuracy for each imaging technique.
Results: A total of 112 patients were included (88.4% female, mean age 48.7 years). Cisternoscintigraphy was performed in 44 patients (14 positive, 31%), and CT cisternography in 68 patients (16 positive, 23%). Clinical follow-up confirmed the diagnostic validity of both techniques. Cisternoscintigraphy showed a sensitivity of 81% CI 95%(0.62-1.00), specificity of 96% CI 95% (0.90-1.03), PPV of 93% CI 95% (0.79-1.06), and NPV of 90% CI 95% (0.19-1.01)(p = 0.044) statistically significant. CT cisternography showed a sensitivity of 55% CI 95%(0.34-0.75), specificity of 91% CI 95% (0.83-0.99), PPV of 75%, and NPV of 81% (p = 0.048).
Conclusions: Cisternoscintigraphy demonstrated higher sensitivity and diagnostic accuracy than CT cisternography, particularly in low-volume leaks. While both techniques are useful, cisternoscintigraphy is recommended in cases with high clinical suspicion of SIH and inconclusive MRI findings. This study provides valuable evidence to improve SIH diagnostic strategies in the Colombian healthcare context.

Conflict of Interest
I declare that I have no conflicts of interest and the current project has not received any financial support.

Graphic

Imagen 2.

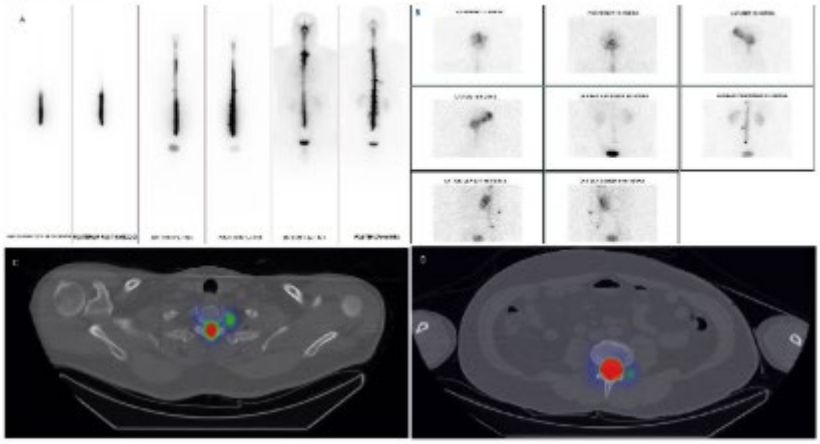

A. Imágenes planares: Se observó ascenso lento del radiofármaco por el neuroeje, visualización precoz del sistema urinario (siluetas renales y vejiga) a las 4-6 horas, y múltiples quistes raquídeos (divertículos meníngeos). **B. Imágenes tardías:** Captación paraespinal focal sostenida asimétrica de alta intensidad en los niveles de T1-T2 (izquierda), T9-T10 (derecha) y L3-L4 (izquierda) que corresponden a fístula activa de LCR a la altura de la raíz izquierda de T1, derecha de T9 e izquierda de L3. **C. Imagen SPECT/CT corte axial cervicotorácica:** Fuga de LCR a nivel de T1-T2 (izquierda) que corresponde a fístula activa de la raíz nerviosa izquierda de T1. **D. Imagen SPECT/CT corte axial torácica:** Fuga de LCR a nivel de L3-L4 (izquierda) que corresponde a fístula activa de la raíz nerviosa izquierda de L3.

Table

Cisternogammagrafía

Índices de validez interna. Prueba patrón ("Gold Standard").

Prueba	Enfermedad	No enfermedad	Total
Positiva	13	1	14
Negativa	3	27	30
Total	16	28	44

Llene las casillas con el número resultados de la prueba, positiva o negativa, para los estados de enfermedad o no enfermedad.

		IC AL 95%	
		LI	LS
Prevalencia	0.36		
Sensibilidad	0.81	0.62	,1.00
Especificidad	0.96	0,90	1.03
VP+	0.93	0.79	1.06
VP-	0,90	0.79	1.01
CP+	22.75	3.27	158.1(
CP-	0.19	0.07	0.54

Estimación para su paciente
Rellene la Probabilidad preprueba (prevalencia) estimada para su paciente.
Este valor debe ser mayor que 0 y menor que 1.

Prevalencia (Probabilidad preprueba)	0.5

PROBABILIDAD POSTPRUEBA

		IC al 95 %	
		LI	LS
Para un resultado +	0.96	0.77	0.99
Para un resultado -	0.16	0.07	0.35

Citernografía por CT

Índices de validez interna. Prueba patrón ("Gold Standard").

Prueba	Enfermedad	No enfermedad	Total
Positiva	12	4	16
Negativa	10	42	52
Total	22	46	68

Llene las casillas con el número resultados de la prueba, positiva o negativa, para los estados de enfermedad o no enfermedad.

		IC AL 95%	
		LI	LS
Prevalencia	0.32		
Sensibilidad	0.55	0.34	0.75
Especificidad	0.91	0.83	0.99
VP+	0.75	0.54	0.96
VP-	0.81	0,70	0.91
CP+	6.27	2.28	17.24
CP-	0,50	0.31	0.81

Estimación para su paciente
Rellene la Probabilidad preprueba (prevalencia) estimada para su paciente.
Este valor debe ser mayor que 0 y menor que 1.

Prevalencia (Probabilidad preprueba)	0.5

PROBABILIDAD POSTPRUEBA

		IC al 95 %	
		LI	LS
Para un resultado +	0.86	0,70	0.95
Para un resultado -	0.33	0.24	0.45

O03

Beyond clinical assessment: The value of combined metabolic and dopaminergic mapping with PET/CT for the differential diagnosis of parkinsonian syndromes

Dr. Abigail Arriaga Contreras[1], Dr. Rodrigo Hernández Ramírez[1], Dr. Juan Pablo Chávez Torres[1], Dr. Miguel Angel Corza Ayala[1], Dr. Francisco Jesús Solano Caballero[1], Dr. Oscar Enrique Lucio Baez[1], Dra. Blanca Estela López Graciano[1]
[1]Instituto Nacional De Ciencias Médicas y Nutrición Salvador Zubirán, Ciudad De México, Mexico

Oral Presentations 1: Neurology, Radiopharmacy and Chemistry, Arsenal Room, February 13, 2026, 14:00 - 16:00

Background/Aims: The differential diagnosis between Parkinson's disease and atypical parkinsonian syndromes is challenging due to overlapping clinical symptoms, yet an accurate diagnosis is crucial for appropriate treatment. While conventional MRI has limited sensitivity, molecular imaging with [^{18}F]-FDOPA (presynaptic) and [^{18}F]-FDG (postsynaptic) PET plays a key role in differentiating these disorders. This study aimed to determine the utility of a dual PET/CT protocol using both tracers in the differential diagnosis of degenerative parkinsonian syndromes.
Material and Methods: We retrospectively reviewed the database of 35 patients with parkinsonian syndromes who underwent dual 18F-FDOPA and 18F-FDG PET/CT between January 2021 and January 2025. All included patients had at least six months of clinical follow-up with a specialist after the imaging was performed. McNemar's test was used for statistical analysis to compare the diagnostic agreement between the initial clinical, PET/CT, and final follow-up diagnoses.
Results: comparing the initial diagnoses with the definitive diagnosis established during follow-up, the initial clinical diagnosis was concordant in 20 out of 35 patients (58%). Meanwhile, the diagnosis obtained via dual PET/CT showed concordance with the definitive diagnosis in 29 out of 35 patients (83%), providing key information to the diagnostic process.
The diagnostic agreement analysis (McNemar's test) revealed a statistically significant difference between the initial clinical impression and the definitive follow-up diagnosis ($p=0.035$).
In this context, dual PET/CT proved to be a highly consistent tool, as its diagnosis showed no significantdifferences with the follow-up outcome ($p=0.423$), indicating a high concordance between them.
Conclusions: Dual PET/CT with FDOPA/FDG in the differential diagnosis of neurodegenerative parkinsonian syndromes, particularly for distinguishing between Parkinson's disease and atypical parkinsonian syndromes, proves to be robust and highly concordant with patients' clinical and follow-up diagnoses. It is a valuable tool for achieving early and accurate diagnoses, which are essential for optimizing patient management and treatment outcomes.

Conflict of Interest
No conflict of interest.

O04

"Semiquantitative difference in the uptake of the pineal gland of [18F]fluorodopamine in patients with Parkinson's disease versus atypical parkinsonism."

Dr. Kinari Ortega[1], Dr. Manlio Gerardo Gama[1], Dr. Gustavo Vázquez[1], Dr. Miguel Ángel Olarte Casas[1]
[1]National Autonomous University of Mexico, CDMX, Mexico

Oral Presentations 1: Neurology, Radiopharmacy and Chemistry, Arsenal Room, February 13, 2026, 14:00 - 16:00

Background/Aim. Parkinson's disease is the leading cause of parkinsonism, characterized by resting tremor, bradykinesia, and postural instability. It is one of the most common neurodegenerative diseases in adulthood [1]. Atypical parkinsonisms include progressive supranuclear palsy, Lewy bodies dementia, multiple system atrophy, and corticobasal degeneration. Pathophysiologically, they share depletion of dopaminergic neurons of the nigrostriatal pathway, induced by chemical, structural, or, more often, degenerative abnormalities in the presynaptic pathway that produce loss of control of voluntary movements [2]. Presynaptic dopaminergic imaging supports the differential diagnosis between neurodegenerative parkinsonian syndromes and etiologies of parkinsonism without dopamine deficiency [3]. Some studies discuss the relationship between the depletion of dopiminergic neurons in the striatum and an increase of L-aminoacid decarboxylase in the pineal gland as a compensatory extrastriatal mechanism [4,5]. The aim of this study was to evaluate the difference in the uptake pattern of the pineal gland, using SUVmax, SUVmean and SUVpeak on PET/CT with [18F]fluorodopamine in patients with Parkinson versus atypical parkinsonism.
Methods. From 2022 to 2025, we selected patients with standardized PET/CT [18F] fluorodopamine protocols for movement disorder studies; patients without dual PET/CT were excluded. The study population were ten patients in the Parkinson group and six in the atypical parkinsonism group. The average and median of the semi-quantitative variables were analyzed.
Results. In the pineal gland the average SUVmax, SUVmean and SUVpeak for the Parkinson group were 3.62, 1.84 and 1.81 respectively. For the second group average SUVmax was 2.88, SUVmean 1.6 and SUVpeak 1.67. There was a percentage difference of 22.76% in the SUVmax, 13.9% for the SUVmean, and 8.04% for the SUVpeak between both groups.
Conclusions. Pineal gland uptake in average is higher in patients with Parkinson which could correlate with the degree of dopaminergic neuron loss in this pathology.

References:
[1] Jankovic, J. Epidemiology, pathogenesis, and genetics of Parkinson disease. UpToDate. 2024. Recovered 5 april 2025, https://www.uptodate.com/contents/epidemiology-pathogenesis-and-genetics-of-parkinson-disease
[2] Munhoz RP, Tumas V, Pedroso JL, Silveira-Moriyama L. The clinical diagnosis of Parkinson's disease. Arq Neuropsiquiatr. 2024;82(6):1-10. Disponible en: http://dx.doi.org/10.1055/s-0043-1777775
[3] Morbelli S, Esposito G, Arbizu J, Barthel H, Boellaard R, Bohnen NI, et al. EANM practice guideline/SNMMI procedure standard for dopaminergic imaging in Parkinsonian syndromes 1.0. Eur J Nucl Med Mol Imaging. 2020;47(8):1885-912. Disponible en: http://dx.doi.org/10.1007/s00259-020-04817-8
[4] Ghaemi M, Rudolf J, Hilker R, Herholz K, Heiss WD. Increased pineal Fdopa uptake is related to severity of Parkinson's disease--a PET study. J Pineal Res. 2001;30(4):213-9. Available 0n: http://dx.doi.org/10.1034/j.1600-079x.2001.300404.x
[5] Hazut Krauthammer, S.;Cohen, D.; Even-Sapir, E.; Lerman, H.Beyond Visual Assessment of BasalGanglia Uptake: Can AutomatedMethod and Pineal Body UptakeAssessment Improve Identification of Nigrostriatal Dysfunction on18F-DOPA PET/CT? Int. J. Mol. Sci.2023, 24, 5683. https://doi.org/10.3390/ijms24065683
Conflict of Interest
None

O05

In vitro biological evaluation of a 99mTc tricarbonyl complex derived from Erlotinib for molecular imaging in triple negative breast cancer

Dr. María Emilia Tejería Pérez[1], Romina Rossi[1], Ana María Rey Ríos[1]
[1]Área Radioquímica/ Facultad de Química, Montevideo, Uruguay

Oral Presentations 1: Neurology, Radiopharmacy and Chemistry, Arsenal Room, February 13, 2026, 14:00 - 16:00

Introduction/ Objectives: Triple negative breast cancer is a global public health problem. 60% of these tumors overexpress the epidermal growth factor receptor (EGFR), making this molecular target very promising for improving diagnostic and therapeutic strategies. Our group proposes the development and the evaluation of a potential radiopharmaceutical derived from Erlotinib for breast cancer imaging.
Methods: The complex C was obtained in 2 steps: preparation of the precursor fac-[99mTc(I)(CO)3(H2O)3]+ (30-50 mCi) and substitution with L (0.3 mg, 30 min at 75°C 3-6 mCi). Radiochemical purity (RCP) was evaluated by HPLC. Phisicochemical, Stability and in vitro studies were performed.
Results: Complex C is a 99mTc tricarbonyl complex where the metal is coordinated through the N,N,O chelating system of the Erlotinib derivative. The RCP was more than 90% after purification by HPLC. C was stable in the labeling milieu and in human plasma for at least 4 hours. Lipophilicity (log P octanol/ phosphate buffer 0.1M pH=7.4) was 0.9±0.1 and protein binding was 53±9%. In vitro biological studies were performed in MDA-MB-231 triple negative breast cancer cells and in MCF-7 as a negative control for 1 hour of incubation (37°C 5%CO2), 1.8x105 cells and 10 µCi of C. The membrane uptake was 0.31±0.03% and 0.40±0.03% for MCF-7 and MDA-MB-231 cells, respectively. The internalization for both cell lines was 0.24 ±0.03%. Uptake and internalization did not change with increasing the incubation time, the amount or C or the cell number.
Conclusions: A 99mTc complex derived from Erlotinib was obtained with high RCP, adequate physicochemical properties, and good stability. In vitro cells studies did not show significant uptake or internalization. Consequently, the group will redesign the molecule in order to improve biological behavior.
Acknowledges: Joaquín Afonso, Gonzalo Carrau, Daniela Gamenara, ANII (POS_NAC_2022_1_173941), Despegue-Científico-PEDECIBA, CMNIM, Facultad de Medicina, Udelar, Consultorio de Medicina Nuclear Ferrari-Ferrando-Paéz.

Conflict of Interest
No conflict of interest

O06

Results From a First-In-Human Phase I Trial of [68Ga]Ga-OncoCAIX in ccRCC: Safety, Dosimetry, Pharmacokinetics and Preliminary Diagnostic Performance

Dr. Fabrizia Gelardi[1], Prof Martina Sollini[1,2], Dr Cristiano Pini[2], Rita Petrelli[1], Alessia Tudda[1], Prof Paola Anna Erba[3,4], Jacqueline Mock[5], Samuele Cazzamalli[5], Dario Neri[5], Prof Arturo Chiti[1,2]

[1]IRCCS San Raffaele Hospital, Milano, Italy, [2]Vita-Salute San Raffaele University, Milano, Italy, [3]School of Medicine and Surgery, University of Milano-Bicocca, Milano, Italy, [4]Nuclear Medicine Unit, ASST Papa Giovanni XXIII Hospital, Bergamo, Italy, [5]Philochem AG, Otelfingen, Switzerland

Oral Presentations 1: Neurology, Radiopharmacy and Chemistry, Arsenal Room, February 13, 2026, 14:00 - 16:00

Background/Aims: Carbonic anhydrase IX (CAIX), a transmembrane protein overexpressed in clear cell renal cell carcinoma (ccRCC), is a promising imaging target for accurately characterising and staging ccRCC. [^{68}Ga]Ga-OncoCAIX is a novel, small-molecule radiopharmaceutical with high affinity to CAIX, tumour-specific uptake and favourable biodistribution in preclinical models. We present the preliminary results of a multicentre, prospective phase I trial investigating the safety, dosimetry, pharmacokinetics, and diagnostic performance of [^{68}Ga]Ga-OncoCAIX in patients with suspected ccRCC.
Methods: We plan to enrol up to 20 patients with suspected ccRCC. Participants are assigned to either Cohort A (primary renal tumours only, n = 6) or Cohort B (including patients with possible metastatic disease). A single intravenous injection of [^{68}Ga]Ga-OncoCAIX is administered (250 MBq), followed by PET/CT scans at 0–30 minutes, 60 minutes and 120 minutes post-injection. Blood and urine samples are collected for pharmacokinetic and excretion analysis. Adverse events (AEs) are monitored and graded according to CTCAE v5.0. Where available, PET findings are correlated with histopathology.
Results: As of 15 September, nine patients had undergone imaging, with one more scheduled. Eight of these patients presented with incidental renal masses, while two presented with possible ccRCC recurrence. No AEs were observed. [^{68}Ga]Ga-OncoCAIX showed favourable biodistribution, with renal clearance and minimal uptake in healthy kidney tissue. High physiological uptake was observed in the gastrointestinal tract, particularly in the stomach. The patients' characteristics and the diagnostic performance results of [^{68}Ga]Ga-OncoCAIX PET are detailed in Table 1. Patients with positive PET results showed uptake in renal lesions early at the post-injection acquisition, with increasing intensity at 60- and 120-minutes scan.
Conclusion: [^{68}Ga]Ga-OncoCAIX has been shown to be safe and well tolerated, with favourable biodistribution. Histopathological validation is ongoing to confirm its diagnostic potential for detecting ccRCC and its clinical applicability.

Conflict of Interest

JM and SC: employees of Philochem AG. DN: founder and shareholder of Philogen S.p.A. AC: advisory role for Blue Earth Diagnostics, Telix Pharmaceuticals and InnovaRadi Therapeutic; Speaker's Bureau for Bracco Diagnostics, General Electric, Novartis, Telix Pharmaceuticals and United Imaging.

Table

Patient	Sex	Age	Lesion site	Clinical setting	Previous treatments	[^{68}Ga]Ga-OncoCAIX PET result	Scheduled intervention	AP results
1	F	78	Right kidney	Characterisation	None	Positive	Partial nephrectomy	Pending
2	M	68	Right kidney	Characterisation	None	Negative	Tumorectomy	Chromophobe RCC (TNM pT1a; pNX)
3	M	78	Left kidney	Characterisation	None	Positive	Radical nephrectomy	ccRCC (TNM pT3a; pNX)
4	M	45	Right kidney	Characterisation	None	Positive	Partial nephrectomy	Pending
5	M	78	Right kidney	Suspicious relapse on MRI	Cryoablation	Negative	Radiological FU	NA
6	M	48	Left kidney + lymph node renal hilum	Characterisation	None	Negative	Tumorectomy	Renal Oncocytoma + leiomyosarcoma G1
7	F	57	Right kidney (multiple lesions)	Suspicious relapse on CECT	Radical nephrectomy (left)	Positive	Radical nephrectomy (right)	Pending
8	M	48	Left kidney	Characterisation	None	Negative	Biopsy	Pending
9	M	68	Bilateral	Characterisation	None	Negative	Biopsy	Pending
10	M	75	Bilateral	Characterisation	None	Pending	TBD	Pending

O07

Ampelomins radiolabelled with Tc-99m and F-18: Synthesis and functionalization of tracers for imaging infectious processes

Quim. Carolina Brindisi[1,2], Dr. Javier Giglio[2,3], **Dra. Mariella Adriana Terán Gretter**[2], Dra. Margarita Brovetto[1]
[1]Química Orgánica (DQO) - Universidad de la República, Montevideo, Uruguay, [2]Área Area Radioquímica (DEC) - Universidad de la República, Montevideo, Uruguay, [3]Centro Uruguayo de Imagenología Molecular (CUDIM), Montevideo, Uruguay

Oral Presentations 1: Neurology, Radiopharmacy and Chemistry, Arsenal Room, February 13, 2026, 14:00 - 16:00

Background/Objectives: Early detection of occult infections remains a clinical challenge, particularly in immunocompromised patients. Molecular imaging with radiopharmaceuticals offers a non-invasive approach to localize infectious foci and monitor treatment response. Carbasugars have emerged as promising scaffolds for new radiotracers due to their structural similarity to microbial metabolites. This study aimed to design, synthesize, and evaluate ampelomycin derivatives, a class of carbasugars with α-glucosidase inhibitory activity as potential imaging agents labelled with 99mTc and 18F.
Methods: Synthetic pathways based on the Pendent Approach were developed, incorporating spacers and triazole rings to enable coordination with 99mTc or nucleophilic substitution with 18F. The resulting ligands were labelled using the precursor fac-[99mTc][$Tc(CO)_3(H_2O)_3$]+ or through nucleophilic fluorination. Physicochemical properties (stability in plasma and reaction medium, lipophilicity, plasma protein binding) were assessed, alongside in vitro binding to Staphylococcus aureus and Candida albicans cultures.
Results: 99mTc-labelled complexes (compounds 3 and 4) were obtained with >95% radiochemical purity and remained stable for up to 4 hours. They exhibited hydrophilic profiles (log P: -0.070 ± 0.001 for 3; -0.026 ± 0.001 for 4) and low plasma protein binding (12 ± 1% for 3; 9.2 ± 1% for 4). However, both showed minimal or undetectable microbial binding under assay conditions. Labelling with 18F was inefficient, with low yields and 1.6% radiochemical purity, precluding further evaluation.
Conclusions: This study established a robust synthetic platform for ampelomycin-derived carbasugars and enabled successful 99mTc radiolabelling, yielding stable complexes with favorable physicochemical characteristics. Despite low microbial affinity in vitro, the findings offer valuable insights for future ligand design. 18F-labeling limitations highlight the need for alternative strategies to improve radiochemical outcomes.
Acknowledgements: CSIC Project 2325, CAP scholarship, Hospital de Clínicas, Consultorio Ferrari-Ferrando-Páez

Conflict of Interest
None

Graphic

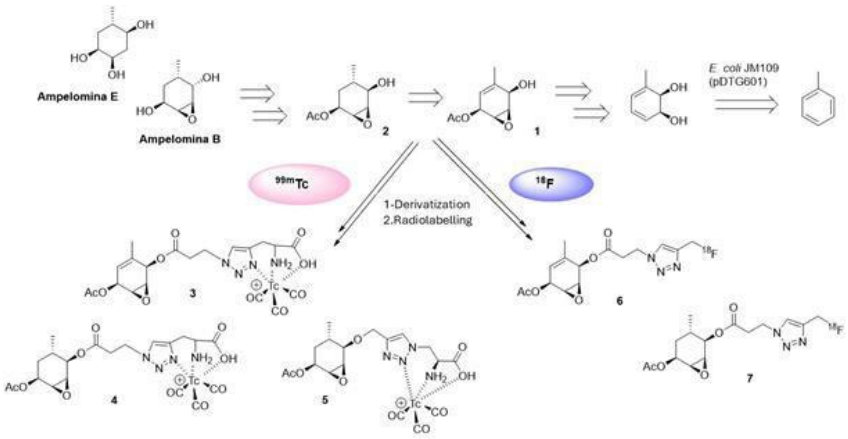
Ampelomina E
Ampelomina B
E. coli JM109
(pDTG601)
99mTc
18F
1-Derivatization
2.Radiolabelling

O08

Radiosensitization of Theranostics for Pancreatic Ductal Adenocarcinoma

Dr. Moralba Dominguez Garcia[1], Alexa Michel[1], Mohamed Hussien[1], Amy Morrison[2], Dr. Jason S. Lewis[1]
[1]Memorial Sloan Kettering Cancer Center, New York, United States, [2]King's College London, London, United Kingdom

Oral Presentations 1: Neurology, Radiopharmacy and Chemistry, Arsenal Room, February 13, 2026, 14:00 - 16:00

Background: Pancreatic ductal adenocarcinoma (PDAC) is one of the most lethal cancers, with a five-year survival rate of 9%. While surgery remains the main treatment, only 15–20% of patients are eligible. A major barrier to effective treatment is PDAC's hypoxic tumor microenvironment, which limits radiotherapy efficacy by reducing the formation of reactive oxygen species (ROS) essential for inducing a permanent DNA damage. To overcome this challenge, we propose an innovative strategy: selective radiosensitization of hypoxic tumor cells via radiolabeled antibody-radiosensitizer conjugate.
Methods: We have synthesized two novel molecule (Compound 35 and 39), each featuring an azobenzene-based hypoxia-sensitive linker and a potent cytotoxic and radiosensitizer monomethyl auristatin E (MMAE). Compound 39 also has incorporated a deferoxamine (DFO) chelator for radiometal labeling. Both compounds were conjugated to 5B1, a human monoclonal antibody targeting CA19.9, a biomarker overexpressed in PDAC. Thus, three conjugates were produced: 5B1-DFO, 5B1-35-DFO, and 5B1-39, which were radiolabeled with Zirconium-89 to generate the corresponding [^{89}Zr]Zr-radioimmunoconjugates. In vivo evaluation (approved by MSKCC) was performed in BxPC3 xenograft mouse models by using PET imaging to assess tumor targeting and biodistribution.
Results: The synthesis of compounds 35 and 39 was successful, and all antibody conjugates showed high radiochemical purity (< 98%). PET imaging showed high tumor uptake for 5B1-DFO (73 ± 4 %ID/g), while 5B1-35-DFO and 5B1-39 exhibited reduced tumor targeting (56 ± 12 %ID/g and 32 ± 4 %ID/g, respectively) with some liver uptake, which has been observed in some ADC.
Conclusions: This strategy represents a novel and promising direction in radiotheranostics by integrating targeted antibody delivery, hypoxia-triggered MMAE release, and radiotherapy synergy. Despite some liver uptake, these new radiolabeled conjugates show potential to enhance radiotherapy outcomes in PDAC. Currently, we are conducting a pilot therapeutic study using CHX-A''-DTPA in place of DFO for Lutetium-177 labeling to assess therapeutic efficacy.

Conflict of Interest
All conflict of interest are disclosed. Chemical structures and concept application have been submitted for patent protection via the Sofia platform (SK2025-047). Also this project is funding by Geoffrey Beene Cancer Research Cancer (ID:FP00009492)

Graphic

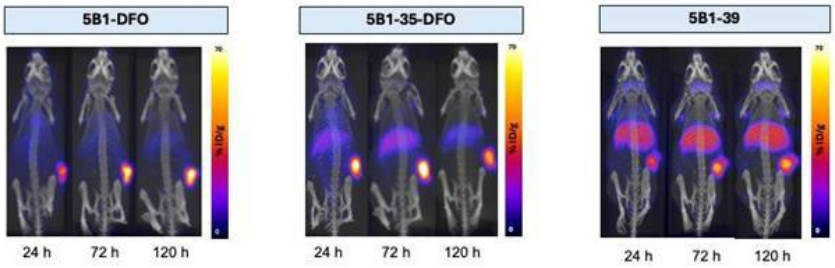

Figure 1. Five-day post-injection PET images of xenograft female nude mice bearing BxPC3 pancreas tumor.

O09

Validation of an Alternative Analytical Technique for Determining the Radiochemical Purity of 99mTc-HMDP

Mr. Eliecer Cantillo[1], Mr. Renzo Guardo[1], Mr. Juan Balanta[1], Ms. Viviana Montoya[1], Mr. Giovani Naranjo[1]
[1]Hospital Universitario Fundación Valle Del Lili, Cali, Colombia

Oral Presentations 1: Neurology, Radiopharmacy and Chemistry, Arsenal Room, February 13, 2026, 14:00 - 16:00

Background: In Colombia, the National Institute for the Surveillance of Medicines and Food (INVIMA) has required the validation of analytical techniques for the quality control of technetium-labeled radiopharmaceuticals for over a decade. Currently, Resolution 560 of 2024 is in force. This regulation has prompted radiopharmacies to adapt their validation methods, taking into account the specific characteristics of radiopharmaceuticals, such as the presence of particular impurities: free technetium and reduced-hydrolyzed technetium.
Methodology: A validation protocol was designed to assess the radiochemical purity of 99mTc-HMDP, based on international guidelines (ICH Q2(R1) [1], USP [2], EANM [3]).
Bibliographic references were consulted regarding impurities [4], as well as previous studies involving similar methods [5]. A chromatographic system was employed using Whatman No. 3 paper as the stationary phase, with acetone and 0.9% saline solution as mobile phases. Parameters evaluated included specificity, linearity, intermediate precision, repeatability, limit of quantification, and robustness. Samples were applied to Whatman No. 3 paper chromatography strips and analyzed using a mathematical formula to calculate the percentage of radiochemical purity.
Results: The technique clearly distinguished the impurities, meeting the purity specification (>95%) across all batches. Linearity demonstrated an appropriate correlation between concentration and activity. Intermediate precision and repeatability showed low coefficients of variation (1.0% and 0.9%, respectively). The limit of quantification was validated with consistent results. Robustness was confirmed by varying the dimensions and composition of the stationary phase without significantly affecting the outcomes.
CONCLUSIONS: The validated alternative analytical technique is reliable, meets regulatory criteria, and can be routinely implemented in radiopharmacy laboratories. Its use enhances operational efficiency without compromising quality. It is recommended to expand its evaluation through multicenter studies to strengthen its applicability.

References

1. European Medicines Agency. ICH Harmonised Tripartite Guideline Q2(R1): Validation of Analytical Procedures: Text and Methodology. London: EMA; 1995. CPMP/ICH/381/95.
2. United States Pharmacopeial Convention. <825> Radiopharmaceuticals—Preparation, Compounding, Dispensing, and Repackaging. In: United States Pharmacopeia and National Formulary (USP 47–NF 42). Rockville, MD: USP; 2024.

3. Gillings N, Todde S, Behe M, et al. EANM guideline on the validation of analytical methods for radiopharmaceuticals. EJNMMI Radiopharmacy and Chemistry. 2020;5(7).
https://doi.org/10.1186/s41181-019-0086-z.
4. Vásquez M, Ramos B. Validación de un método analítico por TLC-scanner para la determinación de pureza radioquímica del pertecnetato de sodio 99mTc solución inyectable. Inf. Cient. Tec. 2016;16(2):15-21.
5. Ekoume FP, Boersma HH, Dong à Zok D, Rubow SM. Validation of a cost-effective alternative for a radiochromatography method to be used in a developing country. EJNMMI Radiopharmacy and Chemistry. 2020;5(9). https://doi.org/10.1186/s41181-020-0092-1

Conflict of Interest

The authors declare that there is no conflict of interest in the presentation of this work. This study was sponsored and guided exclusively by the team of workers at the Hospital Universitario Fundación Valle del Lili, with no involvement from external entities or commercial interests.

O10

R1 from 18F-PR04.MZ as a proxy for cerebral blood flow in degenerative parkinsonisms: comparison with 15O-H2O PET/CT

Dr. Andres Damian[1,2], Dr. Ignacio Amorin[3], Dr. Vasko Kramer[4], Dr. Juan R. Higgie[3], TRI. Ismael Cordero[1,2], Dr. Luis Gutierrez[2], Dr. Eduardo Savio[1], Dra. Thalia Arias[2], Dr. Omar Alonso[1,2], Dr. Rodolfo Ferrando[1,2]
[1]Centro Uruguayo De Imagenología Molecular - Cudim, Montevideo, Uruguay, [2]Unidad Académica de Medicina Nuclear e Imagenología Molecular, Hospital de Clínicas, Universidad de la República, Montevideo, Uruguay, [3]Instituto de Neurología, Hospital de Clínicas, Universidad de la República, Montevideo, Uruguay, [4]Nuclear Medicine and PET/CT Center PositronMed, PositronPharma SA., Santiago, Chile

Oral Presentations 1: Neurology, Radiopharmacy and Chemistry, Arsenal Room, February 13, 2026, 14:00 - 16:00

Background/Aims: 18PR04.MZ is an effective dopamine transporter (DAT) tracer for detecting dopaminergic depletion in degenerative parkinsonisms (DP). R1 images derived from dynamic 18PR04.MZ studies have been proposed as a proxy for cerebral blood flow (CBF), but no study has directly compared R1 with perfusion measured by 15O-H2O PET/CT, the gold standard for non-invasive CBF assessment. Aim: To evaluate the relationship between R1 from 18PR04.MZ and CBF assessed by 15O-H2O PET/CT in patients with parkinsonian syndromes.
Methods: Fourteen patients with degenerative parkinsonism (11 Parkinson's disease, two multiple system atrophy, one progressive supranuclear palsy) underwent 18PR04.MZ and 15O-H2O PET/CT within two weeks. Specific Uptake Ratios (SURs) of caudate, putamen, and substantia nigra were compared with 17 healthy controls (HC). Parametric images of R1 (18PR04.MZ) and absolute perfusion maps (15O-H2O) were generated by compartmental analyses. Correlations were assessed across cortical and subcortical regions.
Results: SURs were significantly reduced in patients compared to HC (caudate: 8.7 ± 4.2 vs. 17.9 ± 2.9; putamen: 5.3 ± 4.5 vs. 22.3 ± 3.1; substantia nigra: 0.91 ± 0.71 vs. 4.7 ± 1.4; all $p < 0.0001$). Significant correlations between R1 and CBF were found in the putamen (correlation coefficient= 0.717, $p = 0.0058$), parietal (CC= 0.673, $p = 0.0117$), frontal (CC= 0.631, $p = 0.0209$), and occipital cortices (CC = 0.573, $p = 0.0407$).
Conclusions: Dynamic 18F-PR04.MZ PET with kinetic analysis provides complementary information on CBF and may serve as a useful proxy for perfusion imaging in degenerative parkinsonism, with potential applications in the differential diagnosis of parkinsonian syndromes.

Conflict of Interest
None

O11

Evaluation of cortical amyloid burden and tau deposition in cognitively normal and preclinical Alzheimer's disease through positron emission tomography

Mr. Phelipi Nunes Schuck[1], Dr Ana Maria Marques da Silva[1,2]
[1]Faculdade de Medicina FMUSP, Universidade de Sao Paulo, São Paulo, Brazil,
[2]Medical Imaging & Data Analytics (MEDIIMA), Porto Alegre, Brazil

Oral Presentations 1: Neurology, Radiopharmacy and Chemistry, Arsenal Room, February 13, 2026, 14:00 - 16:00

Background/Aims: Preclinical Alzheimer's disease (pAD) precedes manifestation of cognitive impairment symptoms associated with AD [1]. The assessment of amyloid burden and tau deposition through PET provides valuable prognostic information regarding AD progression [2]. This study aims to quantitatively assess amyloid and tau deposition within the total brain cortex through PET imaging in pAD and cognitively normal (CN) subjects.
Materials and Methods: 194 CN individuals (69±8yo, max: 91yo, min: 46yo; MMSE: 29±1, max: 30, min: 23) and 96 pAD (77±7yo, max: 98yo, min: 56yo, MMSE: 27±3, max: 30, min: 21) were selected from public dataset Open Access Series of Imaging Studies
(OASIS-3: https://sites.wustl.edu/oasisbrains/). [^{11}C]PIB, [^{18}F]AV45 and [^{18}F]AV1451 PET images [3] were smoothed (8mm FWHM) to reduce inter-scanner differences. Motion correction was performed using vector-gradient algorithm. Brain regions were segmented using Freesurfer (v. 5.3; http://surfer.nmr.mgh.harvard.edu/) on date-matched MRI acquired within 300 days from PET. Standardized uptake value ratios (SUVR) were calculated for amyloid-PET (Amy-PET; [^{11}C]PIB: 30–60 min; [^{18}F] AV45: 50–70 min) and tau-PET ([^{18}F]AV1451: 80–100 min), using cerebellar cortex as reference. Statistical differences between groups were assessed through Student's 2-sample t-test for Amy-SUVR and Tau-SUVR (CI=95%). Reference intervals were investigated using age as fixed variable for each group [4].
Results: Amy-SUVR was significantly higher in pAD than in CN individuals (CN: 1.19 ± 0.45; pAD: 1.88 ± 0.89; $p < 0.0001$) (Fig. 1A). CN reference interval for Amy-SUVR matches the amyloid positivity cutoff (OASIS-3 Cutoff=1.42; Measured Cutoff 95%CI=1.39) while the measured cutoff (95%CI) is 2.10 for pAD (Fig 1-B,C). No statistical differences were found between CN and pAD for Tau-SUVR either for group analysis or age-specific reference intervals.
Conclusion: Cortical amyloid burden assessed through PET can be an early phase indicator of preclinical Alzheimer's disease. Ongoing longitudinal analyses will clarify regional tau and amyloid involvement and its prognostic value in pAD.

References
[1]. Dubois B, Hampel H, Feldman HH, Scheltens P, Aisen P, Andrieu S, Bakardjian H, Benali H, Bertram L, Blennow K, Broich K. Preclinical Alzheimer's disease: definition, natural history, and diagnostic criteria. Alzheimer's & Dementia. 2016 Mar 1;12(3):292-323.
[2]. Rafii MS, Aisen PS. Detection and treatment of Alzheimer's disease in its preclinical stage. Nature aging. 2023 May;3(5):520-31.
[3]. LaMontagne PJ, Benzinger TL, Morris JC, Keefe S, Hornbeck R, Xiong C, Grant E, Hassenstab J, Moulder K, Vlassenko AG, Raichle ME. OASIS-3: longitudinal neuroimaging, clinical, and cognitive dataset for normal aging and Alzheimer disease. medrxiv. 2019 Dec 15:2019-12.
[4]. Altman DG (1993) Construction of age-related reference centiles using absolute residuals. Statistics in Medicine 12:917-924.
Conflict of Interest
Data were provided by OASIS-3: Principal Investigators: T. Benzinger, D. Marcus, J. Morris; NIH P50AG00561, P30NS09857781, P01AG026276, P01AG003991, R01AG043434, UL1TR000448, R01EB009352. AV-45 doses were provided by Avid Radiopharmaceuticals, a wholly owned subsidiary of Eli Lilly.

Graphic

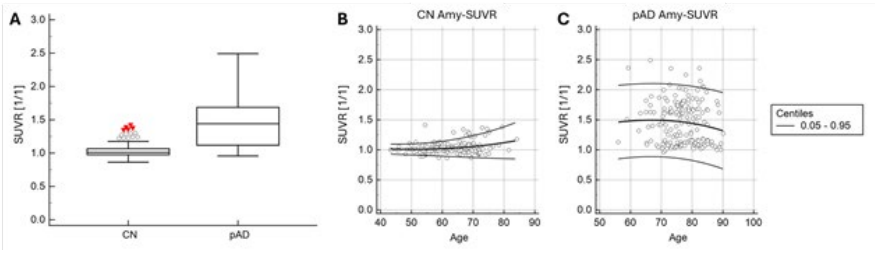

O12

Influence of EEG Discharges During FDG-PET Cerebral Metabolism Assessment in Patients with Pharmacoresistant Epilepsy

Dr. Valentino Mendez[1], Dr Andrés Damian[1,2,3], LIC Maria Pages[3], Dra Mariana Legnani[3], Dr Andrés Bertinat[3], Dra Patricia Braga[3], Dr Omar Alonso[1,2], Dr Rodolfo Ferrando[1,2,3]

[1]Unidad Académica de Medicina Nuclear e Imagenología Molecular, Hospital de Clínicas, Universidad de la República, Montevideo, Uruguay, [2] Centro Uruguayo de Imagenología Molecular (CUDIM), Montevideo, Uruguay, [3]Programa de Cirugía de Epilepsia del Hospital de Clínicas, Montevideo, Uruguay

Oral Presentations 1: Neurology, Radiopharmacy and Chemistry, Arsenal Room, February 13, 2026, 14:00 - 16:00

Background: Accurate localization of the epileptogenic zone is essential for successful surgery in pharmacoresistant epilepsy. However, few studies have investigated the impact of epileptic activity during FDG injection on cerebral metabolism.
Objective: To assess the value of EEG monitoring during radiotracer injection for evaluating cerebral metabolism with FDG-PET.
Methods: Retrospective analysis of pharmacoresistant epilepsy patients undergoing 18F-FDG PET with simultaneous EEG during radiotracer injection. EEG was recorded 20 minutes before and after FDG injection (3 MBq/kg). PET imaging commenced 40 minutes post-injection. EEG findings were compared with PET metabolic patterns.
Results: Seventy-nine patients were included (age range 3–59 years, 44 females). EEG abnormalities during FDG injection were detected in 49 patients (62%): mild interictal activity (<10 spikes/min) in 34 (43%), moderate activity in 9 (11%), and electroclinical seizures in 6 (8%). Temporal lobe involvement was noted in 29 cases (37%). PET was able to lateralize or localize the epileptogenic focus in 45 patients (57%). Concordance between EEG findings and PET hypometabolism was observed in 21 patients (27%). Five of the six patients that had electroclinical seizures during injection showed decreased cortical metabolism in the postulated epileptogenic focus. No significant association was found between the presence of EEG activity and hypometabolism detection in the epiletogenic zone (p=0.98). Nineteen patients underwent surgery (8 with focal cortical dysplasia, 5 with mesial temporal sclerosis, 2 gliomas, 4 other etiologies). Sixteen resected lesions exhibited FDG-PET abnormalities, and seven also showed EEG abnormalities.
Conclusions: EEG monitoring during radiotracer injection revealed significant epileptogenic activity. However, the lack of an overall association between EEG abnormalities—even at rates >10/min—and hypometabolism did not appear to influence the sensitivity of FDG-PET in detecting the epileptogenic zone.

References
-Theodore WH. Presurgical focus localization in epilepsy: PET and SPECT. Semin Nucl Med. 2017;47(1):44–53.
-Hong KS, Lee DS, Lee MC, et al. Asymmetry of interictal spikes during FDG-PET scanning in temporal lobe epilepsy. J Nucl Med. 2002;43(8):1118–1124.
-Bansal R, Kumar A, Bhatia R, et al. Interictal PET hypermetabolism in pediatric epilepsy: Clinical and imaging correlation. J Pediatr Neurosci. 2016;11(3):184–189.
-Bittar RG, Olivier A, Andermann F, et al. Interictal spikes increase cerebral glucose metabolism and CBF: A PET study. Epilepsia. 1999;40(12):1701–1706.
Conflict of Interest
I declare that I have no conflicts of interest.

O13

Evaluation of a murine model of metastatic castration resistant prostate cancer for combination radioligand therapy and immunotherapy

Dr. Cindy Rodriguez[1], Alexa Michel[1], Moralba Dominguez Garcia[1], Angelique Loor[1], Yana Reshetnyak[2], Jason S. Lewis[1]
[1]Molecular Pharmacology Program Memorial Sloan Kettering Cancer Center, New York, United States, [2]Department of Physics University of Rhode Island, Kingston, United States

Oral Presentations 1: Neurology, Radiopharmacy and Chemistry, Arsenal Room, February 13, 2026, 14:00 - 16:00

Background/Aims: Prostate specific membrane antigen (PSMA)-targeted radioligand therapy has become a promising method for treatment of patients with metastatic castration-resistant prostate cancer (mCRPC), yet ~50% of patients with mCRPC do not respond well, possibly due to PSMA expression heterogeneity.
The pH low insertion peptide (pHLIP) can target and insert itself intro the cell membrane with high affinity in the acidic tumor microenvironment. pHLIP can be modified at either the N-or C-terminus to deliver a cytotoxic payload to the tumor cell.
We propose a combination approach harnessing the advantages of (PSMA)-targeted radioligand therapy and pHLIP-based immunotherapy (pHLIP-STINGa) to amplify the therapeutic response and overcome issues with tumor heterogeneity in +PSMA mCRPC.
Methods: Male C57BL/6 mice were implanted with either RM1-WT or RM1(+PSMA) murine PC cells. Tumors were allowed to grow until ~200 mm3 and randomly sorted into imaging (n=4) or treatment (n=5) groups.
Imaging Studies: Mice were administered 68Ga-PSMA-11 and imaged by positron emission and computed tomography 2 h post-injection.
The following day, the same mice were administered 89Zr[Zr]-DFO-pHLIP and imaged 48 h post-injection.
Pilot treatment study: Treatment groups include saline, pHLIP alone, STINGa alone, pHLIP-STINGa, and 177Lu[Lu]-PSMA-617 (low, mid, and high). Tumor sizes are measured twice-weekly by caliper and retro-orbital blood collection performed weekly. This study is currently ongoing.
All animal studies were reviewed and approved by Institutional Animal Care & Use Committee at Memorial Sloan Kettering Cancer Center (MSKCC).
Results: Mice with +PSMA tumors obtained significantly higher uptake of the tracer compared to WT tumors with 68Ga[Ga]-PSMA-11, and similar uptake of the 89Zr[Zr]-DFO-pHLIP peptide in both tumor types.
Conclusion: The combination of radioligand- and immuno-therapy may provide increased therapeutic efficacy in late stage mCRPC.
Acknowledgments: This work was supported by NIH 3R35CA232130-07S1 (JSL/CR), and the Small Animal Imaging and Radiochemistry & Molecular Imaging Probes cores at MSKCC.

Conflict of Interest
JSL and YR are co-inventors of MSK intellectual property licensed to pHLIP Inc.

Graphic

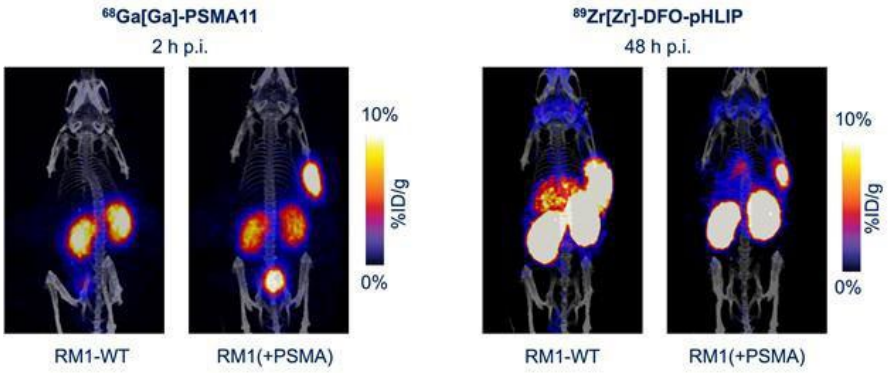
68Ga[Ga]-PSMA11
2 h p.i.
10%
%ID/g
0%
RM1-WT
RM1(+PSMA)
89Zr[Zr]-DFO-pHLIP
48 h p.i.
10%
%ID/g
0%
RM1-WT
RM1(+PSMA)

O14

Optimizing Pretargeted Radiotheranostics: From PET to Therapy

Mr. Mike Cornejo[1,2,3], Zachary V. Samuels[1,2,3], Gina Dehlavi[1,2,4], Lukas Carter[5], Emilia Strugala[1], Brian M. Zeglis[1,2,4,6]
[1]Department of Chemistry, Hunter College, The City University of New York, New York, United States, [2]Ph.D. Program in Chemistry, Graduate Center of the City of New York, New York, United States, [3]Department of Radiology, Memorial Sloan Kettering Cancer Center, New York, United States, [4]Ph.D. Program in Biochemistry, Graduate Center of the City University of New York, New York, United States, [5]Department of Medical Physics, Memorial Sloan Kettering Cancer Center, New York, United States, [6]Department of Radiology, Weill Cornell Medical College, New York, United States

Oral Presentations 1: Neurology, Radiopharmacy and Chemistry, Arsenal Room, February 13, 2026, 14:00 - 16:00

Background: Monoclonal antibodies (mAbs) have long been an attractive vector for delivering radionuclides to tumor tissue; however, their slow pharmacokinetic profiles pose limitations, particularly with respect to radiation dose rates to healthy tissues. In vivo pretargeting helps alleviate these issues by decoupling the antibody from the radionuclide payload, allowing the former to accumulate in the tumor before the administration of the radioligand. This radioligand then travels through the body quickly and either binds to the tumor-bound antibody or clears from circulation. The optimization of the radioligand is crucial to the safety and efficacy of in vivo pretargeting strategies. Herein, we explore the pharmacokinetic profiles of three 64/67Cu-labeled sarcophagine-tetrazine radioligands for pretargeted PET and radioimmunotherapy.
Methods: Sarcophagine-tetrazine radioligands - SarAr-Tz, SarAr-PEG5-Tz, and SarAr-PEG10-Tz - were labeled with 64/67Cu using standard protocols, and their purity and stability were assayed via radio-iTLC and radio-HPLC. The in vivo performance of the trio was evaluated via 64Cu-PET imaging 6, 12, and 24 h after the administration of the radioligand in a murine model of colorectal cancer. The safety and efficacy of the most promising radioligand were further explored in longitudinal 67Cu-pretargeted radioimmunotherapy therapy studies.
Results: SarAr-Tz, SarAr-PEG5-Tz, and SarAr-PEG10-Tz were successfully synthesized and radiolabeled with 64/67Cu in radiochemical yields and purities of >99% and specific activities of 15-20 MBq/μg. All three radioligands showed excellent PET contrast, with [^{64}Cu]Cu-SarAr-PEG10-Tz achieving the best tumor-to-tissue concentration ratios. The SarAr-PEG10-Tz was further explored in a longitudinal therapy study demonstrating promising efficacy and safety in mouse model.
Conclusion: We have synthesized and radiolabeled SarAr-Tz, SarAr-PEG5-Tz, and SarAr-PEG10-Tz with 64/67Cu in high yield and purity. Pretargeted PET and biodistribution experiments enabled us to identify SarAr-PEG10-Tz as the best candidate for 67Cu-based pretargeted radioimmunotherapy. Our findings showed that PRIT using [67Cu]Cu-SarAr-PEG10-Tz had a good safety profile and demonstrated a dose-dependent therapeutic effect.

References
1. Keinanen, O.; Fung, K.; Brennan, J. M.; Zia, N.; Harris, M.; van Dam, E.; Biggin, C.; Hedt, A.; Stoner, J.; Donnelly, P. S.; et al. Harnessing (64)Cu/(67)Cu for a theranostic approach to pretargeted radioimmunotherapy. Proc Natl Acad Sci USA 2020, 117 (45), 28316-28327.

Conflict of Interest

BZ holds intellectual property related to the approach to in vivo pretargeting described. Other authors have declared that no competing interest exists.

This work was supported by funding from the National Institutes of Health (1R01CA244327, 1RO1CA281801, 1R01AI175417, and 1R21CA280595 to BMZ) and the National Science Foundation under (DGE-2151945). The authors thank the MSKCC Small Imaging Core Facility and Radiochemistry and Molecular Imaging Probe Core, which are supported by NIH awards P30CA008748-48, S10OD016207-01, and S10RR020892-01. The authors declare no competing financial interest.

All animals were treated according to guidelines approved by the Research Animal Resource Center and the Institutional Animal Care and Use Committees of Memorial Sloan Kettering Cancer Center, Weill Cornell Medical College, and Hunter College.

Graphic

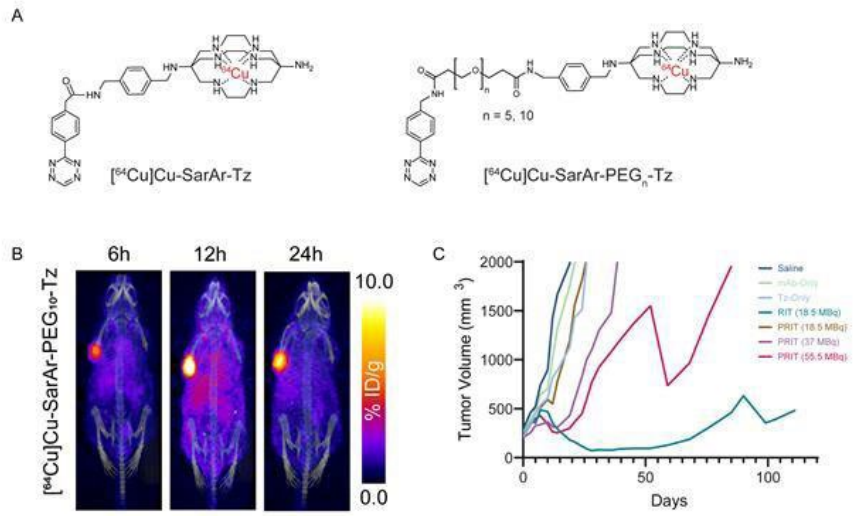

O15

Design and Astatination of Radioligands for the Pretargeted Delivery of Astatine-211

Mr. Mike Cornejo[1,2,3], Cindy Rodriguez[2], Zachary Samuels[1,2,3], Yutian Feng[5], Michael R. Zalutsky[5], Brian M. Zeglis[1,2,3,4]
[1]Department of Chemistry, Hunter College, The City University of New York, New York, United States, [2]Department of Radiology, Memorial Sloan Kettering Cancer Center, New York, United States, [3]PhD. Program in Chemistry, Graduate Center of the City University of New York, New York, United States, [4]Department of Radiology, Weill Cornell Medical College, New York, United States, [5]Department of Radiology, Duke University Medical Center, Durham, United States

Oral Presentations 1: Neurology, Radiopharmacy and Chemistry, Arsenal Room, February 13, 2026, 14:00 - 16:00

Background: Short-lived *α*-emitting radionuclides such as ^{211}At have great potential for targeted radionuclide therapy because they deliver high-linear energy transfer radiation over short path lengths. However, their short half-life is not compatible with the long serum residence time of macromolecular targeting vectors like monoclonal antibodies. Pretargeting can circumvent this problem by allowing for the accumulation of the immunoconjugate at the tumor site prior to the administration of the therapeutic radioligand, and relying on bioorthogonal ligations — such as the inverse electron demand Diels-Alder reaction between tetrazine and trans-cyclooctene — for the in vivo combination of these two components. In this project, we focused on the development of astatinated stannyl-modified tetrazine radioligands bearing a residualizing prosthetic group for in vivo pretargeting.
Methods: Boc2-iso-GMTB-PEG6-Tz and Boc2-iso-GMTB-Tz were synthesized, purified via high-performance liquid chromatography (HPLC) with >98% purity, and characterized using mass spectroscopy and 1H-NMR. The two tetrazine-modified radioligands were astatinated under acidic conditions using chloramine-T as the oxidizing agent. The radiolabeling process was monitored and purified using radio-HPLC. Following purification, the deprotection of the two radioligands was performed under acidic conditions, resulting in iso-[211At]GMAtB-PEG6-Tz and iso-[211At]GMAtB-Tz as the final products.
Results: Boc2-iso-[211At]GMAtB-PEG6-Tz and Boc2-iso-[211At]GMAtB-Tz were produced in >99% radiochemical conversion and radiochemical purity. After deprotection and purification, iso-[211At]GMAtB-PEG6-Tz and iso-[211At]GMAtB-Tz were produced in 35% overall radiochemical yield.
Conclusion: We have synthesized, purified, and characterized iso-[211At]GMAtB-PEG6-Tz and iso-[211At]GMAtB-Tz with a final isolated radiochemical yield of 35%. Preliminary in vivo pretargeting experiments using athymic nude mice bearing SW1222 colorectal cancer xenografts are currently in progress.

Conflict of Interest
BZ holds intellectual property related to the approach to in vivo pretargeting described. Other authors have declared that no competing interest exists.

This work was supported by funding from the National Institutes of Health (1R01CA244327, 1RO1CA281801, 1R01AI175417, and 1R21CA280595 to BMZ) and the National Science Foundation under (DGE-2151945). The authors thank the MSKCC Small Imaging Core Facility and Radiochemistry and Molecular Imaging Probe Core, which are supported by NIH awards P30CA008748-48, S10OD016207-01, and S10RR020892-01. The authors declare no competing financial interest.

Graphic

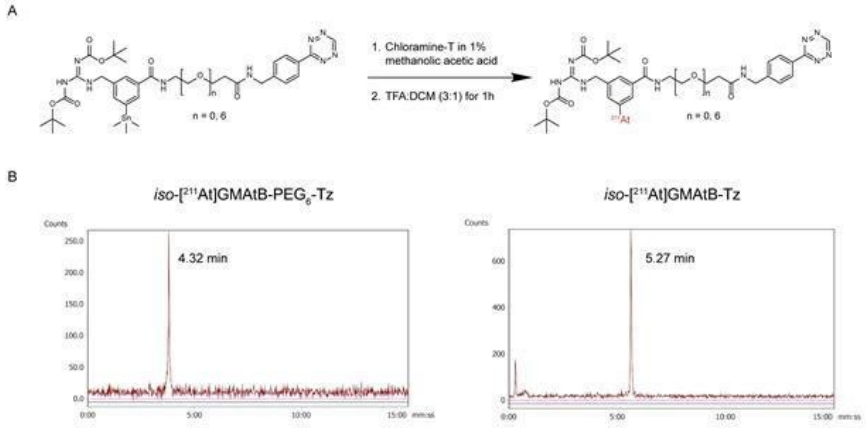

O16

Combining deep learning and kinetic modeling for cerebral PET parametric imaging with reduced-time dynamic acquisitions

Lic. Santiago Burgos[1], Dr. Arturo Avendaño[1,2], Dr. Miguel Ávila[1,2]
[1]Unidad Radiofarmacia-Ciclotrón, División de Investigación, Facultad de Medicina, Universidad Nacional Autónoma de México, Ciudad De México, México, [2]Centro de Investigación sobre el Envejecimiento, CINVESTAV Sede Sur, Ciudad de México, México

Oral presentations 2: Physics and Technology, Arsenal Room, February 14, 2026, 8:00 - 10:00

Background/Aims: Kinetic analysis of PET images requires prolonged dynamic acquisitions to estimate physiological parameters such as binding potential (BP), which is impractical in clinical settings. In this work, we propose a strategy that combines a simple Deep Learning (DL) architecture with quantitative PET analysis, aiming to shorten the duration of brain PET studies without compromising quantitative accuracy.
Methods: This is a retrospective study; the database was consolidated from 16 dynamic PET/CT scans (60 min) using [^{11}C]DTBZ, previously acquired at the PET/CT Unit of UNAM. Data augmentation techniques were applied to expand the training set. Images were processed with PMOD (v4.4), and the DL model was based on a lightweight architecture combining 2D convolutional LSTM and 3D convolutional layers to predict final frames, intentionally omitted to resemble shortened dynamic acquisitions. Kinetic analysis was performed using the Logan reference tissue model (LRTM), with manually defined regions of interest in the striatum and occipital lobe as reference.
Results: The model was able to reconstruct late frames from shortened dynamic acquisitions while preserving differential uptake in the striatum. Parametric images obtained from the DL-based studies closely matched the reference images obtained with complete dynamic acquisitions (SSIM=0.9939±0.0015, RMSE=0.0230±0.0021). The bias between the BP values obtained from DL-based studies and the reference (left striatum:2.85±2.54%, right striatum:3.62±2.85%) was lower than that observed when comparing the shortened study (last frames removed) with the reference (left striatum:5.88±2.96%, right striatum:5.95±5.10%).
Conclusions: A simple DL model was implemented as a proof-of-concept to generate late frames in dynamic cerebral PET studies. Quantitative results derived from the generated studies (13 minutes shorter) were comparable to those obtained from full acquisitions, suggesting that this approach not only demonstrates feasibility but could potentially allow for much greater reductions in scan duration. This research study was supported by DGAPA-UNAM research grant PAPPIT-IT201623.

Conflict of Interest
NA

Graphic
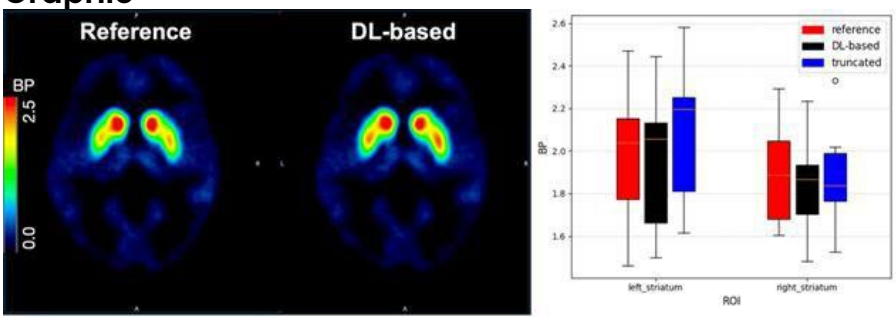

O17

High throughput scanning with a vertical and compact Walk-Through flat panel PET

Prof. Stefaan Vandenberghe[1], Dr. Jens Maebe[1], Msc Maya Abi Akl[1], Ir. Boris Vervenne[1], Msc Rabia Aziz[1], Ir. Thibault D'Hulster[1], Ir. Florence Marie Muller[1,3], Prof Dr. Nadia Withofs[2], Prof. Dr. Christian Vanhove[1]
[1]MEDISIP, Ghent University, Gent, Belgium, [2]CHU Liege, Liege, Belgium, [3]PET instrumentation group, University Pennsylvania, Philadelphia, USA

Oral presentations 2: Physics and Technology, Arsenal Room, February 14, 2026, 8:00 - 10:00

The Walk-Through PET (WT-PET) is a novel long axial field-of-view (LAFOV) PET system design using two vertically aligned flat detector panels (height 106 cm) positioned around an upright standing patient. The scanner gap has been optimized to 50 cm and the width to 71 cm based on ergonomic data and PET-CT patient databases. Patients can enter the scanner through the side gaps and position themselves. By removing the patient bed, the WT-PET streamlines workflow, increases throughput, and minimizes staff involvement.
The system is based on monolithic detectors with high spatial resolution, DOI, and TOF. Simulations show that it delivers more uniform image resolution (< 2 mm) than cylindrical PET and good image quality in 30 seconds. The planar design reduces detector area (and system cost) by 50%, while maintaining comparable sensitivity (120 kcps/Mq) to cylindrical LAFOV scanners (176 kcps/MBq). It also has a much smaller footprint than current PET.
Challenges include (1) patient motion in the upright position, (2) quantitative reconstruction without CT, (3) limited-angle sampling, and (4) scanning bedridden patients. Motion is minimized through rapid acquisition, ergonomic headrest, hand supports adjustable to their heights and real-time feedback. Lack of CT is compensated by deep learning–based attenuation correction. Transverse limited angle sampling effects are reduced by the large axial opening angle and DOI/TOF–enhanced sampling combined with deep learning corrections. Finally, bedridden patients can be scanned by sliding the bed horizontally through the WT-PET with a gap adjusted to 70 cm.
This design is interesting for countries with high demand for PET. Efficient patient positioning + high sensitivity leads to high patient throughput (up to 12 patients/hr). Another advantage of fast scanning is the more efficient use of tracer (66% reduction in ordered tracer dose/patient). After simulations of phantoms, the reconstruction was optimised and the system is now under construction.

Conflict of Interest
Stefaan Vandenberghe
is Editor-in-Chief EJNMMI Physics (Springer Nature)
is One of the founders of Nuclivision.com (Ghent, Belgium)
has Patents with Ugent used by Molecubes (acquired by Bruker)

Graphic

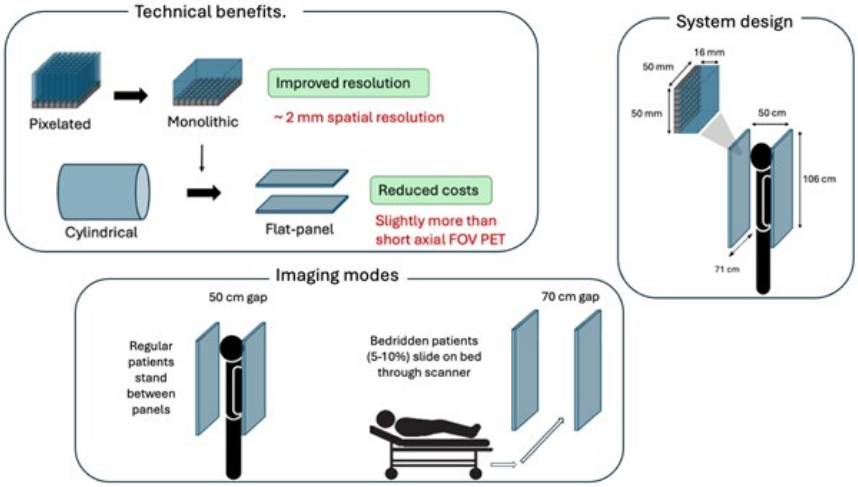

O18

Internal Dosimetry Calculation for PET/CT with ^{18}F-PSMA-1007 Using OpenDose Software

Prof. Kelly Sandoval Sandoval[1], Prof. M. José Abarzua[1], Prof. Jose Ceballos[1]
[1]Fundación Arturo Lopez Perez, Santiago, Chile

Oral presentations 2: Physics and Technology, Arsenal Room, February 14, 2026, 8:00 - 10:00

Background: The radiopharmaceutical ^{18}F-PSMA-1007 offers advantages over other PSMA ligands, such as favorable biodistribution and low urinary excretion, which enhance PET/CT image quality in patients with prostate cancer. However, current evidence is largely based on small sample sizes and heterogeneous methodologies. Therefore, this study aims to estimate the internal dosimetry of ^{18}F-PSMA-1007 using the open-source software OpenDose3D, with the goal of generating standardized and locally relevant data.
Methods: A total of 63 patients with a diagnosis or suspicion of prostate cancer who underwent PET/CT with ^{18}F-PSMA-1007 at Fundación Arturo López Pérez between June and July 2024 were selected. Cases with absent organs or imaging acquisition times outside the optimal range (60–90 minutes) were excluded. The images were processed using OpenDose3D, with automatic organ segmentation and generation of dose-time curves (ADR). Absorbed dose rates per organ and per patient were calculated, followed by descriptive statistical analysis.
Results: A total of 115 anatomical structures were contoured. The organs receiving the highest absorbed doses were the trachea, gallbladder, and kidneys, confirming their role as critical organs in the dosimetry of ^{18}F-PSMA-1007. The gallbladder showed the highest interindividual variability (standard deviation of 0.149 mGy/MBq). Other parenchymal organs such as the liver, spleen, and duodenum also showed relevant but more homogeneous dose values.
Conclusion: This study demonstrates that OpenDose3D enables accurate and reproducible estimation of ^{18}F-PSMA-1007 PET/CT dosimetry. The identification of critical organs with high dosimetric variability underscores the need for personalized approaches. Additionally, the use of open-access tools promotes multicenter standardization, enhances patient safety, and supports the development of more effective theranostic therapies.

Conflict of Interest
no

Table

Organ	Mean (mGy/MBq)	STD
Trachea	0.277	0.045
Gallbladder	0.230	0.149
Right Kidney	0.129	0.029
Right Lung	0.124	0.036
Liver	0.120	0.027
Left Kidney	0.114	0.030
Duodenum	0.100	0.035
Spleen	0.075	0.022

Table 1. Mean absorbed dose results per organ for ^{18}F-PSMA-1007. Source: Own elaboration based on data obtained with OpenDose3D.

O19

Quantitative Evaluation of Scatter Correction Strategies in Long Axial Field-of-View PET/CT

Dr. Mohammadreza Teimoorisichani[1], Dr. Inki Hong[1]
[1]Siemens Medical Solutions USA Inc., Knoxville, United States

Oral presentations 2: Physics and Technology, Arsenal Room, February 14, 2026, 8:00 - 10:00

Background: Scatter correction in PET and especially in long axial field-of-view (LA-FOV) PET systems is required to maintain quantitative accuracy in the reconstructed images. A common approach employs single-scatter simulation (SSS) [1]. However, since SSS inherently models only first-order scatter, accurate scaling is essential. This study compared four scatter scaling strategies in terms of bias, robustness, and sensitivity to PET/CT mismatch.
Methods: Four scatter correction methods were implemented:
(1) absolute scaling: where SSS sinograms were directly applied,
(2) tail-fitting (TF): where scaling factors were estimated by fitting large radial bins of the scatter to net trues,
(3) maximum likelihood scatter scaling (MLSS): in which scale factors were derived using a discrete data-consistency condition [2],
(4) exponential model scaling (EXM): which employed an exponential model to approximate higher-order scatter. Performance was evaluated using an 18F-FDG patient scan acquired on an LA-FOV PET/CT system. All procedures were IRB-approved with informed consent. Reconstructions were repeated with 45-cm transaxially truncated CT data to simulate PET/CT mismatch. Images were assessed qualitatively and quantitatively with VOIs placed in multiple organs.
Results: As summarized by the Table and Figure, absolute scaling consistently underestimated scatter, leading to a bias in PET images. With full CT, TF, MLSS and EXM yielded comparable results. However, under truncation, TF produced severe artifacts due to inflated scale factors from mismatched tails. In contrast, MLSS and EXM preserved quantitative accuracy. Importantly, CT truncations introduced attenuation-related artifacts in the arms independent of scatter.
Conclusions: Absolute scaling leads to systematic underestimation, while TF is highly sensitive to PET/CT mismatch. Methods that incorporate data within the patient contour, like MLSS and EXM, mitigate bias and maintain accuracy even under challenging conditions. These methods enhance the reliability of activity recovery and image quality in LA-FOV PET, supporting their clinical translation for quantitative and diagnostic applications.

References
[1]-https://doi.org/10.1109/TNS.2007.901227
[2]-https://doi.org/10.1109/NSSMIC.2012.6551685
Conflict of Interest
All authors are full-time employee of Siemens Medical Solutions USA, Inc.

Graphic

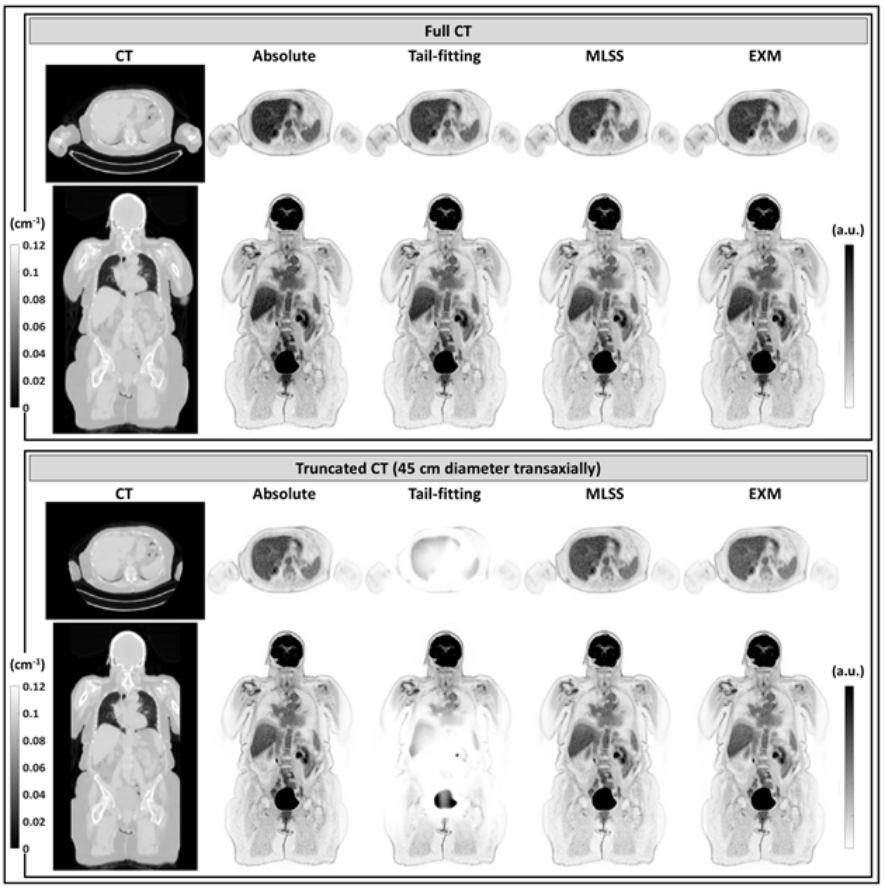

Figure. Sample axial and coronal slices through the images of an ^{18}F-FDG patient data reconstructed with full (top) and 45-cm transaxially truncated (bottom) CT data and different scatter correction techniques.

Table

Table. Percentage difference in organ uptake for various scatter correction methods using full or transaxially truncated CT images. Values are expressed as percent difference relative to images reconstructed with full CT and the tail-fitting scatter correction method.

Scatter Correction Method	CT Data	Brain	Liver	Lungs
Absolute	Full CT	2.49	7.89	12.48
	Truncated CT	1.14	-9.97	-4.74
Tail-fitting	Full CT	0	0	0
	Truncated CT	3.22	-78.87	-67.70
MLSS	Full CT	0.34	-1.49	-6.09
	Truncated CT	-0.94	-11.07	-12.10
EXM	Full CT	1.37	1.46	4.51
	Truncated CT	0.25	-15.53	-11.81

O20

A Quantitative CT-less Reconstruction Workflow for Long-axial Field-of-view PET Scanners with Enhanced Scaling

Dr. Mohammadreza Teimoorisichani[1], Dr. Josh Schaefferkoetter[1], Dr. Hasan Sari[2,3]
[1]Siemens Medical Solutions USA Inc., Knoxville, United States, [2]Department of Nuclear Medicine, Inselspital, Bern University Hospital, Bern, Switzerland, [3]Siemens Healthineers International AG, Zurich, Switzerland

Oral presentations 2: Physics and Technology, Arsenal Room, February 14, 2026, 8:00 - 10:00

Background: The joint estimation problem in maximum likelihood estimation of activity and attenuation (MLAA) is ill-posed and non-unique, leading to scaling issues in MLAA-reconstructed images. While time-of-flight (TOF) improves spatial localization and mitigates scaling, it may not fully resolve the issue, particularly with inconsistent or noisy data. This work introduces an improved quantitative CT-less reconstruction workflow based on TOF-MLAA, incorporating a novel approach to address scaling.
Methods: The proposed method is designed for PET scanners with lutetium-based scintillators. We use attenuation maps (μ-maps) derived from lutetium background radiation as an initial condition in TOF-MLAA as proposed in [1].
To further mitigate scaling issues, a partially known μ-map is employed to determine and apply a scaling factor to reconstructed images. In the absence of ground-truth μ-maps in CT-less PET, we utilize a deep learning (DL)-based organ segmentation algorithm to segment non-attenuation-corrected PET images. The mean attenuation coefficient of an organ minimally affected by MLAA cross-talk (the liver in 18F-FDG studies) is then compared to a nominal value (0.1 cm^{-1} for the liver). The resulting offset is used to calculate and apply a scaling factor within MLAA. This approach is particularly suited for long-axial field-of-view PET scanners, where the high lutetium background radiation flux allows for a transmission reconstruction with acquisitions as short as a few minutes. We evaluated the proposed CT-less reconstruction framework on three patients (written consents provided) scanned with 18F-FDG using a long-axial FOV PET/CT scanner.
Results: Reconstructed μ-maps from MLAA showed excellent agreement with CT-based μ-maps, with minimal inconsistencies due to cross-talk. The final PET images were comparable to reference images both qualitatively and quantitatively, with individual organ uptake values within 5% of those from CT-based reconstructions.
Conclusions: The proposed CT-less reconstruction workflow in this work in can be a practical solution to ultra-low dose PET scans.

References

1. Medical Physics 49 (1), 309-323, 2022

Conflict of Interest

M. Teimoorisichani and J. Schaefferkoetter are full time employee of Siemens Medical Solutions USA Inc. H. Sari is a part time employee of Siemens Healthineers International AG, Zurich, Switzerland

O21

High-Precision PET/CT: Optimization and Quality strategies led by the Nuclear Medicine Technologist

Sra. Andrea Milena Bautista Beltran[1]
[1]Clínica De Marly, Bogotá Dc, Colombia

Oral presentations 2: Physics and Technology, Arsenal Room, February 14, 2026, 8:00 - 10:00

Introduction: PET/CT image quality is essential for accurate diagnosis and treatment planning. Variables such as patient preparation, technical acquisition, and routine equipment quality control directly affect reproducibility and clinical interpretation. The nuclear medicine technologist plays a decisive role in optimizing these processes. This work analyzes the technologist's impact on image optimization and diagnostic accuracy in PET/CT using different radiopharmaceuticals.
Methods: A literature review (IAEA [1], EANM [2], SNMMI [3]) was integrated with practical experience in PET/CT acquisition using 18F-FDG, 18F-PSMA, and 18F-FET. Three critical stages were assessed: (1) patient preparation (fasting, glycemic control, hydration); (2) acquisition parameters (time per bed position, BMI-adjusted protocols, iterative and time-of-flight reconstruction); and (3) quality control (daily uniformity, resolution, calibration). Special attention was given to radiopharmaceutical biodistribution: 18F-FDG shows physiological uptake in brain, myocardium, and urinary tract; 18F-PSMA in salivary glands, kidneys, and liver; and 18F-FET with low background activity in healthy brain tissue, improving tumor to background contrast.
Results: Optimized protocols reduced motion and attenuation artifacts, enhanced signal to noise ratio, and improved discrimination between physiological and pathological uptake. Correct anticipation of biodistribution patterns minimized false positives, particularly distinguishing urinary excretion in FDG studies and physiological glandular uptake in PSMA imaging. In neuro-oncology, the favorable biodistribution of FET improved lesion delineation. Repeat scans were reduced, decreasing patient radiation exposure and improving institutional efficiency.
Conclusions: The nuclear medicine technologist is a central actor in PET/CT optimization. Their role ensures accurate differentiation of normal biodistribution from pathological uptake, enhances diagnostic confidence, and promotes protocol standardization across centers. Continuous education in radiopharmaceutical kinetics and advanced imaging techniques is essential to maintain high standards of image quality, patient safety, and clinical reliability.

References
1. IAEA. Quality assurance for PET and PET/CT systems. IAEA Human Health Series No. 1. Vienna: International Atomic Energy Agency; 2009.
2. Boellaard R, et al. EANM procedure guidelines for tumour PET imaging: version 2.0. Eur J Nucl Med Mol Imaging. 2015;42:328–354.
3. SNMMI Procedure Standards. PET/CT imaging. Society of Nuclear Medicine and Molecular Imaging; 2021. High-Precision PET/CT: Optimization and Quality Strategies Led by the Nuclear Medicine Technologist

Conflict of Interest

No conflict of interest

O22

Brain MRI-guided PET Reconstruction in a New PET/MRI System with <200ps TOF resolution

Dr. Jorge Cabello[1], Dr Karen Kettless[2], Dr Patrick Lehmann[2,3], Dr Anders Rodell[2], Dr Joshua Schaefferkoetter[1], Dr Ian Law[4], Prof Flemmin Littrup Andersen[4,5], Dr Thomas Lund Andersen[4,5], Dr Paul Schleyer[1]
[1]Siemens Medical Solutions USA, Knoxville, United States, [2]Siemens Healthcare A/S, Ballerup, Denmark, [3]Research & Clinical Translation, Magnetic Resonance, Siemens Healthineers AG, Erlangen, Germany, [4]Department of Clinical Physiology and Nuclear Medicine, Copenhagen University Hospital—Rigshospitalet, Copenhagen, Denmark, [5]Department of Clinical Medicine, University of Copenhagen, Copenhagen, Denmark

Oral presentations 2: Physics and Technology, Arsenal Room, February 14, 2026, 8:00 - 10:00

PET imaging inherently exhibits limited spatial resolution and high image noise. Recent improvements in Time-of-Flight (TOF) performance have resulted in significantly better image quality. Simultaneous PET/MRI acquisition provides spatially overlapping metabolic/functional and soft tissue anatomical information at the same time point. By leveraging anatomical MR-images as prior information in the PET reconstruction, MRI-guided (MRIg) MAP-EM PET reconstruction reduces image noise, and improves spatial resolution and quantification accuracy. The current work presents preliminary results of MRIg-MAP-EM PET reconstruction of several brain FDG-PET datasets acquired on the BIOGRAPH One, a second-generation PET/MRI system (Siemens Healthineers) with best-in-class TOF performance.
Several subjects were injected with FDG, and underwent a brain PET scan in the PET/MRI system, while simultaneously acquiring multiple MRI sequences. PET data were acquired in list-mode format and rebinned to different scan lengths. The datasets were reconstructed using OP-OSEM and MRIg-MAP-EM reconstruction, based on the Bowsher prior combined with a novel algorithm to adaptively calculate the anatomical strength, using an MPRAGE MRI sequence as anatomical reference.
Results demonstrated that MRI-guided PET reconstruction yielded lower image noise and enhanced delineation of brain structures, compared to OP-OSEM. This improvement enabled a reduction in scan time by up to 75% without perceptible degradation in image quality. While the high TOF resolution OP-OSEM reconstructions exhibited high image quality, MRIg-MAP-EM further improved image sharpness and reduced noise.
In conclusion, the TOF resolution achieved by this new PET/MRI system significantly improved image quality compared to non-TOF reconstruction, resulting in more precise visualization and delineation of small structures within the brain. Moreover, the integration of anatomical information further refined spatial resolution and reduced image noise. This synergistic approach not only maintains high image quality but also enables reduced scan times or lower radiation doses, thereby improving patient comfort and safety without compromising diagnostic accuracy.

Conflict of Interest
Cabello J., Kettless K., Lehmann P., Rodell A.B., Schaefferkoetter J., and Schleyer P. are employess of Siemens Healthineers.

Graphic

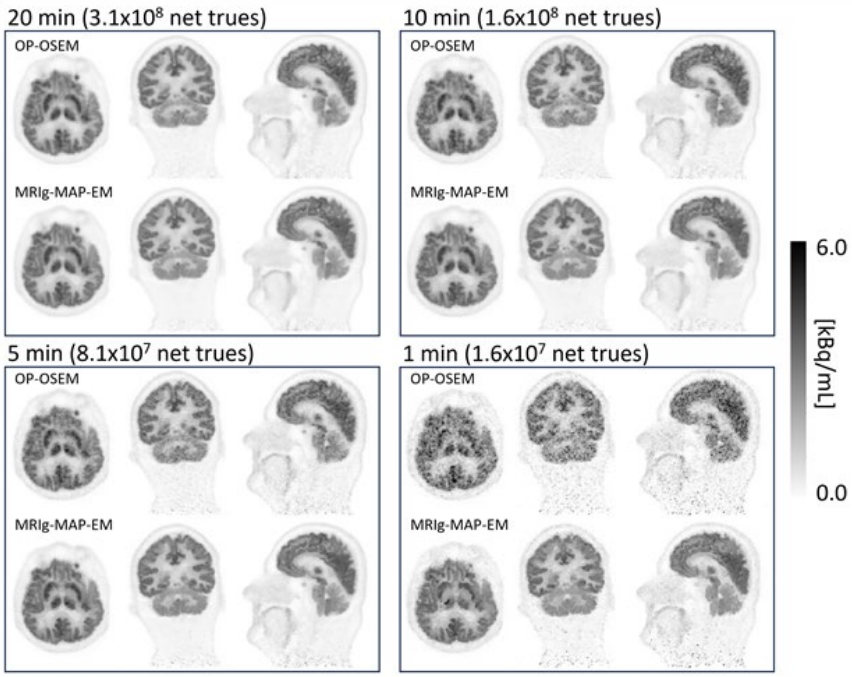

O23

Colombian Guide for the support of Radiological Events in Nuclear Medicine and Radiopharmacy

Mrs. Lorena Sandoval Castillo[1,2], Mrs. Eliana Franco[1,3], Mrs. Angela Londoño[1,4], Mrs. Stephany Calderón[1,5], Mrs. Erika Xiomara Cely[1,6], Mrs. Patricia Rico[1,7], Mrs. Nathalia Nuñez[1,7], Mr. Harley J. Orjuela B.[1,8], Mrs. Claudia Blanco[1,9], Mr. Omar Patiño[1,10]
[1]Asociación Colombiana De Física Médica- ACOFIMED, Bogotá, Colombia, [2]Clínica del Country, Bogotá, Colombia, [3]Hospital Universitario Mayor Méderi, Bogotá, Colombia, [4]Medicina nuclear, Clínica de Occidente, Cali, Colombia, [5]Medicina Nuclear S.A., Valledupar, Colombia, [6]Servicio de medicina nuclear, Clínica Internacional de alta tecnología -Clinaltec, Ibagué, Colombia, [7]Grupo de Física Médica, Fundación Valle de Lili, Cali, Colombia, [8]Área de Física Médica, Hospital Serena del Mar, Cartagena de Indias, Colombia, [9]Servicio Geológico Colombiano, Bogotá, Colombia, [10]Física Médica Hospitalaria, Hospital Universitario de Caldas, Manizales, Colombia

Oral presentations 2: Physics and Technology, Arsenal Room, February 14, 2026, 8:00 - 10:00

Background/Aims: In Latin America, the lack of specific protocols for managing radiological events in medical settings poses a significant risk. This is the current situation in Colombia, despite some progress in national regulations. To address this limitation, a group of clinical medical physicists from the Colombian Association of Medical Physics (ACOFIMED) led the development of the country's first technical and practical guide, adapted to its specific regulatory and operational conditions.
The document's primary objective is to create a technical and practical guide that strengthens the response capabilities of radiation protection officers and specialized personnel in the face of radiological events within services like conventional nuclear medicine, PET, metabolic therapies, and radiopharmacy.
Methods: The guide was developed through a comprehensive review of current national regulations, international guidelines, and scientific literature. This was complemented by the authors' real-world experiences in Colombian clinical settings. The technical writing and editing focused on the most relevant scenarios: metabolic therapies, radiopharmacy, and conventional nuclear medicine (SPECT, SPECT/CT, and PET/CT). Each chapter was reviewed by a dedicated working group and an external expert to ensure its accuracy and relevance.
Results: The final document provides detailed guidance for first responders, covering everything from the classification of events (incident, accident, and emergency) to notification procedures. It includes the required components of an emergency kit and the technical parameters for evaluating radiation exposure (external, internal, and contamination). Furthermore, it outlines the criteria for action based on the type of exposure and the affected party (patient, worker, public, or the environment), which facilitates rapid and effective adaptation in clinical practice.

Conclusion: This guide represents a significant advancement for radiological safety in Colombia. Its practical and contextualized approach strengthens institutional preparedness and promotes a culture of safety in facilities that handle radioactive materials

Conflict of Interest

The authors, [Lorena Sandoval, Eliana Franco, Angela Londoño, Stephany Calderón, Erika Xiomara Cely, Patricia Rico, Nathalia I. Nuñez, Harley J. Orjuela, Claudia Blanco, Omar Patiño], declare that there are no conflicts of interest—whether personal, financial, commercial, academic, or of any other nature—that could have affected the impartiality of the results and analysis presented in this work. The research has been conducted independently and without receiving sponsorship or support from any public or private entity with interests in the topic.

O24

Comparison of Patlak imaging with SUV imaging in metastatic uveal melanoma patients with a long axial field-of-view (LAFOV) PET/CT

Dr. Leyun Pan[1], Prof. Dr. Christos Sachpekidis[1], Prof. Dr. Antonia Dimitrakopoulou-Strauss[1]
[1]German Cancer Research Center, Heidelberg, Germany

Oral presentations 2: Physics and Technology, Arsenal Room, February 14, 2026, 8:00 - 10:00

Aim/Introduction: New Long Axial Field-of-View (LAFOV) PET-CT scanners allow, for the first-time, whole-body (WB) dynamic scanning, as well as WB pharmacokinetic studies and WB parametric imaging. We, herein, aimed to evaluate whether WB direct Patlak imaging is feasible with the LAFOV Biograph Vision Quadra PET/CT system (106 cm FOV) and whether it improves lesion detectability compared to 50-60 min and 70-80 min images in patients with multiple liver metastases from uveal melanoma prior to tebentafusp therapy, which is a first-in-class TCR-CD3 bispecific immunotherapy.
Materials and Methods: 17 uveal melanoma patients with 89 liver lesions were enrolled in the study. All patients underwent [18F]FDG PET/CT (skull to upper thigh). Three sets of images were compared: direct Patlak Ki images, 70-80 min SUV (late SUV) images, and 50-60 min SUV (early SUV) images. All three sets of images were visually (qualitatively) reviewed by the reading physicians. Furthermore, 89 liver lesions were quantitatively analyzed using the target-to-background (TBR).
Results: No significant differences were observed between the three group of images regarding the number of liver lesions. However, we found two discordant results: two true positive liver lesions were identified on Patlak Ki images, one in each of the two patients, which were not delineated on the SUV images. Quantitatively, parametric imaging showed that direct Patlak Ki images and late SUV images had superior TBR compared to early SUV images (2.3- and 1.3-fold mean increase in TBR, respectively).
Conclusion: Dynamic LAFOV PET/CT scanner allows the calculation of Patlak Ki images with better lesion contrast than SUV images, but does not significantly increase the lesion detection rate. In addition, late (70-80 min) SUV images have better contrast than early (50-60-min) SUV images. In a small number of cases, Patlak images revealed discordant findings compared to SUV images, adding further useful clinical information.

Conflict of Interest
None.

Graphic

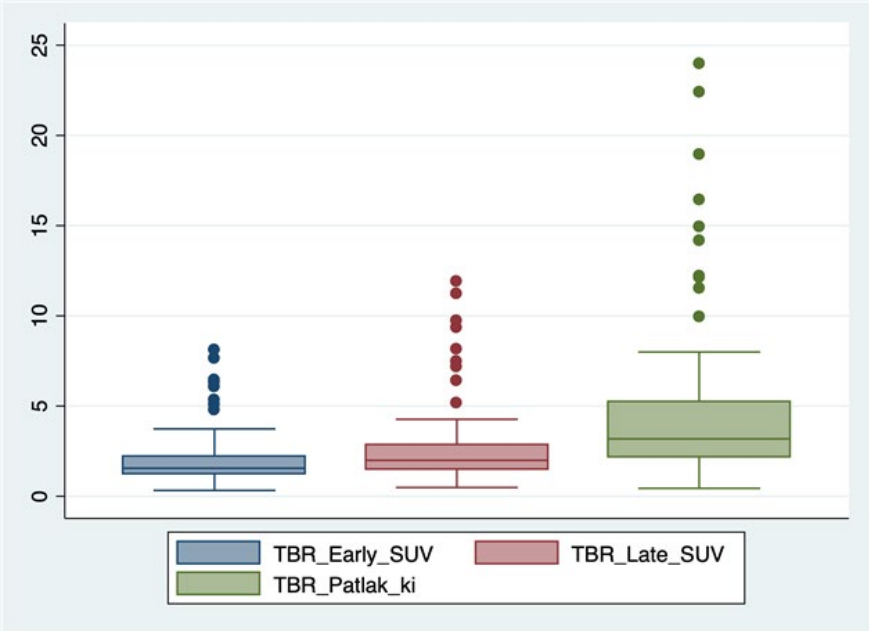

O25

Clinical validation of deep learning denoising for low-count PET/CT: preserving SUV accuracy and image quality

Dr. Mauro Namías[1], **PhD Yamila Rotstein Habarnau**[1], Dr Nicolás Bustos[1], Dr Paola Corona[1], Dr Christian González[1], Dr Sonia Traverso[1], Dr Federico Matorra[1], BSc Francisco Funes[2], BSc Juan Martín Giraut[1], PhD Laura Pelegrina[2], Dr Gabriel Bruno[1]
[1]Fundación Centro Diagnóstico Nuclear, Buenos Aires, Argentina, [2]Comisión Nacional de Energía Atómica, Buenos Aires, Argentina

Oral presentations 2: Physics and Technology, Arsenal Room, February 14, 2026, 8:00 - 10:00

Background and objectives: Optimizing image quality in positron emission tomography (PET) while minimizing radiation dose and costs remains a central challenge. Reducing radiotracer activity or acquisition time lowers patient exposure but compromises signal-to-noise ratio. We report the first clinical validation of a novel artificial-intelligence–based denoising solution designed to recover high-quality PET images from low-count acquisitions.
Methods: A total of 258 patients referred for oncological fluorodeoxyglucose positron emission tomography/computed tomography (18F-FDG PET/CT)were prospectively enrolled under Institutional Review Board (IRB)approval and informed consent. Standard-of-care images (100%) from GE Discovery 710 and 610 scanners were reconstructed according to the most recent European Association of Nuclear Medicine standards (EARL2 [1-3]). Half-count statistics datasets were generated from list-mode data and processed with the artificial intelligence (AI)software (50%+AI). Lesion detectability, false positives, standardized uptake value (SUV) accuracy, and subjective image quality were assessed. All lesions were segmented manually or automatically on both image sets. Quantitative agreement of maximum SUV (SUVmax)was evaluated using Bland-Altman analysis. Two experienced readers blindly and independently scored image quality on 5-point scales.
Results: 1,649 lesions were analyzed from 198 studies with positive findings. 50%+AI images demonstrated 99.9% sensitivity for lesion detection, with only one false positive reported. SUVmax concordance between 100% and 50%+AI images showed excellent agreement, with a bias of –1.01% and 95% limits of agreement within ±12.5%. Importantly, image quality of 50%+AI datasets was rated as equal or superior to standard-of-care images in all cases.
Conclusions: This AI-based denoising tool enables routine oncological 18F-FDG PET/CT at half counting statistics, maintaining diagnostic sensitivity and quantitative reliability while reducing radiation exposure and examination costs. Clinical integration appears safe and effective, supporting a paradigm shift toward lower-dose PET imaging without compromising diagnostic confidence.

References

1. https://earl.eanm.org/accreditation-specifications/
2. Boellaard et al (2015). EJNMMI 42(2), 328–354.
3. Koopman et al (2016). EJNMMI Physics, 3(1), 22

Conflict of Interest

The AI tool reported in this abstract was developed at Fundación Centro Diagnóstico Nuclear, and is commercially available in Argentina.

Graphic

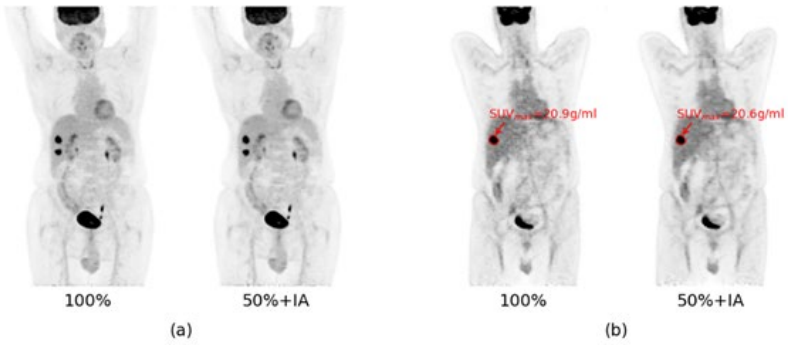

Figure 1: Male patient, 77 years old, 84 kg, diagnosed with colon cancer. Injected activity: 330.5 MBq. Scanner: GE Discovery 610. Maximum intensity projection (MIP) view (a) and coronal view (b) of the 100% counting statistics image and the 50%+IA image. One oncologic lesion is delineated and its SUV_{max} is report

Table

Scanner	SUV_{max} differences [g/ml]			SUV_{max} relative differences [%]		
	Bias	95% LoA	MAE	Bias	95% LoA	MAE
GE Discovery 610	-0.10	[-1.64,1.43]	0.57	-0.90	[-12.52,10.71]	4.62
GE Discovery 710	-0.05	[-1.19, 1.10]	0.45	-1.47	[-17.09, 14.15]	6.04
GLOBAL	**-0.09**	**[-1.56, 1.38]**	**0.54**	**-1.01**	**[-13.51, 11.48]**	**4.90**

Table 1: Bias, 95% limits of agreement (LoA) and mean absolute errors (MAE) on SUV_{max} absolute and relative differences for all scanners separately and combined (GLOBAL).

O26

Rapid scan assessment with non-quantitative FastPET: Generalizability to different tracers and count levels

Naveen Murthy[1], Dr. Yifan Zheng[1], Dr. Vladimir Panin[1], Dr. Deepak Bharkhada[1], Dr. Paul Schleyer[1]
[1]Siemens Medical Solutions, USA, Inc., Knoxville, United States

Oral presentations 2: Physics and Technology, Arsenal Room, February 14, 2026, 8:00 - 10:00

Background:Fast assessment of PET scans is essential for improving patient throughput. Technologists typically rely on reconstructed images to determine if a scan has been completed successfully (e.g. absence of patient motion), but this could take several minutes post-acquisition (especially for long axial FOV (LAFOV) scanners). We recently introduced ultraFastPET [1], a deep-learning method for near real-time non-diagnostic scan assessment, and showed preliminary results for [^{18}F]FDG data. This abstract explores its generalizability across tracers and count levels.
Methods:UltraFastPET is a lightweight, non-quantitative version of FastPET [2], based on a 3-D U-Net with residual blocks. It is trained in a patch-based manner, with PET histo-images as input, and non-attenuation corrected (NAC) MLEM reconstructions as targets. Histo-images correspond to an alternate data format, where listmode events are directly histogrammed into image space, instead of projection space. The training dataset included 20 [^{18}F]FDG whole-body static scans acquired on the Biograph Vision Quadra (Siemens Healthineers) LAFOV PET/CT scanner [3], with acquisition times of 4–10 minutes (635 million to 4.6 billion prompts).
Results:To investigate the generalizability of ultraFastPET (trained only using high-count FDG data), we tested it on scans with [^{82}Rb], [^{90}Y], [^{68}Ga]PSMA, [^{68}Ga]DOTA and [^{18}F]Flutemetamol, acquired on the Biograph Vision Quadra (Siemens Healthineers). Figure 1(a) shows input histo-images, ultraFastPET outputs, and clinical NAC recons (OSEM: 4 iterations, 5 subsets). The ultraFastPET images are visually comparable to the NAC recons. For low-count evaluation, we decimated a 30-second frame (~47 million prompts) from a high-count FDG scan to 50%, 25% and 10% counts. Figure 1(b) shows that ultraFastPET produces reasonable tracer distributions even at very low counts.
Conclusions:UltraFastPET enables rapid (~4 seconds on NVIDIA RTX 3090 for a single histo-image) non-diagnostic scan assessment. Despite being trained only on high-count FDG data, we show that it generalizes well across tracers and count levels.
Acknowledgements: The authors would like to thank Bern University Hospital's Inselspital Department of Nuclear Medicine for providing anonymized patient data.

References
[1] Murthy, N., Millardet, M., Zheng, Y., Bharkhada, D., Panin, V., Schleyer, P., 2025. Fast, non-quantitative imaging for near real-time scan assessment using end-to-end deep learning, In 2025 IEEE NSSMIC.
[2] Millardet, M., Bharkhada, D., Raj, J., Schaefferkoetter, J., Panin, V., Conti, M. and Matej, S., 2025. Improved Quantification in end-to-end Deep Learning FastPET Reconstruction Using Multi-View Histo-Images of Attenuation Correction Factors. IEEE Trans. on Rad. and Plas. Med. Sc. 2025.
[3] Prenosil, G.A., Sari, H., Fürstner, M., Afshar-Oromieh, A., Shi, K., Rominger, A. and Hentschel, M., 2022. Performance characteristics of the Biograph Vision Quadra PET/CT system with a long axial field of view using the NEMA NU 2-2018 standard. J. of Nucl. Med., 63(3), pp.476-484.
Conflict of Interest
No, there are no conflicts of interest.

Graphic

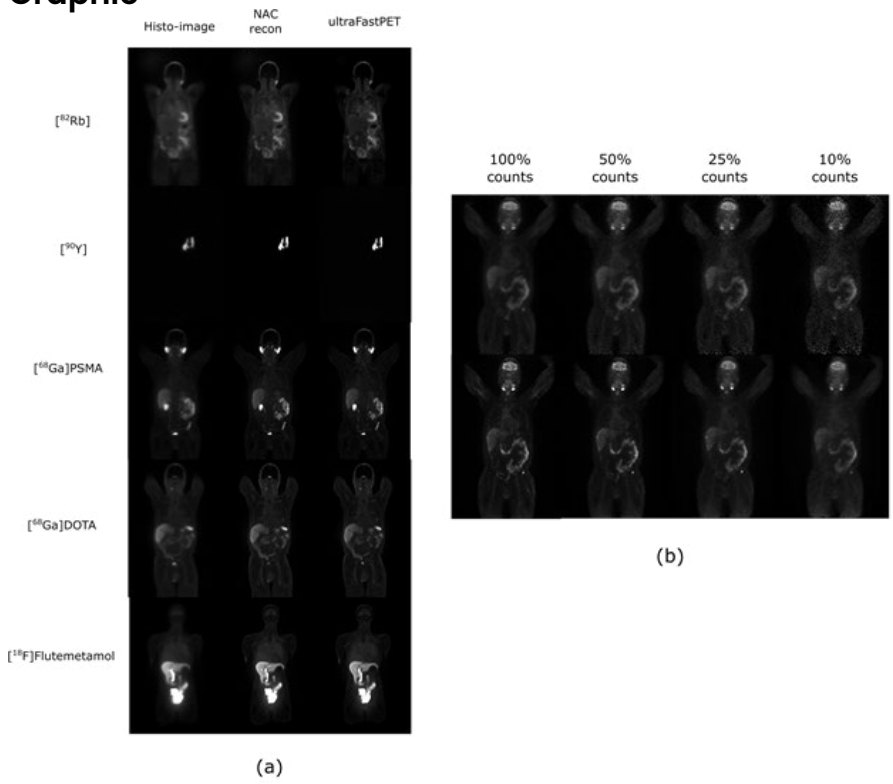

Figure 1: Generalizability of ultraFastPET. (a) Comparison of input histo-image vs. clinical NAC reconstruction vs. ultraFastPET output for different tracers. (b) Comparison of histo-images (top) vs ultraFastPET (bottom) for different count levels for an FDG acquisition.

O27

Deep learning-based dose estimation for radionuclide therapy: a feasibility study

Dr. Yamila Rotsein Habarnau[1], Dr. Mauro Namías[1]
[1]Fundación Centro Diagnóstico Nuclear, Ciudad Autónoma de Buenos Aires, Argentina

Oral presentations 2: Physics and Technology, Arsenal Room, February 14, 2026, 8:00 - 10:00

Background and objectives: Internal dosimetry for radiopharmaceutical therapy aims at determining the amount of radiation dose deposited in tumors and healthy tissues. Typically, estimation of the absorbed dose rate is performed for electrons only with convolution or local deposition methods. The photonic dose rate estimation typically requires Monte Carlo methods, which is time consuming for clinical applications. In this study, we propose the implementation of a deep learning method to accelerate the estimation of photon dose rate in radionuclide therapies.
Methods: We implemented different variants of a UNet-3D[1] network for patient-specific and voxel level photon dose estimation (Figure 1). The inputs of the network are the patient's computed tomography (CT) and the radiopharmaceutical activity image. We generated hundreds of random point sources inside the body region to train the network. The output of the network is the absorbed dose rate image. Ground truth dose rate images were obtained from Monte Carlo simulations, using GATE software[2]. The CT images were taken from the AutoPET MICCAI 2023 Challenge dataset[3]. We tested different network configurations and compared relative errors in the absorbed dose in vertebral bodies, segmented using TotalSegmentator[4].
Results: Table 1 shows the results for a subset of configurations: with/without skip connections on the branch of the network that processes the CT image and with/without instance normalization blocks. We found that adding skip connections and normalization blocks improved the performance. Inference only takes a few seconds, making it suitable for implementation in clinical practice. These preliminary results serve as guidance for optimizing the method.
Conclusions: We found that it is possible to train a deep learning method to estimate the photonic component of dose deposition in radionuclide therapies.

References

1.Çiçek et al., LNCS,vol.9901,2016.
2.Jan et al., Phys Med Biol,vol.49,2004.
3.Gatidis et al., Sci Data,vol.9,2022.
4.Wasserthal et al., Radiol Artif Intell,vol.5,2023.

Conflict of Interest

None

Graphic

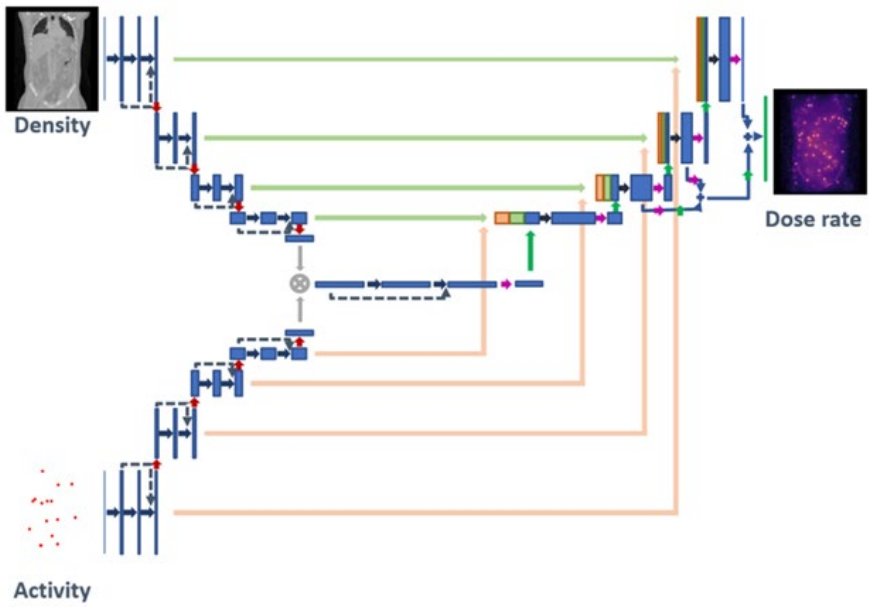

Figure 1: Network architecture. One encoder branch processes the CT image, the other one processes the activity map and they combine to obtain the dose rate map.

Table

Vertebrae	Relative error [%]			
	Skip connections: False Normalization: True	Skip connections: True Normalization: True	Skip connections: True Normalization: False	Skip connections: False Normalization: False
C1-C7	11.47 ± 4.15 [7.07,16.02]	10.80 ± 8.22 [0.41,37.64]	48.21 ± 64.66 [0.85,261.82]	62.80 ± 14.40 [34.23,89.54]
T1-T12	13.40 ± 1.72 [11.31,15.28]	6.51 ± 4.56 [0.16,22.40]	34.31 ± 21.67 [2.07,147.72]	53.73 ± 7.78 [33.90,71.57]
L1-L5	19.61 ± 2.75 [16.36,21.99]	7.08 ± 5.78 [0.23,20.14]	35.75 ± 17.29 [5.16,69.60]	60.02 ± 9.78 [41.32,78.93]

Table 1: Percentual relative error between Monte Carlo simulation and prediction of the network for the absorbed dose in vertebral bodies, for different network configurations: with/without skip connections on the branch of the network that processes the CT image and with/without normalization blocks.

O28

Assessment of the impact of gastrointestinal motion on PET quantification due to mismatched CT

Dr. Giordana Salvi De Souza[1], Maria Giulia Toro[1], Samaneh Mostafapour[1], Johannes H. van Snick[1], Adrienne H. Brouwers[1], Charalampos Tsoumpas[1]
[1]Nuclear Medicine and Molecular Imaging, University of Groningen, University Medical Center Groningen, Groningen, The Netherlands

Oral presentations 2: Physics and Technology, Arsenal Room, February 14, 2026, 8:00 - 10:00

Introduction: Quantification of gastrointestinal (GI) organs in PET is challenging due to physiological motion and variable intraluminal air. Such motion may cause mismatch between CT (used for attenuation correction, AC) and PET data. This study quantified GI motion and segmentation reproducibility over a 10-minute interval and evaluated its impact on PET quantification through AC mismatches.
Methods: Seven patients undergoing oncological [^{18}F]FDG PET/CT (after ≥4h fasting) received two CT scans 10 minutes apart on a long axial view PET/CT scanner (Ethics approval: UMCG - 10946). The second CT was acquired with ultra-low dose [1]. GI organs, including stomach, duodenum, small bowel, and colon, were automatically segmented using TotalSegmentator. Segmentation agreement and reproducibility were evaluated with Dice Similarity Coefficient (DSC), Relative Volume Difference (RVD), and 95% Hausdorff Distance (HD95). In four patients, manual displacement of GI organs and colonic segments (ascending, transverse, descending) was measured, along with AC map differences.
Results: Segmentation reproducibility was moderate across organs (DSC 0.6–0.7). Colon showed the best agreement (RVD 7.3±4.1%), while the duodenum and small bowel were less consistent (RVD 21.1±25.3% and 16.1±9.3%). Stomach demonstrated intermediate reproducibility (RVD 15.8±10.0%) but exhibited the largest superior–inferior displacement (23.5mm). HD95 values ranged from 11 to 15 mm, indicating contour variability. Manual displacement analysis revealed organ-specific motion often exceeding 10 mm, equivalent to 20–60% of the organ diameter. These shifts, driven by intraluminal air, led to PET–CT mismatches and AC differences ranging from -28.3% to +46.3%.
Conclusion: Within 10 minutes, GI motion caused mismatches between PET and CT leading to AC differences of up to 46% and apparent displacements exceeding 10 mm. These findings may differ in non-fasted patients and are likely even more pronounced during longer (e.g. 60-minute) dynamic PET acquisitions. The results highlight the necessity for motion correction strategies to ensure accurate PET quantification of GI organs.

References

[1] Mostafapour et al. Ultra-low dose CT scanning for PET/CT. Med Phys. 2024.

Conflict of Interest

None.

Graphic

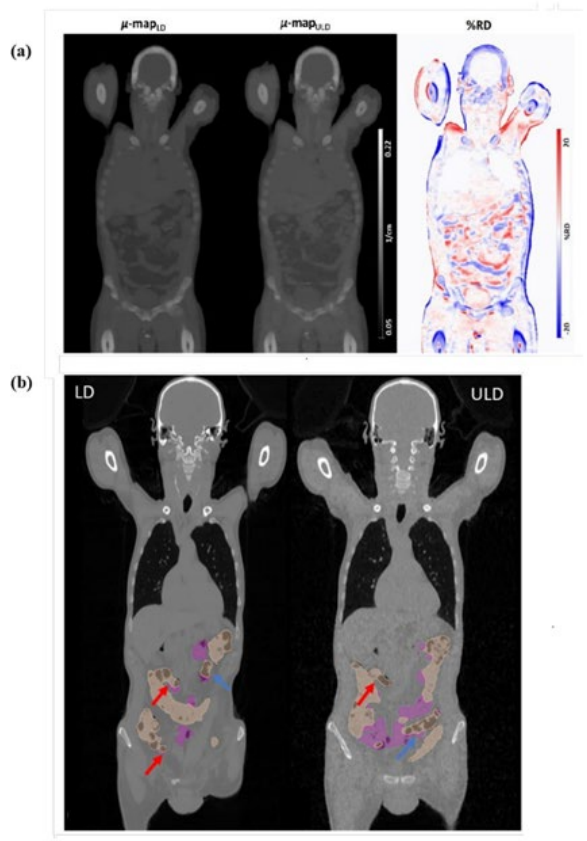

Figure 1: (a) Attenuation maps from low-dose (LD) and ultra-low-dose (ULD) CT scans, with the corresponding relative difference (%RD) map. **(b)** Coronal LD (left) and ULD (right) CT slices with automatic segmentations of colon (beige) and small bowel (purple). Red arrows highlight displaced air-related protrusions, and the blue arrow indicates misclassification between small bowel and colon.

Table

Table 1. Segmentation reproducibility and GI displacement measurements

Organ	Dice (mean ± SD)	RVD (%) (mean ± SD)	95% Hausdorff (mm, mean ± SD)	Displacement SI (mm, median [range])	Displacement AP (mm, median [range])	Displacement LR (mm, median [range])
Stomach	0.7 ± 0.1	15.8± 10.0	12.1 ± 3.6	11.3 [7.0 – 23.5]	−0.7 [−7.7 – 8.6]	−1.1 [−13.2 – 10.9]
Duodenum	0.5 ± 0.2	21.1 ± 25.3	10.9 ± 4.6	4.7 [−7.0 – 11.9]	−4.3 [−5.9 – 8.9]	4.0 [−11.5 – 7.5]
Small bowel	0.6 ± 0.1	16.1 ± 9.3	14.4 ± 3.8	4.4 [−8.6 – 9.7]	−0.04 [−9.6 – 6.0]	−4.7 [−8.5 – 8.4]
Colon / Ascending colon	0.7 ± 0.1	7.3 ± 4.1	15.2 ± 3.3	3.4 [−9.1 – 18.6]	1.6 [−14.7 – 7.6]	1.6 [−9.4 – 12.0]
Transverse colon				9.3 [4.9 – 15.7]	−3.4 [−4.6 – 4.8]	—
Descending colon				1.4 [−9.3 – 8.1]	−4.6 [−9.6 – 6.0]	−6.2 [−22.4 – 8.7]

Legend: DSC = Dice Similarity Coefficient; RVD = absolute Relative Volume Difference; HD_{95} = 95% Hausdorff Distance; SI = superior-inferior; AP = anterior-posterior; LR = left-right.

O29

Optimization of pet/ct acquisition parameters for pregnant patients: phantom study with reduced dose and preserved image quality

Mr. Yann Cras[1], MD. Mariagiulia Longo[1], MD. Camilo Garcia[1], Pr. Désirée Deandreis[1], MD. Theophraste Henry[1]
[1]Gustave Roussy, Villejuif, France

Oral presentations 2: Physics and Technology, Arsenal Room, February 14, 2026, 8:00 - 10:00

Background/Aims
Performing PET/CT in pregnant patients requires minimizing radiation exposure while maintaining diagnostic image quality. A 40% reduction in injected activity and at least 65% reduction in CT dose are targeted. Theoretical models suggest compensating for reduced activity by increasing PET acquisition time and adjusting CT parameters (kV, mAs, pitch). This study aimed to determine, on a phantom, optimal PET and CT acquisition settings adapted to our digital time-of-flight PET/CT system and compare them with theoretical predictions.
Methods
A NEMA IEC phantom was filled with 50 MBq of F-18 (hot background, six hot spheres, contrast ratio 10.3). PET acquisitions were performed at three reference activity levels and at delayed time points to simulate 40% activity reduction (equivalent to lowering from 2.5 to 1.5 MBq/kg for pregnancy). Acquisition times were adjusted according to theoretical proportionality and compared with +/- 20% variations. Background variability, sphere contrast, and activity recovery were assessed. For CT, acquisitions were performed with the reference protocol (120 kV, 20 mAs, pitch 1.3) and with reduced-dose parameters derived from theory (100 kV, 11 mAs, pitch 1.5). Other parameters are inchanged.
Results
For PET, the optimal acquisition time to achieve noise levels equivalent to reference images was 13 min 03 s, compared with 13 min 30 s predicted theoretically. Contrast recovery and sphere-to-background contrast remained stable across conditions. For CT, adjusted parameters achieved a dose-length product reduction of 65.7%, close to the 66.9% theoretical estimate (-1.2% difference).
Conclusions
A PET acquisition time of 13.05 minutes ensures preserved image quality despite a 40% reduction in injected activity. CT dose reduction goals (>65%) can be achieved with adapted acquisition parameters. These optimized settings provide practical guidelines for performing PET/CT safely in pregnant patients.

Conflict of Interest
Nothing to disclose

O30

Implementation of Innovative Toilet Filtration Systems for Radionuclide Therapy Effluents: First Latin American Clinical Experience

MSc Eduardo Antonio Gonzalez Villa[1], MSc Cristhoper Camacho Herrera[2], Dr. Dany Mena Cortes[1,2], Bart Boots[3], Mattijs Maris[3], **Lic. Yesenia Saldierna Martinez**
[1]Oncologia San José, Hermosillo, Mexico, [2]Nuclear Medicine World, Ciudad de Mexico, Mexico, [3]Zereau, Netherlands

Oral presentations 2: Physics and Technology, Arsenal Room, February 14, 2026, 8:00 - 10:00

Background/Aims:During radionuclide therapy, patients treated with iodine-131 (I-131) or lutetium-177 (Lu-177) excrete significant fractions of administered activity through urine and feces. *Studies on Lu-177-octreotate therapy show that patients excrete roughly 46 % of the administered activity within four hours [1]*. According to Mexico's NOM-041-NUCL-2013, radioactive liquid effluents must meet strict release limits *[2]*, typically requiring shielded decay tanks. This study reports the first Latin-American clinical experience implementing an innovative toilet filtration system designed to retain therapeutic radionuclides directly at the source.
Methods: At Oncología San José (OSJ), a "toilet filter system – all in one" unit was installed upstream of the sanitary drain. It operates like a conventional toilet but incorporates automated sorbent dosing, micro-filtration, vacuum dewatering, and liquid absorption filtration. The system managed effluents from patients receiving I-131 (3700–5550 MBq, ±10 %) and Lu-177 (7400 MBq, ±5 %). Filters were replaced weekly, stored in lead-shielded containers, and quantified via planar SPECT imaging using AI-based count-to-activity conversion. Residual activity was compared with decay-tank samples.
Results: The system captured > 90 % of excreted radionuclide activity, achieving effluent concentrations well below regulatory limits. Waste volume was reduced by > 95 %, eliminating the need for shielded tanks and enabling therapy in standard rooms. Dose rates around the filters were markedly lower than near decay tanks.
Conclusions: This filtration system provided safe, hygienic, and cost-effective management of I-131 and Lu-177 therapeutic effluents, transforming aqueous waste into compact solid cartridges and offering a practical alternative to decay tanks.
Financial Support: This work was supported by institutional collaboration between Oncología San José and Nuclear Medicine World.

References

[1] Secretaría de Energía. Norma Oficial Mexicana NOM-041-NUCL-2013, Límites anuales de incorporación y concentraciones en liberaciones (2013)
[2] Calais PJ et al. Radiation safety of outpatient Lu-177-octreotate radiopeptide therapy of neuroendocrine tumors. Ann Nucl Med (2014)

Conflict of Interest

None to be reported

O31

Cocaine-dependent patients with depressive symptoms and suicide risk studied with brain perfusion SPECT and systemic inflammatory markers

Dr. Teresa Massardo[1], Dr. Juan Carlos Quintana[2], Dr. Carlos Ibáñez[1], Dr. Jonathan Veliz[1], Dr. Rodrigo Jaimovich[2], Dr. Claudia S Saez[2], Dr. Jaime Pereira[2], Dr. Francisco Javier Gomez[1], Dr. Isabel Berrocal[3], Dr. Rene Fernandez[1]
[1]Hospital Clínico Universidad De Chile, Santiago, Chile, [2]Hospital Clínico Pontificia Universidad Catolica De Chile, Santiago, Chile, [3]hospital San Juan De Costa Rica, San Jose, Costa Rica

Oral Presentations 3: Cardiology, Infection and Inflammation, Arsenal Room, February 14, 2026, 14:00 - 16:00

Patients with cocaine dependence may present symptoms of mood disorders and even self-harm,not initially clearly differentiated from the substance acute side effects . There is evidence that both cocaine and major depression are related to a proinflammatory state[1-3].
Goal: To compare cerebral perfusion and systemic inflammatory markers in cocaine-dependent individuals without therapy, with and without suicidal behavior or depressive symptoms upon entering abstinence.
Methods: Forty-nine patients with no history of MD and cocaine dependence according to DSM-IV were studied, 24 with depressive symptoms and/or suicidal attempts or ideation (Group A) and 25 without these conditions (Group B) at baseline using SPECT cerebral perfusion tomography, measuring the percentage of cerebral hypoperfusion (<66% of the maximum). Systemic inflammation was analyzed using markers of endothelial dysfunction and platelet activation (circulating endothelial cells, RANTES, MCP-1, sICAM and p-Selectin).
Main results: In group B, basal prefrontal hypoperfusion correlated with age of onset and, at 4 weeks, duration of use correlated with global cortical and left prefrontal hypoperfusion, as well as with degree of use to a greater extent with prefrontal and cingulate cortex (r=0.47; p=0.027 in the latter).
Markers of endothelial dysfunction and platelet activation were significantly altered in the entire group compared to controls without cocaine use (p<0.05) and showed no difference between subgroups A and B (p>0.05).
A significant correlation was observed between cerebral hypoperfusion in patients in group A and sICAM and p-Selectin, mainly in the prefrontal and cingulate cortex (r=0.63; p=0.0089 in the latter with sICAM). In group B, all parameters had p=ns.
Conclusion: Cocaine addicts with depressive symptoms were older and began their addiction later than those without depression. All presented alterations in systemic inflammatory parameters with no differences between subgroups, although the cerebral cortex, mainly prefrontal and cingulate, correlated significantly with systemic inflammation markers. This may have therapeutic implications.

References
[1]Massardo T, Quintana JC. et al. Changes in regional cerebral blood flow are associated with endothelial dysfunction markers in cocaine-dependent patients under recent abstinence. J Addict Med. 2015 Mar-Apr;9(2):139-46.
[2]Massardo T, Quintana JC, et al. Effect of Low-Dose Statins in Addition to Standard Therapy on Brain Perfusion and Neurocognitive Performance in Patients with Major Depressive Disorder. Neuropsychobiology. 2022;81(4):271-285.
[3]Massardo T, Quintana JC, et al. Regional Brain Perfusion Is Associated with Endothelial Dysfunction Markers in Major Depressive Disorder. Neuropsychobiology. 2021;80(3):214-224
Conflict of Interest
None

Table

Brain hypoperfusion and systemic inflammatory markers (endothelial dysfunction and paltelet activation)		
	With depressive symptoms	Without depressive symptoms
Global brain	ICAM r: -0,6263 p=0.0094	all ns
Global Cortex	ICAM r: -0,6264 p=0.0094	
Prefrontal bilateral cortex	ICAM r: -0,5793 p=0.0187 P-selectina r: 0,5792 p=0.029	
Left Prefrontal	ICAM r: -0,5670 p=0.0220	
Right Prefrontal	ICAM r: -0,5831 p=0.0177 P-selectina r: 0,8592 p=0.0132	
Cingulate cortex	ICAM r: -0,6297 p=0.0089	

O32

Radiosynoviorthesis with Erbium-169 Following Surgery for Ankle Pigmented villonodular synovitis: A Rare Disease Series with more than 5 Year Follow-Up

Prof. Ioannis Iakovou[1], MD Evanthia Giannoula[1], MD Paraskevi Exadaktylou[1], MD Efthalia Gatzouli[1], MD Panos Charalambous[1], MD Kyriaki Papadopoulou[1], MD Agni Tsangaridi[1], Prof Argyrios Doumas[1], Prof Christos Sachpekidis[2]
[1]Aristotle University of Thessaloniki, Thessaloniki, Greece, [2]German Cancer Research Center, Heidelberg, Germany

Oral Presentations 3: Cardiology, Infection and Inflammation, Arsenal Room, February 14, 2026, 14:00 - 16:00

Background / Aims: Pigmented villonodular synovitis (PVNS) of the ankle is a rare, aggressive synovial disorder characterized by local proliferation and a high risk of recurrence after surgical excision. Radiosynoviorthesis (RSO) with erbium-169 (169Er) is well-established for inflammatory joint conditions but has not been widely studied in proliferative synovial tumors such as PVNS.
Objective: To evaluate the long-term efficacy and safety of adjuvant 169Er-RSO following surgical excision of ankle PVNS in young, physically active individuals.
Methods: Between January 2015 and June 2024, 27 athletes (aged 19–36) with histologically confirmed ankle PVNS underwent surgical excision—22 arthroscopically and 5 via open surgery—followed by intra-articular administration of 169Er-RSO. Clinical outcomes were assessed using the Foot Function Index (FFI) and the Visual Analog Scale (VAS) for pain. Patients were followed prospectively for a median of 63 months (range 12–125), with final evaluation in June 2025.
Results: All patients reported sustained pain relief and full functional recovery. Median FFI improved from 77% (pre-treatment) to 0.5% (post-treatment). Median VAS decreased from 4 to 0.
No recurrences or major complications were observed.
All five open-surgery patients reported a final VAS of 1. Among patients over 30 years old at final follow-up (n = 16), four reported a VAS increase from 0 to 1, attributed to early degenerative changes rather than PVNS recurrence.
Conclusions: Adjuvant 169Er-RSO following surgery appears to be a durable, safe, and effective strategy for managing ankle PVNS, with no disease recurrence over extended follow-up. These findings support expanding the role of 169Er beyond inflammatory arthritis, demonstrating its potential in rare, locally aggressive synovial disorders and reinforcing the importance of multidisciplinary treatment approaches.

Conflict of Interest
none

Table

Patient No	date of rso	Gender	Age	Age @ 6/25	Sport	Time between Synovectomy and RSO	Side-Effects	Duration of Follow-Up (6/2025)	FFI pre rso	FFI 6/25	Duration of Follow-Up (6/2025)	VAS Score Pre-RSO	VAS Score at 3 Months	VAS Score at 6 Months	VAS Score at 12 Months	VAS Score Minimum Follow-Up: 3 yrs	VAS Score on 6/2025
1	Jan-15	M	36	46	volleyball	5 months	None	125	0,77	0,005	125	3	1	0	0	0	1
2	Apr-15	M	32	42	football (soccer)	3 months	Pain, edema (3 weeks)	122	0,85	0,060	122	7	6	2	1	1	1
3	Jul-15	F	25	34	track and field	3 months	None	119	0,73	0,005	119	4	3	1	1	1	1
4	Oct-15	F	20	29	rhythmic gymnastics	3 months	None	116	0,85	0,005	116	5	1	1	0	0	0
5	Jun-16	F	28	37	track and field	4 months	None	108	0,71	0,005	113	4	1	0	1	0	1
6	Feb-17	F	20	28	rhythmic gymnastics	3 months	Pain, edema (3 wks)	100	0,77	0,000	100	4	2	2	1	1	1
7	Sep-17	F	25	32	jogging	3 months	none	93	0,71	0,005	93	3	1	0	0	0	0
8	Jun-18	F	36	43	jogging	2 months	none	84	0,85	0,060	84	7	5	2	1	1	1
9	Dec-18	M	28	34	track and field	4 months	Pain (2 wks)	78	0,77	0,005	79	5	1	0	0	0	0
10	Mar-19	F	32	38	cycling	3 months	none	75	0,77	0,005	75	4	1	0	0	0	0
11	Dec-19	M	19	34	rhythmic gymnastics	3 months	none	66	0,71	0,000	66	3	1	0	0	0	0
12	May-20	F	24	29	soccer	3 months	Pain, edema 3wks	61	0,71	0,000	61	4	1	1	0	0	0
13	Nov-20	F	19	23	rhythmic gymnastics	3 months	none	55	0,71	0,000	55	3	1	0	0	0	0
14	Dec-20	M	36	40	volleyball	5 months	None	54	0,77	0,005	54	3	1	0	0	0	1
15	Apr-21	M	32	36	football (soccer)	3 months	Pain, edema (3 wks)	50	0,85	0,060	50	7	6	2	1	1	1
16	Jul-21	F	25	28	track and field	3 months	None	47	0,73	0,005	47	4	3	1	1	1	1
17	Sep-21	M	35	38	jogging	4 months	Pain 3wks	45	0,71	0,005	45	4	2	1	1	1	1
18	Oct-21	F	20	23	rhythmic gymnastics	3 months	None	44	0,85	0,005	44	5	1	1	0	0	0
19	Nov-21	F	22	25	rhythmic gymnastics	3 months	none	43	0,73	0,005	43	4	3	1	0	0	0
20	Dec-21	M	24	27	football (soccer)	3 months	none	42	0,77	0,005	42	3	1	0	0	0	0
21	Mar-21	F	35	39	track and field	4 months	Pain (2 wks)	39	0,85	0,005	50	7	7	1	1	1	1
22	Jun-22	F	28	31	track and field	4 months	None	36	0,71	0,005	36	4	1	0	1	0	0
23	Feb-23	F	19	21	rhythmic gymnastics	3 months	none	28	0,85	0,005	28	5	1	1	0	0	0
24	Jun-23	F	25	27	track and field	3 months	none	24	0,73	0,005	24	4	3	1	1	0	1
25	Dec-23	M	35	36	track and field	3 months	Pain 3wks	18	0,77	0,000	18	3	1	0	0		0
26	Apr-24	F	27	28	cycling	5 months	Pain edema 3wks	14	0,71	0,060	14	4	3	2	1		1
27	Jun-24	M	31	32	jogging	2 months	none	12	0,85	0,060	12	7	6	2	1		1

O33

Deep-learning-based positron range correction (PRC) for Rb-82 cardiac PET

Dr. Yifan Zheng[1], Nerea Encina-Baranda[2], **Dr. Jorge Cabello**, Maurizio Conti[1], Joaquin López Herraiz[2]
[1]Siemens Medical Solutions USA, Inc., Knoxville, United States, [2]Nuclear Physics Group and IPARCOS, University Complutense of Madrid (IdISSC), Madrid, Spain

Oral Presentations 3: Cardiology, Infection and Inflammation, Arsenal Room, February 14, 2026, 14:00 - 16:00

Background: Positron range (PR) describes the distance traveled by a positron in tissue prior to annihilation, introducing image blurring and degrading spatial resolution in Positron Emission Tomography (PET). The effect is particularly pronounced in Rb-82 cardiac imaging, as its high-energy positrons exhibit long ranges in tissue. Conventional positron range correction (PRC) approaches, such as analytical or deconvolution-based methods, are either limited by isotropic assumptions or high computational cost, restricting their clinical utility. Deep learning (DL) methods have emerged as promising alternatives, offering improved computational efficiency while better capturing the anisotropic nature of positron transport.
Methods: We propose a DL-based PRC framework tailored for Rb-82 cardiac PET imaging. The network was trained using GATE Monte Carlo simulations derived from 20 clinical N-13 ammonia PET/CT studies acquired on the Biograph Vision PET/CT scanner, including both rest and stress conditions. For each patient, Rb-82 images were simulated from the measured N-13 source distributions (which can be effectively considered free of PR effects). The simulated Rb-82 images served as the input and the clinical N-13 images as the target in the supervised training of a DL model that learns the transformation from PR-blurred Rb-82 images to their corrected N-13 counterparts.
Results: The results demonstrate that the proposed method effectively restores myocardial structures and improves spatial resolution while preserving noise characteristics. As shown in Figure 1, representative coronal and transverse slices show that the network output closely reproduces the N-13 ground truth distribution. Line profile analysis further confirms the recovery of myocardium activity, where the corrected images align well with the N-13 target and outperform the uncorrected Rb-82 input.
Conclusions: The deep-learning-based PRC recovers spatial resolution in Rb-82 cardiac imaging without compromising quantitative fidelity and texture properties, highlighting the clinical relevance of DL-based PRC as a practical post-processing solution for Rb-82 cardiac PET imaging.

Conflict of Interest
Yifan Zheng, Jorge Cabello, and Maurizio Conti are employees of Siemens Healthineers. All other authors declare no conflicts of interest.

Graphic

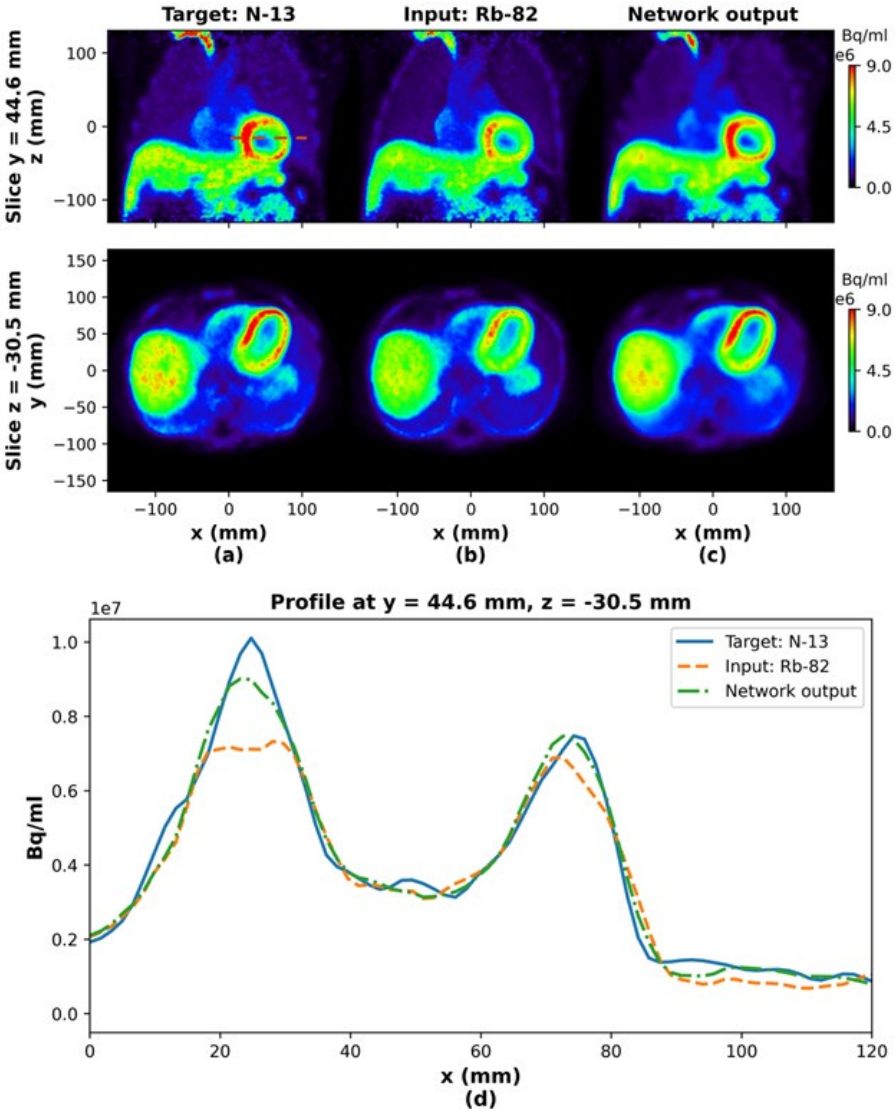
Target: N-13
Input: Rb-82
Network output
Slice y = 44.6 mm
z (mm)
Slice z = -30.5 mm
y (mm)
Bq/ml
e6
9.0
4.5
0.0
x (mm)
(a)
(b)
(c)
Profile at y = 44.6 mm, z = -30.5 mm
1e7
Target: N-13
Input: Rb-82
Network output
Bq/ml
x (mm)
(d)

O34

Analysis of the Prognostic Value of Myocardial Perfusion Imaging – SPECT/CT Stratified by the AHA/ASCN 2021 Risk Algorithm

Dr. Sebastián Rojas Lara[1]
[1]Fundación Universitaria Sanitas, BOGOTÁ, D.C., Colombia

Oral Presentations 3: Cardiology, Infection and Inflammation, Arsenal Room, February 14, 2026, 14:00 - 16:00

Background: Coronary artery disease (CAD) remains the leading cause of death worldwide. Myocardial perfusion imaging (MPI) using SPECT/CT is a non-invasive diagnostic tool that evaluates myocardial blood flow and has significant prognostic value. Several studies have shown that abnormal perfusion is associated with a higher risk of major adverse cardiac events (MACE). Given the growing emphasis on appropriate medical resource use, the AHA/ASCN 2021 risk stratification algorithm proposes classifying patients into risk groups to optimize clinical decision-making.
Objective: To analyze the prognostic value of myocardial perfusion imaging (MPI) SPECT/CT stratified by the AHA/ASCN 2021 risk algorithm in patients treated at Colsanitas clinics during the 2023–2024 period.
Methodology: An observational analytical study was conducted using a retrospective cohort design. Patients who underwent MPI-SPECT/CT with Tc-99m MIBI at three reference centers were included. They were classified into low, intermediate, and high-risk groups according to the AHA/ASCN 2021 algorithm. Clinical follow-up was performed over 6 to 30 months to assess the occurrence of MACE through medical record review. Hazard ratios were calculated for each outcome.
Preliminary Results: Out of 16,729 studies performed, 240 patients showed abnormal perfusion. Of these, 77% were classified as high risk, 14% as intermediate risk, and 9% as low risk. The high-risk group had significantly higher rates of death (11.3% vs. 2.6% at intermediate risk and 1.3% at low risk; hazard ratio: 2.1; $P = 0.04$), cardiac death (21.8%), myocardial infarction (16.7%), revascularization (23.7%), and cerebrovascular events (4.7%), with hazard ratios ranging from 2.1 to 4.1 ($p < 0.05$).
Discussion: The results validate the AHA/ASCN 2021 algorithm as an effective tool for identifying patients at higher risk of MACE, enabling better stratification and clinical decision-making.
Conclusions: Implementing the AHA/ASCN 2021 algorithm in MPI-SPECT/CT improves cardiac event prediction, optimizes resource use, and promotes personalized, cost-effective care.

Conflict of Interest
I declare that I have no conflicts of interest and the current project has not received any financial support.

Graphic

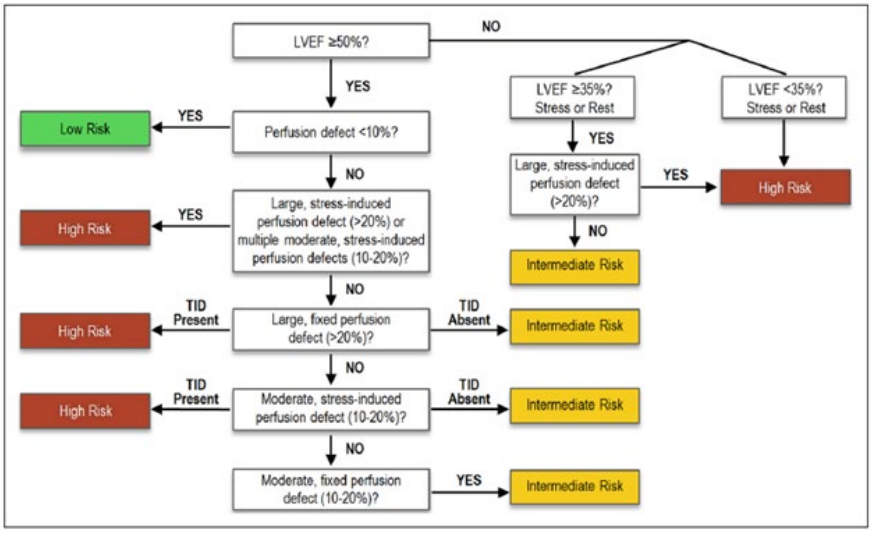

Table

Event	High Risk (%)	Intermediate Risk (%)	Low Risk (%)	Hazard Ratio	P-value
Death	11.3	2.6	1.3	2.1	0.04
Cardiac Death	21.8	3.3	2.6	2.3	0.01
Myocardial Infarction	16.7	9.7	1.7	2.7	0.05
Revascularization	23.7	2.7	2.3	4.1	<0.011
Cerebrovascular Event	4.7	7.2	3.2	4.1	<0.02

O35

Towards a new classification of therapeutic response in IgG4-related disease: A cluster approach based on 18F-FDG PET/CT

Dr. Miguel Angel Corza Ayala[1], Dr Rodrigo Hernandez Ramírez[1], Dr Joel Vargas Ahumada[1], Dr Eduardo Martín Nares[1], Dra Gabriela Aurora Hernández Molina[1], Dr Juan Pablo Chávez Torres[1]
[1]Instituto Nacional De Ciencias Médicas Y Nutrición Salvador Zubirán, Mexico CIty, Mexico

Oral Presentations 3: Cardiology, Infection and Inflammation, Arsenal Room, February 14, 2026, 14:00 - 16:00

Background/Objectives: IgG4-related disease (IgG4-RD) is a chronic systemic fibroinflammatory disease characterized by systemic and immune-mediated involvement [1]. Although 18F-FDG PET/CT is a useful tool for evaluating lesions, there is no standardized classification for assessing the response disease [2],[3],[4].
Objective: To establish a new classification of therapeutic response in IgG4-related disease using a cluster approach with 18F-FDG PET/CT.
Methods: The research protocol was approved by the institutional review committee. No financial support was provided.
This was an observational, descriptive, longitudinal, retrospective study. Inclusion: Patients with IgG4-RD, two 18F-FDG PET/CT studies, and IgG4 levels from January 1, 2017 to July 1, 2025.
The Shapiro-Wilk, Mann-Whitney U, and Chi-square tests were used. Similar response patterns (with number of affected organs and SUVmax) were identified by hierarchical cluster analysis (Ward's method) with a dendrogram and K-means for patient assignment. Analysis of variance (ANOVA) was used to evaluate differences between the identified groups. SPSS v26 software was used.
Results: Thirty-three patients were included: 20 men and 13 women, with a mean age of 51.7 years. The most common phenotype was Mikulicz disease (48.5%). A significant association was found between metabolic response (SUVmax) and the number of affected organs ($p<0.05$); there was no association between IgG4 response and the number of affected organs ($p>0.05$).
Cluster analysis identified three distinct groups (Table 1). ANOVA confirmed that these groups were biologically significant in terms of metabolic intensity ($p<0.05$), but not in terms of disease extent ($p>0.05$).
Conclusions: Treatment response is not a uniform phenomenon, but can be grouped into distinct profiles. The findings confirm that metabolic intensity (SUVmax) is the main factor distinguishing patients with a favorable response from those with disease progression. A new system for assessing treatment response is proposed. This knowledge is crucial for guiding future treatment strategies and defining more precise risk profiles.

References
[1] F. A. G. Pinheiro, I. A. Pereira, A. W. S. de Souza, H. A. M. Giardini, and R. A. Cordeiro, "IgG4-related disease—rare but you should not forget it," Advances in Rheumatology, vol. 64, no. 1, p. 35, 2024, doi: 10.1186/s42358-024-00374-y.
[2] L. Peng et al., "The development and initial validation of IgG4-related disease damage index: a consensus report from Chinese IgG4-RD Consortium," RMD Open, vol. 10, no. 1, p. e003938, Mar. 2024, doi: 10.1136/rmdopen-2023-003938.
[3] C. Y. L. Tang, W. M. Chua, L. T. J. Cheng, W. Fong, S. Zaheer, and W. W.-C. Lam, "18F-FDG PET/CT Manifestations of IgG4-related Disease," British Journal of Radiology, vol. 94, no. 1124, p. 20210105, Aug. 2021, doi: 10.1259/bjr.20210105.
[4] S. S. Hedgire, S. McDermott, D. Borczuk, A. Elmi, S. Saini, and M. G. Harisinghani, "The Spectrum of IgG4-Related Disease in the Abdomen and Pelvis," American Journal of Roentgenology, vol. 201, no. 1, pp. 14–22, Jun. 2013, doi: 10.2214/AJR.12.9995.

Conflict of Interest
No conflicts of interest to declare

Graphic

Figure 1. Examples of ER-IgG4 PET/CT ^{18}F-FDG evaluation.

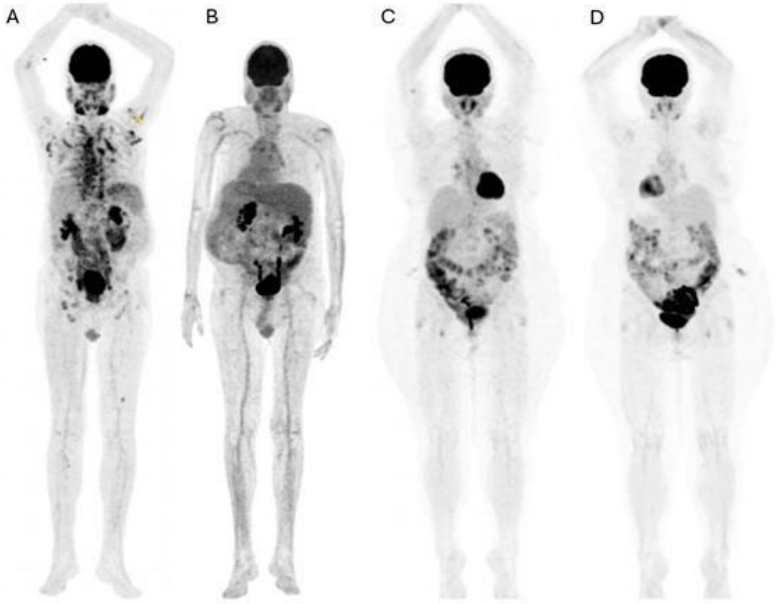

A/B) Favorable response: a 58-year-old male patient with Mikulicz/systemic phenotype who presented decreased anatomical activity in 8 sites and a decreased IgG4 level of 65% (3807-1328 mg/dL) and a 51% decrease in SUVmax. **C/D) Stable disease:** 52-year-old female patient with Mikulicz/systemic phenotype, the same sites of metabolic activity persisted and presented a decrease in IgG4 levels of 82% (188-33.20 mg/dL) and a 1.6% decrease in SUVmax. The difference between each PET/CT was 6 months.

Table

Table 1. 18F-FDG PET/CT assessment criteria in IgG4-ER

Response	Description	N=33 Patients (%)	Mean change in SUVmax	Mean change in number of lesions
Favorable response	Reduction of lesions (>1) and decrease in metabolic activity (SUVmax<50%)	11 (33.3%)	Mean -72.14% (SD 23.0)	Mean -2.73% (SD 2.33)
Stable disease	Stable lesions (±1) without significant changes in metabolic activity (SUVmax <50%)	6 (18.2%)	Mean -13.99% (SD 16.40)	Mean -0.38% (SD 0.62)
Metabolic progression	Stable lesions (±1) with significant increase in metabolic activity (SUVmax >50%)	16 (48.5%)	Mean +69.08% (SD 21.08)	Mean -0.80% (SD 1.1)
Other response profiles	Patients with atypical or mixed responses, such as metabolic progression without anatomical extension, or metabolic remission with progression of extension.	Classification proposed to cover atypical or mixed scenarios.		

O36

[99mTc]Tc-iFAP SPECT/CT as a new radiotracer for the evaluation of lesions in IgG4-related disease: Comparison with 18F-FDG PET/CT

Dr. Miguel Angel Corza Ayala[1], Dr. Rodrigo Hernández Ramírez[1], Dr. Joel Eduardo Vargas Ahumada[1], Dr. Eduardo Marín Nares[1], Dra. Gabriela Aurora Hernández[1], Dr. Juan Pablo Chávez Torres[1], Dra Myrna Luna Gutierrez[2], Dr. Sebastián Salvador Medina Ornelas[1], Dr. Daniel Carrillo Vázquez[1], Dra. Abigail Arriaga Contreras[1]
[1]Instituto Nacional de Ciencias Médicas y Nutrición Salvador Zubirán, Mexico CIty, Mexico, [2]Instituto Nacional de Investigaciónes Nucleares, Mexico CIty, Mexico CIty

Oral Presentations 3: Cardiology, Infection and Inflammation, Arsenal Room, February 14, 2026, 14:00 - 16:00

Background/Objectives:IgG4-related disease (IgG4RD) is a chronic systemic fibroinflammatory disease characterized by systemic and immune-mediated involvement [1]. Although 18F-FDG PET/CT is a useful tool for assessing lesions [2],[3], it does not distinguish between fibrosis and inflammation. In IgG4RD, fibroblasts overexpress fibroblast-activating protein (FAP); FAP inhibitor-related markers (FAPi), which are potentially useful [4].
Objective: To compare the lesion detection rate on [99mTc]Tc-iFAP SPECT/CT with 18F-FDG PET/CT in the initial evaluation, recurrence, and response to treatment.
Methods: The research protocol was approved by the institutional ethics, research, and biosafety committee. No financial support was provided.
Prospective, comparative cohort study. Patients with IgG4-ER who underwent 18F-FDG PET/CT and consented to an extension study with [99mTc]Tc-iFAP SPECT/CT from January 1, 2015, to September 1, 2025, were included.
The number and sites of lesions detected by each method were analyzed. Statistical tests were used to determine a significant difference in the detection rate, and Bland-Altman and the Intercalase Comparison Coefficient were used to determine the agreement between the two measurements. SPSS v26 software was used.
Results: Fifteen patients were included. The most common phenotype was Mikulicz disease (57%). No statistically significant differences were found between the two studies (McNemar $p>0.05$), and good agreement was found between the two studies, with a very good ICC (0.9). Using [99mTc]Tc-iFAP, lesions with little or no 18F-FDG uptake were identified.
Conclusions: This study demonstrated that the use of the [99mTc]Tc-iFAP radiopharmaceutical using SPECT/CT is a reliable tool for evaluating ER-IgG4 lesions. Adequate concordance with standard 18F-FDG PET/CT was found, and in some cases, the new radiopharmaceutical demonstrated diagnostic superiority. These findings are relevant for more detailed molecular analysis and suggest its potential as a substitute for or complement to PET/CT.

References
[1] F. A. G. Pinheiro, I. A. Pereira, A. W. S. de Souza, H. A. M. Giardini, and R. A. Cordeiro, "IgG4-related disease—rare but you should not forget it," Advances in Rheumatology, vol. 64, no. 1, p. 35, 2024, doi: 10.1186/s42358-024-00374-y.
[2] L. Peng et al., "The development and initial validation of IgG4-related disease damage index: a consensus report from Chinese IgG4-RD Consortium," RMD Open, vol. 10, no. 1, p. e003938, Mar. 2024, doi: 10.1136/rmdopen-2023-003938.
[3] C. Y. L. Tang, W. M. Chua, L. T. J. Cheng, W. Fong, S. Zaheer, and W. W.-C. Lam, "18F-FDG PET/CT Manifestations of IgG4-related Disease," British Journal of Radiology, vol. 94, no. 1124, p. 20210105, Aug. 2021, doi: 10.1259/bjr.20210105.
[4] Boschi A, Urso L, Uccelli L, Martini P, Filippi L. 99mTc-labeled FAPI compounds for cancer and inflammation: from radiochemistry to the first clinical applications. EJNMMI Radiopharm Chem [Internet]. 2024;9(1):36. https://doi.org/10.1186/s41181-024-00264-0

Conflict of Interest
No conflict of interest to declare

Graphic

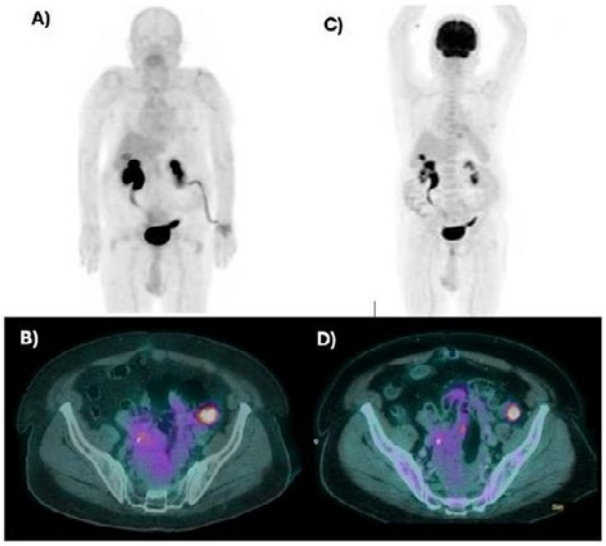

A 79-year-old male patient was diagnosed with IgG4-ER. A/B) [99mTc]Tc-iFAP SPECT/CT identified presacral solid tissue that extends and loses the interface between the common iliac vessels, distal ureters, the middle and upper third of the rectum, as well as the distal portion of the sigmoid colon, which presents greater uptake intensity than the 18F-FDG PET/CT images (C/D).

O37

Nitrate-enhanced technetium-99m-sestamibi single photon emission tomography for myocardial viability assessment: eleven-year single center experience

Dr. Eduardo Lischinsky[1], Dr. Mauricio Basantes[1], Dr. Manuel Román[1], Dr. Gerardo Dos Santos[1], PhD MD Omar Alonso[1]
[1]CMNIM, Hospital De Clínicas "Dr. Manuel Quintela" - Universidad De La República, Montevideo, Uruguay

Oral Presentations 3: Cardiology, Infection and Inflammation, Arsenal Room, February 14, 2026, 14:00 - 16:00

Background/Objectives: While fluorine-18 fluorodeoxyglucose positron emission tomography (18F-FDG PET/CT) remains the gold standard for myocardial viability assessment, nitrate-enhanced technetium-99m-sestamibi single photon emission computed tomography (SPECT) offers a widely accessible alternative in settings where positron emission tomography is unavailable or cost-prohibitive. Despite documented effectiveness, real-world clinical experience with this technique remains underreported. This study aimed to evaluate our institution's experience with nitrate-enhanced sestamibi imaging for myocardial viability detection.
Methods: Following institutional ethics committee approval, we conducted a retrospective analysis of 29 consecutive patients who underwent nitrate-enhanced technetium-99m-sestamibi SPECT viability assessment between 2009-2019 at a university hospital nuclear medicine center. The standardized protocol consisted of stress/rest SPECT followed by nitrate protocol on a separate day (1-5 day interval). Viability was defined as improved tracer uptake in previously fixed defects reported as infarct territory. The 20-segment model endorsed by ASNC (American Society of Nuclear Cardiology) was used. Viability grading was performed qualitatively.
Results: Myocardial viability was detected in 18 of 29 patients (62.1%). Territorial distribution showed higher frequency in anterior territory (55.6%), followed by septal (44.4%), inferior (44.4%), lateral (33.3%) and apical (16.7%). Qualitative grading showed mild viability (61.1%), moderate (22.2%) and extensive (16.7%). Nitrate protocol allowed identification of viable segments not detected in baseline study, demonstrating its utility for differentiation between hibernating myocardium and scar tissue.
Conclusions: This single-center experience demonstrates that nitrate-enhanced sestamibi SPECT yields viability detection rates consistent with published international studies (58-65% range). The technique showed reliable performance across multiple myocardial territories with comprehensive regional distribution. Our findings suggest the continued clinical utility of nitrate-enhanced sestamibi as a practical alternative when 18F-FDG PET/CT is not available, providing valuable diagnostic information for guiding revascularization decisions in patients with ischemic cardiomyopathy.

Conflict of Interest
No conflict of interest

Graphic

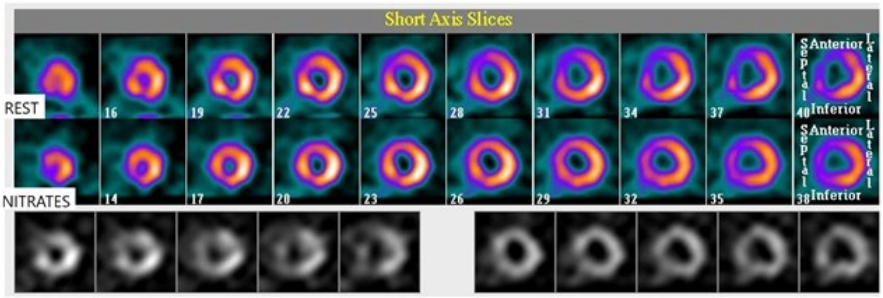

Figure 1. Female patient from the cohort who presented significant viability in the lower segments of the anteroseptal region using nitrate-enhanced ^{99m}Tc-MIBI SPECT.

Table

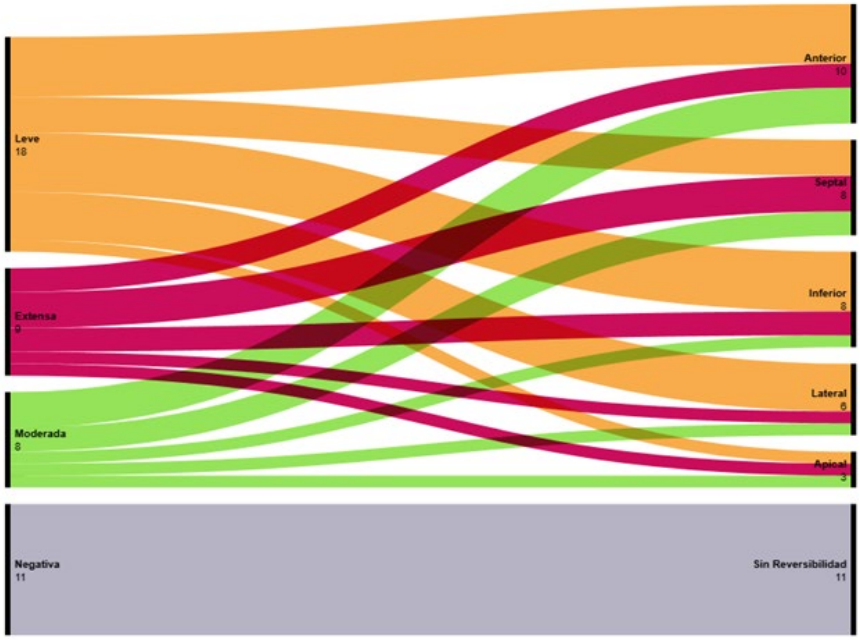

O38

Myocardial perfusion patterns and ventricular function in patients with chagas disease, analysis at a regional reference center in eastern colombia

Dr. Marvin Holman Anderson Achicanoy Botina[1], Ivan Camilo Ospina Florez[1], Jose Fernando Silva Llanos[1], Cesar Augusto Garcia Quintanilla[1,2], Lizeth Catherine Rodriguez Corredor[3]
[1]Nuclear Medicine Postgraduate Program - Universidad Autónoma De Bucaramanga (UNAB), Bucaramanga, Colombia, [2]SPECT Medicina Nuclear S.A.S., Bucaramanga, Colombia, [3]Faculty of Health Sciences - Universidad Autónoma De Bucaramanga (UNAB), Bucaramanga, Colombia

Oral Presentations 3: Cardiology, Infection and Inflammation, Arsenal Room, February 14, 2026, 14:00 - 16:00

Background/Aims: To evaluate the association between imaging patterns, functional parameters, and clinical variables in patients with Chagas disease undergoing myocardial perfusion gated-SPECT between January 2020 and August 2025.
Methods: A cross-sectional study was conducted in 34 patients with Chagas disease and symptoms suggestive of cardiovascular involvement, recording clinical, imaging, and functional data. Descriptive analysis calculated absolute and relative frequencies, means, and standard deviations. Bivariate analysis employed Fisher-exact test and Mann-Whitney U test, adopting $p<0.05$ as the significance threshold.
Results: The main characteristics of the cohort are shown in the accompanying table; the mean summed difference score was 1.3±2.7 and the transient ischemic dilatation index was 0.99±0.16, with inferior, inferolateral, and apical walls most frequently involved (50.0%, 41.2%, and 32.4%). Resting and stress left ventricular ejection fraction were 57.1±17.9 and 55.6±18.0, respectively, with a decrease of at least five-percentage points in half of the patients; global hypokinesia occurred in 23.5% and frequent ventricular extrasystoles in 8.8%; while 61.1% of those with wall thickening abnormalities (n=18) improved under stress. Significant differences were found between perfusion defects and their location (apex, inferior, inferolateral, and anterolateral; p=0.001). No significant differences were observed in wall-thickening response by stress modality (p=0.280), although 72.7% of those who improved had received pharmacologic stress. Higher summed difference score was associated with lower stress left ventricular ejection fraction (≤1: 61.8±14.2; ≥7: 21.5±12.0; p=0.014) and with greater end diastolic (p=0.002) and end systolic (p=0.0001) volumes.
Conclusions: Greater perfusion defect severity is directly associated with left ventricular systolic dysfunction and volumetric compromise. Predominant inferior, inferolateral, and apical involvement reflecting the characteristic pattern[1-2]; the observed reduction in ejection fraction under stress in half of the cohort indicates impaired contractile reserve[3], whereas improvement in global wall thickening in most abnormal cases suggests myocardial viability[4]. Gated-SPECT is a useful tool for evaluation in this population.

References

1. Regueiro A, García-Álvarez A, Sitges M, Ortiz-Pérez JT, De Caralt MT, Pinazo MJ, Posada E, Heras M, Gascón J, Sanz G. Myocardial involvement in Chagas disease: insights from cardiac magnetic resonance. Int J Cardiol. 2013 Apr 30;165(1):107-12. doi:10.1016/j.ijcard.2011.07.089. Epub 2011 Sep 9. PMID:21907431.
2. Barbosa MM, Costa Rocha MO, Vidigal DF, Bicalho Carneiro Rde C, Araújo RD, Palma MC, Lins de Barros MV, Nunes MC. Early detection of left ventricular contractility abnormalities by two-dimensional speckle tracking strain in Chagas' disease. Echocardiography. 2014 May;31(5):623-30. doi:10.1111/echo.12426. PMID:25232573.
3. Ciampi Q, Villari B. Role of echocardiography in diagnosis and risk stratification in heart failure with left ventricular systolic dysfunction. Cardiovasc Ultrasound. 2007 Oct 2;5:34. doi:10.1186/1476-7120-5-34. PMID:17910744; PMCID:PMC2064911.
4. Zhang F, Wang J, Shao X, Yang M, Qian Y, Yang X, Wu Z, Li S, Xin W, Shi Y, Liu B, Yu W, He Z, Zhou W, Wang Y. Incremental value of myocardial wall motion and thickening to perfusion alone by gated SPECT myocardial perfusion imaging for viability assessment in patients with ischemic heart failure. J Nucl Cardiol. 2021 Dec;28(6):2545-56. doi:10.1007/s12350-020-02040-4. Epub 2020 Feb 14. PMID:32060856; PMCID:PMC10961704.

Conflict of Interest

None of the authors reported any conflicts of interests.

Table

Variable	Mean	Std. dev.
Age (years)	67.1	10.9
	Freq	**Percent**
Sex		
Female	16	47.1
Male	18	52.9
Stress modality		
Ergometric (Exercise)	15	44.1
Pharmacologic (Dipyridamole)	19	55.9
Reported symptoms		
Asymptomatic	8	23.5
Dyspnea	12	35.3
Chest pain	12	35.3
Chest pain + dyspnea	1	2.9
Palpitations	1	2.9
Perfusion defects		
None	14	41.2
Fixed	7	20.6
Reversible	1	2.9
Mixed	12	35.3
Summed Difference Score (SDS)		
≤1	23	67.6
2-4	6	17.6
5-6	3	8.8
≥7	2	5.9
Transient Ischemic Dilatation index (TID)		
≥1.2	2	5.9
<1.2	32	94.1
LVEF classification		
Severely reduced (<35%)	5	14.7
Moderately reduced (35-45%)	2	5.9
Mildly reduced (46-49%)	4	11.8
Low normal (50-55%)	5	14.7
Normal (56-69%)	8	23.5
Hyperdynamic (≥70%)	10	29.4
LVEF drop ≥5%		
No	17	50.0
Yes	17	50.0
Global wall thickening (stress)		
No change	17	50.0
Worsens	6	17.6
Improves	11	32.4
Left ventricle dilatation		
No	20	58.8
Yes	14	41.2
Hypertrophy changes		
None	20	58.8
Global	6	17.6
Segmental	8	23.5
Right ventricle uptake		
Not Visible	13	38.2
Visible	21	61.8
Defect extent		
≤9%	1	5.0
10-19%	5	25.0
20-39%	8	40.0
≥40%	6	30.0

Main characteristics of the population studied.
LVEF (Left ventricle ejection fraction)

O39

Assessment of CCR2-Related Inflammatory Activity in Abdominal Aortic Aneurysms with 99mTc-HYNIC-CCR2-L and SPECT/CT

Dr. Jorge Rodríguez[1], Dr Javier Anaya Ayala, Dr Joel Eduardo Vargas Ahumada, Dr Rodrigo Hernandez Ramirez, Dr Felipe de Jesús Rodríguez Hernández
[1]Instituto Nacional de Ciencias Médicas y Nutrición, Mexico City, Mexico

Oral Presentations 3: Cardiology, Infection and Inflammation, Arsenal Room, February 14, 2026, 14:00 - 16:00

Introduction: Histological studies of abdominal aortic aneurysms (AAA) demonstrate mural neovascularization and macrophage infiltration; however, the pathophysiology of AAA remains incompletely understood.
Objective: To evaluate the expression of C-C chemokine receptor type 2 (CCR2) in AAA using single-photon emission computed tomography (SPECT/CT) with the radiotracer 99mTc-HYNIC-CCR2-L.
Methods: We prospectively included patients with atherosclerotic, asymptomatic AAA and a history of smoking. Patients with a known family history of aortic aneurysmal disease were excluded. SPECT/CT imaging was performed after injection of 99mTc-HYNIC-CCR2-L. Regions of interest (ROIs) were drawn on the aneurysmal wall, left ventricular blood pool (LV), and gluteal muscle (GM). Target-to-background ratios (TBR) were calculated using LV and GM as background references to quantify focal tracer uptake in the aneurysm wall. Figure 1.
Results: Nine patients were included. Patients with focal uptake showed significantly higher TBR values compared to those without focal uptake (LV-TBR: median 1.59 vs 1.08, p = 0.016; GM-TBR: median 2.56 vs 1.18, p = 0.016) Table1 .
Conclusion: 99mTc-HYNIC-CCR2-L SPECT/CT demonstrated increased CCR2-mediated inflammatory activity in the aneurysmal wall compared to non-affected regions. This targeted molecular imaging approach may assist in evaluation of biological activity and potential risk of aneurysm progression and rupture. Larger studies comparing tracer uptake with aneurysm growth rates are needed to validate these findings.

Conflict of Interest
No conflict

Graphic

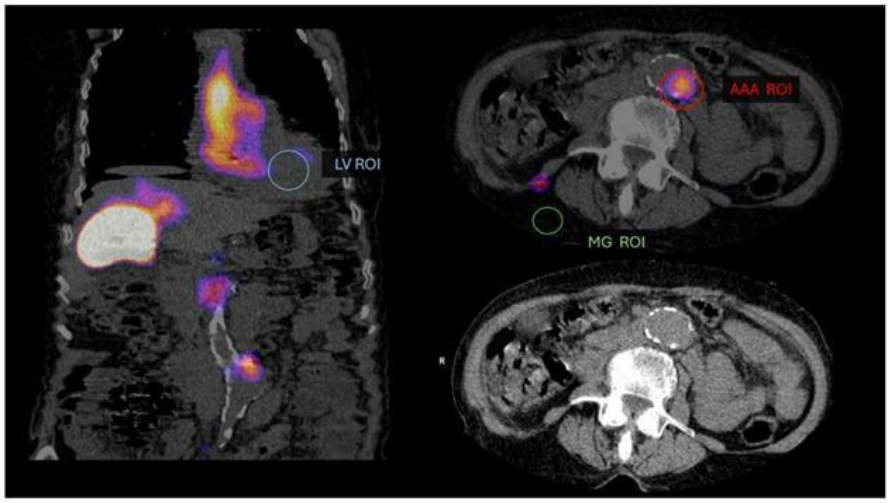

Figure 1. *Regions of interest (ROIs) delineated on SPECT/CT images. ROIs were drawn on the aneurysmal wall (red), left ventricular blood pool (LV, blue), and gluteal muscle (GM, green) to calculate target-to-background ratios (TBR).*

Table

Patient	*Focal Uptake (Y/N)*	*LV-TBR*	*MG-TBR*
1	Yes	1.56	1.99
2	Yes	2.05	2.46
3	Yes	1.54	12.6
4	Yes	1.62	2.65
5	No	1.02	1.02
6	No	1.09	1.2
7	No	1.04	1.08
8	No	1.08	1..16
9	No	1.24	1.38

Table 1. LV-TBR: target-to-background ratio using the left ventricular blood pool as reference; GM-TBR: target-to-background ratio using gluteal muscle as reference. "Focal uptake" indicates visually increased 99mTc-HYNIC-CCR2-L accumulation in the aneurysm wall on SPECT/CT. Values represent individual patient measurements.

O40

SPECT/CT with [99mTc]Tc-UBI 29-41 in challenging-to-diagnose infections: clinical concordance and impact on redefining the initial diagnosis

Dr. Hernando Andres Benavides Jimenez[1], Dr Luz Kelly Anzola Fuentes[3], Dr Viviana Andrea Daza Betancourt[1], Dr Cristian Camilo Vargas Lopez[1], Dr Sebastian Rojas Lara[1], Dr Sergio Moreno Lopez[4], Dr Carlos Alvarez Moreno[2]
[1]Fundacion Universitaria Sanitas, Bogota, Colombia, [2]Clinica Reina Sofia, Bogota, Colombia, [3]Clinica Universitaria Colombia, Bogota, Colombia, [4]Universidad Nacional de Colombia, Bogota, Colombia

Oral Presentations 3: Cardiology, Infection and Inflammation, Arsenal Room, February 14, 2026, 14:00 - 16:00

Introduction: Diagnosing complex infections remains difficult due to the limited specificity of conventional imaging and clinical assessment. The antimicrobial peptide [99mTc] Tc-UBI 29-41 binds selectively to bacterial membranes, offering a molecular approach that may enhance diagnostic accuracy and guide clinical decisions.
Objective: To evaluate the concordance between SPECT/CT with [99mTc] Tc-UBI 29-41 and the definitive clinical diagnosis (post-test) in patients with suspected complex infection.
Methods: We conducted an observational, analytical, cross-sectional study including imaging data from130 patients with suspected infection of challenging etiology. A total of 286 SPECT/CT studies with [99mTc] Tc-UBI 29-41 were performed. Concordance between the imaging-based diagnosis and the post-test clinical diagnosis was analyzed using Cohen's kappa coefficient; 95% confidence intervals (CI) were estimated by bootstrapping with 1,000 replications.
Results: Median age was 61 years (IQR: 43–72), 53.9% were women. Main clinical indications were osteomyelitis (13.3%), infected arthroplasty (10.1%), and spondylodiscitis (8.7%); additional indications included fever of unknown origin and vascular prosthesis infections. SPECT/CT with [99mTc] Tc-UBI 29-41 showed an overall agreement of 95.5% with the final clinical diagnosis (kappa: 0.89; 95% CI: 0.83–0.95). Imaging findings led to a change in the initial pre-test diagnosis in 21.7% of patients, directly influencing clinical management. Performance was consistent across osteoarticular infections, prosthetic joint infections, and spondylodiscitis, including cases with initially uncertain diagnoses.
Conclusions: SPECT/CT with [99mTc] Tc-UBI 29-41 demonstrates high concordance with the final clinical diagnosis and provides clinically relevant information that changes the diagnostic approach in about one out of five patients with suspected infection. Incorporating this technique may improve the evaluation of complex infections when standard methods are inconclusive. Larger prospective studies are warranted to strengthen the current evidence and better define its role within diagnostic algorithms for musculoskeletal and prosthetic infections.

Conflict of Interest
Conflict of interest: The authors declare no conflicts of interest.

O41

Splenic uptake in dipyridamole stress and rest tc-99m mibi spect: a potential vasodilatory marker

Dr. Paula Aristov[1], Dr. Andrés Damián[1], Dr. Rodolfo Ferrando[1], Dr. Omar Alonso[1], Dr. Federico Ferrando[1], Técnico Aldo Sanchez[1], Técnico Pablo Bracesco[1]
[1]Servicio Medicina Nuclear, Hospital De Clinicas, Montevideo, Uruguay

Oral presentations 3: Cardiology, Infection and Inflamation, Arsenal Room, February 14, 2026, 14:00 - 16:00

Background: Myocardial perfusion SPECT with pharmacological stress using dipyridamole is a valuable tool to assess the presence of ischemia. However, objectively confirming the vasodilatory response to dipyridamole remains a challenge. The splenic switch-off has been described as a marker of vasodilatory efficacy in PET and MRI, but this effect has not yet been evaluated in SPECT. Objective: To assess the presence of splenic switch-off in Tc-99m MIBI SPECT in patients with confirmed vasodilatory response. Methods Prospective, observational, and longitudinal study of patients referred for myocardial ischemia assessment. A two day protocol with dipyridamole (0.56 mg/kg) and rest conditions followed by the endovenous injection of Tc-99m MIBI was performed. Static abdominal images were acquired in both conditions in posterior position at 10-30 min after the Tc-99m MIBI injection, in addition to the standard myocardial perfusion SPECT at 45 min. A spleen-to-liver ratio and the Splenic Response Ratio (SRR) was quantified. Results Ten patients were recruited (5 women, 5 men; 42–81 years). All studies were indicated to rule out myocardial ischemia. Seven patients showed ischemia on perfusion SPECT, while 3 were normal. All patients presented a clinical response to dipyridamole (10 by changes in blood pressure and heart rate, and 3 by presence of ischemia). In all cases, a lower spleen-to-liver ratio was observed during pharmacological stress compared to the rest conditions. The spleen-to-liver ratio was 0.5 ± 0.1 under stress and 0.71 ± 0.16 at rest ($p<0.001$). The mean SRR was 0.71 ± 0.09 .Conclusions: The splenic switch-off can be evaluated in Tc-99m MIBI myocardial perfusion SPECT and has the potential to serve as a marker of dipyridamole-induced vasodilation. Validation in a larger cohort will confirm its value as an objective marker of vasodilatory response and optimize diagnostic interpretation, reducing false negatives.

References

[1] Bami, K., et al. Splenic switch-off as a marker of adenosine response in rubidium-82 myocardial perfusion PET/CT. Journal of Nuclear Cardiology. 2019. [2] Okada, R. D., Glover, D. K., et al. Cardiac imaging and myocardial kinetics of technetium-tertiary butyl-isonitrile during dipyridamole-induced hyperemia. Journal of the American College of Cardiology. 1988;12(5):1279-1288. [3] Henzlova, M. J., Duvall, W. L., Einstein, A. J., Travin, M. I., Verberne, H. J. ASNC imaging guidelines for SPECT nuclear cardiology procedures: Stress, protocols, and tracers. Journal of Nuclear Cardiology. 2016;23(3):606-639. [4] Slart, R. H. J. A., et al. Procedural recommendations of cardiac PET/CT imaging: Standardization by the EANM/ASNC/SNMMI. European Heart Journal – Cardiovascular Imaging. 2015;16(4):340-349. [5] Germano, G., Kavanagh, P. B., Slomka, P. J., Berman, D. S. Myocardial perfusion SPECT: Technical principles and clinical applications. Radiology. 2021;301(3):599-611.

Conflict of Interest: Declaro no tener conflictos de intereses.

O42

Cannabidiol prevents age-related cognitive decline and neuroinflammation, and enhances brain metabolism in a Down syndrome animal model

Dr. Lidia Spelta[1], Chiara Righini[1], Jean Brizola[1], Dr. Carlos Buchpiguel[1], Dr. José Alexandre Crippa[2], Dr. Daniele de Paula Faria[1]
[1]Laboratory of Nuclear Medicina, Faculty of Medicine, University of São Paulo (USP), São Paulo, Brazil, [2]Department of Neurosciences and Behavior, Faculty of Medicine from Ribeirão Preto, University of São Paulo (USP), Ribeirão Preto, Brazil

Oral Presentations 3: Cardiology, Infection and Inflammation, Arsenal Room, February 14, 2026, 14:00 - 16:00

Introduction: Individuals with Down syndrome (DS) experience premature aging due to the inherent effects of trisomy 21, which causes the overexpression of genes associated with oxidative stress, mitochondrial dysfunction and inflammatory responses. Age-related diseases are likely to manifest significantly earlier in individuals with DS than in the general population. Given the need to improve aging outcomes in DS, cannabidiol (CBD), with its anti-inflammatory and neuroprotective properties, emerges as a potential intervention. Therefore, we aimed to evaluate the effect of CBD on aging in a DS animal model using positron emission tomography (PET).
Methods: Male and female trisomic Ts65Dn mice (CEUA-1811/2022) were treated with CBD (20mg/kg, i.p.) or vehicle for 30 days, starting at 7 months of age. Longitudinal PET imaging with [^{18}F]FDG and [^{11}C]PK11195 was performed at 4, 8, 12, and 18 months to assess brain metabolism and neuroinflammation. Cognitive function was evaluated using the novel object recognition test; and immunohistochemistry for astrocytes and neurons was conducted, alongside plasma cytokine quantification.
Results: CBD prevented age-related neuroinflammation observed in the vehicle group ($p<0.0001$) and increased brain glucose metabolism ($p=0.03$). The treatment also improved short- and long-term memory at 12 ($p=0.058$ and $p=0.025$) and 18 months ($p=0.002$ and $p=0.004$) compared to vehicle. This effect was accompanied by increased hippocampal neuronal population at 18 months ($p=0.0002$), without changes in astrocytes. Plasma cytokines IL-6 ($p=0.057$), IFN-γ ($p=0.023$), and TNF-α ($p=0.03$) were elevated only in the vehicle group, at 18 months.
Conclusion: These findings suggest that CBD treatment mitigates age-related neuroinflammation. In addition, it enhances brain glucose metabolism and preserves the hippocampal neuronal population, resulting in improved cognitive performance at older ages and highlighting its potential as a therapeutic strategy to slow premature brain aging in Down syndrome.

Conflict of Interest
The authors have declared that they have no conflicts of interest.

Graphic

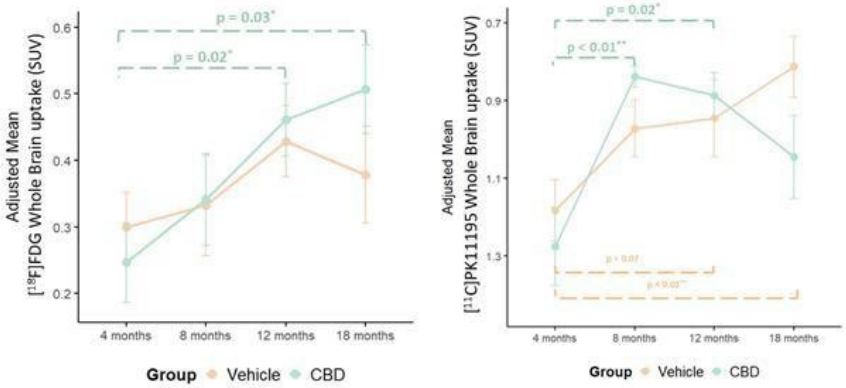
p = 0.03*
p = 0.02*
Adjusted Mean
[18F]FDG Whole Brain uptake (SUV)
0.6
0.5
0.4
0.3
0.2
4 months
8 months
12 months
18 months
Group
Vehicle
CBD
p = 0.02*
p < 0.01**
Adjusted Mean
[11C]PK11195 Whole Brain uptake (SUV)
0.7
0.9
1.1
1.3
4 months
8 months
12 months
18 months
Group
Vehicle
CBD

O43

Quantitative 99mTc-PYP SPECT/CT in ATTR-CA: head-to-head MBR, LV/bone and SUVmax with near-perfect discrimination

Mr. Luciano Santos[1], Mrs. Agustina Pérez[1,2], Mr. Pablo Roman[1,2], Mrs. Karina Bayardo[2], Mr. Federico Ferrando[1,2], Mr. Rodolfo Ferrando[1,2]
[1]Consultorio De Medicina Nuclear Ffp., Montevideo, Uruguay, [2]Centro de Medicina Nuclear e Imagenología Molecular del Hospital de Clínicas, Universidad de la República, Montevideo, Uruguay., Montevideo, Uruguay

Oral Presentations 3: Cardiology, Infection and Inflammation, Arsenal Room, February 14, 2026, 14:00 - 16:00

Background. Quantitative 99mTc-PYP SPECT/CT is increasingly used to support transthyretin cardiac amyloidosis (ATTR-CA) diagnosis, yet the relative value of raw versus normalized indices remains unclear.
Objective. To compare the diagnostic performance of quantitative metrics and their associations with clinical reference.
Methods. We included 50 consecutive patients evaluated for suspected ATTR-CA over the last 18 months. Imaging was performed at 3 h post-injection (median 166 min [IQR 128–179]). Perugini score was assigned on SPECT. LV VOIs were auto-thresholded in visually positive scans and manual segmental VOIs were drawn in negatives; the blood-pool VOI was placed in left atrium (LA); the bone VOI was automatic (spine/ribs/sternum). Metrics: SUVmax(LV); MBRmax = SUVmax(LV)/SUVmean(LA) (myocardium-to-blood); MBRmean = SUVmean(LV)/SUVmean(LA); LV/bone = SUVmean(LV)/SUVmean(bone). Reference was final diagnosis. Logistic regression: log(MBRmax) adjusted for VOI type and post-injection time. Sensitivity models tested log(SUVmax) or log(MBRmean) and VOI size. Effects are OR per SD; model AUCs with 95% CIs. AMB (absolute myocardial burden) and AMB-LA were estimated in positives with automatic LV VOIs.
Results. Of the 50 patients (79.0±7.7 years; 52% male), 17 were positive and 33 negative. Positives were older (p=0.0166), sex was similar. Diagnostic performance was excellent: MBRmax and SUVmax both had AUC 1.00 (cut-points 1.84 and 9.97); LV/bone AUC 0.986 (95% CI 0.947–1.00), cut-point 1.56, sensitivity 94.1%, specificity 100%; MBRmean AUC 0.963 (0.872–1.00), cut-point 1.26, sensitivity 94.1%, specificity 100%. Quantitative measures correlated with Perugini (MBRmax: t_b=0.64; p<0.0001). Logistic models remained near-perfect (AUC 1.00); log(MBRmax) showed OR 7.60 (6.43–8.81), unchanged after adding age; log(SUVmax) OR 11.79 (8.80–14.53). In positives, AMB-LA correlated with MBRmean (p=0.53; p=0.028).
Conclusions. Quantitative 99mTc-PYP SPECT/CT provides excellent discrimination for ATTR-CA. SUVmax and MBRmax delivered comparable, near-perfect classification; LV/bone and MBRmean were strong alternatives. Logistic regression confirmed these findings. In positives, AMB/AMB-LA added volumetric context potentially useful for therapy monitoring.

Conflict of Interest
no

Graphic

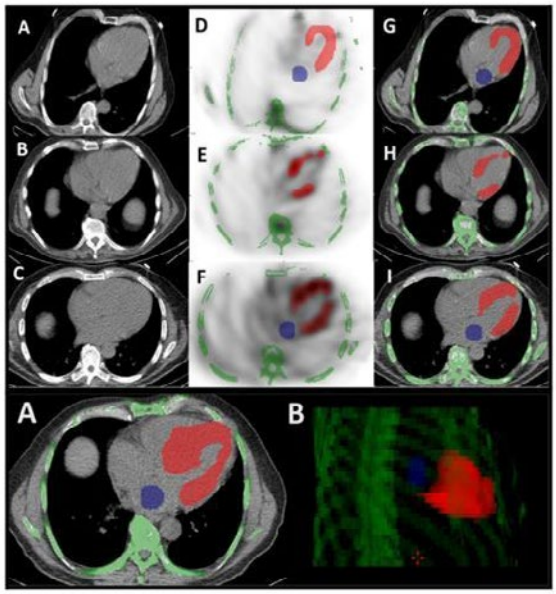

Figure 1. Visual examples and VOI methodology on quantitative ^{99m}Tc-PYP SPECT/CT.

Top row — clinical examples. For three representative patients, axial CT, SPECT, and fused SPECT/CT images are shown (left-to-right in each triplet), illustrating absent, focal high, and diffuse high myocardial tracer uptake, respectively.

Bottom row — quantification workflow. (A) Example of volumes of interest (VOIs) used for fully quantitative analysis. Left-ventricular myocardium (red), left-atrial blood pool (blue), and axial skeleton (green). VOIs for positive scans were generated automatically by thresholding; in negative scans, manual segmental LV VOIs were used. (B) 3-D reconstructions of the same VOIs. These VOIs underpin the study metrics (SUVmax, MBRmax = SUVmax(LV)/SUVmean(LA), MBRmean = SUVmean(LV)/ SUVmean(LA), and LV/bone = SUVmean(LV)/ SUVmean(Bone).

Table

Metric	AUC	95% CI	Cut-point (Youden)	Sensitivity	Specificity
SUVmax (LV)	1.00	1.00–1.00	9.97	1.00	1.00
MBRmax	1.00	1.00–1.00	1.84	1.00	1.00
LV/bone	0.986	0.947–1.00	1.56	0.941	1.00
MBRmean	0.963	0.872–1.00	1.26	0.941	1.00

Table 1. Diagnostic performance vs. final diagnosis.

O44

Myocardial perfusion imaging: When is not just supine, not just prone

Dr. Romina Lorena Romero[1], Dr. Karina Quintero[2], Dr. María del Carmen Alak[1], Dr. César Mendez[1], Lic. Hernan Policella[1], Lic. Antonio Casares[1], Lic. Macarena Montaño[1]
[1]Hospital Británico De Buenos Aires, Buenos Aires, Argentina, [2]Hospital de Pediatría Dr. Juan P. Garrahan, Buenos Aires, Argentina

Oral Presentations 3: Cardiology, Infection and Inflammation, Arsenal Room, February 14, 2026, 14:00 - 16:00

Background: Myocardial perfusion imaging is a widespread method for evaluation of coronary heart disease in routine practice. But when dextrocardia may be encountered during imaging, difficulties and artifacts during acquisition and processing may arise because of altered position and orientation of the heart. Its diagnosis in adult life is usually incidental.
Goals: Since dextrocardia is a rare clinical condition, general experience regarding acquisition,
processing, and interpretation of cardiac single photon emission computed tomography (SPECT) studies is limited.
The aim of our report is to show our experience of how from usual protocols already established, they would require modification, to prevent the emergence of artefactual defects with this group of patients.
Methods: One day rest-stress protocol was used for the 99mTc sestamibi myocardial perfusion Gated SPECT. SPECT imaging was realized by a dual head gamma camera, using 64x64 matrix and 30 projections (rest:25seconds, stress:20seconds). For ECG-gated study, camera acquisition was triggered to R-wave, 8 frames collected per R-R interval [1].
Results: It is important to review the raw data. Each patient requires careful selection of the arc of
rotation, the heart should be kept in the center of it. Image 1.Table.
Conclusions: Although Dextrocardia is a rare cardiac malposition, this group of patients may be referred to for the evaluation of myocardial perfusion imaging in nuclear medicine practice. The incidence of coronary heart disease and the life expectancy of patients with isolated dextrocardia and no other congenital cardiac abnormalities are the same as in the general population. Its importance lies in the association with other congenital pathologies which increases morbidity and mortality. Whatever the patient positioning and acquisition method used, it is essential to know the exact details of the orientation of the heart and its chambers so that correct interpretation of the images is possible.

References
1-Dorbala S, Ananthasubramaniam K, Armstrong IS, et al. Single photon emission computed tomography (SPECT) myocardial perfusion imaging guidelines: instrumentation, acquisition, processing, and interpretation. J Nucl Cardiol. 2018;25: 1784–1846
2-Arcilla RA, Gasul BM. Congenital dextrocardia: clinical, angiocardiographic, and autopsy studies on 50 patients. J Pediatr. 1961;58:251–262.
Conflict of Interest
None

Graphic

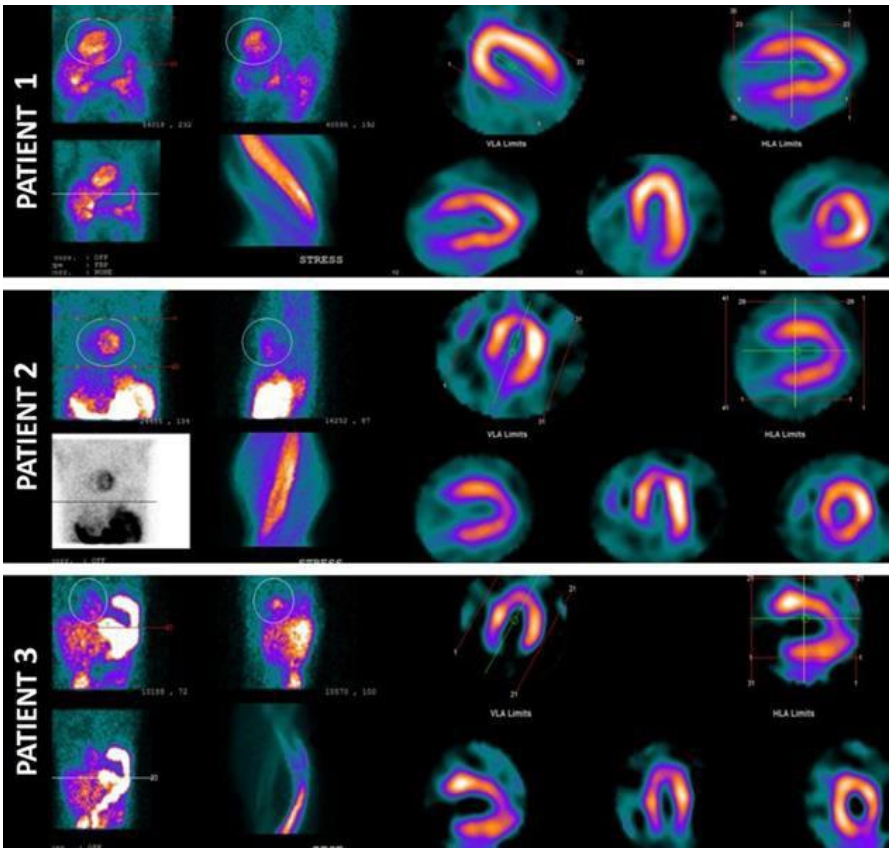

Table

VARIABLE	PATIENT 1	PATIENT 2	PATIENT 3
AGE (YEARS)	50	44	66
SEX	MALE	MALE	MALE
PRESENTATION	TYPICAL CHEST PAIN Poor acoustic window ultrasound	UNCONTROLLED HYPERTENSION, DYSLIPIDEMIA Poor acoustic window ultrasound	CARDIOVASCULAR RISK FACTORS, CONTINUE SPORTS ACTIVITY Poor acoustic window ultrasound
TYPE OF DEXTROCARDIA (Arcilla and Gasul) [2] Base to ápex axis orientation in the thorax	II COMPLETE INCIDENTAL FINDING Base-to-apex axis of the heart is pointed towards the right	IV INCIDENTAL FINDING Base-to-apex axis of the heart is pointed vertically	V LEFT PULMONARY AGENESIS Right-sided displacement, leftward orientation
SITUS INVERSUS	NO	NO	NO
PATIENT POSITIONING	FEET FIRST SUPINE	FEET FIRST SUPINE	FEET FIRST SUPINE
IMAGING ARC DURING ACQUISITION :180|DEGREES , L-MODE CIRCULAR ORBIT	CLOCKWISE 45°LEFT ANTERIOR OBLIQUE PROYECTION-135°RIGHT POSTERIOR OBLIQUE PROYECTION	COUNTERCLOCKWISE 180° RIGHT LATERAL TO LEFT LATERAL	CLOCKWISE 45°LEFT ANTERIOR OBLIQUE PROYECTION-135°RIGHT POSTERIOR OBLIQUE PROYECTION
PROCESSING SPECT	ORIENTATION WAS CORRECTED	PROCESSED AS USUAL	PROCESSED AS USUAL
PERFUSION	NORMAL	NORMAL	NORMAL
EJECTION FRACTION	59%	64%	57%

O45

Standardized Formulation of a Business Case for a PET-CT Nuclear Medicine Service in Colombia

Dr. Saule Karanauskas[1], Ingeniera Lenys Roncancio[1], Dr. María Martínez[1]
[1]Medicina Nuclear Diagnostica, Villavicencio, Colombia

Oral Presentations 3: Cardiology, Infection and Inflammation, Arsenal Room, February 14, 2026, 14:00 - 16:00

Introduction: In Colombia, the demand for PET-CT studies continues to rise as an essential diagnostic tool for oncologic and non-oncologic diseases; however, the availability of these services remains limited to main cities, generating long waiting times. Expanding Nuclear Medicine services is therefore a public health priority, yet establishing new PET-CT facilities requires not only high-cost technology but also a comprehensive evaluation of clinical, operational, regulatory, and financial aspects. A standardized process is necessary to ensure sustainable and evidence-based investment decisions.
Objective: To describe the implementation of a standardized process for developing a business case to evaluate the clinical, operational, and financial feasibility of a new PET-CT Nuclear Medicine service prior to investment.
Methods: A systematic approach was applied based on international and national best practices (IAEA, Ministry of Health, PMI). The model included regional epidemiological and demand analysis, assessment of service supply and access gaps, operational and clinical design, capital and operational cost projections (CAPEX and OPEX), financing structure, financial indicators (IRR, NPV), and regulatory risk analysis.
Results: The standardized process allowed the integration of clinical, technical, regulatory, and financial components into one document. A 10-year cash flow projection and scenario analysis (optimistic, conservative, and pessimistic) were developed to support decision-making.
Conclusion: Applying a standardized business case formulation provides a robust foundation for investment decisions, aligning the project with public health needs, regulations, and optimal resource allocation.
Keywords: Business case; Nuclear Medicine; Standardized process; Public health; Early detection; PET-CT.

References

Referencias Bibliográficas
1. Project Management Institute. (2015). The standard for business analysis. Project Management Institute.
2. Project Management Institute. (2021). A guide to the project management body of knowledge (PMBOK® guide) (7th ed.). Project Management Institute.
3. Project Management Institute. (2015). Business analysis for practitioners: A practice guide. Project Management Institute.
4. Instituto de Evaluación Tecnológica en Salud. (2022). Manual de evaluación para la incorporación de tecnologías sanitarias en instituciones prestadoras de servicios de salud [Documento técnico]. Ministerio de Salud / IETS

5. International Atomic Energy Agency. (2006). Nuclear Medicine Resources Manual. IAEA.
6. International Atomic Energy Agency. (2024). Guidance on Setting Up a Comprehensive Nuclear Medicine and PET/CT Service. IAEA.
7. Ministerio de Salud y Protección Social. (s. f.). Guía para la evaluación de tecnologías de salud (ETS) en instituciones prestadoras de servicios de salud (IPS). https://www.minsalud.gov.co/sites/rid/1/Guia_evalucaion_de_tecnoclogias_en_salud.pdf
8. Ministerio de Salud y Protección Social. (2019). Resolución 3100 de 2019: Por la cual se definen los procedimientos y condiciones de inscripción de los prestadores de servicios de salud y de habilitación de los servicios de salud y se adopta el Manual de Inscripción de Prestadores y Habilitación de Servicios de Salud. https://www.minsalud.gov.co/sites/rid/Resolucion-3100-de-2019.pdf
9. Ministerio de Salud y Protección Social. (2025). Resolución 1633 de 2025: Por la cual se determina el marco técnico de infraestructura y equipamiento de edificaciones destinadas a la prestación de servicios de salud. Diario Oficial de la República de Colombia.

Conflict of Interest

No Conflict of Interest

O46

[177Lu]Lu-DOTA-ATWLPPR/(D-Lys6-LHRH) peptide heterodimer as a potential theragnostic agent for prostate and breast cancer

Dr. Ximena Camacho[1], MSc. Carolina Perroni[1], Dr. Mirel Cabrera[1], Dr. Lucía Alfaya[1], Dr. Marcos Tassano[1], MSc. Ana Laura Reyes[2], Tech. Andrea Paolino[2], Dr. Eduardo Savio[2], Dr. Juan Pablo Gambini[1,2], Dr. Pablo Cabral[1]
[1]Universidad de la República, Montevideo, Uruguay, [2]Centro Uruguayo de Imagenología Molecular, Montevideo, Uruguay

Oral presentations 4: Therapy and Radioguided Procedures, Barahona Room 2, February 15, 2026, 8:00 - 10:00

Background/Aims: Neuropilin-1 (NRP-1) and luteinising hormone-releasing hormone (LHRH) receptors are highly overexpressed in prostate and breast cancers (PC and BC), making them attractive targets for diagnosis and therapy. Heterodimeric peptides—combining ligands for different tumor markers—are gaining attention due to their enhanced affinity and specificity compared to monomeric analogs. We report the design, synthesis, and preclinical evaluation of a novel heterodimeric peptide targeting NRP-1 and LHRH, radiolabeled with lutetium-177, as a potential theranostic agent for PC and BC.
Methods: The heterodimeric peptide [ATWLPPR-Ahx-DOTA-Ahx-(D-Lys6)-LHRH] and the respectively monomers were purchased from GenScript, USA. 20 ug of all peptides were mixed with 0.5 M NH4Ac buffer (pH 5), radiolabeled with [177Lu] LuCl3 (74-185 MBq) at 95 °C for 15 and analysed by HPLC Log D and stability in serum, PBS, DTPA, EDTA, and FeCl3 were evaluated up to 72 hs. In vitro cell binding studies were done in different PC and BC cell lines (PC3, LnCap, DU145, MCF-7, BT-474, MDA-MB-231 and 4T1) up to 60 min. Biodistribution studies were developed in normal Swiss and Balb/C mice at 1 and 24 h p.i. (n = 4) (Ethics Approval: No. 240011-501407-21 and 240011-500866-21).
Results: [177Lu]Lu-labeled heterodimer showed high radiochemical purity (98.35 ± 1.53%), good hydrophilicity (Log D = -1.70 ± 0.13), and stability in all tested conditions. Specific binding was observed across all PC and BC cell lines, with prominent membrane association and limited internalization. In vivo biodistribution showed notable uptake in kidneys, liver, and gastrointestinal tract.
Conclusions: [177Lu]Lu-DOTA-labeled ATWLPPR-LHRH heterodimer exhibits favorable stability, specificity, and biodistribution profiles, supporting its potential as a novel theranostic agent for prostate and breast cancer.
Acknowledged: ANII-Uruguay (FMV_3_2022_1_172303) and DICYT/MEC-Uruguay (FVF_2023_ 444).

Conflict of Interest
No potential conflicts of interest relevant to this abstract were reported.

O47

Targeted ROR1 protein degradation combined with PET imaging reveals the role of ROR1 in overcomes EGFR Resistance in NSCLC

Mr. Bo Mei[1], Prof Zhi Yang[1], Prof Lei Xia[1]
[1]Peking University Cancer Hosiptal, Beijing, China

Oral presentations 4: Therapy and Radioguided Procedures, Barahona Room 2, February 15, 2026, 8:00 - 10:00

Objectives: Non-small cell lung cancer (NSCLC) faces clinical challenges due to recurrence and tyrosine kinase inhibitor (TKI) resistance. ROR1, a tumor-specific receptor tyrosine kinase, sustains caveolae integrity and EGFR-driven survival pathways. This study developed a ^{125}I-labeled imaging probe ([^{125}I]I-Zilovertamab) and a lysosomal-targeted ROR1 degrader (Zilovertamab-CMA) to dynamically monitor therapy response and combat resistance.
Methods: The [^{125}I]I-Zilovertamab probe was synthesized via N-bromosuccinimide oxidation and purified by size-exclusion chromatography. Radiochemical purity (RCP) and stability were assessed using radio-TLC under physiological conditions (PBS, 5% HSA). In vitro binding specificity was evaluated in ROR1-high NCI-H1975 cells via y-counting, with competitive blocking using unlabeled Zilovertamab. Subcutaneous H1975 xenografts in nude mice underwent micro-PET/CT imaging to assess tumor targeting. Zilovertamab-CMA, engineered by conjugating Zilovertamab to a lysosome-targeting peptide, was administered to evaluate ROR1 degradation. Western blot and multiplex immunofluorescence quantified ROR1, Cavin-1, and EGFR pathway markers. Therapeutic response was correlated with PET signal changes pre-/post-degrader treatment.
Result:Probe Characteristics: The [^{125}I]I-Zilovertamab exhibited RCP >95% and retained >95% stability over 96 h. In vitro binding assays showed specific uptake in ROR1-high H1975 cells (1.88 ± 0.5% ID/g vs. 0.3 ± 0.02% in ROR1-low controls; $p < 0.01$), with 85% inhibition by excess unlabeled antibody ($p < 0.001$).
In Vivo Imaging: Micro-PET/CT revealed rapid tumor uptake (1.89 ± 0.6 SUV at 96 h post-injection) and high tumor-to-muscle ratios (T/NT = 1.95 ± 1.1), resolving intratumoral heterogeneity. Signal intensity declined by 52% ($p < 0.01$) post-degrader treatment, aligning with therapeutic response.
Conclutions:This study establishes [^{125}I]I-Zilovertamab as a high-precision imaging tool for ROR1-positive NSCLC, enabling real-time monitoring of therapeutic response. Zilovertamab-CMA effectively degrades ROR1, disrupts Cavin-1/EGFR signaling, and reverses TKI resistance. The dual theranostic strategy offers a transformative approach to NSCLC treatment, addressing both tumor heterogeneity and drug resistance. These findings pave the way for clinical translation of ROR1-targeted therapies in EGFR-resistant malignancies.

Conflict of Interest
There is no conflict of interest

Graphic

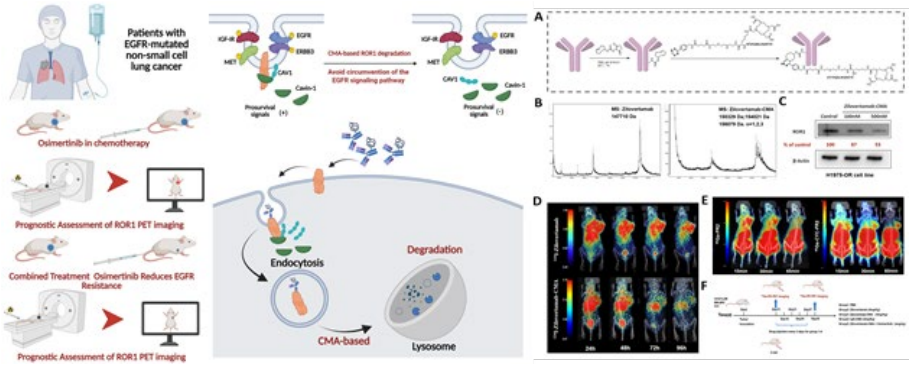

O48

Preclinical evaluation of ^{212}Pb-labeled CXCR4 peptides for targeted alpha therapy in colorectal carcinomatosis

Mr. Richard Whiteside[1], Nasrin Abbasi-Gharibkandi[1], Fabio Gallazzi[1], Jessica Newton-Northup[1], Meltem Ocak[1], David Bauer[1]
[1]The University of Missouri, Columbia, United States

Oral presentations 4: Therapy and Radioguided Procedures, Barahona Room 2, February 15, 2026, 8:00 - 10:00

Background. Colorectal cancer (CRC) is a leading cause of cancer-related death worldwide, with incidence rising particularly among younger populations. [1]Recurrence and therapy resistance remain major clinical challenges, and intraperitoneal (IP) carcinomatosis represents a frequent and lethal route of disease progression that is poorly addressed by current therapies. The chemokine receptor CXCR4 is upregulated in most CRC cases and is strongly linked to metastatic spread and poor prognosis[2], making it a rational target for intervention. Because of its role in peritoneal dissemination, antagonizing this receptor may provide a therapeutic benefit in locoregional therapy. If administered IP, targeted alpha therapy (TAT) employing ^{212}Pb-labeled CXCR4 ligands offers the potential to eradicate micrometastatic disease in the abdominal cavity by delivering highly cytotoxic, short-range alpha particles.
Methods. Eight CXCR4-targeting peptides were designed based on the clinically validated[3] tracer PentixaFor and refined based on current literature[4] to enhance ^{212}Pb chelation and prolong peritoneal retention. Radiolabeling, purification, and in vivo stability were established using in-house–produced ^{212}Pb. Pharmacokinetics and clearance will be assessed by planar gamma imaging at 1-, 4-, and 24-hours post-injection. Two CRC models, using HT-29 and SW620 luciferase-expressing CRC cells, were engrafted intraperitoneally and subcutaneously in athymic nude mice, with bioluminescence and imaging and caliper measurements used to quantify and correlate tumor burden and growth patterns. All animal procedures were approved by the University of Missouri IACUC.
Results. To this date, HT-29-Luc growth kinetics were established, confirming robust formation of intraperitoneal lesions suitable for therapy evaluation. CXCR4-targeted peptides were successfully radiolabeled with ^{212}Pb, characterized, and initial imaging studies demonstrated distinct clearance profiles following intraperitoneal administration.
Conclusion. We report the development of a reliable intraperitoneal CRC model alongside a novel panel of ^{212}Pb-labeled CXCR4 tracers. Ongoing biodistribution and imaging studies will identify the most promising candidate for therapeutic evaluation in upcoming dose-escalation studies.

References

[1] Siegel RL, Wagle NS, Cercek A, Smith RA, Jemal A. Colorectal cancer statistics, 2023. CA Cancer J Clin. 2023; 73(3): 233-254. DOI:10.3322/caac.21772

[2] Ottaiano A, Santorsola M, Del Prete P, Perri F, Scala S, Caraglia M, Nasti G. Prognostic Significance of CXCR4 in Colorectal Cancer: An Updated Meta Analysis and Critical Appraisal. Cancers (Basel). 2021 Jun 30;13(13):3284. DOI: 10.3390/cancers13133284
[3] Eleni G, Oliver D, Margret S, Calogero D.A, Stefan S, Ingrid D, Udo S, Markus S, Horst K, Wester H.J. PET of CXCR4 Expression by a 68Ga-Labeled Highly Specific Targeted Contrast Agent. Journal of Nuclear Medicine. 2011; 52 (11) 1803-1810. DOI: 10.2967/jnumed.111.098798
[4] Osl T, Schmidt A, Schwaiger M, Schottelius M, Wester H.J. A new class of PentixaFor and PentixaTher-based theranostic agents with enhanced CXCR4 targeting efficiency. Theranostics. 2020; 10(18): 8264-8280. DOI: 10.7150/thno.45537

Conflict of Interest

There are no Conflicts of Interest to disclose.

Graphic

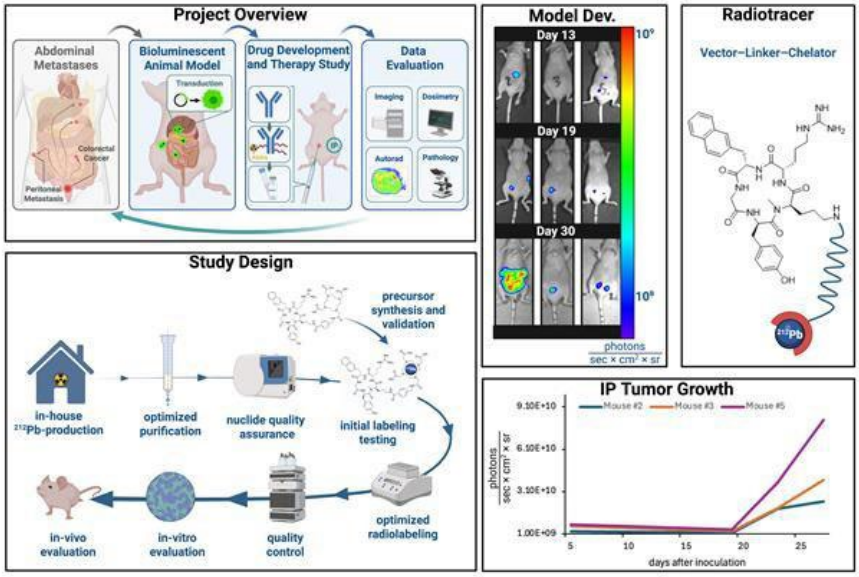

O49

Intraoperative Sentinel Lymph Node Mapping with Dual Modality (Radioisotopic/Optical) Using 99mTc-ICG Nanocolloid: Improved Precision and Overcoming Clinical Limitations

Mrs. Carolina Furtado Prieto[1,2], Ms Bettina Martinucci[1], Ms Mirel Cabrera[2], Ms Ximena Camacho[2], Mr Marcos Tassano[2], Mr Omar Alonso[1], Mr Gustavo Burroso[3], Mr Pablo Duarte[3], Mr Alarico Rodríguez[3], Mr Pablo Cabral[2], Mr Juan Pablo Gambini[1,3]
[1]UA Medicina Nuclear e Imagenología Molecular, Hospital de Clínicas Dr. Manuel Quintela, Facultad de Medicina, UdelaR, Montevideo, Uruguay, [2]Centro de Investigaciones Nucleares, Facultad de Ciencias, UdelaR, Montevideo, Uruguay, [3]Centro Uruguayo de Imegenología Molecular, Montevideo, Uruguay

Oral presentations 4: Therapy and Radioguided Procedures, Barahona Room 2, February 15, 2026, 8:00 - 10:00

Background: Accurate intraoperative identification of sentinel lymph nodes (SLN) is essential in oncology to reduce surgical morbidity. Conventional techniques are limited by low anatomical resolution and suboptimal real-time visualization. Combination of radionuclides and fluorophores in a single hybrid tracer, like 99mTc-indocianine green (ICG) nanocolloid, represents a promising solution for improving precision and visualization.
Methods: A hybrid tracer of nanocolloid labeled with 99mTc and ICG was administered by peritumoral subcutaneous injection to 10 patients. SLN uptake was assessed preoperatively with planar scintigraphy and SPECT/CT. During surgery, a gamma probe (Oncovision) and a proprietary near-infrared (NIR) visualization system were used. This dual-modality technique allowed the radioisotopic and optical detection of the SLN, guiding its resection with minimally invasive approach.
Results: The use of the hybrid tracer and its complementary detection modality allowed precise localization of SLNs, with concordance between radioactive and fluorescent signals. Approximately 38 nodes were removed, an average of 3.8 per patient. Real-time ICG visualization facilitated dissection, reduced manipulation of normal tissue, vascular and nervous structures and optimized the surgical procedure. In a breast cancer case where the patient did not tolerate preoperative imaging, infrared camera allowed direct visualization of lymphatic drainage on skin surface, enabling the optimization of the exploratory incision and successful resection. Furthermore, the fluorescence assisted pathologists in the rapid and specific localization of the SLN in the resected specimen.
Conclusions: The hybrid technique with 99mTc-ICG nanocolloid offers superior precision and significant advantages in intraoperative SLN detection, even in patients with complex approaches. The dual modality of the technique, combining long-range guidance with high-resolution visualization, not only benefits surgeons but also optimizes the diagnostic-surgical workflow and extends the benefit of SLN mapping to patients with preoperative barriers. This positions it as a highly effective technique with potential to become the method of choice for SLN resection surgeries.

Conflict of Interest
No poseo conflicto de intereses

Graphic

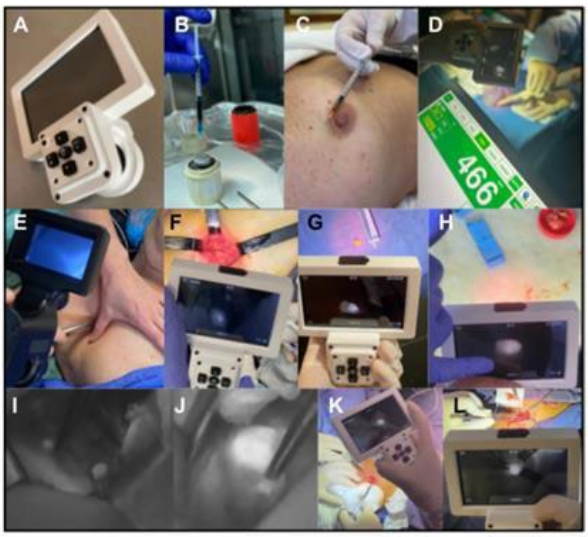

FIGURA 1. Intraoperative sentinel lymph node mapping in oncology with dual modality using ^{99m}Tc-ICG-Nanocolloid.
(A)Portable NIR fluorescence camera.
(B-C)Labeling of hybrid tracer in hospital radiofarmacy according to GMP and subcutaneous administration of hybrid tracer.
(D)Dual modality detection of resected SLN.
(E)Lymphatic vessel pathway observed in skin using near-infrared visualization system.
(F-G)SLN intraoperative mapping and correlation with observation of the resected structure using near-infrared camera.
(H) Use of indocyanine green to assist the pathologist in dissecting the specimen.
(I-J-K-L) Intraoperative SNL mapping obtained with a near-infrared camera.

O50

Intraoperative near-infrared lymphatic mapping in thyroid cancer using intrathyroidal indocyanine green

Mrs. Carolina Furtado Prieto[1,2], Ms. Bettina Martinucci[1], Ms. Carolina Guarneri[3], Mr. Ulises Parada[3], Mr. Pablo Duarte[4], Mr. Omar Alonso[1], Mr. Gustavo Burroso[4], Mr. Alarico Rodríguez[4], Mr. Pablo Cabral[2], Mr. Juan Pablo Gambini[1,4]
[1]UA Medicina Nuclear e Imagenología Molecular, Centro de Investigaciones Nucleares - Universidad de la República, Montevideo, Uruguay, [2]Centro de Investigaciones Nucleares, Facultad de Ciencias, UdelaR, Montevideo, Uruguay, [3]Unidad Académica Clínica Quirúrgica A, Hospital de Clínicas Dr. Manuel Quintela, Facultad de Medicina, UdelaR, Montevideo, Uruguay, [4]Centro Uruguayo de Imagenología Molecular, Montevideo, Uruguay

Oral presentations 4: Therapy and Radioguided Procedures, Barahona Room 2, February 15, 2026, 8:00 - 10:00

Background/Objectives: Precise lymphatic mapping is essential to optimize the extent of central neck dissection in thyroid cancer, improving oncological completeness while minimizing morbidity. Near-infrared (NIR) fluorescence with indocyanine green (ICG) provides real-time, high-contrast visualization of lymphatic drainage, offering a complementary approach to conventional surgical and nuclear medicine techniques. This study evaluated the feasibility, safety, and intraoperative value of intrathyroidal ICG injection for bilateral lymphatic mapping in differentiated thyroid carcinoma.
Methods: In a single-center feasibility series, three women with aggressive differentiated thyroid carcinoma undergoing total or subtotal thyroidectomy with central and bilateral lymph node dissection received intrathyroidal ICG (≈1 mL, 2.5 mg/mL) before thyroid removal. A portable NIR camera was employed for real-time surgical guidance (Figure 1) Primary endpoints were feasibility (fluorescence detection and nodal localization) and safety; secondary endpoints included concordance with pathology and qualitative impact on dissection. Institutional ethics approval and patient consent were obtained.
Results: Intrathyroidal ICG consistently generated prompt, stable fluorescence delineating bilateral central neck lymphatic pathways. Fluorescence enhanced surgical orientation, reduced manipulation of neurovascular structures, and facilitated targeted lymphadenectomy. Across the cohort, >50 lymph nodes were resected; pathology confirmed metastatic disease in 35–66% per patient. Fluorescence signals correlated with pathological findings, supporting accuracy of intraoperative mapping. No ICG-related adverse events occurred. Postoperative imaging corroborated completeness of nodal clearance.
Conclusions: Intrathyroidal ICG-guided NIR imaging is a safe and feasible technique that augments intraoperative lymphatic mapping in thyroid cancer. By supporting selective, anatomy-sparing dissections and improving identification of metastatic nodes, this hybrid optical-surgical approach has the potential to enhance the precision of thyroid cancer surgery. Integration with nuclear medicine concepts of lymphatic mapping positions this modality within a broader theranostic framework, warranting validation in larger controlled studies

Conflict of Interest
No conflict of interest

Graphic

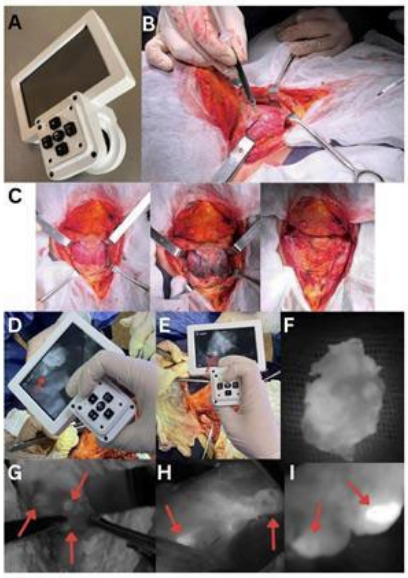

Figure 1. Intraoperative lymph node mapping in thyroid cancer using intrathyroidal indocyanine green (ICG) and near-infrared (NIR) imaging.
(A) Portable NIR fluorescence camera.
(B) Intrathyroidal multipuncture administration of ICG.
(C) Thyroid gland exposed before and after ICG injection, with improved delineation of the surgical field.
(D–E) Real-time lymphatic mapping with NIR imaging.
(F–I) Fluorescent lymph nodes visualized intraoperatively, facilitating selective dissection while preserving surrounding neurovascular structures.

O51

Diagnostic Accuracy of Robotic Arm assisted Real time PET-CT guided Biopsy of Abdomino-pelvic lesions including Retroperitoneal lesions

Dr. Arun Ravi John[1], Dr. Jeenu Varghese[1], Dr. Srivallabh Dande[1], Dr TVSVGK Tilak[1]
[1]Command Hospital Air Force, Bengaluru, India

Oral presentations 4: Therapy and Radioguided Procedures, Barahona Room 2, February 15, 2026, 8:00 - 10:00

Background/Aim: This study aimed to assess the diagnostic accuracy of real-time PET/CT-guided biopsies of abdominal and pelvic lesions, including retroperitoneal lesions, with the assistance of a robotic arm.
Methods: This retrospective study involved 54 patients (32 men and 22 women; mean age-49.6 ± 12.3 years; range, 22–74 years) who underwent real-time PET/CT-guided biopsies of FDG or FAPI avid lesions in the abdomen and pelvis from June 2023 to June 2025. The biopsies were performed using an automated robotic arm with real-time PET-CT guidance. Histopathology reports were used to evaluate the diagnostic performance. Clinical and/or imaging follow-up for up to six months confirmed negative results. The diagnostic accuracy of the guided biopsy was assessed by comparing it with a composite diagnosis. This diagnosis was established through pathological analysis and corroborated by clinico-radiological follow-up. Results were classified as true-positive if histopathology confirmed either malignant or benign pathology. Results were true-negative if no evidence of disease was identified through pathology or follow-up. A false-positive result occurred when histopathology incorrectly indicated an alternative pathology. A false-negative result occurred when histopathology failed to reveal a diagnosis including non-representative and inconclusive results.
Results: Of 54 patients, lesions were successfully targeted and diagnosed pathologically in 50 (92.6%). Of these, 38 were malignant and 12 benign. Three cases of mild residual FDG uptake post-malignant treatment were true negatives, confirmed by six months of follow-up. Diagnostic results included 47 true positives, 3 true negatives, 4 false negatives, and no false positives. The sensitivity was 92.1%, specificity 100%, positive predictive value 100%, negative predictive value 42.8% and accuracy 92.5%. There were no serious complications or life-threatening events.
Conclusions: The use of real-time PET-CT guidance with a robotic arm for percutaneous biopsy of metabolically active lesions in the abdomen and pelvis offers a precise, safe, and accurate method for pathological diagnosis[1,2].

References

[1] Kumar, R., Mittal, B.R., Bhattacharya, A. et al. Diagnostic performance of real-time robotic arm-assisted 18F-FDG PET/CT-guided percutaneous biopsy in metabolically active abdominal and pelvic lesions. Eur J Nucl Med Mol Imaging 46, 838–847 (2019). https://doi.org/10.1007/s00259-018-4133-x
[2] Li, X., Zhang, W. Clinical application of real-time PET/CT guided targeted retroperitoneal masses biopsy in diagnosing malignant tumors. BMC Cancer 23, 829 (2023). https://doi.org/10.1186/s12885-023-11334-y

Conflict of Interest
Nil

Graphic

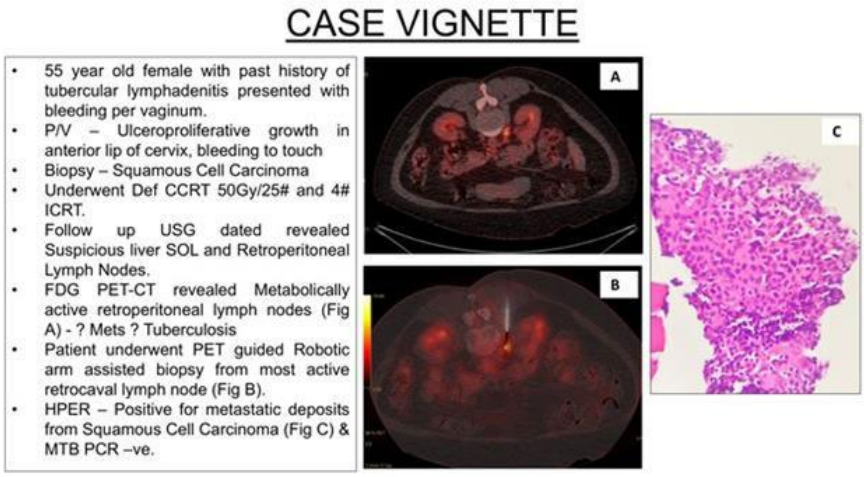

O52

Bridging Vision and Practice: The Journey to Implementing a Theranostics Centre at the University Health Network in Toronto, Canada

Dr. Luke Brzozowski[1]
[1]University Health Network, Toronto, Canada

Oral presentations 4: Therapy and Radioguided Procedures, Barahona Room 2, February 15, 2026, 8:00 - 10:00

The growing pipeline of radiopharmaceuticals moving toward regulatory approval and standard-of-care (SOC) status is driving a substantial increase in demand for theranostic services. At the University Health Network (UHN), a large multi-site Canadian hospital system, a strategic and interdisciplinary initiative was launched to support the transition of theranostics from clinical research into mainstream care.
Recognizing the operational and systemic complexities of this transition, UHN developed a multi-year implementation roadmap grounded in research experience and informed by real-world healthcare delivery needs. This roadmap addresses key components including capacity forecasting, infrastructure development, government reimbursement for compounds and associated delivery costs, fundraising strategies, and governance structures required to sustain a theranostics program.
By drawing on insights from clinical trial operations and fostering strong hospital–industry partnerships, UHN is facilitating the integration of theranostics into routine practice. This presentation will outline the centre's development journey—from initial vision to implementation—highlighting the models, challenges, and enablers that have shaped a scalable, interdisciplinary approach to delivering theranostics as a standard of care.

Conflict of Interest
No conflict of interest

O53

Real-world efficacy: first prospective study in Argentina of the effectiveness and safety of 177Lu-DOTATATE in GEP-NET

Dr. Silvina Racioppi[1], Dr. Eduardo Cardozo[2], Lic. Mariano Portillo[1], **Lic. Mariano Portillo**[1], Dr. Martina Musumeci[1], Lic. Marcos Mussio[1], Dr. Federico Esteso[2], Dr. Juan Manuel OConnor[2]
[1]Servicio de Medicina Nuclear, Instituto Alexander Fleming, Buenos Aires, Argentina, [2]Servicio de Oncología Clinica, Instituto Alexander Fleming, Buenos Aires, Argentina

Oral presentations 4: Therapy and Radioguided Procedures, Barahona Room 2, February 15, 2026, 8:00 - 10:00

177Lu-DOTATATE is a treatment option for gastroenteropancreatic neuroendocrine tumors (GEP-NETs) with somatostatin receptor overexpression. It demonstrated benefits in overall survival (OS) and objective response rate (ORR) in the NETTER 1 and 2 studies.
There are limited data on the effectiveness of this treatment in Latin America. The treatment sequence in GEP-NETs and factors used to define these are not yet standardized. Our objective was to evaluate clinical characteristics, ORR, and OS in patients with GEP-NETs.
This was a prospective, single-institutional cohort study. Patients with metastatic GEP-NETs with somatostatin receptor overexpression were included. Patients received four doses of 177Lu-DOTATATE between April 2018 and July 2024. Response was assessed by 68Ga-DOTATATE PET-CT starting 3 months after the fourth dose. Descriptive statistics were used, and survival was calculated using the Kaplan-Meier method.
The therapeutic regimen consisted of administering 200mCi of 177Lu-DOTATATE in co-infusion with amino acids using an automatic pump every 8+/-2 weeks, according to guidelines. Gamma camera SPECT scans, interdose laboratory and clinical monitoring, and end-of-treatment imaging were performed starting 3 months after the last dose. The median follow-up was 1 year.
The ORR was reported at 42%, similar to the NETTER-2 rate of 43%. The most frequently reported adverse events (AEs) were myelotoxicity (17%) and asthenia (18%). There were no discontinuations due to serious AEs. There were no statistically significant differences in PFS (p=0.77) between the use of 177Lu-DOTATATE in earlier lines (1-2ºL vs >2ºL) and according to primary tumor site or functioning status of the tumor.
The first prospective study in Argentina with efficacy and safety data for 177Lu-DOTATATE in GEP-NET reported an ORR similar to that of NETTER-2 with excellent tolerability, with a trend toward benefit observed with the use of 177Lu-DOTATATE in earlier lines. Longer follow-up is required to draw conclusions regarding OS.

References

1. Treatment with 177Lu-DOTATATE showed significant efficacy in patients with midgut neuroendocrine tumors (Strosberg et al., 2017).
2. A recent phase 3 trial in advanced G2–G3 gastroenteropancreatic NETs confirmed these findings (Singh et al., 2024)

Conflict of Interest

The authors declare not to have any conflict of interest.

Graphic

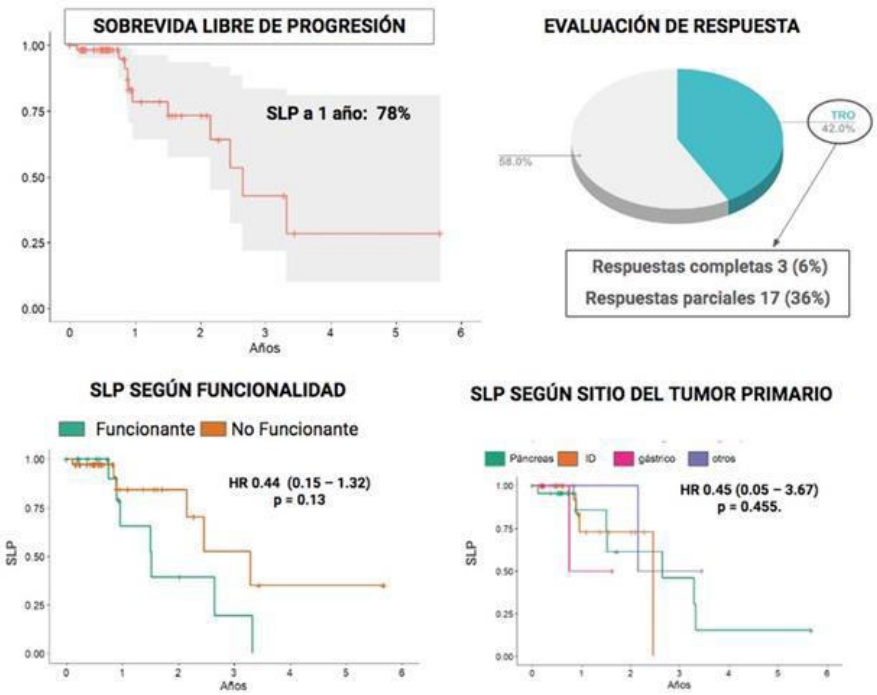

O54

Intraoperative metabolic assessment (PET-CT) of surgical margins in breast cancer: a novel challenge in oncologic surgery

Dr. John Orozco Cortés[1], Dr. Jorge Sabater Sancho[2], Dr. Elvira Buch Villa[3], Dr. Ernesto Muñoz Sornosa[3], Dr. Vicente LópezFlor[3], Dr. Tomas Mut Dolera[3], Dr. Líria Térradez Mas[3], Dr. Octavio Burgués Gaisón Burgués Gaisón[3], Dr. Marcos Adrianzen Vargas[3], Dr. RRafael DíazExpósito[4]
[1]Hospital Universitario Dr. Peset, Valencia, Spain, [2]Consorcio Hospitalario Provincial de Castellón, Castellon, Spain, [3]Hospital Clínico Universitario de Valencia, Valencian, Spain, [4]Hospital Universitario y Politecnico la Fe, Valencia, Spain

Oral presentations 4: Therapy and Radioguided Procedures, Barahona Room 2, February 15, 2026, 8:00 - 10:00

Background/Aims: Intraoperative assessment of surgical margins in breast cancer remains a major challenge, as positive margins can lead to reoperation and compromise oncologic outcomes. This study aimed to evaluate the feasibility and diagnostic accuracy of ex vivo positron emission tomography/computed tomography (PET/CT) with ^{18}F-fluorodeoxyglucose (^{18}F-FDG) for intraoperative evaluation of surgical specimens, and to determine its concordance with conventional histopathology.
Methods: Eight patients with histologically confirmed breast carcinoma underwent surgery (six breast-conserving and two mastectomy). A preoperative intravenous injection of 0.8 MBq/kg ^{18}F-FDG was administered. After resection, surgical specimens were scanned ex vivo using a standardized PET/CT protocol, without interfering with surgical workflow or subsequent pathological processing, which was performed separately and blinded. Six margins per specimen (n = 48) were analyzed. Focal FDG uptake was considered indicative of margin involvement. Sensitivity, specificity, positive predictive value (PPV), negative predictive value (NPV), and overall concordance with histopathology were calculated. Ethical approval was obtained from the institutional review board.
Results: The mean age of patients was 65 years (range 52–79). Three received neoadjuvant chemotherapy and five underwent sentinel lymph node biopsy. Lesions were predominantly located in the right breast (7/8). Histopathology revealed six invasive ductal carcinomas, one invasive lobular carcinoma, and one ductal carcinoma in situ. Molecular subtypes included Luminal A (3), Luminal B (2), HER2-positive (1), triple-negative (1), and one case with no residual disease after neoadjuvant therapy. Necrosis was present in 3/8 patients, and multifocality in 2/8. Among 48 evaluated margins, concordance between PET/CT and histopathology was 93.8%. Sensitivity was 83.3%, specificity 95.2%, PPV 71.4%, and NPV 97.6%.
Conclusions: Ex vivo PET/CT is a promising technique for intraoperative margin assessment in breast cancer. Its high negative predictive value, together with seamless integration into surgical workflow, supports its potential to reduce reoperation rates and improve oncologic safety.

Conflict of Interest
None.

O55

Freehand-SPECT augmented reality navigation compared with planar scintigraphy for sentinel lymph node biopsy in breast cancer

Dr. John Orozco Cortés[1], Dr. Franco Jose Cavagna Matti[1], Dr. Angela Esteban Hurtado[2], Dr Georgina Bonino[1], Dr PPedro AbreuSanchez[1], Dr. Jose Rafael Infante de la Torre[1], Dr Fabrizio Montenegro Muñoz[1], Dr. Laura Casas Calabuig[1], Dr. Maria Dolores Reyes Ojeda[1], Dr Elisa Veronica Caballero Calabuig[1]
[1]Hospital Universitario Dr. Peset, Valencia, Spain, [2]Centre Medic Alomar, Barcelona, Spain

Oral presentations 4: Therapy and Radioguided Procedures, Barahona Room 2, February 15, 2026, 8:00 - 10:00

Background/Aims: Freehand-SPECT (declipse SPECT®; SurgicEye, Munich, Germany) has emerged as a viable alternative for sentinel lymph node biopsy in breast cancer. In addition to conventional planar scintigraphy, it enables direct visualization of radiotracer distribution and accurate lesion depth measurement after a short scan. The aim of this study was to evaluate the correlation in the number of sentinel nodes detected between Freehand-SPECT and conventional planar scintigraphy.
Methods: A total of 103 patients with newly diagnosed invasive breast cancer and no clinical evidence of nodal involvement prospectively underwent sentinel lymph node biopsy. Preoperative evaluation included Freehand-SPECT imaging 15 minutes post-injection and planar gamma camera images at 25 minutes (early) and 60 minutes (late). A concordance study was performed between the number of sentinel nodes detected with Freehand-SPECT and planar scintigraphy, as well as between early and late planar scintigraphy.Results
Overall, there was high concordance between Freehand-SPECT and scintigraphy: 72% between Freehand-SPECT and early scintigraphy, and 85% between Freehand-SPECT and late scintigraphy. Concordance analysis showed moderate agreement between Freehand-SPECT and early scintigraphy (kappa = 0.42), and moderate to high agreement between Freehand-SPECT and late scintigraphy (kappa = 0.60). No significant differences were found between these comparisons (p = 0.16).
Conclusions: Freehand-SPECT may be considered a valid alternative for the presurgical evaluation of sentinel lymph nodes in breast cancer. Its moderate to high concordance with conventional scintigraphy supports its potential as an innovative imaging tool for surgical navigation.

Conflict of Interest
non

Graphic

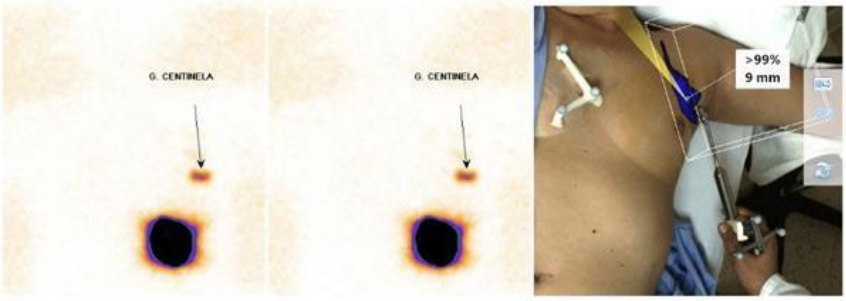

Fig 1: A) Single left axillary sentinel node in early scintigraphy; B) Single left axillary sentinel node in late scintigraphy; C) Single left axillary sentinel node 9 mm deep in Freehand-SPECT.

Table

Table 1: Cohen's kappa coefficient using different methods of weighting between Freehand-SPECT and early and late scintigraphy.

	FH-SPECT vs early scintigraphy			FH-SPECT vs late scintigraphy		
	Observed proportion of agreement	Kappa (CI 95%)	SE	Observed proportion of agreement	Kappa (CI 95%)	SE
Quadratic weighted kappa	0,97 vs 0,94	0,42* (0,19 – 0,65)	0,116	0,98 vs 0,95	0,60* (0,38 – 0,82)	0,112

*p-value < 0,05
FE-SPECT: freehand SPECT; SE: estandar error.

O56

First experience with molecular surgery in pancreatic and hepatic cancer using PET radiopharmaceuticals

Dr. John Orozco Cortés[1], Dr. Jorge Sabater Sancho[2], Dr Luis Sabater Ortí[3], Dr. Antonio Stacey Solis[3], Dr. Elena Muñoz Forner[3], Dr Maria del Puig Cozar Santiago[3], Dr. Marina Garces Albir[3], Dr. CaCarolina Castillorias[3], Dr Maria Carmen Redal peña[3], Dr. Rafael Díaz Expósito[4]
[1]Hospital Universitario Dr. Peset, Valencia, Spain, [2]Consorcio Hospital Provincial de Castellon, Castellon, Spain, [3]Hospital Clinico Universitario de Valencia, Valencia, Spain, [4]Hospital Universitario y Politecnico la Fe, Valencia, Spain

Oral presentations 4: Therapy and Radioguided Procedures, Barahona Room 2, February 15, 2026, 8:00 - 10:00

Background/Aims:Molecular surgery using PET radiopharmaceuticals is a novel approach that can assist in planning and intraoperative assessment in oncologic surgery. The objective of this study was to describe the initial experience in pancreatic and hepatic cancer using ^{18}F-fluorodeoxyglucose (^{18}F-FDG) to evaluate its utility for surgical planning and intraoperative and postoperative evaluation.
Methods: Four patients diagnosed with pancreatic adenocarcinoma (n = 3) and hepatic metastases from colorectal adenocarcinoma (n = 1) were included between April and May 2024, after providing written informed consent. A baseline preoperative PET was performed to confirm tumor metabolic activity. On the day of surgery, 1 mCi of ^{18}F-FDG was administered before the procedure. A flexible drop-in laparoscopic probe was used intraoperatively to identify hypermetabolic lesions relative to healthy parenchyma. After resection, PET/CT of surgical specimens was performed to evaluate margin status, and results were compared with histopathology.Results
In pancreatic adenocarcinoma cases, there was 100% concordance between PET/CT margin assessment and histopathology. In the patient with hepatic metastases, the laparoscopic probe detected an additional lesion in segment V, later confirmed as metastasis with negative surgical margins. All intraoperatively identified hypermetabolic lesions were visible on specimen PET/CT, which was performed in the Nuclear Medicine Department.
Conclusions: This first experience demonstrates that PET radiopharmaceuticals such as ^{18}F-FDG are valuable tools for surgical planning, intraoperative navigation, and postoperative specimen evaluation in oncologic molecular surgery. The high concordance with histopathology supports further research in this innovative field.

Conflict of Interest
non

O57

Impact of fixed suv thresholds on lesion segmentation in psma pet/ct: methodological implications for recip response assessment to lu177-psma-617 therapy

Mr. Yann Cras[1], MD. Khalil Trabelsi[1], MD. Adam Bekkhoucha[1], MD. Tarek Kamoun[1], MD. Mehdi Borsali[1], Pr. Désirée Deandreis[1], DR. Camilo Garcia[1]
[1]Gustave Roussy, Villejuif, France

Oral presentations 4: Therapy and Radioguided Procedures, Barahona Room 2, February 15, 2026, 8:00 - 10:00

Background/Aims: In castration-resistant prostate cancer (mCRPC), PSMA PET/CT selects candidates for Lu177-PSMA-617, enables whole-body lesion segmentation. This process determines total metabolic tumor volume (TMTV), a parameter for response evaluation according to RECIP criteria. Segmentation relies on a threshold of 3 SUVbw, but the effect of alternative thresholds has not been systematically assessed. This study investigated how thresholds influence TMTV quantification and RECIP-based response categorization in patients treated with Lu177-PSMA-617.
Methods: Sixty mCRPC patients enrolled in the Gustave Roussy PSMADose registry, treated with Lu177-PSMA-617 between January 2023 and August 2025 were analyzed. Baseline and follow-up PSMA PET/CT scans (after cycles 2, 4, 6 when available) were segmented using thresholds of 3, 4, 5 SUVbw (minimum 0.5 mL) with the LesionID workflow (MIM Software). All lesions were validated by a senior nuclear medicine physician. TMTV changes were computed relative to baseline, with response defined as ≥30% decrease and progression ≥20% following RECIP criteria. Baseline SUVmean was recorded.
Results: Raising the threshold from 3 to 5 SUVbw reduced tumour volumes and modified RECIP classification. Responders showed higher baseline median SUVmean, increasing from 9.46 at 3 SUVbw to 12.31 at 5 SUVbw (+30%), while non-responders generally remained below 10. No responders at 3 SUVbw was reclassified as non-responder at higher thresholds; 4 and 7 patients (12% and 21%) initially classified as non-responders at 3 SUVbw were reclassified as responders at thresholds of 4 and 5. The proportion with median SUVmean >10 rose with thresholds (46%, 65%, 77%), whereas most non-responders had SUVmean <10 (71%, 65%, 50%).
Conclusions: The choice of SUV threshold in PSMA PET/CT impacts TMTV quantification and RECIP categorization in patients treated with Lu177-PSMA-617. These findings highlight the need for standardized segmentation protocols before RECIP-based metrics can be reliably applied in trials or practice. Correlations with biomarkers, imaging, outcomes will be presented.

Conflict of Interest
Nothing to disclosed

O58

Limitations of applying the hänscheid single-time-point method to 177lu-psma-617 organ dosimetry: toward psma-specific simplified protocols

Mr. Yann Cras[1], MD. Khalil Trabelsi[1], MD. Adam Bekkhoucha[1], MD. Tarek Kamoun[1], MD. Mehdi Borsali[1], Pr. Désirée Deandreis[1], MD. Camilo Garcia[1]
[1]Gustave Roussy, Villejuif, France

Oral presentations 4: Therapy and Radioguided Procedures, Barahona Room 2, February 15, 2026, 8:00 - 10:00

Background/Aims: The single-time-point (STP) approximation by Hänscheid[1], supports late quantitative measurement (~96 h) to estimate absorbed doses in organs/NET lesions. Its validity depends on mono-exponential kinetics and tissue half-lives. Transposition to 177Lu-PSMA ligands is uncertain due to different biodistribution. STP is feasible only with PSMA-specific time points or prior models. We compared multi-time-point (MTP) dosimetry with STP and assessed detector influence (Anger/CZT).
Methods: Forty metastatic castration-resistant prostate cancer patients included in the PSMADOSE prospective registry, underwent whole-body quantitative SPECT/CT at D0, D1, and D5-7 after the first 177Lu-PSMA-617 cycle using Anger or CZT cameras. Acquisition times reflected center logistics: same-day post-therapy (D0), single 24-h return (D1), and delayed scan within the week (D5-7); intermediate acquisitions (48-72 h) were not possible. Kidneys, salivary glands, and liver were segmented on CT and mapped to SPECT. Absorbed doses were calculated with MIM software using both MTP and Hänscheid STP methods (Voxelised S-values Convolution Algorithms). Primary endpoint: STP deviation from MTP. Organ effective half-lives were estimated in 10 patients.
Results: D1-based STP produced the lowest deviations versus MTP (<20% kidneys/salivary glands; <10% liver), whereas D0 and D5-7 exceeded 25%. Effective half-lives varied widely, deviated from mono-exponential kinetics, invalidating direct Hänscheid scaling for Lu177-PSMA-617. Detector type had minimal clinical impact. Findings support PSMA-specific STP protocols: ~48 h for organs, ≥72 h for tumors, or "STP-prior" using first-cycle MTP data to guide subsequent STP acquisitions.
Conclusions: Under logistic constraints limiting acquisitions to D0, D1, and D5-7, a single 24-h acquisition offered the most consistent STP approximation for organ dosimetry. Previous reported data suggest that acquisitions at 48-72 h would likely yield more accurate absorbed dose estimates for organs and tumors due particular kinetics. Hänscheid's model cannot be directly applied to PSMA ligands, highlighting the need for PSMA-specific protocols combining initial MTP data with optimized single-time-point follow-up.

References

[1] Hänscheid et al. "Dose Mapping After Endoradiotherapy with 177Lu-DOTATATE/DOTATOC by a Single Measurement After 4 Days" THE JOURNAL OF NUCLEAR MEDICINE • Vol. 59 • No. 1 • January 2018

Conflict of Interest

Nothing to disclose

O59

Selection of Patients for Lutetium-177 DOTATATE Therapy Using Tc-99m HYNIC-TOC Scintigraphy: Preliminary Experience in a Peruvian Center

Dr. Shirley Alarcon[1], Dr. Estuardo Paredes
[1]Clinica Ricardo Palma, Lima, Perú

Oral presentations 4: Therapy and Radioguided Procedures, Barahona Room 2, February 15, 2026, 8:00 - 10:00

Introduction: Peptide receptor radionuclide therapy (PRRT) with 177Lu-DOTATATE has demonstrated efficacy in well-differentiated neuroendocrine tumors (NETs). Patient selection requires confirmation of somatostatin receptor expression. In settings where DOTA-based PET tracers are not widely available, Tc-99m HYNIC-TOC scintigraphy represents an alternative. This study aimed to evaluate its utility for PRRT selection.
Materials and Methods: A retrospective descriptive study was performed including patients with NETs who underwent Tc-99m HYNIC-TOC scintigraphy between 2024–2025. Demographic data, histological grade (WHO 2019), Ki-67 index and Krenning score. Inclusion criteria for PRRT were uptake ≥ liver (Krenning ≥3), absence of discordant lesions, and preserved organ function.
Results: Twenty-eight patients were included. Mean age was 55.5 years (range 13–77), with female predominance (61%). Histological grades were: G1 in 36%, G2 in 50%, and G3 in 14%. Median Ki-67 was 5% (range 1–90%). Krenning score was 0 in 36%, 1 in 7%, 2 in 18%, 3 in 14%, and 4 in 25%. Overall, 11 patients (39%) achieved Krenning ≥3, meeting criteria to be considered eligible for PRRT. Main exclusion causes were insufficient uptake (61%), impaired organ function, or discordant lesions.
Discussion: Our findings are consistent with previous studies demonstrating high sensitivity and specificity of Tc-99m HYNIC-TOC for NET imaging [1,3]. Although 68Ga-DOTATATE PET remains the most sensitive and accurate modality for staging and detection of occult primaries [2], its limited availability in developing countries supports the use of Tc-99m EDDA/HYNIC-TOC as a valid and accessible alternative [4]. In our cohort, approximately 4 out of 10 patients were eligible for PRRT, underscoring its clinical impact in patient selection.
Conclusion: Tc-99m HYNIC-TOC scintigraphy identified 39% of patients with NETs as candidates for 177Lu-DOTATATE therapy. This method represents a feasible and accessible approach in clinical practice, with the potential to expand theranostic access in Latin America.

References

1. Al Bulushi N, Al Suqri B, Al Aamri M, Al Hadidi A, Al Jahdami H, Al Zadjali M, Al Risi M. Diagnostic accuracy of technetium-99m-octreotide in imaging neuroendocrine tumors: Oman hospital experience with literature review. World J Nucl Med. 2019;18(2):137–142. doi:10.4103/wjnm.WJNM_36_18

2. Etchebehere EC, de Oliveira Santos A, Gumz B, et al. 68Ga-DOTATATE PET/CT, 99mTc-HYNIC-octreotide SPECT/CT, and whole-body MR imaging in detection of neuroendocrine tumors: a prospective trial. J Nucl Med. 2014;55(10):1598–1604. doi:10.2967/jnumed.114.144543
3. Liepe K, Becker A. 99mTc-Hynic-TOC imaging in the diagnostic of neuroendocrine tumors. World J Nucl Med. 2018;17(3):151–156. doi:10.4103/wjnm.WJNM_6_18
4. Briganti V, Cuccurullo V, Berti V, Di Stasio GD, Linguanti F, Mungai F, Mansi L. 99mTc-EDDA/HYNIC-TOC is a new opportunity in neuroendocrine tumors of the lung (and in other malignant and benign pulmonary diseases). Curr Radiopharm. 2020;13(3):166–176. doi:10.2174/1874471013666191230143610

Conflict of Interest
No disclosures

O60

Biochemical Variability in the Response to [177Lu]Lu-iPSMA in Heavily Pretreated Patients: Real-World Experience

Dr. Edgar Hernandez[1], Dr. Francisco Osvaldo García Pérez[1], Dra. Irma Soldevilla Gallardo[2], Dra. Quetzali Gabriela Pitalua Cortés[3], Dra. Sofía Denisse Gonzalez Rueda[1]
[1]INCan, Cdmx, México, [2]ABC, CDMX, México, [3]Medica Sur, CDMX, México

Oral presentations 4: Therapy and Radioguided Procedures, Barahona Room 2, February 15, 2026, 8:00 - 10:00

Introduction: Prostate-specific membrane antigen (PSMA)–targeted radioligand therapy, particularly with [177Lu]Lu-iPSMA, has demonstrated clear benefits in overall survival and quality of life. However, real-world experience shows that outcomes can vary considerably depending on patient selection profiles. Patients receiving radioligand therapy are typically heavily pretreated with chemotherapy, next-generation hormonal agents, or PARP inhibitors. This heterogeneity influences response, tolerability, and the duration of clinical benefit, making the evaluation of outcomes outside the controlled environment of clinical trials crucial to understanding the true impact of this therapy.
Objective: To assess the effectiveness of [177Lu]Lu-iPSMA in real-world settings in patients with castration-resistant prostate cancer (mCRPC), through biochemical response of prostate-specific antigen (PSA).
Methodology: This was an observational, retrospective, analytic, multicenter study across three institutions in Mexico City, including 63 patients with mCRPC previously treated with ADT, next-generation antiandrogen, and/or taxane-based chemotherapy between 2019 and 2025. The median age was 70 years (range: 53–92). Patients received between 1 and 6 cycles of targeted therapy based on VISION trial selection criteria, with PSA measured pre- and post-therapy.
Results: Among the 63 patients, a PSA reduction greater than 50% was observed in 42.8% (n=27); PSA increase greater than 50% in 39.6% (n=25); and 17.4% (n=11) had changes between −49% and +49%. Fig. 1. There were no significant differences in hemoglobin, platelet, or leukocyte values postherapy. 35 of patients experienced fatigue (55%), 12 abdominal pain (19%), 10 nausea (15%), and 7 diarrhea (11%).
Conclusions: [177Lu]Lu-iPSMA–based therapies show good biochemical correlation with a decrease in the tumor marker PSA. However, response rates are lower compared to controlled studies; this underestimation may be explained by the use of previous treatment regimens and the presence of disease.

References

1. Sartor O, de Bono J, Chi KN, Fizazi K, Herrmann K, Rahbar K, et al. Lutetium-177–PSMA-617 for Metastatic Castration-Resistant Prostate Cancer. New England Journal of Medicine [Internet]. 2021 Jun 23;385(12):1091–103. Available from: https://www.nejm.org/doi/full/10.1056/nejmoa2107322.
2. National Comprehensive Cancer Network. (2025). NCCN Clinical Practice Guidelines in Oncology (NCCN Guidelines®): Prostate Cancer (Version 2.2025, April 16, 2025).

Conflict of Interest
we don´t have conflict of interest in this paper

Graphic

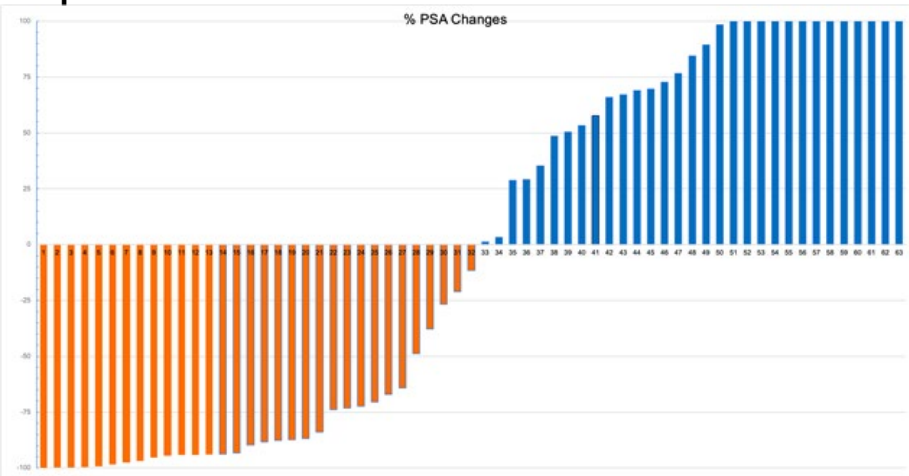

O61

Role of 18F-PSMA-(Pylclari) and 68Ga-PSMA-11 PET-CT in the staging of high-risk prostate cancer

Javier Jesus Robles Barba[1], Juan José Martín Marcuartu[1], **Dr. Carlos Andrés Tapias Mesa**[1], Jorge Luis Díaz Moreno[1], Andrea Bagan Trejo[1], Marta Zamorano Rivas[1], David Durany Lara[2], María Pane Foix[3], Jose Francisco Suarez Novo[4], Montserrat Cortes Romera[1]

[1]Servicio de Medicina Nuclear / PET (IDI). Hospital Universitario de Bellvitge, L'Hospitalet de Llobregat, Spain, [2]Servicio de Radiología. Hospital Universitario de Bellvitge, L'Hospitalet de Llobregat, Spain, [3]Servicio de Anatomía Patológica. Hospital Universitario de Bellvitge, L'Hospitalet de Llobregat, Spain, [4]Servicio de Urología. Hospital Universitario de Bellvitge, L'Hospitalet de Llobregat, Spain

Oral presentations 5: Oncology 1 (NETs and Prostate), Arsenal Room, February 15, 2026, 12:15 - 14:15

Background/Aims: To assess the usefulness of PET-CT with 18F-PSMA-(Pylclari) and 68Ga-PSMA-11 in the staging of high-risk prostate cancer (HRPC): its impact on therapeutic management, concordance with pathology (PA) and conventional imaging techniques (CIT), and a comparative study of the performance of both radioligands.
Methods: Fifty patients (age range: 53-79, median 67) performed a PET-CT for HRPC staging on a GE Discovery MI PET-CT, with 18F-PSMA-(Pylclari) (29/50) or 68Ga-PSMA-11 (21/50). Agreement with PA (PAA), in-site agreement (ISA) in prostate with MRI, and out-site agreement (OSA) in the whole-body imaging with the available CIT (CT, bone scintigraphy or MRI) were assesed. Discrepancies were classified as major (only one of the techniques was positive) or minor (both techniques positive but showing different number of lesions or degree of extension). Change in therapeutic management attributable to PSMA-PET was assessed. Efficacy of both radioligands was compared.
Results: All patients had a positive local test (50/50, PAA 100%). ISA with MRI was 78% (39/50), with minor discrepancies in 10/11 cases and major discrepancy in 1 case (negative on MRI, positive on PET-PSMA with confirmatory PA). OSA with TIC was 62% (31/50); all discrepancies found here were major, 11/19 due to dissemination not visible on TIC (upstaging); 7/19 due to negative PSMA PET of suspicious lesions described in TIC (downstaging), and 1/19 due to the presence of a synchronous tumor of non-prostatic origin (chondrosarcoma). PSMA-PET led to changes in therapeutic management in 32% (16/50), with no significant differences between 18F-PSMA-(Pylclari) (31%) and 68Ga-PSMA-11 (33%).
Conclusions: PET-CT with PSMA radioligands proved to be highly useful in staging HRCP, showing high local agreement with AP and MRI, and improved performance compared to CIT in the whole-body study. This led to a change in therapeutic management in one-third of patients, with no significant differences found when using 18F-PSMA-(Pylclari) or 68Ga-PSMA-11.

Conflict of Interest
None

O62

99mTc-HYNIC-iPSMA SPECT/CT in Prostate Cancer: A Real-World Data Multicentric Study in 457 Mexican Patients

Dr. Joel Vargas Ahumada[1], Dr. Luis Vargas Rodriguez[1], Dr. Sergio López Buenrostro[2], Dr. Paola Vallejo Armenta[1], Dr. Ana L. Calderón Ávila[3], Dr. Eleazar Ignacio Álvarez[4], Dr. Fabrio A. Sinisterra Solis[1]
[1]Imagenologia Diagnóstica, Xalapa, México, [2]Unidad de Patología Clínica, Guadalajara, México, [3]Centro Médico Nacional Siglo XXI, Ciudad de México, México, [4]Hospital Almater, Mexicali, México

Oral presentations 5: Oncology 1 (NETs and Prostate), Arsenal Room, February 15, 2026, 12:15 - 14:15

Background / Objectives: In developing countries, PET/CT access is limited due to high costs and scarce availability, restricting advanced molecular imaging in prostate cancer (PCa). SPECT/CT with 99mTc-labeled PSMA ligands is a cost-effective alternative. This multicentric study evaluated the diagnostic performance and clinical impact of 99mTc-HYNIC-iPSMA SPECT/CT in Mexican patients.
Methods: Retrospective multicentric study(3 centers) included 457 patients with histologically confirmed or clinically suspected PCa who underwent 99mTc-HYNIC-iPSMA SPECT/CT between 2023–2025. Indications were clinical suspicion (n=52), staging (n=287), restaging (n=26), biochemical recurrence (BCR)(n=50), treatment response (n=18), hormone-sensitive (n=12), and castration-resistant PCa (CRPC)(n=12). Clinical data, imaging findings, lesion distribution, and therapeutic impact were analyzed. Target-background ratio (TBR) and PRIMARY scores were correlated with clinical and histopathological variables.
Results: Mean age was 69.7 ± 8.4 years; mean PSA 10.7 ng/dl. PSMA-avid lesions were detected in 99.7% of staging cases, 96.2% in restaging, 70% in BCR, and 100% in CRPC. Bone involvement was higher in CRPC (66.7%) ($p<0.001$). In 22% of cases with prior imaging, management changed in 63.6% after SPECT/CT. Secondary malignancies were detected in 5%. TBR correlated with ISUP grade ($p<0.001$). In BCR, detection rates according to PSA were: 44% for <0.5 ng/ml, 63% for 0.5–1.0, 92% for 1.1–4.99 and 100% for ≥5.0. Clinical suspicious cases with PRIMARY scores of 1 and 2 had a negative biopsy result (100%); those with PRIMARY scores 3, 4, and 5, 50%, 72%, and 100% had a positive biopsy. A TBR ≥8.79 indicated significant malignancy (sensitivity 80%; specificity 100%; NPV58.8%; PPV 100%).
Conclusions: 99mTc-HYNIC-iPSMA SPECT/CT demonstrated high detection rates across diverse clinical scenarios, influenced therapeutic decisions, and identified secondary malignancies. The use of PRIMARY score yielded outstanding diagnostic accuracy in patients with suspected PCa. Considering its lower cost and wider accessibility, this modality represents a valuable diagnostic tool for PCa management in resource-limited healthcare systems.

Conflict of Interest
There is no conflict of interest

Graphic

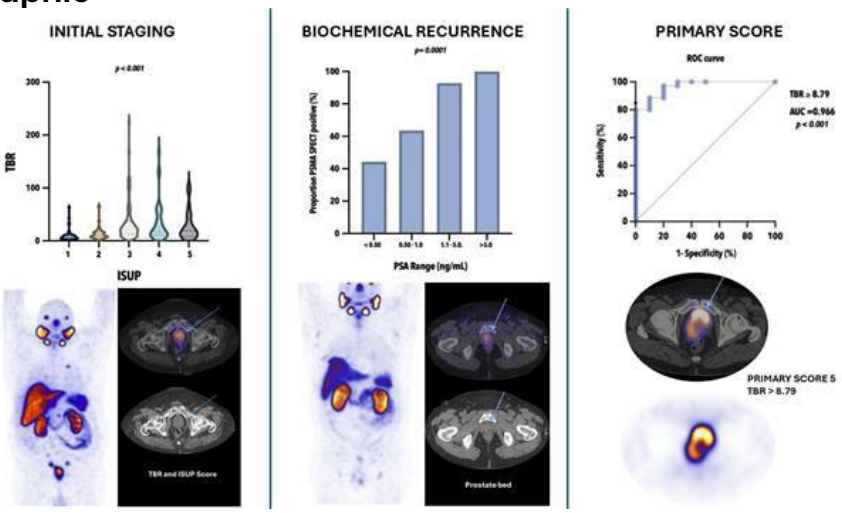

Table

Table 1. Analysis of SPECT/CT with ^{99m}Tc-iPSMA in prostate cancer scenarios

Number of bone lesions	PSA elevation n= 52	Staging n= 287	Re-staging n= 26	BCR n= 50	HSPC n= 12	CRPC n= 12	Treatment response n= 18	p
≥1 positive lesion	37 (71.2)	286 (99.7)	25 (96.2)	35 (70)	9 (75)	12 (100)	11 (61.1)	<0.001*
Uptake								
No	5 (9.6)	2 (0.7)	3 (11.5)	24 (48)	4 (33.3)	3 (25)	8 (44.4)	
Prostate	47 (90.4)	285 (99.3)	23 (88.5)	12 (24)	8 (66.7)	9 (75)	10 (55.6)	<0.001*
Prostate bed	0	0	0	14 (28)	0	0	0	
Extra prostatic (seminal vesicles, bladder and/or rectum)	12 (23.1)	97 (33.8)	7 (26.9)	3 (6.0)	2 (16.7)	5 (41.7)	6 (33.3)	0.281*
Locoregional lymph nodes	5 (9.6)	68 (23.7)	8 (30.8)	6 (12)	4 (33.3)	4 (33.3)	3 (16.7)	0.695*
Lymph nodes M1	2 (3.8)	44 (15.3)	6 (23.1)	4 (8.0)	4 (33.3)	7 (58.3)	4 (22.2)	0.002*
Bone	4 (7.7)	42 (14.6)	10 (38.5)	4 (8.0)	4 (33.3)	8 (66.7)	6 (33.3)	<0.001*
Number of bone lesions 1	0	9 (3.1)	2 (7.7)	3 (6.0)	1 (8.3)	1 (8.3)	0	<0.001*
2 – 5	0	11 (3.8)	2 (7.7)	1 (2.0)	1 (8.3)	1 (8.3)	0	
6 – 20	1 (1.9)	8 (2.8)	3 (11.5)	0	0	1 (8.3)	0	
> 20 or diffuse	3 (5.8)	14 (4.9)	3 (11.5)	0	2 (16.7)	5 (41.7)	6 (33.3)	
Visceral	0	5 (1.7)	0	1 (2.0)	1 (8.3)	1 (8.3)	0	0.235*
Lung	0	4 (1.4)	0	1 (2.0)	1 (8.3)	0	0	0.069*
Liver	0	0	0	0	0	1 (8.3)	0	
TBR in prostate °	14.30 (7.30 – 37.90)	14.80 (7.70 – 27.70)	19.40 (9.75 – 56.20)	10.40 (7.34 – 23.87)	7.60 ± 3.62 (4.57 – 10.63)	10.60 (5.20 – 25.44)	9.0 (4.87 – 18.87)	0.076

° Mediana (percentil 25 – 75), prueba U Mann Whitney

* The chi-square test for linear trend

O63

Prospective head-to-head comparison of 18F-PSMA -1007 and 18F-DCFPyl PET/CT for primary skeletal staging in high risk prostate cancer

Dr. Marko Seppänen[1], Simona Malaspina[1], Ekaterina Saukko[2], Tommi Noponen[3], Jukka Kemppainen[1], Mikael Anttinen[4], Suvi Hartikainen[5], Janne Salonen[6], Peter Boström[4], Otto Ettala[4]

[1]Turku PET Centre, University of Turku, Turku University Hospital, Turku, Finland, [2]Department of Radiology, Turku University Hospital and University of Turku, Turku, Finland, [3]Department of Clinical Physiology, Nuclear Medicine, Turku PET Centre and Medical Physics, Turku University Hospital, Turku, Finland, [4]Department of Urology, University of Turku and Turku University Hospital, Turku, Finland, [5]Department of Clinical Physiology and Nuclear Medicine, Kuopio University Hospital, Kuopio, Finland, [6]Department of Nuclear Medicine, University of Helsinki and Helsinki University hospital, Helsinki, Finland

Oral presentations 5: Oncology 1 (NETs and Prostate), Arsenal Room, February 15, 2026, 12:15 - 14:15

Background/Aims: Nonspecific bone uptakes (UBU) without anatomical correspondence are frequently reported, particularly with 18F-PSMA-1007 tracer, which may lead to inappropriate disease upstaging. The aim of this prospective study is to characterize the nature of 18F-PSMA-1007 PET-CT skeletal uptakes using 18F-DCFPyL PET-CT as a reference in primary staging of high-risk prostate cancer.
Methods: This ongoing study enrolled 34 men with high-risk prostate cancer (EUDRA-CT 2021-000486-33; NCT06219746). Most patients had ISUP grade 4 or 5 (88%), and the median PSA level was 9 ng/mL (IQR 9–23). All participants underwent 18F-PSMA-1007 and 18F-DCFPyL PET/CT scans within one week. Images were reviewed side-by-side, and the maximum standardized uptake value (SUVmax) of lesions in identical skeletal locations—both with and without anatomical correspondence—were analyzed and classified according to the PROMISE criteria.
Results: A total of 141 bone uptakes were identified, of which 50 (35%) had anatomical correspondence, while 91 (65%) did not. For uptakes with anatomical correspondence, the median SUVmax on 18F-PSMA-1007 PET was 23 (IQR 17–30), and 18 (IQR 14–22) on 18F-DCFPyL PET ($p < 0.001$). For uptakes without anatomical correspondence, the median SUVmax on 18F-PSMA-1007 PET was 5.2 (IQR 4.3–6.6), also higher than the median SUVmax of 1.8 (IQR 1.5–2.4) on 18F-DCFPyL PET ($p < 0.001$).
Most 18F-PSMA-1007 PET uptakes without anatomical correspondence (N = 84, 92%) had a PSMA expression score of 0 or 1, and none of these had a score greater than 1 on 18F-DCFPyL PET. Of the remaining uptakes, five that scored 2 and two that scored 3 on 18F-PSMA-1007 PET corresponded to scores of 1 (n=5), 2 and 3 on 18F-DCFPyL PET, respectively.

Conclusions: UBUs on 18F-PSMA-1007 PET that are lower than spleen and lack anatomical correspondence should be interpreted as benign. However, further research is needed to determine when these uptakes may represent true metastases.

Conflict of Interest
Invited lecturer by GE Healthcare, Astellas, Janssen-Cilag Oy, and Bayer.

O64

Validation of PET/CT with 18F-NOTA-Oc and 18F-FDG for obtaining the "NETPET score" as a prognostic biomarker in neuroendocrine neoplasms

Dr. Francisco Jesus Solano Caballero[1], Dr. Rodrigo Hernández Ramírez[1], Dr. Juan Pablo Chávez Torres[1], Dra. Natalia Ramírez Pedraza[1], Dra. Ailan Hitandhui Barrientos Priego[1], Dr. Miguel Angel Corza Ayala[1], Dra. Abigail Arriaga Contreras[1]
[1]Instituto Nacional De Ciencias Médicas Y Nutrición Salvador Zubirán, Tlalpan, Mexico

Oral presentations 5: Oncology 1 (NETs and Prostate), Arsenal Room, February 15, 2026, 12:15 - 14:15

Background/Aims: Neuroendocrine neoplasms (NEN) are rare tumors with heterogeneous clinical behavior. Dual-tracer PET/CT with ^{18}F-NOTA-Oc (a somatostatin analog tracer) and ^{18}F-FDG allows calculation of the NETPET score, a five-category grading scheme proposed as a prognostic biomarker in NEN. The aim of this study was to assess the prognostic value of the NETPET score in NEN patients by correlating it with survival outcomes.
Methods: A retrospective, analytical study was conducted in 51 patients with histologically confirmed NEN at a tertiary center (2020–2025). All patients underwent dual PET/CT with ^{18}F-NOTA-Oc and ^{18}F-FDG. The NETPET score was calculated for each case and categorized as low (P1–P3) or high (P4–P5). The association between NETPET score and survival was analyzed using contingency tables, Kaplan-Meier curves, and log-rank tests.
Results: All patients with a low NETPET score (P1–P3) were alive at last follow-up, whereas the majority with a high score (P4–P5) had died[6]. A high NETPET score was associated with worse prognosis, with significantly shorter overall survival compared to the low-score group (log-rank $p < 0.0001$). The estimated median survival for the high NETPET group was ~12.5 months, whereas median survival was not reached in the low-score group (not attained due to low mortality).
Conclusions: The NETPET score obtained from dual-tracer PET/CT proved to be a useful non-invasive prognostic biomarker in NEN. A high NETPET score correlated with higher mortality and shorter survival, whereas a low score indicated a favorable prognosis. These findings support the use of the NETPET score for prognostic risk stratification of NEN patients in clinical practice.

Conflict of Interest
The authors declare no conflict of interest.

Graphic

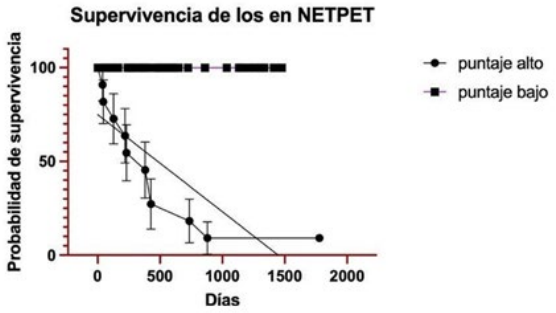

Gráfica 1. Probabilidad de supervivencia Kaplan-Meier con IC del 95% en pacientes con puntaje alto y bajo.

O65

[99mTc]Tc-HYNIC-PEG4-ATWLPPR/Tricine peptide as a potential diagnostic agent for prostate cancer: In vitro evaluation

Mrs. Carolina Perroni Zanoniani[1], Dr Ximena Camacho[1], Dr Mirel Cabrera[1], Dr Lucía Alfaya[1], Dr Marcos Tassano[1], Dr Juan Pablo Gambini[3], Dr Pablo Cabral[1]
[1]Departamento de Radiofarmacia, Centro de Investigaciones Nucleares, Facultad de Ciencias, Universidad de la República, Montevideo, Uruguay, [2]Centro Uruguayo de Imagenología Molecular, Montevideo, Uruguay, [3]Centro de Medicina Nuclear e Imagenología Molecular Hospital de Clínicas, Facultad de Medicina, Universidad de la República, Montevideo, Uruguay, Montevideo, Uruguay

Oral presentations 5: Oncology 1 (NETs and Prostate), Arsenal Room, February 15, 2026, 12:15 - 14:15

Background/Aims: The heptapeptide (Ala-Thr-Trp-Leu-Pro-Pro-Arg) ATWLPPR anti-Neuropilin-1 (NRP-1) is one of the inhibitors of tumor angiogenesis process. It is capable of increasing VEGF/VEGFR-2 binding by up to 10 times and promoting vascularization in prostate tumors. NRP-1 is highly overexpressed in prostate cancer (PC) subtypes. We report the in vitro evaluation of a novel peptide targeting NRP-1, radiolabeled with [99mTc]Tc, as a potential diagnostic agent for PC.
Methods: The peptide [HYNIC-PEG4-ATWLPPR] was radiolabeled with [99mTc] TcO_4^- (74-300 MBq) using Tricine as coligand (50°C, 10 min). Radiochemical purity (RCP) was assessed by HPLC and ITLC-SG. Lipophilicity (Log D) was determined via octanol/PBS partition. Stability studies were performed in human serum, PBS, and L-Cysteine (0.1 and 1 mM) at 37°C for 24 h. For testing cell adhesion, PC cell lines (LnCap and PC3) were exposed to the radiotracer at 37°C. The assessment of membrane attachment and internalization was done at intervals of 15, 30, 60, 90, and 120 min employing an acid wash method using 0.2 M glycine buffer (pH of 2. 8), and lysis (1M NaOH). Specificity was confirmed by blocking with excess unlabeled peptide.
Results: Radiolabeling achieved RCP 98% (HPLC). Log D (-2.10 ± 0.15) confirmed high hydrophilicity. The peptide remained stable in serum (over 95% RCP at 24 h) and PBS, with minimal transchelation in L-Cysteine (over 5% and 10% degradation). Time-dependent binding was observed in evaluated cell lines. Internalization was limited (<5% at 120 min), with predominant membrane localization. Blocking reduced binding by <50%, confirming receptor specificity.
Conclusions: The [99mTc]Tc-HYNIC-PEG4-ATWLPPR/Tricine peptide demonstrates excellent in vitro performance: high radiochemical yield, favourable hydrophilicity, stability in biological media, and specific, high-affinity binding to PC cells. Its minimal internalization supports rapid target-to-background contrast for SPECT imaging, validating its potential as a diagnostic radiotracer for BC, particularly for tumors expressing NRP-1.
Acknowledged: ANII-Uruguay (POS_NAC_2024_1_183380), PEDECIBA-QUIMICA, CSIC-Uruguay.

Conflict of Interest
All authors manifest no conflict of onterest

O66

Results from a Prospective Phase I Clinical Trial on [68Ga]Ga-OncoACP3 in Prostate Cancer: Safety, Dosimetry, Pharmacokinetics and Diagnostic Performance

Dr. Cristiano Pini[1], Dr. Fabrizia Gelardi[1], Prof. Martina Sollini[1,2], Dr. Anna Piai[3], Dr. Rita Petrelli[2], Prof. Paola Anna Erba[4,5], Dr. Jacqueline Mock[6], Dr. Samuele Cazzamalli[6], Dr. Dario Neri[6], Prof. Arturo Chiti[1,2]

[1]Vita-salute San Raffaele University, Milan, Italy, [2]Department of Nuclear Medicine, IRCCS Ospedale San Raffaele, Milan, Italy, [3]Medical Physics Department, IRCCS Ospedale San Raffaele, Milan, Italy, [4]School of Medicine and Surgery, University of Milano-Bicocca, Milan, Italy, [5]Nuclear Medicine Unit, ASST Papa Giovanni XXIII Hospital, Bergamo, Italy, [6]Philochem AG, Otelfingen, Switzerland

Oral presentations 5: Oncology 1 (NETs and Prostate), Arsenal Room, February 15, 2026, 12:15 - 14:15

Background/Aims: Acid Phosphatase 3 (ACP3) is an emerging promising theranostic target in prostate cancer (PCa), expressed on PCa cells across most primary and metastatic lesions. ACP3 shows higher, more homogeneous expression than PSMA in low- and high-ISUP-grade tumours and in metastases, while not being expressed in healthy organs such as salivary glands, kidneys, and gastrointestinal tract.
We present data from a multicentre, prospective phase I clinical trial investigating safety, dosimetry, pharmacokinetics, and diagnostic performance of [68Ga]Ga-OncoACP3, a high-affinity ligand of ACP3 discovered from DNA-Encoded Chemical Libraries, in PCa.
Methods: We plan to enrol 20 patients with a confirmed diagnosis of PCa in two cohorts: Cohort A, 5 patients with primary tumour only; Cohort B, 15 patients with or without metastatic disease.
Patients receive an intravenous administration of 250 MBq [68Ga]Ga-OncoACP3, followed by PET/CT imaging at 0-20, 60-, and 120-min post-injection. Blood and urine samples are collected to assess pharmacokinetics. Adverse events are reported per CTCAEv5.0.
When available, results are compared to PSMA PET and correlated with follow-up data and pathological findings.
Results: As of September 15th, 17 patients completed [68Ga]Ga-OncoACP3 PET imaging: 8 for initial staging, 7 for biochemical relapse, and 2 for metastatic disease.
No adverse events occurred.
[68Ga]Ga-OncoACP3 showed mixed hepatobiliary/renal excretion, with no uptake in salivary glands.
All confirmed PSMA-positive lesions were evident at [68Ga]Ga-OncoACP3, in most cases with a higher tumour-to-background. In three cases, [68Ga]Ga-OncoACP3 PET detected additional PCa lesions. No area of unspecific bone uptake at PSMA PET was evident at [68Ga]Ga-OncoACP3. Details on patient characteristics, PSMA and ACP3 PET results are presented in Table 1.

Conclusion: [68Ga]Ga-OncoACP3 resulted safe and showed favourable biodistribution and targeting for PET imaging of PCa. [68Ga]Ga-OncoACP3 may outperform current PSMA-targeting modalities across the whole natural history of the disease, and particularly in theranostic applications.

Conflict of Interest

A. Chiti: Advisor to Telix Pharmaceuticals, Blue Earth Diagnostic, Innova Radi Thrapeutic; Speaker for Bracco Diagnostics, General Electric, Novartis, Telix Pharmaceuticals, United Imaging

J. Mock, S. Cazzamalli, A. Ciamarone, F. Migliorini, D. Neri: Employees of Philochem AG D. Neri: Shareholder of Philogen S.p.A.

Table

Patient	Age	Disease status	Previous treatments	ISUP-GG	PSA	PSMA results	ACP3 results
#1	74	BCR	RP+LAD	3	0.26	Positive for local relapse	Positive for local relapse
#2	61	Metastatic disease	RP+LAD; salvage RT; RT su 3 bone lesions; enantone	5	5.26	Faint uptake on paracaval adenopathy and bone lesion	Intense uptake on paracaval adenopathy and bone lesion
#3	64	Metastatic disease	RP+LAD; RT on choline-PET+ N; enantone	3	8.9	Multiple adenopathies, bone lesions, lung lesion	Multiple adenopathies, bone lesions, lung lesion
#4	78	Staging	None	2	5.67	Inhomogeneous prostate uptake; multiple UBUs	Diffuse intense prostate uptake; no UBUs
#5	64	Staging	None	2	3.564	Inhomogeneous faint prostate uptake	2 areas of focal prostatic uptake
#6	70	Staging	None	2	3.16	Inhomogeneous faint prostate uptake	Inhomogeneous faint prostate uptake
#7	62	BCR	RP+LAD	2	0.25	Faint uptake on bone lesion	Intense uptake on bone lesion
#8	63	BCR	RP+LAD	5	1.982	Multiple locoregional adenopathies	Multiple locoregional adenopathies
#9	77	BCR	RP+LAD; salvage RT	3	0.611	Negative; multiple UBUs	Uncertain focal post-surgical uptake on abdominal wall; no UBUs
#10	63	Staging	None	2	4.02	Inhomogeneous prostate uptake; UBUs	Intense focal prostate uptake; no UBUs
#11	64	Staging	None	5	19.6	Multifocal prostate uptake; locoregionals adenopathies	Multifocal prostate uptake with seminal vesicle invasion; locoregionals adenopathies
#12	49	Staging	None	5	7.9	Multifocal prostate uptake	Multifocal prostate uptake
#13	60	BCR	RP+LAD	3	0.21	2 adenopathies; 1 bone lesion	2 adenopathies; 1 bone lesion
#14	72	BCR	RT	1	0.3	Negative; multiple UBUs	Negative; no UBUs
#15	70	BCR	RP+LAD	3	1.05	Local relapse; UBUs	Local relapse; no UBUs
#16	69	BCR	RP+LAD	4	0.23	Single bone metastasis	Single bone metastasis
#17	75	Staging	None	4	6.09	Negative	2 areas of focal prostatic uptake

Table 1. Baseline characteristics, PSMA and [^{68}Ga]Ga-OncoACP3 PET results of enrolled patients.

Abbreviations. BCR: biochemical relapse; ISUP-GG: international society of urological pathology grade group; PSA: prostate-specific antigen; RP+LAD: radical prostatectomy and lymphadenectomy; RT: radiotherapy; UBUs: unspecific bone uptakes.

O67

Prostate Tumor Volume by 68Ga-PSMA PET/CT as a Predictor of Lymph Node Metastases in High-Risk Prostate Cancer

Dr. Angie Paola Llanos Cuellar[1], Ana Milena Gualdrón-Naranjo[1], Liliana Patricia Torres-Agredo[2], Humberto Varela-Ramirez[2], Alejandra Gomez-Marting[1], Helen Johanna Mejia-Efeer[1], Milton Yesid Gomez-Buitrago[1], Marco Antonio Parra-Pérez[1]
[1]Fundación Universitaria Sanitas, Bogotá, Colombia, [2]Instituto Nacional de Cancerología, Bogotá, Colombia

Oral presentations 5: Oncology 1 (NETs and Prostate), Arsenal Room, February 15, 2026, 12:15 - 14:15

Background /Aims: Prostate cancer is the most common malignancy in men and a growing public health concern in Colombia. Precise staging is critical for therapeutic decisions. 68Ga-PSMA PET/CT has shown superiority over conventional imaging in detecting lymph node metastases. Prostate tumor volume (PSMA-TV) has emerged as a biomarker of metastatic burden, but evidence in Latin American populations is limited. This study aimed to evaluate the association between PSMA-TV and lymph node metastases in high-risk prostate cancer patients at initial staging.
Methods: We performed a retrospective study of 45 high-risk patients treated at the National Cancer Institute (2020–2024). All underwent 68Ga-PSMA PET/CT followed by radical prostatectomy with lymphadenectomy. Clinical, biochemical, and histopathological data were analyzed. ROC curve analysis was applied to determine the optimal PSMA-TV cutoff predicting nodal metastases.
Results:Mean age was 63.9 years and mean PSA was 25.9 ng/ml. PSMA PET/CT detected lymph node metastases in 35.6% of patients, while histopathology confirmed nodal involvement in 33.3%. Mean SUVmax was 12.6 and mean PSMA-TV 15.9 cm^3. ROC analysis identified a PSMA-TV cutoff ≥9 cm^3, yielding 66.7% sensitivity and 55.6% specificity (AUC 0.5; 95% CI 0.3–0.7). Patients above this threshold showed a higher probability of nodal disease, confirming a significant correlation between PSMA-TV and regional spread.
Conclusions: PSMA-TV quantified by 68Ga-PSMA PET/CT correlates significantly with lymph node metastases in high-risk prostate cancer. These findings highlight its potential as a prognostic biomarker and complementary tool in initial staging, providing pioneering evidence from Latin America to optimize therapeutic decision-making.

Conflict of Interest
The authors declare no conflicts of interest

Graphic

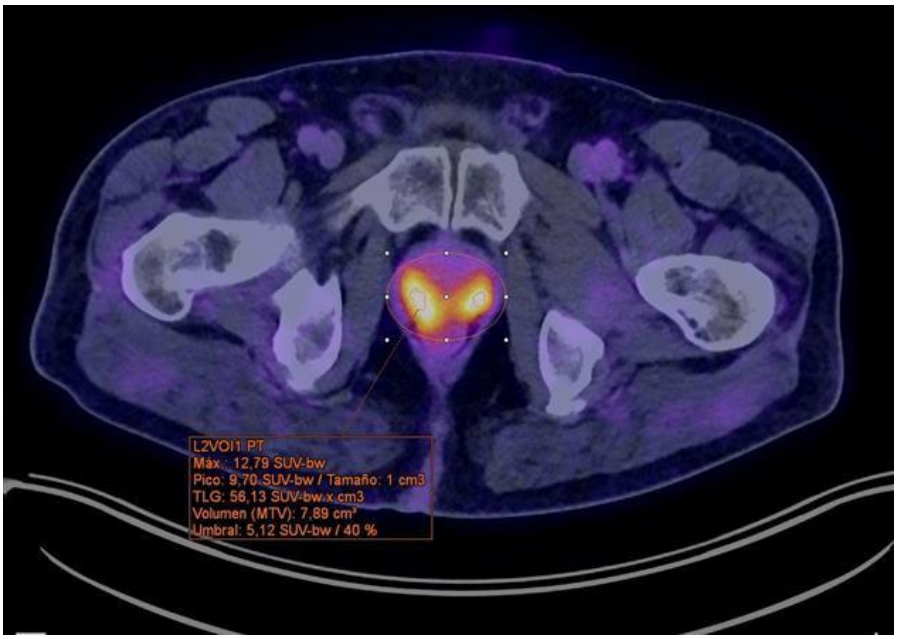

Table

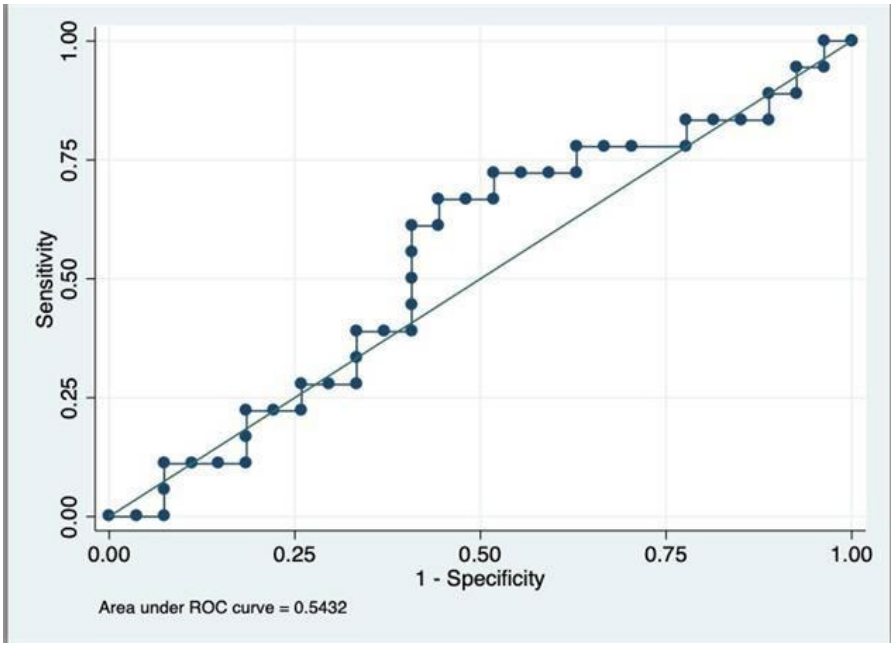

O68

Usefulness of Fluoride PET CT 18F-Alf Nota on suspicion of well-differentiated neuroendocrine tumors (NETs)

Dr. Francisco Gomez[1], Dr. Alejandro Rojas[1], Dr. Juan Dupouy[1], Dr. Teresa Massardo[1], Dr. Jose Tomas Donoso[1], Dr. Paloma Peña[1], Dr. Evelyn Ortiz[1], Dr. Francisco Tortorolo[1], Dr. Rocio Hidalgo[1], Ms. Sofia Rivas[1]
[1]Hospital Clinico Universidad De Chile, Santiago, Chile

Oral presentations 5: Oncology 1 (NETs and Prostate), Arsenal Room, February 15, 2026, 12:15 - 14:15

Introduction: Current guidelines state that somatostatin receptor (SSTR) PET is not indicated for screening without prior histological confirmation. This recommendation is based on the low prevalence of NETs in the general population and the potential for false positives. In MEN-1 carriers, there is good performance, up to 91% detection. In Chile, we dispose of 18FAlf-Nota (FAN). Goal: To assess PET-CT FAN usefulness in patients with clinical and morphological high suspect of well-differentiated NET.
Method: Since May 2023, we performed 88 SSTR PET-CT and 25 corresponded to NET suspicion; FAN images were reported and the features were classified by organ, local and distant dissemination as well as biopsies recorded when available and also their subsequent change of management. Age range:34-81 y.o (12 males/13 females).
Results: Most patients presented abdominal discomfort or gastrointestinal bleeding and had abdominal imaging, mostly CT, with a possible NET lesion. FAN was positive in 17/25 cases, with focal uptake in pancreas(8), ileum(5), jejunum(1), cecum(1) and stomach(1); positive lymph nodes were present in 11 cases and distant uptake observed in 2. We obtained histological confirmation of Grade I or II NET in 9/10 biopsies concordant with the report. Change of management was conducted in 60% of 23 patients with follow-up. Interestingly, PET-CT detected 2 cases with focal uptake in solid thyroid nodules, requiring posterior assessment; 1 intrapancreatic splenulus and 1 ectopic pancreas all with marked FAN uptake. Two GIST were resected, 1 with contained perforation with mild uptake reported as negative for NET.
Conclusion: Although performing SSTR PET in the workup of NETs is not an established indication, in this small case series with FAN, this exam was relevant for confirming the diagnosis in 68%, leading to an important change in management. This reinforces the idea that in well-selected patients/high clinical suspicion, this exam could be considered.

References

[1] Haeger A, et al. Al[18F]F-NOTA-Octreotide Is Comparable to [68Ga]Ga-DOTA-TATE for PET/CT Imaging of Neuroendocrine Tumours in the Latin-American Population. Cancers (Basel). 2023 Jan 10;15(2):439.

[2] Kostiainen I, et al. Pancreatic imaging in MEN1-comparison of conventional and somatostatin receptor positron emission tomography/computed tomography imaging in real-life setting. Eur J Endocrinol. 2023;188(5):421-429.

Conflict of Interest

none

O69

[18F]SiTATE in neuroendocrine neoplasia (NEN): first Latin America experience in prostate, lung and colon NEN patients

Dr. Emiliano Michel Sánchez[1], Dr. Vikas Prasad[2], MSc Eduardo Antonio González Villa[1], BSc. Francisco Rafael Peres Anaya[1], Dr. Danny Roberto Mena Cortes[1]
[1]Oncologia San Jose, HERMOSILLO, Mexico, [2]Mallinckrodt Institute of Radiology, St. Louis, US

Oral presentations 5: Oncology 1 (NETs and Prostate), Arsenal Room, February 15, 2026, 12:15 - 14:15

Background/Aims: Neuroendocrine tumor (NET) imaging with somatostatin receptors radiotracers is widely used, frequently with 68Ga tracers. In Latin America 68Ga is not available in many regions. 18F radiopharmaceuticals development is necessary to expand the use of PET in NEN. We report our first experience with [18F] SiTATE, novel 18F-labeled somatostatin receptor-targeting radiopharmaceutical. We report here the production steps and quality control (QC) of [18F]SiTATE, as well as first results of PET/CT performance via tumor-to-mediastinal blood pool ratios in prostate, lung, and colon neuroendocrine tumors (NETs).
Methods: [18F]Fluoride was produced using a 9.6 MeV cyclotron via 18O(p,n)18F reaction on enriched [18O]water (CortecNet, France). Synthesis occurred in an automated synthesis module. Four patients (mean age 46 years; 3 male, 1 female) with suspected/confirmed NETs received 185 MBq [18F]SiTATE IV (0.1 mCi/kg). PET/CT acquired 60 min post-injection with IV contrast CT; OSEM reconstruction; Tracer uptake in lesions, mediastinal blood pool, liver, spleen, uncinate process of pancreas, pituitary and adrenal glands were analyzed. Tumor-to-blood pool ratio was calculated.
Results: Production yielded 21.9% uncorrected radiochemical yield and 100% purity (TLC). QC met GMP standards: pH 6.5-7.5, >99% purity, <400 ppm volatiles, sterile, <5 EU/mL endotoxins. No adverse events reported. Vital signs (BP, pulse, respiration) monitored during and 30 min post-infusion remained stable. Assessed for infusion reactions, hypersensitivity, nausea, and cardiovascular changes. Physiological biodistribution: mediastinal pool 2.1±0.8, liver 5.2±1.7, spleen 12.8±3.1.
Patient data showed high tumor detection with favorable contrast, detailed in a separate table.
Conclusions: In our first experience scanning four patients, [18F]SiTATE was well tolerated with no adverse events and demonstrated excellent image quality, as evidenced by high tumor-to-mediastinal blood pool ratios (2.9-12.9) and modified Krenning scores 3-4 in positive cases. These preliminary findings position [18F] SiTATE as a promising SSTR tracer to improve PET/CT accessibility for NEN in Latin America, where 68Ga availability remains limited.

Conflict of Interest
No conflicts of interest are declared

Graphic

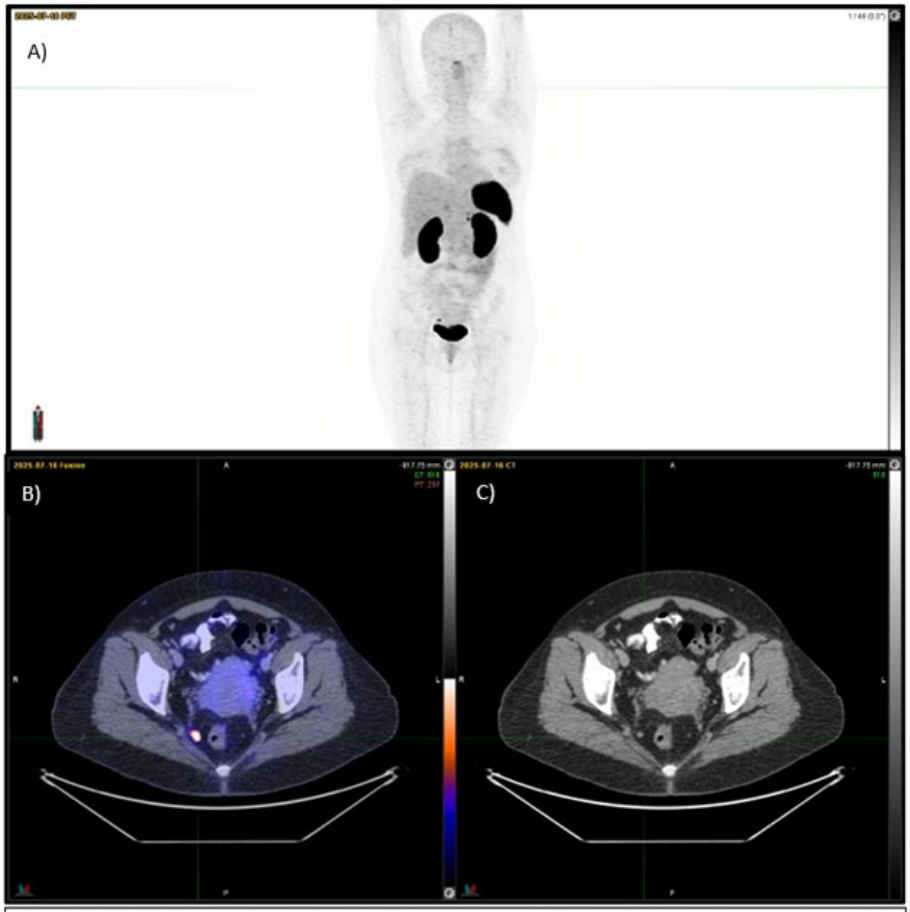

Figure 1. [18F]-SiTATE PET/CT in a 40-year-old female patient with rectal neuroendocrine tumor (restaging post-surgery and somatostatin analog). A) Whole-body MIP image showing physiological biodistribution (SUVmax spleen 15.0, liver 3.1) and a focal area of somatostatin receptor overexpression in the right pelvic region. B) Axial PET/CT fusion slice of the right mesorectum, with intense uptake in the lymph node (SUVmax 10.0, arrow; vs. mediastinal pool SUVmax 3.4 and liver 3.1), consistent with Krenning score 3. Isolated finding with no other lesions detected. C) Axial CT slice of the right mesorectum revealing a subcentimetric lymph node (7.1 mm).

Table

Patient	Diagnosis	Key Lesion	SUVmax Lesion	Mediastinal Pool	Tumor/ Pool Ratio	Krenning Score
1 (39M)	Prostate NEC	Femoral	10.0	2.2	4.5	3
2 (56M)	Pulmonary NET	Hilar mass	18.0	1.4	12.9	4
3 (48M)	Suspected gastrinoma	Negative	-	1.4	-	0
4 (40F)	Rectal NET	Mesorectal node (7.1mm)	10.0	3.4	2.9	3

O70

Clinical Impact Of 18F-PSMA-1007 PET/CT in the Evaluation of Prostate Cancer Patients: Analysis Of 511 Patients in Different Clinical Scenarios

Dr. Gerardo Dos Santos[1,2], Dra. Agustina Banchero[1], Dra. Marta Iraetha[1], Dr. Mauriel Díaz[1], Dr. César Ferreira[2], Dr. Eduardo Lischinky[2], Technician Ismael Cordero[1], Dr. Omar Alonso[1,2]
[1]Uruguayan Center of Molecular Imaging (CUDIM), Montevideo, Uruguay, [2]Nuclear Medicine and Molecular Imaging Center, Clinical Hospital "Dr. Manuel Quintela" University of Uruguay, Montevideo, Uruguay

Oral presentations 5: Oncology 1 (NETs and Prostate), Arsenal Room, February 15, 2026, 12:15 - 14:15

Background/Aims: Since the new tracer 18F-PSMA-1007 showed promising features for diagnosing prostate cancer (PCa), our goal was to assess its usefulness (detection rates) in various clinical scenarios.
Methods: 511 patients underwent a 18F-PSMA-1007 PET/CT between Jun/2020-Dic/2024:
-at initial staging (n=130,25.4%; median age: 68.3years; median PSA level: 32.6ng/mL)
-biochemical recurrence (BCR) (n=352,68.9%, median age:70.7years; median PSA level:15.0ng/mL) after radical prostatectomy (n=157, 44.6%) or radiotherapy (n=195, 55.4%);
-or evaluation for treatment of 177Lutetium-PSMA-617 (n=29; 5.7%).
Results: 18F-PSMA-1007 showed hepatobiliary clearance and limited uptake in urinary bladder.
Abnormal findings (positive rate) for Initial Staging and Biochemical Recurrence were 86.1 and 96 % (112/130 and 243/352 patients) respectively.
In the primary staging group, 18F-PSMA-1007 PET/CT detected distant metastases in 57/130 patients, both in lymph nodes (42 patients, 32.3%) and in bone lesions (35 patients, 26.9%). Notably, therapy planning was modified in 43.8% of patients.
In the BCR group, metastases were detected in 163/252 (64%) in the following sites: lymph nodes (n=97;38.5%), bone (n=89;35.3%) and prostate (n=87;48%).
Even at low PSA values (PSA<1 ng/ml), tumor activity was detected in 43/95patients (45.2%)
The detection rates for metastases for PSA levels 0-<0.5, 0.5<1, 1<2, 2<5 and >5 ng/mL were 26.3%, 41%, 35.5%, 43.7% and 61.8% respectively. Respectively values for prostate disease were 22.8%, 35.9%, 42.2%, 48.7% and 66.4%.
In the "Theragnostic" scenario, PET/CT images confirmed PSMA expression in metastatic lesions and post-therapy SPECT/CT images performed 48 hours after the inyection of 7GBq of 177Lu-PSMA-617 allowed follow up.
Conclusions: 18F-PSMA-1007 constitutes a novel and solid PET/CT radiopharmaceutical for the evaluation of PCa patients at Initial Staging and BCR, with the advantage of minimal urinary excretion and high detection rates at low PSA levels.

18F-PSMA-1007 and 177Lu-PSMA-617 seem to be a potential theragnostic tandem, concerning a treatment that have showed a benefit in overall survival and life quality improvement.

References

Gerardo Gabriel dos Santos Loureiro, Pablo Duarte Couto, Juan Pablo Gambini Gonzalez and Omar Alonso Nuñez. Intraindividual Comparison of novel 18F-PSMA-1007 and 18F-AlF-PSMA-HBED-CC PET/CT in the Prospective Evaluation of Prostate Cancer Patients with Biochemical Relapse. International Journal of Clinical Studies & Medical Case Reports. ISSN 2692-5877. DOI: 10.46998/IJCMCR.2025.53.001311. EN IMPRENTA.

Conflict of Interest

No conflict of interest

Table

Table 1. Patients characteristics and analysis.

Total Patients	n=511	100%
Initial Staging	n=130	25,4%
Age (years)	Median: 68.3 y	Range: 44-90 y
PSA (ng/mL)	Median: 32.4 ng/mL	Rangue: 0.04-1000 ng/mL
Gleason Score	Gleason Score > 6	
Treatment	Prior to treatment	
Abnormal findings	n=112/130	86.1%
Unsuspected Metastases	n=57/130	43.8%
Lymph nodes n=42; 32.3%	Bone lesions n=35; 26.9%	Prostate n=113; 86,9%
BCR	n=352	68,9%
Age (years)	Median: 70,7 y	Range: 47-94 y
PSA (ng/mL)	Median: 15 ng/mL	Range: 0.01-659 ng/mL
Treatment	Radical prostatectomy n=82; 45.5%	Radiotherapy n=98; 54.4%
Abnormal findings	n=243/252	96,0%
Metastases	n=163/252	64,0%
Lymph nodes n=97; 38.5%)	Bone lesions n=89; 35.3%)	Prostate lesions n=87; 48.0%
PSA (ng/mL) <1 ng/mL	Prostate tumor activity n=30; 32,2%	Extra-prostate metastases n=41; 44,0%
PSA (ng/mL)	Prostate tumor activity No. /Positive Results (%)	Extra-prostate metastases No. /Positive Results (%)
0 - <0.5 ng/mL	n=13; 22.8%	n=15; 26.3%
0.5 - < 1 ng/mL	n=14; 35.9%	n=16; 41.0%
1 - <2 ng/mL	n=19; 42.2%	n=16; 35.5%
2 - <5 ng/mL	n=39; 48.7%	n=35; 43.7%
>5 ng/mL	n=87; 66.4%	n=81; 61.8%
177Lu-PSMA Treatment	n=29	5,70%
Age (years)	Median: 66,8 y	Range: 50-79 y
PSA (ng/mL)	Median: 100 ng/Ml	Rangue: 64-1000 ng/mL
PET/CT Lesion Regresion	n=16	55%
PSA decrease	n=19	65%
Pain relief	n=17	58,60%
Adverse effects: (xerostomia, nausea, fatigue or thrombocytopenia)		
Mild	n=5	17%
Moderate/Severe	None	.-
Overall Survival	Under analysis	

O71

Magnitude of change in radiotherapy planning in biochemical recurrence of prostate cancer. From theoretical planned to definitive treatment post-PET-TC PSMA

Dr. Pedro Jose Plaza Lopez[1,2], Dr Francesco Amorelli[3], Dr Juan Sebastian Blanco[1], Dra Eliana Carrillo[1], Dra Natali Augusto[4], Dra Palmira Foro[2,3]
[1]Hospital del Mar. Nuclear Medicine Department, Barcelona, Spain, [2]Universitat Pompeu Fabra, Barcelona, España, [3]Hospital del Mar. Radiation Oncology Department, Barcelona, España, [4]Hospital Josep Trueta. Clinical Analysis Department, Girona, España

Oral presentations 5: Oncology 1 (NETs and Prostate), Arsenal Room, February 15, 2026, 12:15 - 14:15

To assess the impact of PET/CT-18F-DCFPyL (PSMA) on radiotherapy planning in patients with biochemical recurrence (BCR) of prostate cancer (PC) after radical prostatectomy (RP).
Materials and Methods: 85 patients with PCa with BCR after RP were retrospectively analyzed. These included patients with PSA levels of 0.2–1.0 ng/mL considered for salvage radiotherapy (SRT) and those with persistent PSA levels despite prior radiotherapy to the prostate bed (PB).
All patients underwent 18F-DCFPyL-PSMA PET/CT.
The magnitude of the impact of PSMA-PET/CT on radiotherapy planning was evaluated from theoretical intention to definitive treatment planning following the PSMA results.
Depending on the positive/negative PSMA-PET results and their location, changes in prior theoretical treatments were made or not.
Results: A total of 85 patients were included (mean age, 69 years). Positive PET/CT-PSMA results were observed in 53% (45/85) of patients. Ninety lesions were identified (21 in the PB, 48 pathological lesions in the LN, 18 bone lesions, and 3 visceral lesions) that were not detected by conventional imaging (Figure 1).
In 84.4% of positive results ($p<0.001$), treatment changes were observed after PSMA-PET/CT. The most significant changes included PSMA-guided SRT in 50% of cases, targeting pelvic LNs or oligometastatic lesions, often combined with ARSI (29%). The most commonly used radiotherapy regimens were 24Gy in 3 fractions for SBRT, 45-46Gy in PRT (dose-escalation 55Gy for pathological LN), and 66Gy (2Gy/fraction) in PB with dose escalation to 70-72Gy in PSMA-positive areas. The median change in PSA level after treatment was 0.08 ng/mL ($p<0.001$).
PSMA-PET/CT had a significant impact on radiotherapy planning . A larger volume of pelvic nodal and oligometastatic disease was detected, leading to a greater use of PSMA-guided SBRT, PRT, and PBRT with dose escalation in PSMA-positive areas.

Conflict of Interest
no conflict of interest

Graphic

Figure 1: Positive patient detection rate of PET/TC 18F-DCFPyL PSMA by location (a total of 90 lesions not evidenced by conventional radiological study)

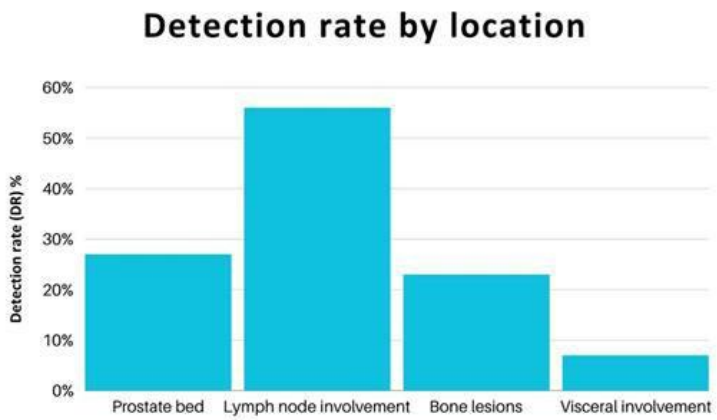

Table

Figure 2: Sankey diagram demonstrating specific change in management per patient (PSMA positives and negatives) from original intention to post-PET/CT with 18F-DCFPyL intention (original intent-to-treat vs. post-PSMA intent-to-treat).

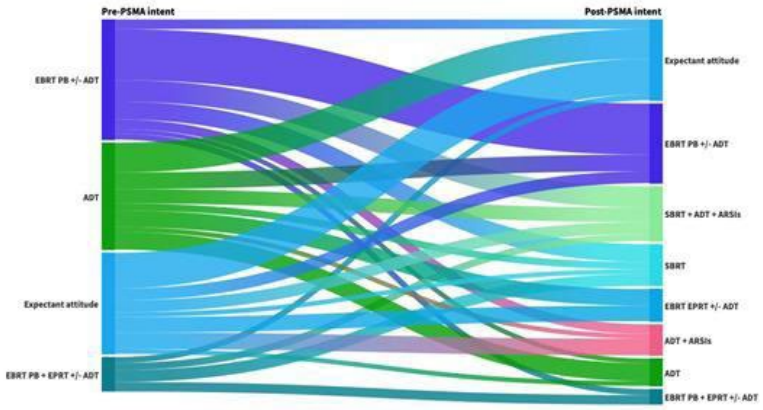

Abbreviations: EBRT (external bean radiation therapy), PB (prostate bed), ADT (Androgen deprivation therapy), EPRT (elective pelvis radiation therapy), PRT (pelvic radiation therapy) SBRT (Stereotactic Body Radiation Therapy), ARSIs (Androgen Receptor Signaling inhibitors)

O72

Biochemical Response Following PSMA-1007 Metabolic Imaging-Guided Radiotherapy in Patients with Biochemical Recurrence of Prostate Cancer After Radical Prostatectomy

Dr. Pedro Jose Plaza Lopez[1,2], Dr. Fracesco Amorelli[3], Dr. Juan Sebastian Blanco[1], Dra. Raquel Valhondo[1], Dra. Cristina Soldevilla[1], Dra Patricia Stefanelli[1], Dra. Palmira Foro[2,3]
[1]Hospital del Mar. Nuclear Medicine Department, Barcelona, Spain, [2]Universitat Pompeu Fabra, Barcelona, España, [3]Hospital del Mar. Radiation Oncology Department, Barcelona, España

Oral presentations 5: Oncology 1 (NETs and Prostate), Arsenal Room, February 15, 2026, 12:15 - 14:15

To evaluate the biochemical response (BR) of patients with biochemically-relapsed prostate cancer (PC) after radical-prostatectomy (RP) treated with positive PSMA-1007 image-guided radiotherapy.
We prospectively included 62 patients with biochemical-recurrence (BCR) of PC who had undergone RP with PSA-levels <0.5ng/mL. Patients were evaluated for salvage radiotherapy (SRT) to prostate-bed (PB) with conventional-radiological-imaging negative. All patients underwent 18F-PSMA-1007-PET/CT. The potential adjustments or changes to radiotherapy-planning fields influenced by PSMA-1007-positive findings were analyzed, as well as their impact on patients' BR, assessed through PSA-levels post-PSMA.
Results: We included 62 patients with a mean-age of 68y. These patients underwent RP and were evaluated for SRT in PB with PSA-values<0.5 ng/mL. Positive-PSMA-1007 results were observed in 64.5% (40/62). Disease-detection-rates were 52.7% local-recurrence, 34.6% nodal-disease, 10.9% bone-metastases, and 1.8% visceral-metastases. The majority of patients had PSA between 0.20-0.50ng/mL with PSA-doubling-time (DT-PSA) <10months. Analysis of ROC-curves identified PSA-values of 0.40ng/mL (AUC 0.60) and DT-PSA of 5.3months (AUC 0.80) as optimal cut-off-points.
Post-PSMA-1007 modifications/changes in radiotherapy-plan were made in 100% of the positive results. Minor-changes were made in 60% of cases included radiotherapy to PB 66Gy (2Gy/Fx) with dose-escalation to 70-72Gy and radiotherapy to pelvic-LN-areas 46Gy (2Gy/Fx) with dose-escalation to pathological-LN to 55Gy. All dose-escalations were guided by positive-PSMA-1007-imaging. Major-changes occurred in 40% of patients (mostly oligometastatic disease), included PSMA-1007 metabolic-volume-guided-SBRT. In patients with negative-PSMA-1007, 66Gy (2Gy/Fx) radiotherapy to PB was performed in 17 patients and watchful-waiting in 5.
After a follow-up of 24months the post-PSMA-1007 BR in the positive group occurred in 85% of patients with a median response of 2 months (95%CI:1.31-4.0) reaching PSA-values <0.003ng/ml. In the negative group, BR occurred in 40% of patients, median response of 4.3 months (95%CI:2.56-9.0). (figure-attached)
Conclusion: The PET/CT-PSMA-1007 allows correct diagnosis of patients with BCR of PC and enables guided metabolic-volume-radiotherapy, achieving early BR in the majority of patients.

References
Amorelli, F.; Foro, P.; Blanco, J.S.; Ocanto, A.; Natali, A.; Fumado, L.; Plaza, P. Diagnostic Capability and Improved Clinical Management of 18F-DCFPyL-PSMA PET/CT in Occult Biochemical Recurrence of Prostate Cancer After Prostatectomy. Cancers 2025, 17, 1272. https://doi.org/10.3390/cancers17081272
Conflict of Interest
no conflict of interest

Graphic

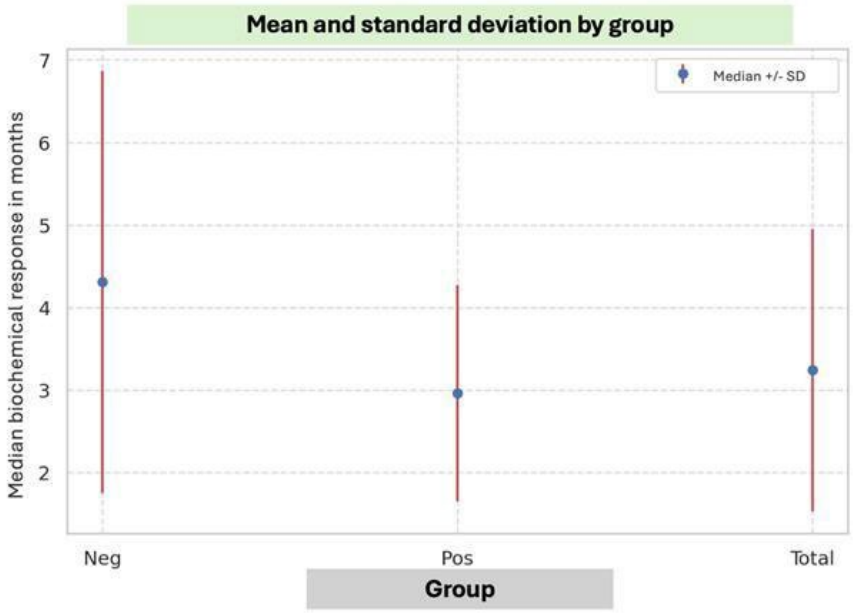

O73

Comparison of 18F-PSMA-1007 and 18F-DCFPyL PET-CT in prostate cancer patients with occult biochemical recurrence with low PSA values

Dr. Pedro Jose Plaza Lopez[1], Dr Francesco Amorelli[3], Dr Juan Sebastian Blanco[1], Dra Eliana Carrillo[1], Dra Raquel Valhondo[1], Sr Guillermo García Álvaro[1], Dra Palmira Foro[2,3]
[1]Hospital del Mar. Nuclear Medicine Department, Barcelona, Spain, [2]Universitat Pompeu Fabra, Barcelona, España, [3]Hospital del Mar. Radiation Oncology Department, Barcelona, España

Oral presentations 5: Oncology 1 (NETs and Prostate), Arsenal Room, February 15, 2026, 12:15 - 14:15

Our porpouse was to compare the diagnostic accuracy and equivocal findings of PET-CT 18F-DCFPyL and 18F-PSMA-1007 in occult biochemical recurrence (BCR) of prostate carcinoma (PCa) with PSA<2ng/ml.
Methods: Sixty-eight patients underwent a PSMA-ligand PET-CT for BCR of PCa evaluation, 18F-DCFPyL or 18F-PSMA-1007.
18F-DCFPyL was synthesized and delivered by Curium Pharma Spain and 18F-PSMA-1007 was synthesized and delivered by IRAB Spain.
After 90 min, a Whole body PET with a diagnostic CT Scan were performed in a Siemens Biograph, following recomendations of EANM Guidelines. Iodine endovenous contrast was given except contraindications. Furosemida was not given.
18F-DCFPyL PET/CT images were reviewed using SyngoVia-20 (Siemens Healthineers) by two experimented nuclear medicine physicians. Imaging standardized evaluation for the interpretation of PSMA-Ligand PET/CT for Prostate Cancer Molecular (PROMISE) were used. Disagreements were resolved by consensus.
Results: 34 patientes (50%) underwent a PET-CT with 18F-PSMA-1007, and the other 34 with 18F-DCFPyL.
Not statistical differences betweeen both groups were found in clinical initial staging (ISUP and PSA values), primary treatments even PSA nadir after primary. PSA values before PET-CT were similar (1007 group median: 0.5; DCFPyL group median: 0.6, p:0.419) and was no statistical differences in PSA doubling time (p:0.524).
Recurrence of PCa was observed in 20 of 34 (58.8%) PET-PSMA-1007 group, and 15 of 34 (45.5%) PET- DCFPyL group, but not statistical differences were found (p:0.332). Locations of the recurrences were similar, p:0.538, (local: 17.6% vs 15.2%; and adenopathy: 32.4% vs 21.2%, respectively).
A statistically significant higher number of non-cancer related bone images (intermediate or high PSMA expresión) was observed in the PET-1007 group (29.4% vs 6.7%, p:0.026), mostly in ribs. Just one extra imagen study (bone MRI) was needed to clarify PET equivocal bone finding.
Conclusion: 18F-PSMA-1007 and 18F-DCFPyL PET-CT show very similar results in the assessment of BCR of PCa.

References
Matthias Eiber, Ken Herrmann, Jeremie Calais, Boris Hadaschik, Frederik L. Giesel, Markus Hartenbach, Thomas Hope, Robert Reiter, Tobias Maurer, Wolfgang A. Weber and Wolfgang P. Fendler. Prostate Cancer Molecular Imaging Standardized Evaluation (PROMISE): Proposed miTNM Classification for the Interpretation of PSMA-Ligand PET/CT Journal of Nuclear Medicine March 2018, 59 (3) 469-478; DOI: https://doi.org/10.2967/jnumed.117.198119
Amorelli, F.; Foro, P.; Blanco, J.S.; Ocanto, A.; Natali, A.; Fumado, L.; Plaza, P. Diagnostic Capability and Improved Clinical Management of 18F-DCFPyL-PSMA PET/CT in Occult Biochemical Recurrence of Prostate Cancer After Prostatectomy. Cancers 2025, 17, 1272. https://doi.org/10.3390/cancers17081272
Conflict of Interest
no conflict of interest

Graphic

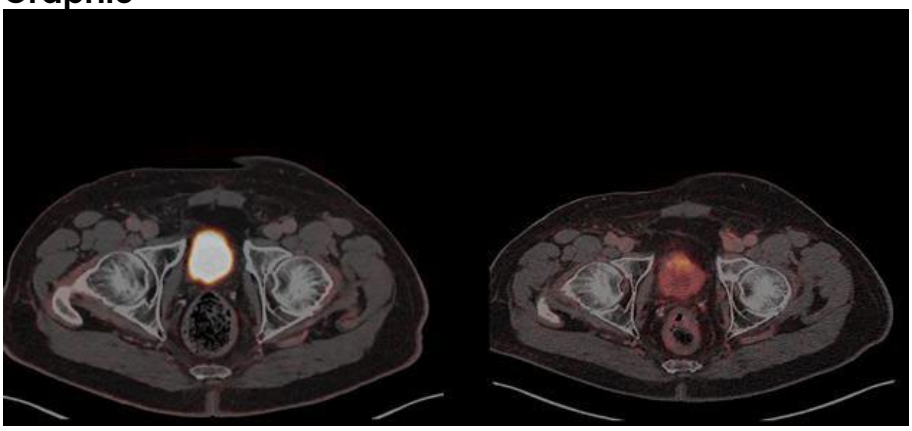

Table

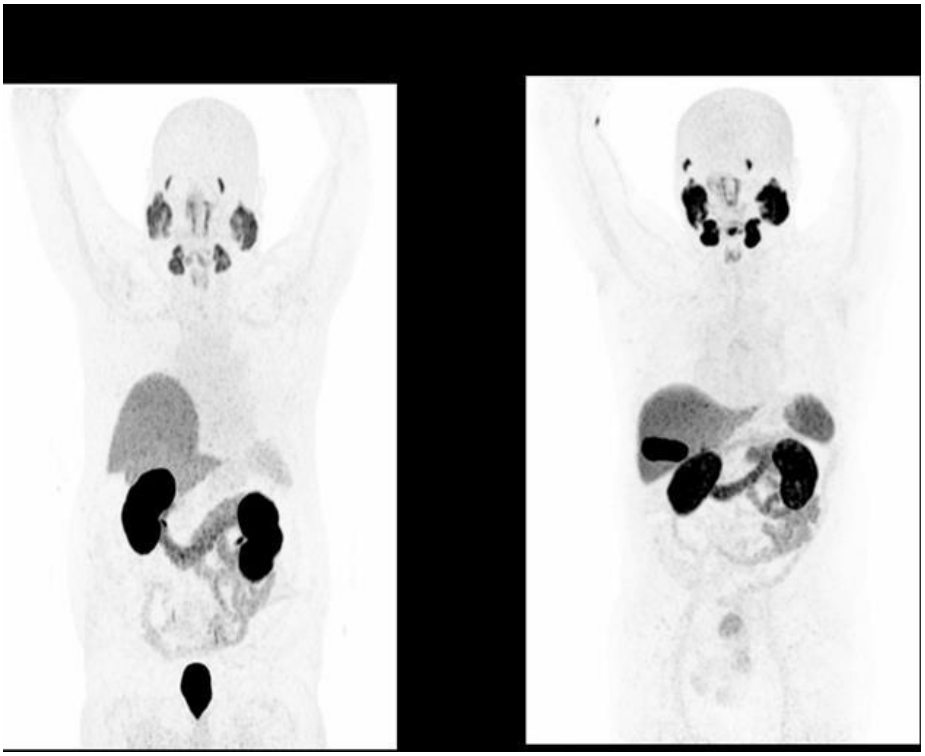

O74

Non-informative [18F]FDG PET/CT studies and rescheduling times as quality indicators in a latin american reference center

Mr. Ismael Cordero[1], Mr. Martin Sabatella[1], Mr. Javier Giglio[1], Mr. Omar Alonso[1], Mr. Gustavo Burroso[1], Mr. Juan Pablo Gambini[1]
[1]Uruguayan Center of Molecular Imaging (CUDIM), Montevideo, Uruguay

Oral presentations 5: Oncology 1 (NETs and Prostate), Arsenal Room, February 15, 2026, 12:15 - 14:15

Background/Aims: Non-informative PET/CT scans reduce diagnostic accuracy, delay treatment, and increase healthcare costs. Although repeat/reject rates of 2-5% have been reported in imaging quality audits [1], no standardized benchmarks exist specifically for PET/CT. Data from Latin America remain limited. At CUDIM, a joint reporting model combining nuclear medicine physicians and radiologists was implemented, in accordance with the IAEA's QUANUM guidelines [2]. This approach enhances diagnostic interpretation by integrating [18F]FDG physiopathology with CT anatomy, reducing uncertainty [3]. Additionally, the Efficient Rescheduling Indicator (ERI) was introduced to monitor delays in repeating non-informative studies.
This study aimed to determine the frequency and main causes of non-informative PET/CT scans, evaluate rescheduling times, and propose improvement strategies to strengthen institutional quality standards.
Methods: A retrospective review was conducted of 39,188 [18F]FDG PET/CT scans performed between May 2016 and May 2025. Studies were classified as non-informative when interpretability was affected by extravasation, hyperinsulinemia, poor preparation, artifacts, brown fat uptake, or muscle activity. Rescheduling times were analyzed in 112 patients. The ERI was calculated using a weighted score: <7 days = 100 points, 8–14 days = 50 points, >14 days = 0 points.
Results: The overall non-informative rate was 0.29%, well below typical international rates. Main causes were extravasation (32.7%), hyperinsulinemia (30.9%), and inadequate preparation (13.4%), accounting for 75.9% of cases. Rescheduling times: <7 days (65.2%, 65.18 points), 8–14 days (24.1%, 12.06 points), >14 days (10.7%, 0 points). Global ERI score: 77.24, rated "good" per IAEA benchmarks.
Conclusions: A low rate of non-informative scans and a strong ERI reflect CUDIM's high diagnostic and operational standards. As most causes were preventable, improvement strategies should focus on reducing delays >14 days, strengthening patient adherence with multimodal reminders, and systematically addressing preventable causes such as extravasation and hyperinsulinemia.

References

[1] Review of Radiologic Physics. 4th Edition. Walter Huda, Author. Philadelphia: Lippincott Williams & Wilkins, 2016.
[2] International Atomic Energy Agency (IAEA). Quality Management Audits in Nuclear Medicine Practices (QUANUM), 3rd. edition. IAEA, Vienna, 2021.
[3] Gatidis, S., et al. (2019). State of affairs of hybrid imaging in Europe: two multi-national surveys.

Conflict of Interest
No conflict of iterest.

O75

Synergy in sight: fusing PSMA PET/CT and mpMRI parameters to enhance prostate cancer risk stratification

Dr. Eva Lorena Valadez Montero[1], Dr Bethsabel Rodríguez Encinas, MD. Irma Soldevilla Gallardo
[1]Centro Medico ABC, Mexico City, Mexico

Oral presentations 5: Oncology 1 (NETs and Prostate), Arsenal Room, February 15, 2026, 12:15 - 14:15

Aims: Accurate risk stratification is crucial for managing prostate cancer. While multiparametric MRI (mpMRI) is standard, combining it with ^{18}F-PSMA PET/CT could improve non-invasive assessment [1, 2]. This study aims to evaluate the combined predictive value of quantitative and volumetric parameters from both imaging modalities for risk stratification in patients with prostate cancer.
Methodology: This analysis from the ABC Medical Center, includes 12 treatment-naïve patients who underwent both ^{18}F-PSMA PET/CT and prostate mpMRI. Key quantitative parameters, including maximum Standardized Uptake Value (SUVmax), Prostate-Specific Membrane Antigen Tumor Volume (PSMA-TV) from PET/CT, as well as Apparent Diffusion Coefficient (ADC) and PI-RADS v2.1 score from mpMRI, were extracted [3, 4]. Spearman's correlation was used to assess relationships between parameters, and the Kruskal-Wallis test was used to compare values across D'Amico risk groups.
Results: Quantitative biomarkers correlated significantly with clinical-pathological factors. A strong positive correlation was found between PSA level and SUVmax_Prostata ($r_s(10)=.78$, $p<.01$), while a robust negative correlation was demonstrated between ADC and the Gleason sum ($r_s(9)=-.82$, $p<.01$). A crucial inter-modal association was identified via a moderate negative correlation between SUVmax_Prostata and ADC ($r_s(9)=-.67$, $p<.05$), suggesting high metabolic activity and cellular density coexist in aggressive tumors. When stratified by D'Amico risk, SUVmax_Prostata increased significantly ($x^2(2)=7.85$, $p=.020$) and ADC decreased significantly ($x^2(2)=7.31$, $p=.026$) with higher risk levels.
Conclusion: Our preliminary findings suggest a significant correlation between the quantitative parameters from PSMA PET/CT and mpMRI, which capture fundamental and complementary biological aspects of the tumor, such as its high disease burden and cellular density. Key parameters like SUVmax and ADC demonstrate strong potential for differentiating between established clinical risk groups. The integration of these metrics could improve non-invasive risk stratification in prostate cancer, allowing for a more precise characterization of tumor aggressiveness.

References

1. Eiber, M., Maurer, T., Souvatzoglou, M., Beer, A. J., Ruffani, A., Gschwend, J. E., Schwaiger, M., & Thalgott, M. (2015). Evaluation of Hybrid ^{68}Ga-PSMA Ligand PET/CT in 248 Patients with Biochemical Recurrence After Radical Prostatectomy. Journal of Nuclear Medicine, 56(5), 668–674.

2. Hofman, M. S., Lawrentschuk, N., Francis, R. J., et al. (2020). Prostate-specific membrane antigen PET-CT in patients with high-risk prostate cancer before curative-intent surgery or radiotherapy (proPSMA): a prospective, randomised, multicentre study. The Lancet, 395(10231), 1208–1216.
3. Chen, M., Zhang, Q., Li, F., et al. (2020). The role of quantitative parameters of PSMA PET/CT in the prediction of prostate cancer aggressiveness: a systematic review and meta-analysis. European Journal of Nuclear Medicine and Molecular Imaging, 47(11), 2626–2636.
4. Woo, S., Kim, S. Y., Cho, J. Y., & Kim, S. H. (2018). The correlation between quantitative parameters of ^{18}F-PSMA-1007 PET/CT and the PI-RADS version 2 for the diagnosis of prostate cancer. European Radiology, 28(7), 3027–3035.

Conflict of Interest

The authors declare no conflicts of interest.

Graphic

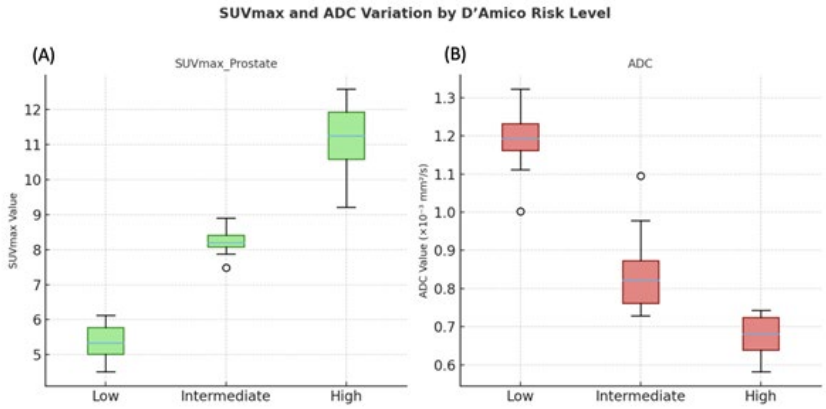

Figure 1. Boxplots illustrating the variation of quantitative imaging biomarkers according to D'Amico risk classification.

(A) SUVmax_Prostate values show a clear upward trend with increasing risk level, indicating higher metabolic activity in more aggressive tumors. The median SUVmax rises markedly from low- to high-risk groups (χ^2 (2) =7.85, p=.020). (B) Apparent Diffusion Coefficient (ADC) values demonstrate an opposite pattern, decreasing significantly as risk increases (χ^2 (2) =7.31, p=.026). This inverse relationship suggests that restricted diffusion, reflecting higher cellular density, is characteristic of high-risk prostate cancer.

Table

Table 1: Comparison of Key Imaging parameters Across D'Amico Risk Groups.

Parameter	Low Risk (n=2)	Intermediate Risk (n=4)	High Risk (n=5)	p-value
	Mean ± SD	*Mean ± SD*	*Mean ± SD*	
SUVmax_Prostate	5.8± 0.3	8.0± 3.9	19.1± 8.2	<0.05
PSMA-TV (cc)	33.9± 3.9	36.4± 10.6	34.0± 30.1	>0.05
ADC Lesion (10–3mm2/s)	0.74± 0.03	0.59± 0.15	0.57± 0.09	<0.05

SD: Standard Deviation; SUVmax: Maximum Standardized Uptake Value; PSMA-TV: PSMA-Tumor Volume; ADC: Apparent Diffusion Coefficient.

O76

KANBAN: Implementation of Software for Patient Traceability in Radioiodine Treatments at the Arturo López Pérez Foundation

Prof. Cristina Gutiérrez Correa[1], Prof Dennys Cuevas Gómez[1], Prof Fernando Navarro[1], Prof Sergio Veliz[1], Prof. Ruben Olave[1], Prof. Miguel Rojas[1], Prof. Luis Madariaga[1], Dra. M. Josefina Jofre[1]
[1]Fundación Arturo Lopez Perez, Santiago, Chile

Oral Presentations 6: Oncology 2 and Endocrinology, Arsenal Room, February 16, 2026, 8:00 - 10:00

Background: Due to the high number of radioiodine treatments for patients with hyperthyroidism and differentiated thyroid cancer at the Nuclear Medicine department of the Arturo López Pérez Foundation, there was a clear need to develop a reliable traceability system.
The objective was to register and track the patient's journey from their initial nuclear medicine consultation to the post-radioiodine treatment whole body scanning, ensuring comprehensive follow-up before and after the procedure.
Methods: In 2023, the creation of this system began in collaboration with the IT, clinical systems, process management, infrastructure, Nuclear Medicine and radiation protection departments. For one year, work was carried out through bi-weekly meetings using a cell-type methodology. Subsequently, a two-month pilot testing phase (soft launch) was conducted, during which modules and functionalities were adjusted until the desired final product was achieved. All relevant treatment variables were analyzed—such as patient personal data, preparation, laboratory tests, critical dates, administered dose, dose rate at discharge, and fall risk assessment—to define the necessary fields of the system and enable effective communication among all stakeholders involved.
Results: The outcome was the implementation of a KANBAN based system for treatments, which optimizes, manages, and ensures traceability from the initial patient care through to the post treatment systemic scan for thyroid cancer patients. This system reduces user induced errors by logging all changes made. It also improves occupancy of metabolic rooms, speeds up dose request processing, and facilitates monitoring of essential tests such as TSH and ß hCG. Additionally, it records radiation exposure levels to support tracking of isolation periods.
Conclusions: In conclusion, this locally designed management software represents a significant innovation that effectively responds to the service's needs, improving patient care times, dose management, and patient satisfaction, resulting in a substantial enhancement of operational efficiency.

Conflict of Interest
No

Graphic

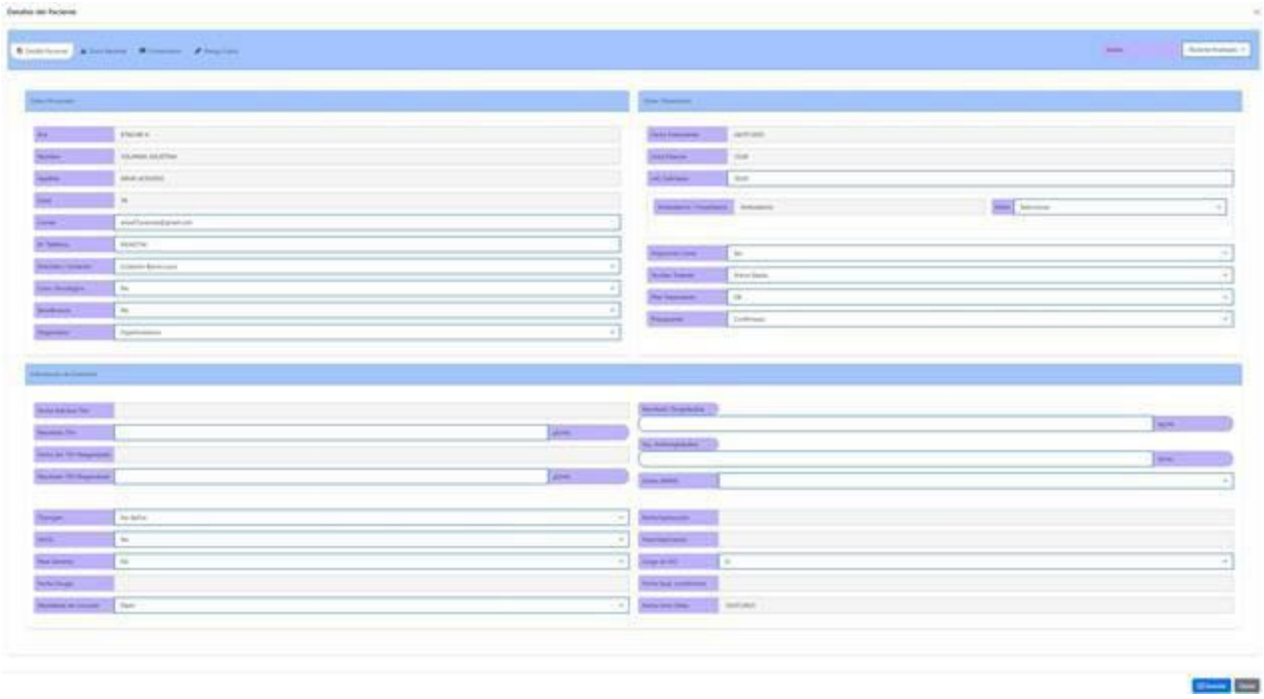

Table

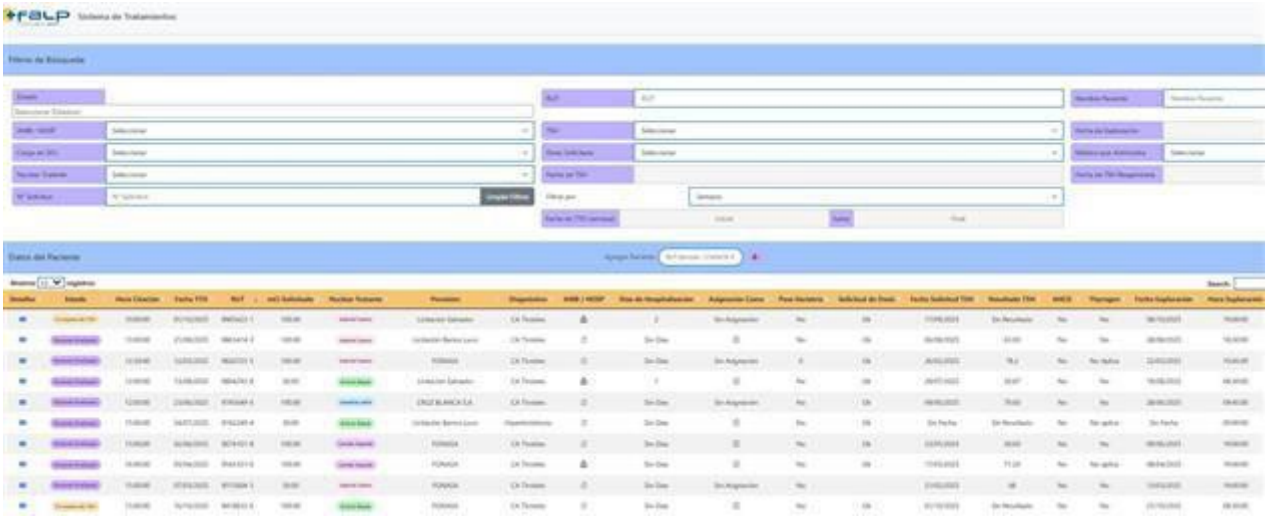

O77

Serum-stimulated thyroglobulin levels before radioactive iodine therapy as a predictive biomarker of disease-negative whole-body scan in differentiated thyroid cancer

Dr. Andres Gamboa[1], Dr. Liset Sanchez[1,2], Dr. Mabel Gomez[1], Dr. Wendy Gallegos[1], Dr. Cesar García[1,2], Dr. Tatiana Morales[1], Dr. Lizeth Rodriguez[1]
[1]Universidad Autónoma de Bucaramanga - UNAB, Bucaramanga, Colombia, [2]SPECT S.A.S, Bucaramanga, Colombia

Oral Presentations 6: Oncology 2 and Endocrinology, Arsenal Room, February 16, 2026, 8:00 - 10:00

Background/Aims: Differentiated thyroid carcinoma (DTC), the most common thyroid cancer, constitutes a significant public health burden [1]. Despite management advances, important prognostic uncertainties remain [2]. Serum thyroglobulin (Tg) serves as a well-established disease biomarker, yet its clinical performance varies across populations [3-5], highlighting the need for regional validation. This study investigated the relationship between pre-radioactive iodine therapy (RIT) stimulated thyroglobulin (Tg) levels and whole-body scan (WBS) findings, and examined the predictive value of Tg for disease detection in a cohort from a Latin American country.
Methods: We conducted a retrospective cohort study including adults with histologically confirmed DTC treated with total thyroidectomy and RIT between January 2020 and June 2025 at a Colombian medical center. Exclusion criteria included medullary or anaplastic carcinoma, incomplete thyroidectomy, metastatic disease, missing data or positive anti-Tg antibodies. WBS positivity was defined as radioactive uptake consistent with locoregional or distant metastases. Descriptive, bivariate, and multivariate analyses were performed; ROC analysis identified the optimal Tg cutoff.
Results: A total of 917 patients (mean age 48 years; 81.7% women; 99.1% papillary type) were analyzed. Most cases were stage I–II and intermediate ATA-2015 risk (59.4%). WBS was negative in 88.8%. Patients with positive WBS had significantly higher pre-RIT Tg levels (33.6 vs. 8.9 ng/mL; $p<0.001$). In multivariate analysis, stimulated Tg remained independently associated with WBS findings ($p=0.005$; Table 1) and a cutoff value of 6.48 ng/mL yielded: sensitivity 42.7%, specificity 75.8%, AUC 0.611 (95% CI: 0.55–0.67; Figure 1); PPV 17.9%, NPV 91.2% (CI 95% 13.3%-23.3%; 88.8% -93.2%).
Conclusions: Pre-RIT stimulated Tg levels independently predicted post-therapy negative scan. The predictive performance observed aligns with previous regional prospective prognostic studies [5]. Our results support Tg's potential role as a reliable postsurgical biomarker for presence of disease. Population-specific validation bolsters the clinical utility of Tg as a predictive and prognostic marker.

References
1. Boucai L, Zafereo M, Cabanillas ME. Thyroid cancer: A review. JAMA. 2024;331(5):425-435. https://doi.org/10.1001/jama.2023.26348
2.Haugen BR, Alexander EK, Bible KC, et al. 2015 American Thyroid Association Management Guidelines for Adult Patients with Differentiated Thyroid Cancer. Thyroid. 2016;26(1):1-133. https://doi.org/10.1089/thy.2015.0020
3.Giovanella L, Milan L, Roll W, et al. Postoperative thyroglobulin as a yard-stick for radioiodine therapy: Decision tree analysis in a European multicenter series of 1,317 patients with differentiated thyroid cancer. Eur J Nucl Med Mol Imaging. 2023;50(9):2767-2774. https://doi.org/10.1007/s00259-023-06239-8
4. Bandeira L, Padovani RP, Ticly AL, et al. Thyroglobulin levels before radioactive iodine therapy and dynamic risk stratification after 1 year in patients with differentiated thyroid cancer. Arch Endocrinol Metab. 2017;61(6):590-599. https://doi.org/10.1590/2359-3997000000308
5. Marín LF, Torres JL, Wandurraga EA, et al. Predictores de recaída en carcinoma diferenciado de tiroides en Colombia: estudio multicéntrico. Rev Colomb Endocrinol Diabetes Metab. 2019;6(2):92-100. https://doi.org/10.53853/encr.6.2.483

Conflict of Interest

All authors declare that they have no conflicts of interest.

Graphic

Figure 1. ROC curve and probability cutoff

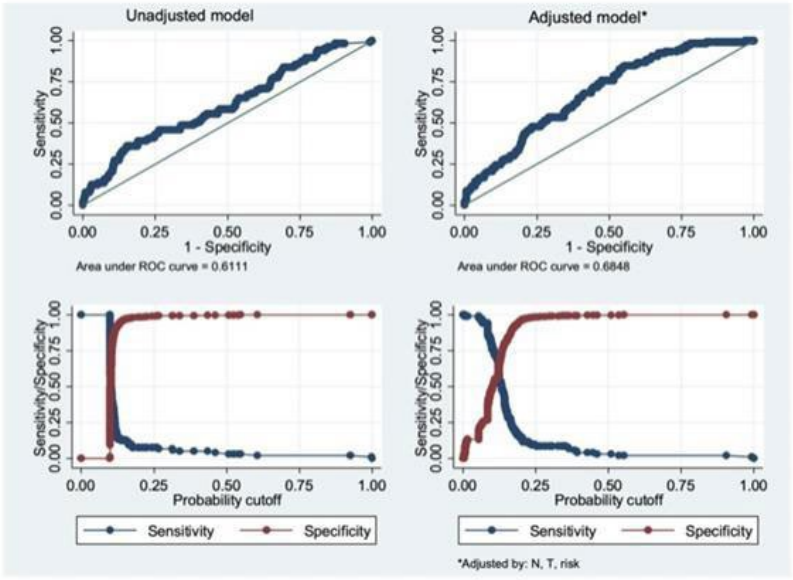

Table

Table 1. Adjusted model of preablative TG and WBS

Number of obs= 917
LR chi2(10) = 49.89
Prob > chi2 = 0.0000
Log likelihood = -297.23949
Pseudo R2 = 0.0774

Variable	Odds Ratio	P > |z|	[95% Conf. Interval]
TG (ng/mL)	1.0073	0.005	1.0022 – 1.0124
N	1.1876	0.485	0.7326 – 1.9252
T (ref: 1a)			
1b	1.6313	0.266	0.6884 – 3.8656
2	2.4187	0.042	1.0317 – 5.6702
3a	3.4156	0.018	1.2334 – 9.4587
3b	2.6618	0.053	0.9869 – 7.1794
4a	2.6020	0.081	0.8886 – 7.6195
4b	6.9908	0.133	0.5547 – 88.1053
Risk			
Intermediate	12.5253	0.013	1.7033 – 92.1055
High	13.5086	0.012	1.7680 – 103.2133

O78

Positron emission tomography/computed tomography radiomics score predicts metabolically active disease and reflects glycolysis-related protein expression in aggressive B-cell lymphomas

Mr. Farid Cury Neto[1,2], Mr. Gabriel de Prince Garcia[2], MSc. Patrik da Silva Vital[1], Dr. Murilo Bonatelli[1], Mr. José Augusto Santanna Otteiro[3], MD., MSc. Flávia Fazzo Barbin[4], MD., MSc. Eduardo Caetano Albino da Silva[4], Dr. Marcelo Wilson Berbone Furlan Alves[5], MD., Dr. Wilson Eduardo Furlan Matos Alves[2,3], Dr. Céline Pinheiro[1,2]
[1]Molecular Oncology Research Center, Barretos Cancer Hospital, Barretos, Brazil, [2]Barretos School of Health Sciences Dr. Paulo Prata, Barretos, Brazil, [3]Department of Nuclear Medicine, Barretos Cancer Hospital, Barretos, Brazil, [4]Department of Pathology, Barretos Cancer Hospital, Barretos, Brazil, [5]Aeronautical Technology Institute, São José dos Campos, Brazil

Oral Presentations 6: Oncology 2 and Endocrinology, Arsenal Room, February 16, 2026, 8:00 - 10:00

Background: Radiomic features derived from ^{18}F-fluorodeoxyglucose positron emission tomography/computed tomography (^{18}F-FDG PET/CT) non-invasively quantify morphology and heterogeneity in intact tumor regions. In aggressive B-cell lymphomas (ABCL), however, their biological basis and ability to identify poor responders remain underexplored. Aims: To evaluate the added value of baseline radiomic features for predicting metabolically active disease (MAD) on end-of-treatment ^{18}F-FDG PET/CT, and to investigate associations between radiomic features and glycolysis-related protein expression. Methods: Clinical and baseline ^{18}F-FDG PET/CT data from 310 ABCL patients were retrospectively analyzed. Data were split into training/test sets (n=247/63), and only repeatable and reproducible radiomic features were retained for feature selection. Predictors of MAD were then selected through redundancy filtering, elastic net, and permutation importance to build the radiomics score (radscore). Machine learning models, including support vector machine (SVM) and random forest (RF), were trained combining radscore, metabolic tumor volume (MTV), and the International Prognostic Index (IPI). Immunohistochemical expression of glucose transporters (GLUT1 and GLUT3), and eight other glycolysis-related proteins were associated with radscore computed from the union of all regions of interest (ROIs) and within the ROI of the biopsy site. This study was approved by the Barretos Cancer Hospital ethics committee. Results: The IPI+MTV+radscore SVM model achieved the highest area under the receiver operating characteristic curve (AUROC) in the test set (0.767), outperforming the IPI RF model (0.720), with significantly greater specificity (0.700 vs. 0.550, p=0.041). Survival analysis showed that radscore remained an independent prognostic factor for overall survival after adjustment for IPI components (hazard ratio=1.272, p=0.040). GLUT1 and GLUT3 expression in fibroblasts, endothelium, and inflammatory cells was significantly higher in patients with low radscore, both in the union ROI and in the biopsy-site ROI (p=0.018/p=0.048). Conclusion: Baseline ^{18}F-FDG PET/CT radiomics enhances risk stratification for treatment response and survival in ABCL and associates with tumor glycolytic biology.

Conflict of Interest

None.

Graphic

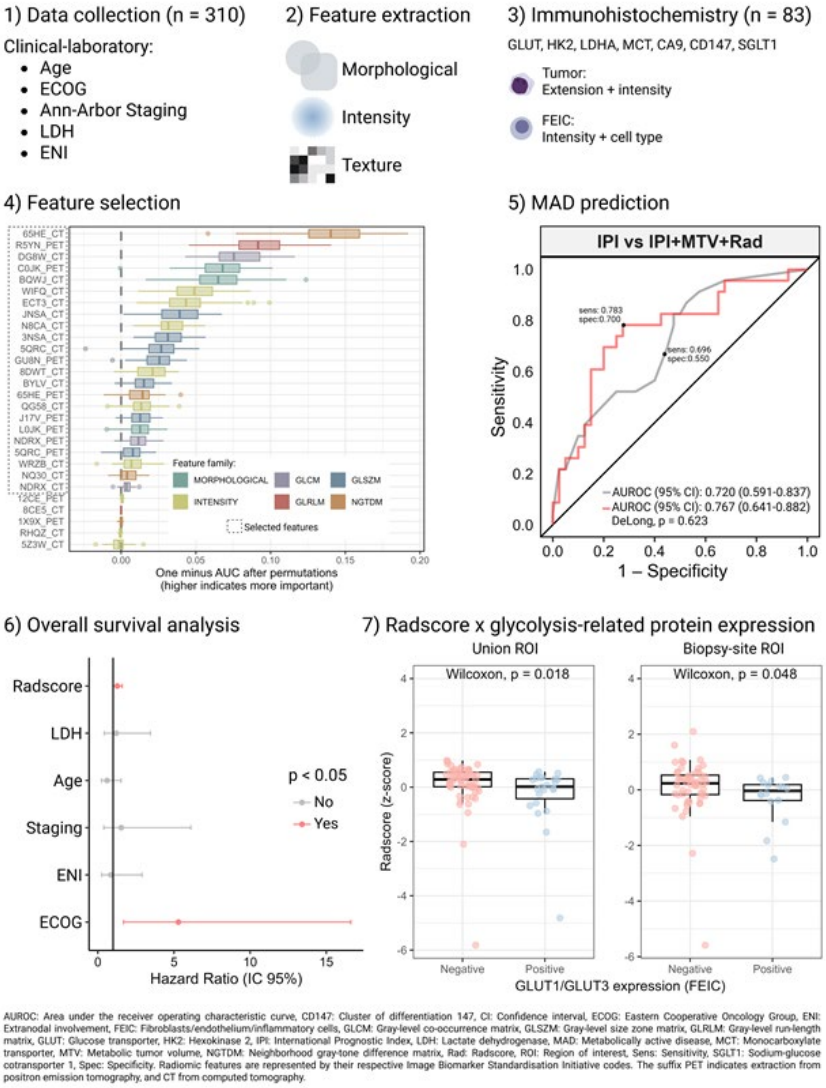

AUROC: Area under the receiver operating characteristic curve, CD147: Cluster of differentiation 147, CI: Confidence interval, ECOG: Eastern Cooperative Oncology Group, ENI: Extranodal involvement, FEIC: Fibroblasts/endothelium/inflammatory cells, GLCM: Gray-level co-occurrence matrix, GLSZM: Gray-level size zone matrix, GLRLM: Gray-level run-length matrix, GLUT: Glucose transporter, HK2: Hexokinase 2, IPI: International Prognostic Index, LDH: Lactate dehydrogenase, MAD: Metabolically active disease, MCT: Monocarboxylate transporter, MTV: Metabolic tumor volume, NGTDM: Neighborhood gray-tone difference matrix, Rad: Radscore, ROI: Region of interest, Sens: Sensitivity, SGLT1: Sodium-glucose cotransporter 1, Spec: Specificity. Radiomic features are represented by their respective Image Biomarker Standardisation Initiative codes. The suffix PET indicates extraction from positron emission tomography, and CT from computed tomography.

Table

Table 1. Performance of IPI, MTV, and Radscore models for complete response vs metabolically active disease classification in aggressive B-cell lymphomas.

	Training (n = 248)							Test (n = 62)						
Model	AUROC	95% CI	AUROC	Sens	Spec	PPV	NPV	AUROC	95% CI	AUROC	Sens	Spec	PPV	NPV
IPI+Radscore RF	0.783	0.757	0.809	0.811	0.647	0.569	0.857	0.744	0.620	0.865	0.826	0.550	0.514	0.846
IPI+Radscore SVM	0.772	0.747	0.797	0.707	0.749	0.617	0.817	0.759	0.632	0.872	0.739	0.725	0.607	0.829
Radscore SVM	0.766	0.738	0.793	0.838	0.535	0.508	0.852	0.659	0.507	0.793	0.870	0.400	0.455	0.842
IPI+Radscore XGB	0.763	0.734	0.792	0.527	0.879	0.714	0.764	0.706	0.571	0.830	0.435	0.800	0.556	0.711
IPI+MTV+Radscore RF	0.761	0.735	0.787	0.540	0.837	0.655	0.760	0.744	0.618	0.860	0.435	0.800	0.556	0.711
IPI+MTV+Radscore SVM	**0.753**	**0.726**	**0.779**	**0.729**	**0.668**	**0.557**	**0.811**	**0.767**	**0.641**	**0.882**	**0.783**	**0.700**	**0.600**	**0.848**
IPI+MTV+Radscore XGB	0.752	0.723	0.781	0.524	0.871	0.700	0.762	0.708	0.573	0.830	0.435	0.800	0.556	0.711
Radscore XGB	0.745	0.716	0.774	0.818	0.545	0.508	0.839	0.711	0.569	0.835	0.870	0.400	0.455	0.842
MTV+Radscore XGB	0.744	0.717	0.771	0.660	0.720	0.574	0.787	0.677	0.544	0.803	0.565	0.625	0.464	0.714
MTV+Radscore SVM	0.734	0.706	0.761	0.633	0.706	0.552	0.771	0.657	0.506	0.794	0.696	0.575	0.485	0.767
Radscore RF	0.723	0.694	0.752	0.864	0.454	0.476	0.854	0.713	0.571	0.836	0.870	0.325	0.426	0.813
MTV+Radscore RF	0.711	0.682	0.740	0.596	0.694	0.528	0.750	0.710	0.574	0.833	0.739	0.625	0.531	0.806
IPI RF	0.690	0.664	0.716	0.787	0.566	0.509	0.822	0.720	0.591	0.837	0.550	0.696	0.759	0.471
IPI XGB	0.671	0.643	0.699	0.847	0.485	0.485	0.847	0.726	0.604	0.840	0.826	0.525	0.500	0.840
IPI+MTV RF	0.671	0.646	0.697	0.789	0.541	0.497	0.817	0.743	0.616	0.856	0.783	0.525	0.486	0.808
IPI+MTV SVM	0.671	0.644	0.698	0.491	0.749	0.529	0.720	0.749	0.629	0.863	0.565	0.800	0.619	0.762
IPI SVM	0.638	0.606	0.671	0.331	0.828	0.525	0.683	0.709	0.571	0.827	0.261	0.925	0.667	0.685
IPI+MTV XGB	0.633	0.603	0.663	0.780	0.418	0.434	0.768	0.758	0.637	0.865	0.957	0.425	0.489	0.944
MTV XGB	0.607	0.575	0.639	0.609	0.578	0.453	0.721	0.697	0.567	0.813	0.739	0.600	0.515	0.800
MTV SVM	0.592	0.552	0.633	0.611	0.450	0.389	0.669	0.689	0.543	0.816	0.348	0.750	0.444	0.667
MTV RF	0.533	0.500	0.566	0.544	0.536	0.402	0.673	0.683	0.547	0.823	0.783	0.575	0.514	0.821

AUROC: area under the receiver operating characteristic curve, CI: confidence interval, IPI: international prognostic index, MTV: metabolic tumor volume, NPV: negative predictive value, PPV: positive predictive value, RF: random forest, Sens: sensitivity, Spec: specificity, SVM: support vector machine, XGB: extreme gradient boost. The model with the highest AUROC in the test set is shown in bold.

O79

Head-to-head intrapatient qualitative comparison of 68Ga-FAPI-04 versus 18F-FDG PET/CT in various oncological pathologies

Dr. Eduardo Lischinsky[1], Javier Giglio[2], Eduardo Savio[2], Ismael Cordero[1,2], Dr. Omar Alonso[1,2], Dr. Gustavo Burroso[2], Dr. Alarico Rodriguez[2], Dr. Juan Pablo Gambini[1,2]
[1]CMNIM, Hospital De Clínicas "Dr. Manuel Quintela" - Universidad De La República, Montevideo, Uruguay, [2]Centro Uruguayo de Imagenología Molecular (CUDIM), Montevideo, Uruguay

Oral Presentations 6: Oncology 2 and Endocrinology, Arsenal Room, February 16, 2026, 8:00 - 10:00

Background/Objectives: While 18F-FDG PET/CT remains the standard for oncological molecular imaging, fibroblast activation protein inhibitor (FAPI) targeting cancer-associated fibroblasts offers complementary diagnostic capabilities in desmoplastic tumors. This study compared the qualitative performance of 68Ga-FAPI-04 versus 18F-FDG PET/CT in the same patients across multiple tumor types.
Methods: A retrospective head-to-head analysis included 13 patients (7 males, 6 females; age range 35-74 years) with various oncological pathologies who underwent both 68Ga-FAPI-04 and 18F-FDG PET/CT within one week. Eleven different tumor types were evaluated. Visual analysis assessed detection rates, tumor-to-background contrast, and identification of additional lesions. Quantitative comparison of SUVmax was not performed due to technical variables including inter-scanner heterogeneity and temporal factors between studies.
Results: 68Ga-FAPI-04 demonstrated superior or equivalent detection rates in 92% of cases (12/13 patients). FAPI detected additional pathological lesions in 46.2% of patients (6/13) not visualized on FDG, including metastatic disease in lung, liver, bone, and soft tissue locations. FAPI showed increased uptake over FDG in renal cell carcinoma, anal canal carcinoma, and tracheal squamous cell carcinoma. FDG demonstrated superior uptake only in Hodgkin lymphoma. Both tracers showed equivalent detection in gastric cancer and non-small cell lung cancer, though FAPI provided superior tumor-to-background contrast. Nonpathologic FAPI uptake was also noted at sites of degenerative bone and joint change, postoperative scarring and dental inflammatory foci, as well as physiologic uterine activity in women, patterns consistently described as benign FAPI avidity and important pitfalls in interpretation.
Conclusions: 68Ga-FAPI-04 PET/CT demonstrated complementary and often superior qualitative performance compared to 18F-FDG across multiple tumor types. The ability to detect additional metastatic lesions and provide enhanced contrast in challenging anatomical locations, along with its pantumoral characteristics, positions FAPI as a valuable adjunct to conventional FDG imaging in precision oncology and its potential for future theranostic applications.

Conflict of Interest
No conflict of interest

Graphic

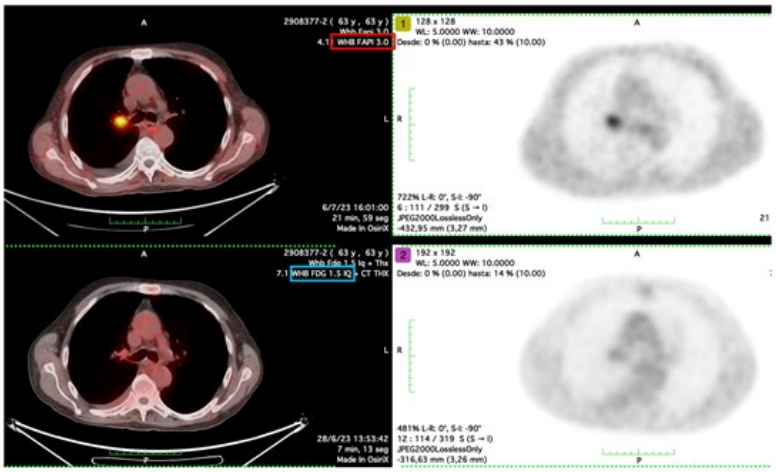

Figure 1. Patient with significant ^{68}Ga-FAPI-04 uptake in right hilar lymph node, previously undetected with ^{18}F-FDG PET/CT

Table

INTRA-PATIENT COMPARISON 68Ga-FAPI-04 vs 18F-FDG PET/CT

Primary tumor	Max. SUVmax FDG	Max. SUVmax FAPI	FDG activity (MBq)	FAPI activity (MBq)	Additional FAPI Findings	Pathological	Remarks
Urothelial carcinoma of the bladder	10,4	13,5	223,5	106,5	None	NA	Equivalent
Non-small cell lung cancer	12,8	12,5	369,4	176	Right adrenal gland	Yes	Equivalent
Hodgkin lymphoma	12,5	7,9	294,5	142,9	Uterus (physiological)	No	FDG superiority
Gastric cancer	47,1	17,2	275	115	Focal uptake in left hepatic lobe	Yes	FDG superiority
Small cell lung cancer	11,3	12,3	318	159	Focal uptake in left ilium	Yes	Equivalent
Renal cell carcinoma	2,7	10,4	242	141	Thoracic spinous processes (degenerative	No	FAPI superiority
Tracheal squamous cell carcinoma	9,8	16,5	228	140	Schmorl's node at L4 (degenerative)	No	FAPI superiority
Non-small cell lung cancer	11,8	19,7	312	148	Focal uptake in right ilium	Yes	FAPI superiority
Vulvar cancer	9,5	13,1	214	110	Left iliacus muscle	Yes	Equivalent
Non-small cell lung cancer	15,2	22,9	274	135	Right hilar lymph node	Yes	FAPI superiority
Anal canal cancer	2,4	12,3	272	176	Osteophyte at T7–T8 (degenerative)	No	FAPI superiority
Cancer of unknown primary	Not measurable	6,4	226	123,4	Sternotomy, alveolodental process	No	FAPI superiority
Penile cancer	6,4	6,8	356	169	None	NA	Equivalent

O80

Comparison of 99mTc-MAA SPECT/CT and CECT with CBCT for Tumor Perfused Liver Volume Segmentation Prior to 90Y Radioembolization

Dr. Leticia Portillo[1], Dr. Rodrigo Hernández Ramírez[1], Dr. Miguel Angel Corza Ayala[1], Dr. Juan Pablo Chávez Torres[1]
[1]Instituto Nacional de Ciencias Médicas y Nutrición Salvador Zubirán, Mexico, Mexico

Oral Presentations 6: Oncology 2 and Endocrinology, Arsenal Room, February 16, 2026, 8:00 - 10:00

Background: For selective internal radiation therapy (SIRT) planning, perfused volume segmentation using cone-beam CT (CBCT), 99mTc-macroaggregated albumin (MAA) SPECT/CT, and contrast-enhanced CT offers distinct advantages and limitations. Accurate perfused volume quantification directly impacts treatment dosimetry and clinical outcomes by influencing target volume selection and dose calculation. The recommended method is CBCT[1].
The objective was to assess the concordance of 99mTc-MAA SPECT/CT and CECT with CBCT for evaluating perfused tumor volume in SIRT with Y90 planning.
Methods: A retrospective, analytical, longitudinal and comparative study (January 2023–September 2025) evaluated patients undergoing selective internal radiation therapy with Y90 glass microspheres for hepatic tumors. Inclusion required available pre-procedural CECT, CBCT, and 99mTc-MAA SPECT/CT images.
All participants provided written informed consent prior to any procedure, in accordance with institutional and ethical standards.
Volumetric perfusion territories were quantified using semi-automated 3D segmentation. Statistical analysis included Student's t-test, Bland-Altman plots, and intraclass correlation coefficient (ICC).
Results: Eleven patients (10 men, 1 woman) with hepatocellular carcinoma were evaluated (mean age 66.27 years, SD 10.66).
The Bland-Altman plot showed inconsistent agreement between measurement methods across value ranges. While mean difference was low, suggesting minimal average bias, dispersion was uneven. Points scattered mostly outside 95% agreement limits, especially for high values.
ICC of single means was 0.975 and median mean 0.987, indicating very high consistency between individual measurements (95% CI, p=0.00).
Conclusions: Although ICC indicates excellent overall reliability between methods, Bland-Altman analysis reveals unacceptable agreement at high volumes, where differences become significant. Use of 99mTc-MAA SPECT/CT as CBCT substitute should be restricted to situations where low volume is expected.

References

1. Giammarile F, Bodei L, Castellani MR, Chiesa C, Krause BJ, Lazzeri E, et al. EANM procedure guideline for the treatment of liver cancer and liver metastases with intra-arterial radioactive compounds. Eur J Nucl Med Mol Imaging. 2011;38(7):1393-406.

Conflict of Interest
No

Graphic

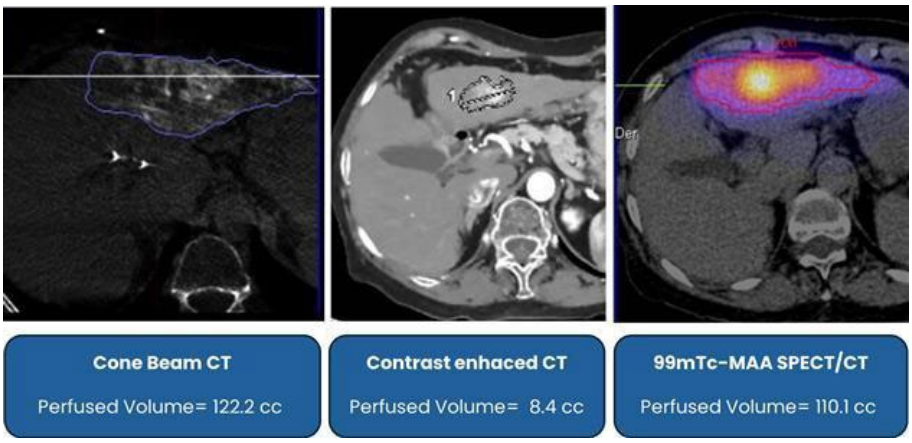

Table

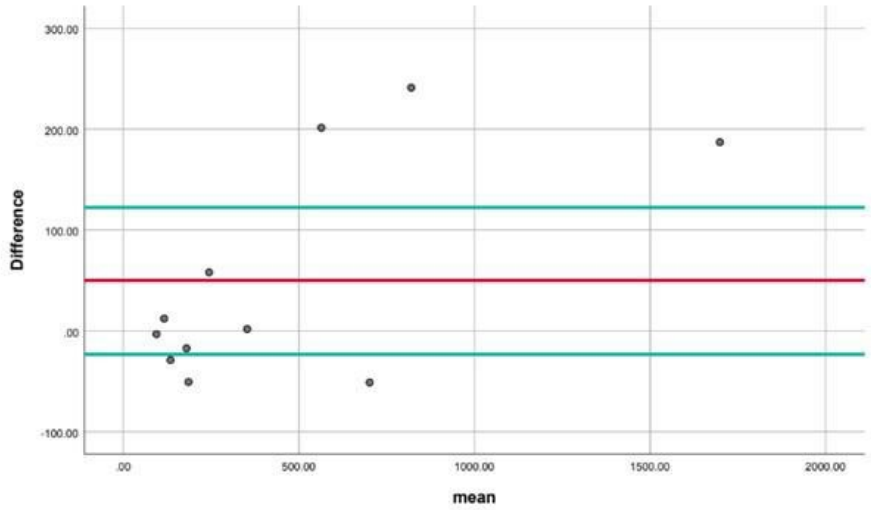

O81

SPECTRA trial: Study of PD-L1 expression and molecular hybrid imaging in triple negative breast cancer: Response prediction and assessement

Dr. Sofía Denisse González Rueda[1,2], Dr. José Antonio García Gordillo[1], Dr. Carlos Arturo González Núñez[1], Dr. Sergio Israel Aguilar Villanueva[1], Dr. Francisco Osvaldo García Pérez[1], Dr. Juan Enrique Bargalló Rocha[1,4], Dr. Paula Anel Cabrera Galeana[1], Dr. Guillermina Ferro Flores[3], Dr. Quetzali Gabriela Pitalúa Cortés[1,2], Dr. Irma Soldevilla Gallardo[1,4]

[1]National Cancer Institute of Mexico, Tlalpan, Mexico, [2]Medica Sur, Tlalpan, Mexico, [3]National Institute of Nuclear Research, Toluca, Mexico, [4]ABC Medical Center, Álvaro Obregón, México

Oral Presentations 6: Oncology 2 and Endocrinology, Arsenal Room, February 16, 2026, 8:00 - 10:00

Introduction: Triple-Negative-Breast-Cancer is characterized for being highly aggressive, proliferative and having a poor-overall-prognosis. Combination of chemotherapy-immunotherapy(ICI) as neoadjuvant treatment has proven better pathological complete response(pCR) and survival rates. Nevertheless, there is currently a lack of known biomarkers that can accurately predict and perform an early identification of patients that would benefit from this approach.
18F-FDG-PET/CT allows metabolic tumour evaluation and volumetric parameters have been associated as predictors of early response and may predict tumour dynamics. On the other hand, novel immuno SPECT/CT(99mTc-iPDL1), makes it possible to qualitatively assess PD-L1 expression invivo and whole-body, considering tumour heterogeneity in a non-invasive way, and not only in a specific sample; which could be predictive within the ICI context.
This trial aims to determine the optimal ΔSUVmax 18F-FDG-PET cut-off value for predicting pCR. Secondary objectives include survival rates, associations between volumetric parameters from both PET/CT,SPECT/CT and tumour biomarkers such as Tumor-Infiltrating-Lymphocytes(TIL's), Ki67, Homologous-Recombination-Deficiency (HRD) and ctDNA dynamics.
Materials and Methods:
Prospective, single-centre, non-randomized, open-labeled, phase II study,that will recruit 50 patients with histologic confirmed breast carcinoma, with ER≤10% and PR≤10%,HER2 negative, clinical stage II-IIIA; basal 18F-FDG-PET/CT and 99mTc-iPDL1-SPECT/CT performed, tissue biopsy and blood sampling, repeated after 3 cycles for response assessment.
Results:
Currently 4 patients have joined the protocol.Tumoral heterogeneity is qualitatively visible from tumor tissue sampling results and qualitative assessment through both hybrid imaging methods: one patient who had mild desmoplasia and 1%TILS, had an intense metabolism uptake and mild iPD-L1 uptake within the primary tumor; whether another patient had an intense uptake from both radiotracers, and pathology showed moderate desmoplasia with high TIL's(30%). Some other data as androgen receptor status,Ki67,HRD,ctDNA, among others are also being collected.

Conclusion:
Patient enrollment began in august 2025, with recruitment expected to continue for 36 months or until the overall expected number is reached, whatever happens first.

Conflict of Interest
No conflict of interest to disclose.

Graphic

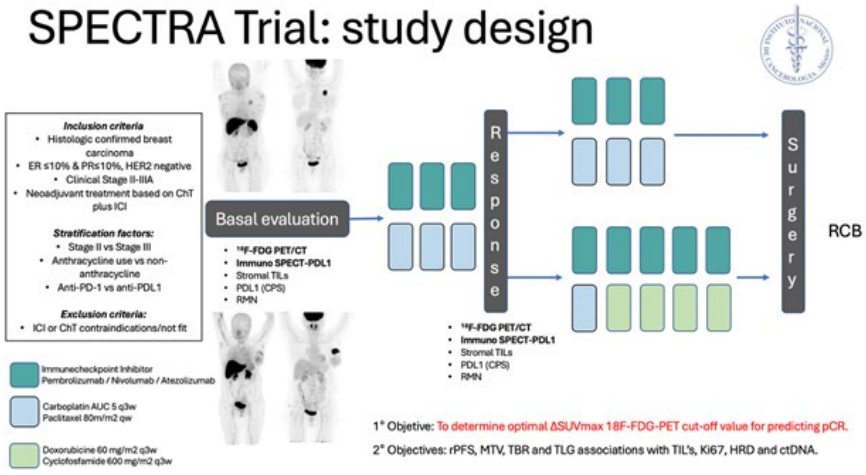

O82

Associated factors with positive [18F]FDG-PET/CT for distant metastasis in breast cancer

Dr. Ada Katerine Franco-ardila[1], Iván Fabricio Vega-González[1,2], Noiver Arbey Graciano-Vera[3], Katerine Montoya-Lezcano[4], Sonia Luz Gómez-Garcés[1], Lina María López-Vélez[2], Indira Díaz-Contreras[1]
[1]Universidad Autónoma De Bucaramanga - Unab, Bucaramanga, Colombia, [2]Clínica Las Américas AUNA, Medellín, Colombia, [3]Instituto de cancerología Las Américas AUNA, Medellín, Colombia, [4]Fundación IDEAS AUNA, Medellín, Colombia

Oral Presentations 6: Oncology 2 and Endocrinology, Arsenal Room, February 16, 2026, 8:00 - 10:00

Background/Objectives: [18F]FDG-PET/CT is a valuable tool for detecting distant metastases in breast cancer patients. Our study aimed to determine the association between tumor biomarkers and other clinicopathological factors with a positive [18F]FDG-PET/CT for metastatic disease during initial staging.
Methods: This case-control study included 272 patients with newly diagnosed breast cancer who underwent [18F]FDG-PET/CT in a specialized oncology center in Medellín, Colombia. We evaluated the association of patient sociodemographic and clinical variables, and tumor histopathological characteristics with the presence of distant metastases. For statistical analysis, we used the chi-squared test or Fisher's exact test for qualitative variables and the Wilcoxon rank-sum test for quantitative variables, estimating Odds Ratios (OR) with 95% Confidence Intervals. Ethical approval was obtained from the institutional authorities. The authors declare that no financial support was received for this work.
Results: A total of 84 patients (30.88%) were diagnosed with distant metastases. Key findings indicate that a positive [18F]FDG-PET/CT was significantly associated with a higher tumor size ($p=0.02$), lymph node involvement (cN, $p=0.02$), higher TNM stage ($p<0.01$), negative estrogen receptor (ER) ($p=0.015$), and positive HER2 status ($p=0.049$). The median SUVmax was significantly higher in patients with positive [18F]FDG-PET/CT. The study highlights that the use of [18F]FDG-PET/CT impacted treatment selection in 19% of cases.
Conclusions: This study reinforces the significant role of [18F]FDG-PET/CT in identifying distant metastases in breast cancer staging. We identified specific factors, including higher clinical stage, tumor size, and negative ER and positive HER2 status, that are associated with metastatic disease. These findings can help select patients who would benefit most from [18F]FDG-PET/CT, optimizing clinical management and treatment pathways.

Conflict of Interest
The authors declare no conflict of interest

Graphic

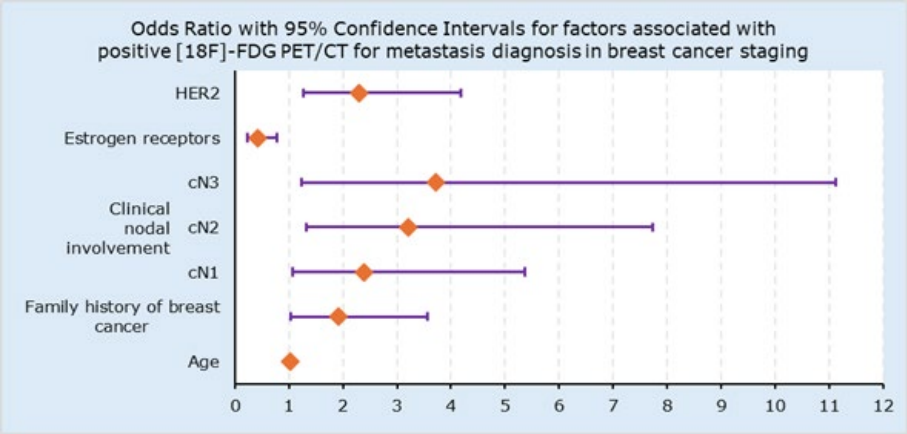
Odds Ratio with 95% Confidence Intervals for factors associated with positive [18F]-FDG PET/CT for metastasis diagnosis in breast cancer staging
HER2
Estrogen receptors
cN3
Clinical nodal involvement
cN2
cN1
Family history of breast cancer
Age
0
1
2
3
4
5
6
7
8
9
10
11
12

O83

Development and Evaluation of a Novel Dual-Targeted ^{68}Ga-FAPI-TTP PET Probe for Enhanced Tumor Imaging

Mrs. Yi-fei Pei[1], Mrs. Xiao-Yi Guo[1], prof Hua Zhu[1], prof Zhi Yang[1]
[1]State Key Laboratory of Holistic Integrative Management of Gastrointestinal Cancers, Beijing Key Laboratory of Carcinogenesis and Translational Research, NMPA Key Laboratory for Research and Evaluation of Radiopharmaceuticals (National Medical Products Administration), Department of Nuclear Medicine, Peking University Cancer Hospital & Institute, Beijing 100142, China, Beijing, China

Oral Presentations 6: Oncology 2 and Endocrinology, Arsenal Room, February 16, 2026, 8:00 - 10:00

Background/Aims: Fibroblast activation protein (FAP), overexpressed on cancer-associated fibroblasts in multiple malignancies, and trophoblast cell surface antigen 2 (TROP2), highly expressed in epithelial tumors, are attractive targets for molecular imaging. However, existing FAP inhibitor (FAPI) PET tracers suffer from rapid clearance and limited tumor retention. To improve targeting efficacy and broaden applicability, we developed a heterodimeric probe, ^{68}Ga-FAPI-TTP, that simultaneously binds FAP and TROP2.
Methods: FAPI-TTP was synthesized by conjugating the quinoline-based FAPI-04 with a high-affinity TROP2-targeting peptide (TTP). Radiochemical purity and stability were assessed via HPLC. Micro-PET/CT imaging and biodistribution studies were performed in murine xenograft models (U87,BXPC3, MDA-MB-468) at 0.5, 1, and 2 hours post-injection, compared with ^{68}Ga-FAPI and ^{68}Ga-TTP. Human organ radiation doses were extrapolated from healthy Balb/c mice.
Results: TTP exhibited high affinity for TROP2 (KD = 0.92 nM). ^{68}Ga-FAPI-TTP was obtained with >95% radiochemical purity and remained stable for over 4 hours. In vivo microPET/CT imaging studies revealed that ^{68}Ga-FAPI-TTP enabled clear and specific tumor visualization across multiple tumor xenograft models. Tumor uptake was significantly enhanced compared to either monomeric ^{68}Ga-FAPI or ^{68}Ga-TTP at all time points evaluated. Furthermore, tracer accumulation patterns observed on PET imaging corresponded well with immunohistochemical analysis, which confirmed co-expression of FAP and TROP2 in tumor tissues, supporting the molecular targeting specificity of the heterodimeric probe. The probe demonstrated rapid clearance from non-target tissues, leading to high tumor-to-background ratios. Radiation dosimetry estimates indicated acceptable safety profiles.
Conclusions: ^{68}Ga-FAPI-TTP is a novel dual-targeted PET probe with favorable radiochemical properties, high stability, and enhanced tumor uptake. Its ability to simultaneously target FAP and TROP2, together with promising biodistribution and safety features, supports its potential as a versatile imaging agent for a broad spectrum of epithelial-derived tumors.

Conflict of Interest
All authors have approved the submission, and we declare no conflicts of interest.

Graphic

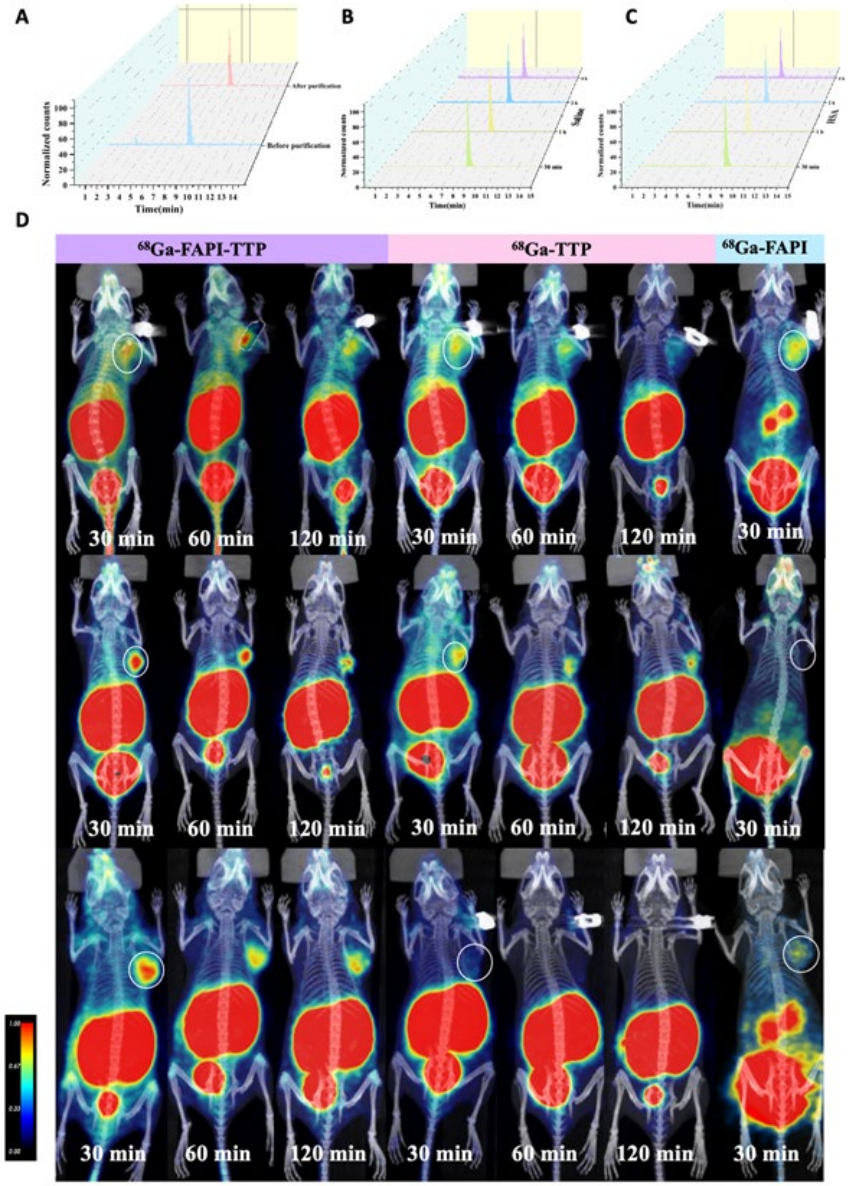
A
B
C
D
68Ga-FAPI-TTP
68Ga-TTP
68Ga-FAPI
30 min
60 min
120 min
30 min
60 min
120 min
30 min
30 min
60 min
120 min
30 min
60 min
120 min
30 min
30 min
60 min
120 min
30 min
60 min
120 min
30 min

O84

Real-life applicability of Fluorocholine PET/CT in primary hyperparathyroidism

Dr. Ivan Vega[1], **Dr. Monica Vidal**[2], Dra. Stefania Cruz[3], Dr. Antonio Rivera[4], Dr. Alejandro Delgado[2], Dra. Indira Diaz[5], Dra. Clara Arango[2], Dra. Carolina Prieto[2], Dr. Carlos Builes[2]
[1]Clínica Las Américas-AUNA, Medellín, Colombia, [2]Hospital Pablo Tobón Uribe, Medellín, Colombia, [3]Universidad Pontificia Bolivariana, Medellín, Colombia, [4]Universidad de Antioquia, Medellín, Colombia, [5]Unidad Gammanuclear , Armenia, Colombia

Oral Presentations 6: Oncology 2 and Endocrinology, Arsenal Room, February 16, 2026, 8:00 - 10:00

Background/Aims: Preoperative localization in primary hyperparathyroidism (PHPT) is crucial for minimally invasive surgery. We compared the performance of ultrasound (US), Tc-99m-Metoxi-isobutil-isonitrilo scintigraphy(SS), and 18F-Fluorocholine/positron-emission-tomography (FCH-PET/CT) for lesion detection and evaluated the ability of FCH-PET/CT to localize adenomas in relation to surgical pathology. We also explored the relationship between parathyroid-hormone (PTH) and the standard uptake value (SUVmax) on detection sensitivity.
Methods: A retrospective study of 75 patients(p) from two hospitals in Medellín-Colombia, previously approved by the ethics committee, with a surgical indication for PHPT with FCH-PET/CT and pathology confirmation. The reference standard was surgical/pathological location and histological confirmation; patients without pathology were excluded. We calculated the sensitivity, specificity, likelihood ratios and accuracy with exact 95% CIs. For localization, sensitivity was estimated at three stringency levels, exact code match, side (right/left), and quadrant (superior/inferior), and category specificity, sensitivity and Cohen's-K (bootstrap CIs). ROC analysis (DeLong) for PTH and SUVmax identified Youden-thresholds and thresholds targeting sensitivity≈0.90.
Results: 68p had pathological detection and underwent FCH-PET/CT 51/68 had US and 61/68 had SS with equivocal or inconclusive results. Sensitivity, specificity and accuracy of diagnostic imaging modalities were presents in Table 1. Of the 61p with positive FCH-PET/CT, 54p had confirmation in surgical pathology. the sensitivity for localization was 88.9% for exact match, 9.44% for side, and 100% for quadrant. Concordance was high (Po:0.889;K:0.849). Localization sensitivity by category ranged from 78.9-100%; macro-average 90.8%. ROC: PTH AUC: 0.669; Youden-threshold: 160.35 pg/mL (Sensitivity 33.9%;Specificity 100%). SUVmax AUC:0.625; Youden-threshold:2.62 (Sensitivity 88.9%;Specificity 50%). FCH-PET/CT sensitivity in surgical cases remained high across PTH quartiles (0.846–1.000) and was uniformly 1.000 across SUVmax quartiles (wide-CIs).
Conclusions: FCH-PET/CT demonstrated superior lesion detection and excellent localization performance compared with US and SS, supporting its role in preoperative PHPT planning and reaffirming like as the preferred imaging modality when precise localization is required.

Conflict of Interest
Not Conflict of interest

Table

Table 1. Sensitivity, specificity and accuracy in preoperative localization in PHPT

IMAGING	PATIENTS (n)	SENSIBILITY (%)	SPECIFICITY (%)	ACCURANCY (%)
US	51	39	71	43
SS	61	17	100	26
FCH-PET/CT	68	92	22	82

O85

Patient-specific factors in radioactive Iodine (I-131) clearance in Differentiated Thyroid Cancer (DTC) treatment

Mr George Thiveos[1], Mr Theofanis Petropoulos[1], Mr John Papantoniou[1], Mrs Agelliki Kokkini-Paschou[1], Mrs Garyfallia Livitsanou[1], Dr Evangelia Skoura[1], Dr Ioannis Datseris[1], **Dr. Ioannis Koutsikos**[1]
[1]Henry Dunant Hospital Center, Athens, Greece

Oral Presentations 6: Oncology 2 and Endocrinology, Arsenal Room, February 16, 2026, 8:00 - 10:00

Background/Aims: I-131 administration in DTC treatment has been proven successful over several decades. High half-life and photon energy of I-131 require strict radiation safety. Estimation of effective half-life (Teff) and clearance of I-131 has attracted research interest for several years. We aim to estimate Teff based on exposure rate measurements and determine whether Teff depends on gender, age or TSH stimulation approach.
Methods: This is a single-center retrospective study. DTC patients treated with radioiodine, following total thyroidectomy, were included. Using a calibrated survey meter, exposure rate measurements at 1 meter were made 24 and 48 hrs post administration, then converted to residual activity (RA) and plotted as percentage of the administered activities against time. Teff was computed from plot exponential line fittings (figure 1). Data analysis was based on gender (F-females / M-males), age (aged 18-39 y.o. group 1, 40-59 y.o. group 2, ≥60 y.o. group 3) and preparation with either recombinant human TSH (rhTSH) or thyroxine withdrawal (TW). Exclusion criteria were repeated treatment and treatment for metastatic disease.
Results: 835 patients, 558 females, 277 males, were included in our study. 288 were in age group 1, 408 in group 2 and 139 in group 3. TW was selected in 655 patients. No significant differences were found between age groups 1 and 2. All our results and statistically significant differences are summarized in attached table.
Conclusions: The lower Teff and faster activity clearance in females might be attributed to better compliance with instructions or differences in hormonal profiles. Activity clearance decreases with increasing age, due to expected declining renal function. Finally, rhTSH prepared patients show faster clearance than thyroxine deprived patients. Understanding these differences, derived from our analysis of a large cohort, can help health professionals tailor treatments and manage patients more effectively, ensuring better outcomes and promoting radiation protection.

Conflict of Interest
No conflict of interest

Graphic

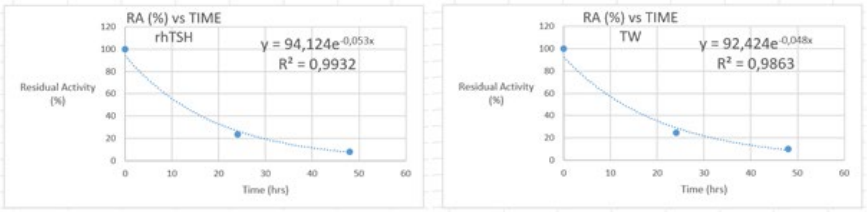

Figure 1: Residual activity exp line fittings for rhTSH and TW patients

Table

	Total	M	F	p-value M/F	Age group 1	Age group 2	Age group 3	p-value age groups 1/2	p-value age groups 1/3	p-value age groups 2/3	rhTSH	TW	p-value rhTSH/TW
Teff (hr)	14.15	14.75	13.86		13.86	13.59	15.75				13.08	14.44	
RA 24h (%)	24.55	25.41	24.12	0.047	23.39	23.89	28.86	NS*	<0.001	<0.001	23.57	24.82	NS*
RA 48h (%)	9.47	10.25	9.09	0.003	9.19	8.84	11.91	NS*	<0.001	<0.001	7.99	9.88	<0.001

*Not significant

O86

Bayesian survival modeling in multiple myeloma: prognostic PET/CT value with missing data imputation, preliminary results

Dr. Eliana Andrea González Artunduaga, Estadistico PhD Nelson Cruz, MD Hematologo Kenny Galvez
[1]Medico Nuclear IDIME, Bogotá, Colombia

Oral Presentations 6: Oncology 2 and Endocrinology, Arsenal Room, February 16, 2026, 8:00 - 10:00

Background / Aims: Prognostic survival models for multiple myeloma (MMND) have traditionally relied on Cox proportional hazards models. However, these approaches often exclude patients with missing data (MD), despite the frequent presence of incomplete datasets in clinical research. This exclusion introduces selection bias, reduces generalizability, and limits clinical application by requiring complete biological or clinical profiles. Advances in Bayesian modeling and multiple imputation strategies provide an opportunity to improve predictive accuracy while maintaining inclusivity.
Methods: We developed a Bayesian survival model (BM) enabling imputation of MD and robust prediction in incomplete datasets. The model was trained and validated using the MicroArray Quality Control II (MAQC-II) project, an international consortium led by the U.S. FDA to assess predictive performance of molecular models. A retrospective cohort of 32 NDMM patients treated at a high-complexity institution in Medellín, Colombia (2017–2024) was analyzed. This study was approved by the Institutional Review Board of Hospital Pablo Tobón Uribe. Eligibility criteria included baseline PET/CT within three months of diagnosis and no prior myeloma-specific treatment. MD were imputed for 47/224 (20%) values, including LDH, beta-2-microglobulin, bone marrow biopsy, and hemoglobin.
Results: The BM achieved a concordance index (C-index) of 71%, comparable to 72% obtained with Cox models in complete-case datasets, supporting its robustness and clinical utility. In the Colombian cohort, median age was 63 years (range 34–92), with 43% male patients. PET/CT was positive in 65.6% of cases. The prognostic variables identified were PET/CT findings and cytogenetic abnormalities, which retained predictive value after imputation.
Conclusions / Perspectives: PET/CT emerges as a critical prognostic tool in NDMM. BM and imputation enhance integration of imaging and clinical data, allowing broader patient inclusion, reducing bias, and supporting individualized risk stratification. These findings pave the way for precision medicine strategies to improve outcomes and optimize resource allocation in practice.

References
[1]Yu B. A Bayesian MCMC approach to survival analysis with doubly-censored data. Comput Stat Data Anal. 2010 Aug 8;54(8):192, [2] MAQC Consortium. The MicroArray Quality Control (MAQC-II) study of common practices for the development and validation of microarray-based predictive models. Nat Biotechnol. 2010;28(8):827–838, [3] R Core Team. R: A language and environment for statistical computing. R Foundation for Statistical Computing, Vienna, Austria, [4] Survival Analysis with R. R Views [Internet] and [5] Ibrahim JG, Chen M-H, Sinha D. Bayesian survival analysis. Springer; 2001.

Conflict of Interest
The authors declare no conflicts of interest.

O87

From Variability to Equity: An Eight-Year Retrospective Analysis of I-131 Therapeutic Practices in a Nuclear Medicine Service

Lic. Mariano Portillo[1], Dr. Martina Musumeci[1], Lic. Marcos Mussio[1], Tec. Delfina Eugeni[1], Dr. Luciana Arburua[1], Tec. Ariel Arispe[1], Dr. Silvina Racioppi[1]
[1]Servicio de Medicina Nuclear, Instituto Alexander Fleming, Buenos Aires, Argentina

Oral Presentations 6: Oncology 2 and Endocrinology, Arsenal Room, February 16, 2026, 8:00 - 10:00

Background and Objectives: Radioiodine therapy (I-131), widely validated for differentiated thyroid cancer, has undergone dose adjustments according to recurrence risk, impacting both professional exposure and the annual administered activity. In our institution, the referral of advanced cases influences the demographic distribution of patients. The aim was to analyze therapeutic implementation with I-131 in relation to the physicians in charge, annual administered activities, and their distribution.
Materials and Methods: A retrospective analysis was performed using the institutional database from April 2017 to August 2025. Paired Student's t-test, Kolmogorov-Smirnov test for normality, and Pearson's correlation coefficient were applied. An annual mean activity index (GBq/procedure) was calculated. Comparisons between physicians were performed using one-way ANOVA followed by Tukey's post-hoc test. Distribution equity was assessed with the Gini index.
Results: A total of 226 procedures were recorded: 65.5% female and 34.5% male patients. Most treatments (89%) were for differentiated thyroid cancer (83% papillary, 6% follicular), while 11% corresponded to benign conditions. The mean total administered activity was significantly higher than the mean annual number of procedures (−51.9; 95% CI: −64.9 to −38.9). A strong positive correlation was observed between both variables ($r = 0.958$; $p < 0.0001$). The activity/procedure index ranged from 2.77 (2018) to 3.70 (2020). ANOVA revealed no significant differences between physicians ($p = 0.2443$). Gini index analysis demonstrated initial concentration of activity (2017 = 0.48), followed by progressive equity from 2021 onwards, reaching near-homogeneous distribution in 2024 (0.02).
Conclusion: Findings confirm consistency in therapeutic practice and variations attributable to evolving dosing strategies. The progressive shift toward equitable distribution of administered activity among physicians represents not only an indicator of organizational efficiency but also a radioprotection strategy that should include the entire multidisciplinary team involved in nuclear medicine.

Conflict of Interest
The authors declare that they have no conflict of interest.

O88

Immunosuppressive molecular mechanisms potentially supporting development and progression of haematological malignancies triggered by abnormal or accidental exposure to nuclear irradiation

Dr Inna Yasinska[1], **Dr. Vadim Sumbayev**[1]
[1]University Of Kent, Chatham Maritime, United Kingdom

Oral Presentations 6: Oncology 2 and Endocrinology, Arsenal Room, February 16, 2026, 8:00 - 10:00

Background and aims. Haematopoietic cells damaged by nuclear irradiation release a protein called HMGB1 (high mobility group box 1) which is a danger signal that would otherwise be located in cell nucleus and will never be released. This protein actively participates in signalling networks associated with development of acute myeloid leukaemia (AML) and other haematological malignancies triggered by abnormal or accidental exposure to nuclear irradiation. Our work aimed to investigate the role of HMGB1 in support of cancer immune evasion machinery focusing on haematological malignancies.
Methods. We used cell cultures and ex vivo models in order to conduct these studies. A wide range of techniques including but not limited to Western blot analysis, ELISA, flow cytometry, qRT-PCRs, On-cell/in-cell Western analysis, a wide range of biochemical assays and synchrotron radiation circular dichroism spectroscopy were employed.
Results. We discovered that HMGB1 triggers the release of tumour necrosis factor alpha (TNF-ą) by primary human AML cells and healthy human monocytes. TNF-ą induced interleukin 1 beta (IL-1ß) production by healthy human leukocytes. Released IL-1ß was inducing expression and secretion of stem cell factor (SCF) by endothelial and epithelial cells. These results were verified in mouse bone marrow and primary human AML blood plasma samples [1]. We also found that HGMB1 induces Toll-like receptor 4 (TLR4)-mediated production of transforming growth factor beta type 1 (TGF-ß), which displays autocrine and paracrine activities. TGF-ß induces production of the immunosuppressive protein galectin-9 in cancer cells. As such, HMGB1 triggers the formation of an autocrine loop which induces galectin-9 expression thus supporting cancer immune evasion machinery of haematological and possibly other malignancies [2].
Conclusions. Our work uncovers biochemical mechanisms which can be potentially employed for development and progression of haematological malignancies triggered by nuclear irradiation. The work also highlights potential therapeutic targets for pharmacological correction of these pathological processes.

References
1) Yasinska IM, Gonzalves Silva I, Sakhnevych SS, Ruegg L, Hussain R, Siligardi G, Fiedler W, Wellbrock J, Bardelli M, Varani L, Raap U, Berger S, Gibbs BF, Fasler-Kan E, Sumbayev VV. High mobility group box 1 (HMGB1) acts as an "alarmin" to promote acute myeloid leukaemia progression. (2018) OncoImmunology, 7(6): e1438109.
2) Teo Hansen Selnø A, Schlichtner S, Yasinska IM, Sakhnevych SS, Fiedler W, Wellbrock J, Berger SM, Klenova E, Gibbs BF, Fasler-Kan E, Sumbayev VV. High Mobility Group Box 1 (HMGB1) Induces Toll- Like Receptor 4-Mediated Production of the Immunosuppressive Protein Galectin-9 in Human Cancer Cells. (2021) Front Immunol, 12: 675731.

Conflict of Interest
The Authors have no conflicts of interest to declare

O89

SPECT-CT in Primary Hyperparathyroidism: The Intermediate Localization Method

Dr. Carlos Collaud[1], Dra. Veronica Santana[1], Dra. Sandra Sunagua[1], Dra. Irene Arma[1], Dra. Isabel Hume[1], Dra. Constanza Cianciarelli[1], Dra. Maria Chacon[1], Dra. Nadia Pabstleben[1], Dra. Ana Mollerach[1], Dra. Ana Wayngarten[1]
[1]Hospital Italiano De Buenos Aires, Buenos Aires, Argentina

Oral Presentations 6: Oncology 2 and Endocrinology, Arsenal Room, February 16, 2026, 8:00 - 10:00

Introduction: Primary hyperparathyroidism is the leading cause of hypercalcemia, and surgery remains the treatment of choice. Successful minimally invasive surgery requires accurate preoperative localization of abnormal glands. Conventional scintigraphy with SPECT (C-SPECT) has been the traditional method, but its sensitivity is variable and often limited. The incorporation of SPECT-CT with diagnostic CT (SPECT-DCT) enables the combination of functional scintigraphic information with the anatomical precision of CT, thereby improving diagnostic accuracy and surgical correlation. In recent years, choline PET-CT has shown superior results and is considered the most sensitive imaging tool; however, its high cost and limited availability restrict its widespread use. Within this context, SPECT-DCT emerges as an intermediate localization method that is more accessible and achieves better results than C-SPECT.
Methods: A total of 117 patients with biochemically confirmed primary hyperparathyroidism and surgical indication were included. Nuclear medicine specialists independently interpreted C-SPECT and SPECT-DCT studies, while ultrasound was performed separately. Detection rates were evaluated and compared among the different modalities.
Results: The cohort included 95% women (111/117), with a mean age of 65 years. Mean serum calcium was 10.5 mg/dL, mean PTH 175.5 pg/mL, and mean vitamin D 36.6 ng/mL. Detection rates were 56% (66/117) for C-SPECT and 78% (89/117) for SPECT-DCT (p=0.0023). In cases with inconclusive C-SPECT, the addition of diagnostic CT allowed reclassification in 20% of patients. Concordance with ultrasound was significantly higher for SPECT-DCT (73.5%, 86/117).
Conclusion: SPECT-DCT significantly improves localization compared with conventional SPECT, representing a robust and accessible imaging option. Although choline PET-CT achieves the highest sensitivity, SPECT-DCT stands as a cost-effective intermediate method with clinically relevant impact on surgical planning in primary hyperparathyroidism.

References

1.- Preoperative parathyroid localization. Relevance of MIBI SPECT-CT in adverse scenarios. https://doi.org/10.1016/j.endinu.2022.02.011
2.- Update on Preoperative Parathyroid Localization in Primary Hyperparathyroidism
3.- Assessment and Comparison of 18F-Fluorocholine PET and 99mTc-sestamibi. Journal of Nuclear Medicine September 2021, 62 (9) 1285-1291; DOI: https://doi.org/10.2967/jnumed.120.257303

Hye-Sun Park1orcid, Namki Hong2, Jong Ju Jeong3, Mijin Yun4, Yumie Rhee2orcid
Endocrinology and Metabolism 2022;37(5):744-755. DOI: https://doi.org/10.3803/EnM.2022.1589
Published online: October 25, 2022
Conflict of Interest
No

Graphic

Image 1: Right paraesophageal and prevertebral parathyroid

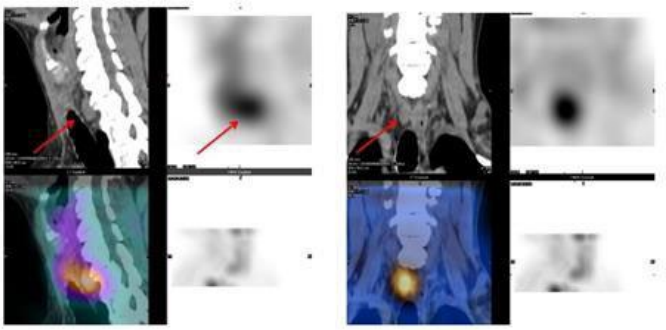

O90

Multiparametric Radiomic Analysis Based on 18F-FDG PET, MRI and Biopsy for Predicting Pathological Complete Response to Breast Cancer Neoadjuvant Chemotherapy

Mr. Marco Guarin[1], Ms. Carolina Tinetti[2], Mr. Mauro Namías[2]
[1]Instituto Nacional De Cancerología, Bogotá, Colombia, [2]Fundación Centro Diagnóstico Nuclear, Buenos Aires, Argentina

Oral Presentations 6: Oncology 2 and Endocrinology, Arsenal Room, February 16, 2026, 8:00 - 10:00

Aim: The aim of this study was to evaluate the ability of a multiparametric radiomic model combining pretreatment PET and Magnetic Resonance imaging with histopathological data to predict pathological complete response (pCR) to neoadjuvant chemotherapy (NAC) in breast cancer patients.
Methods: Thirty patients with biopsy-proven locally advanced breast cancer were included in this prospective study. PET and MRI images were imported into 3DSlicer for lesion annotation using semi-automatic and manual methods, supervised by an expert radiologist. Pretreatment biopsy specimens were analyzed to determine tumor histology, tumor and nuclear grades, and immunohistochemistry. Histopathological results were used to classify patients as pCR or non-pCR. A total of 1702 radiomic features were extracted using PyRadiomics along with 4 biopsy-derived features. Reproducibility against intra- and inter-observer variability was assessed in features extracted from ROI dilation and contraction using the intraclass correlation coefficient (ICC > 0.9). Dimensionality reduction was performed using the minimum redundancy maximum relevance (mRMR) method. The most relevant features were selected through three approaches: Boruta, Wilcoxon, and a Random Forest (RF) machine learning model. Class imbalance was corrected using the adaptive synthetic sampling method (ADASYN). Finally, a supervised RF model was trained and validated with Leave-One-Out cross-validation. The study protocol was reviewed and approved by the Ethics Committee of Instituto Roffo.
Results: The best performance was achieved by an RF model using two variables: estrogen receptor expression (biopsy) and the PET feature “wavelet-HHL_glcm_Imc1” (AUC = 0.95; sensitivity = 90%; specificity = 86%), which demonstrated strong robustness across selection models.
Conclusions: The multiparametric radiomic model showed the ability to predict pCR to NAC in patients with locally advanced breast cancer, thus highlighting its potential to improve pretreatment patient stratification.

Conflict of Interest
None

P001

Myocardial perfusion in patients with suspected coronary artery disease: association with troponin T levels in three centers in Bogotá

Dr. Maria Camila Bedoya Gonzalez[1], Dr. Andrea Carolina Suarez Echavez[1], Dr. Mauricio Andrés Hinojosa Vidal[1], Dr. Alejandro Cortés Polanía[1], Dr. Humberto Varela Ramírez[1]
[1]Fundacion Universitaria De Ciencias De La Salud, Bogotá d.c., Colombia, [2]Fundacion Universitaria Sanitas, Bogotá d.c., Colombia, [3]Clinicas colsanitas, Bogotá d.c., Colombia

Background / Objectives: Diagnosing non ST elevation acute coronary syndrome (NSTE ACS) with negative high sensitivity troponin T (hs TnT) remains challenging. Myocardial perfusion imaging (MPI) with technetium 99m (99mTc) sestamibi/ tetrofosmin can reveal functional ischemia not captured by biomarkers. We aimed to characterize MPI findings and their association with clinical and paraclinical variables in patients presenting with chest pain and negative hs TnT across three institutions in Bogotá in 2023.
Methods: We conducted a retrospective cross sectional study including adults with a clinical diagnosis of unstable angina, negative hs TnT, and inpatient MPI. Sociodemographic, clinical (hypertension, diabetes), laboratory (hs TnT), and imaging variables (MPI positivity and ischemia grade) were collected. Associations were tested with chi square or Fisher's exact tests and Kruskal–Wallis, with statistical significance set at $p<0.05$. Institutional ethics approval was obtained; de identified data were used
Results: Eighty six patients were analyzed (mean age 66.1 years; 61.6% men). MPI was positive in 12.8% and negative in 87.2%. MPI positivity was associated with higher hs TnT values within the negative range ($p=0.047$), a diagnosis of unstable angina ($p=0.004$), hypertension ($p=0.034$), and diabetes mellitus ($p=0.005$); no association with sex was found ($p=0.418$). Among positive studies, ischemia was mild in 27.3%, moderate in 63.6%, and severe in 9.1%.
Conclusions: In patients with chest pain and negative hs TnT, MPI with 99mTc sestamibi/tetrofosmin identifies a subgroup with functional ischemia—particularly when unstable angina and cardiovascular comorbidities are present. Incorporating MPI as a complementary tool may improve risk stratification and support timely clinical decision making in high demand emergency settings.

Conflict of Interest
The authors declare no conflicts of interest.

Graphic

Figure

Myocardial perfusion study results (N=86)

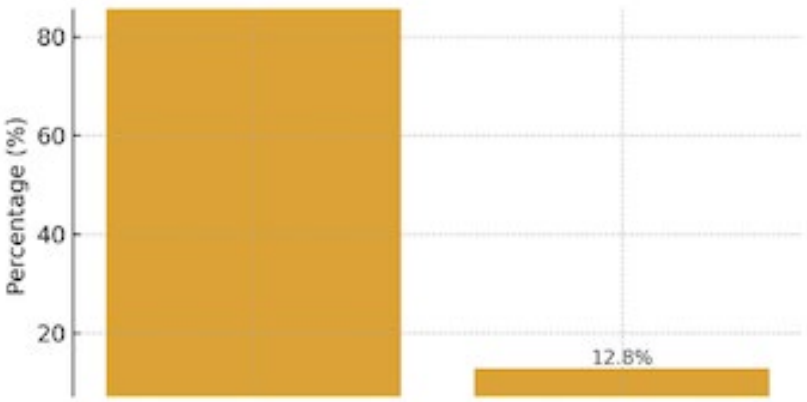

Table

Table

Associations with positive MPI

Variable	Association	p value
hs-TnT (higher, within negative range)	Yes	0.047
Unstable angina diagnosis	Yes	0.004
Hypertension	Yes	0.034
Diabetes mellitus	Yes	0.005
Sex	No	0.418

P002

Agreement of left ventricular ejection fraction by echocardiography and SPECT in patients with chest pain and suspected ischemia

Dr. Angie Cabrera Rojas[1], Dr. César García Quintanilla[2], Dr. Javier Rodríguez Prada[3], Dr. Adriana Reyes González[4]
[1]Universidad Autónoma de Bucaramanga, Floridablanca, Colombia, [2]SPECT Medicina Nuclear SAS, Floridablanca, Colombia, [3]Unidad de Investigación y Educación, Instituto del Corazón de Bucaramanga, Floridablanca, Colombia, [4]Universidad Autónoma de Bucaramanga, Floridablanca, Colombia

Background /Aims: Left ventricular ejection fraction (LVEF) is a key prognostic marker and therapeutic guide in cardiology. Cardiac magnetic resonance is the reference standard for its quantification, but transthoracic echocardiography remains the most widely used technique, with limitations in ventricular geometry and interobserver variability. Gated-SPECT is less operator-dependent but involves radiation exposure. This study aimed to determine agreement between echocardiographic and Gated-SPECT LVEF in patients with chest pain and suspected myocardial ischemia.
Methods: We conducted a retrospective observational study of 279 patients evaluated between 2019 and 2024 at an institution of Nuclear Medicine in Santander (Colombia). Adults ≥18 years with chest pain and suspected myocardial ischemia who underwent both tests within three months, without intervening ischemic events, were included. Since LVEF values did not meet normality assumptions, Spearman correlation, intraclass correlation coefficient (ICC), and Bland-Altman limits of agreement were calculated.
Results: Median age was 69 years (IQR 61–76); 50.2% were women. Median LVEF was 58% (IQR 53–62) by echocardiography and 67% (IQR 59.5–70) by SPECT. Mean bias was −6.2 percentage points (limits −21.9 to 9.5). Spearman correlation was 0.528 ($p<0.001$) and ICC 0.605. Agreement was higher in men (ICC 0.656) and in patients with segmental wall motion abnormalities (ICC 0.635), while moderate in women (ICC 0.467).
Conclusions: There is significant correlation between echocardiographic and SPECT LVEF, but absolute agreement is only moderate, with systematic overestimation by SPECT. Sex and wall motion abnormalities influenced reproducibility. Bland-Altman analysis confirmed clinically relevant variability, indicating the two methods are not interchangeable and results must be interpreted with caution.

Conflict of Interest
There is no conflict of interest

Graphic

Figure 1. Bland-Altman plot for agreement of echocardiographic vs. SPECT LVEF (n=279).

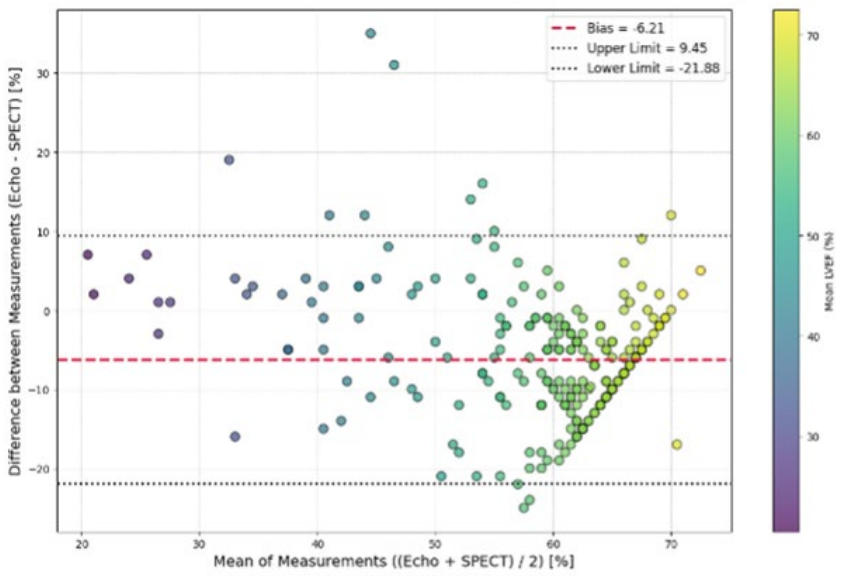

Table

TABLE 1. BIAS AND CORRELATION COEFFICIENTS FOR ECHOCARDIOGRAPHIC VS. SPECT LVEF

Group	N	Bias (LoA 95%)	Spearman ρ (95% CI)	ICC (2,1) (95% CI)
All	279	-6.210 (-21.876 – 9.455)	0.528 (0.429–0.614)	0.605 (0.497–0.686)
Men	139	-4.482 (-22.491 – 13.527)	0.557 (0.406–0.679)	0.656 (0.504–0.755)
Women	140	-7.926 (-20.007 – 4.154)	0.445 (0.258–0.578)	0.467 (0.282–0.598)
Younger than 65 years	93	-4.301 (-23.193 – 14.591)	0.490 (0.309–0.655)	0.644 (0.476–0.772)
65 years or older	186	-7.165 (-20.608 – 6.278)	0.551 (0.432–0.658)	0.576 (0.439–0.672)
Without Segmental Changes	205	-6.442 (-19.955 – 7.071)	0.240 (0.100–0.350)	0.160 (0.051–0.269)
With Segmental Changes	74	-5.568 (-26.112 – 14.976)	0.707 (0.523–0.819)	0.635 (0.473–0.741)

P003

Correlation between Chagas myocartiopathy and heart failure with sudden death over a 10-year period

Lic. Elizabeth Huanca[1], Doctor Raúl Araujo, licenciado Marcelo Torrez, Licenciada Patricia Bernal, Ingeniero Alfredo Zambrana, Doctora Greta Vargas, Doctor Daniel Salinas
[1]Universidad San Francisco Xavier De Chuquisaca, Sucre, Bolivia

Infectious myocarditis secondary to Chagas disease is the leading cause of mortality and morbidity, with the most frequent clinical manifestations being congestive heart failure and sudden cardiac death, the most commonly used diagnostic imaging methods for disease monitoring and prognosis, due to the findings they yield and help establish predictors of death in patients with Chagas disease, are: Echocardiogram, magnetic resonance imaging, and nuclear cardiology.
The research approach is quantitative; prospective, observational and longitudinal survival design was used to analyze the predictor variables of survival time in patients with Chagas disease and dilated cardiomyopathy over a period of ten years, from 2011 to 2021. The total number of Chagas disease patients screened was 47, informed consent was obtained through their relatives.
The study showed that the median survival times for sudden death and death from heart failure in patients with dilated Chagas cardiomyopathy were 5.8 and 5.9 years, respectively, compared to the median survival time for death from cardiac causes, which was 4 years. Of the total deaths (n=37), 45.95% were attributable to sudden death (n=17) and 45.95% to heart failure (n=17), and the remaining 8.10% were attributable to deaths from non-cardiac causes (n=3). Knowledge of the characteristics of the Chagas population, supported by complementary non-invasive tests as radionuclide ventriculography, could provide a strategy to identify patients at high risk of progressing to sudden death and death from heart failure, an essential aspect for reducing the impact of this disease on survival. The presence of regional contractility abnormalities can identify individuals at risk of developing progressive worsening of left ventricular systolic function, leading to mortality from heart failure or sudden death. Diagnosis of LV segmental disorders is essential because it allows for the identification of individuals at risk of worsening LV function and ventricular arrhythmias, which subsequently lead to death.

Conflict of Interest
ninguno

P004

Experience at a university hospital with positron emission tomography using fluorine-18-labeled glucose metabolism in inflammatory/infectious cardiovascular processes

Dr. Teresa Massardo[1], Dr. Juan Dupouy[1], Dr. Alejandro Rojas, Dr. José Tomás Donoso, Dr. Diego Palma, Dr. Daniel Saavedra, Dr. Francisco Javier Gomez[1], Dr. Rocio Hidalgo[1], Dr. WWilfredo Navarrete, Dr. Axel Aranguiz[1], Dr. DaDaniel Schneider Dr. Marcelo Llancaqueo[1]
[1]hospital Clinico Universidad de Chile, Santiago/Chile, Chile, [2]hospital San Juan De Dios, Santiago/Chile, Chile

Background: Findings in positron emission tomography using fluorodeoxyglucose (FDG) are a major criterion for infective endocarditis (IE) in prosthetic as well as in native valves and devices, in current international guidelines. Its usefulness in vasculitis is well recognized in large and medium vessels. Aims: To determine the profile of cases studied with FDG of cardiovascular origin in our practice and correlate them with subsequent management.
Method: Retrospective study from 2023 with 34 FDG cases from 30 patients/850 exams (63% males between 21-84 y.o.) including suspected or confirmed IE, fever of unknown origin (FUO), vasculitis and other inflammatory cardiovascular conditions. Cardiac suppression protocol was employed in suspected EI.
Results: The Table shows the main results according to the final diagnosis in the follow-up: infection (EI and FUO) and inflammation (vasculitis and others) the last corresponded to myocarditis cases. The presence of prosthetic valves or devices including pacemakers is also depicted. One case with recent aortic valve replacement with Surgicel showed moderate nonspecific uptake and another with suspected EI have insufficient preparation. The EI group presented a significant number of distant hypermetabolic lesions remarking 3 spondylodiscitis, and two multifocal pneumonias and septic embolisms. In the vasculitis group we found IgG4, giant cell arteritis, periarteritis nodosa, Behcet's and central nervous system involvement with associated phenomena such as renal/cerebral infarctions. One patient with patchy arteritis and renal failure presented diffuse pericardial hypermetabolism of uremic origin. Another with heterogeneous myocardial hypermetabolism had granulomatous myocarditis. Antibiotics and surgery in the infection group was started or changed and corticosteroids and immunosuppressants in active inflammatory cases. The FDG findings led to a change in therapeutic approach in 72% of infected patients and 50% of the active inflammatory.
Conclusions: Our initial experience with FDG in cardiovascular inflammatory-infectious diseases allowed us a change management in more than two-thirds of cases.

Conflict of Interest
None

Table

Condition	Final Diagnosis	n	FDG positive		Prosthesis grafts/ devices	Bacteria	Conduct change
			Cardiac	Distance			
Infection	EI	15	4 (1nc)	10	11	10	11
	FUO	3	2	2	2	3	4
Inflammation	Vasculitis	10	2	6	0	0	4
	Other: myocarditis	2	2	1	0	0	2
Total		30					21 (70%)

P005

18F-FDG PET/CT for the Detection and Reclassification of Infective Endocarditis in Corrected Congenital Heart Disease

Mrs. Sonia Simona Traverso, MD Roxana Campisi, MD Jessica Herrero, MD Christian Gonzalez, MD Calderon Laura, MD Paola Corona, MD Nicolas Bustos, MD Florencia Arabolaza, MD Gabriel Bruno
[1]Nuclear Diagnostic Center (FCDN), CABA, Argentina

Background:Infective endocarditis (IE) in patients with corrected congenital heart disease (CCHD) is diagnostically challenging due to complex anatomy and diverse prosthetic materials, often located in extracardiac structures. 18F-FDG PET/CT has emerged as a complementary imaging modality for IE. We aimed to evaluate its diagnostic utility in this population.
Methods: We conducted a retrospective observational study of patients with CCHD and clinical suspicion of IE who underwent 18F-FDG PET/CT between January 2017 and December 2024. A preparatory low-carbohydrate, high-fat diet was used to suppress physiological myocardial uptake. Whole-body PET/CT images were acquired. Focal and/or heterogeneous radiotracer uptake around prosthetic material was considered suggestive of infection. Diagnostic thresholds included periprosthetic SUVmax ≥ 5 and SUVmax ratio (periprosthetic/vascular pool) > 2.
Results: Eight male patients were included (mean age 26 ± 15 years, range 9–59). PET/CT reclassified 5 patients (62%) as “definite” IE, with a mean SUVmax of 6.4 ± 0.1 and SUVmax ratio of 3.4 ± 0.9. Of these, only 2 had echocardiographic findings consistent with IE. PET/CT also identified septic emboli in 2 cases, involving pulmonary and splenic territories. Among the 3 patients not reclassified as definite IE, PET/CT contributed to alternative diagnoses: mediastinitis in one and active pulmonary infection in another.
Conclusions: In our group of patients with CCHD and suspected IE, 18F-FDG PET/CT was a valuable diagnostic tool, particularly when echocardiography was inconclusive. It enabled reclassification of IE status, detection of systemic embolic events, and clarification of alternative diagnoses. These findings support the inclusion of PET/CT in the diagnostic workup of IE in this complex patient population.

Conflict of Interest
None

Table

P	Type of Congenital Heart Disease	Type of Surgical Intervention	Prosthetic Material	Time from Last Intervention to PET	Pathogen	Diagnosis After PET/CT	Outcome
1	Duct-dependent pulmonary circulation + pulmonary stenosis	Rastelli surgery + 2 valve replacements	Extracardiac conduit and mechanical valve	7 years	Streptococcus	Definite IE	Surgical treatment performed. Pathology positive for IE. Currently NYHA Class I.
2	Pulmonary atresia + VSD	Patch + RV-PA conduit (homograft)	RV-PA homograft	21 years	Enterococcus faecalis	Definite IE	Two years later: dysfunctional, calcified homograft with severe PI and moderate stenosis, mobile mass on arterial side of homograft. Surgery planned.
3	Transposition of great arteries (TGA)	Arterial switch (Jatene technique + Lecompte maneuver)	None	11 years	None	Definite IE with septic emboli	
4	Bicuspid aortic valve with insufficiency + PDA	Mechanical AVR + mitral valve plasty with patch	Mechanical valve	1 month	*E. faecalis* and MRSA	IE excluded	Completed antibiotics. Currently asymptomatic.
5	Single-ventricle physiology (Fontan-Kreutzer)	Glenn (2005), Fontan (2011), left pulmonary artery stent (2021)	None	3 years	None	IE excluded Active pulmonary infection.	Asymptomatic, NYHA Class I.
6	Atrial septal defect (ASD)	Patch repair	None	3 months	MRSA in mediastinum (not in blood cultures)	IE excluded Mediastinitis.	Occasional palpitations. NYHA Class I.
7	Double outlet right ventricle (DORV) with TGA-type anatomy, coarctation, VSD, and tricuspid valve stranding	Stansel procedure + mechanical AVR during reintervention	Extracardiac conduit and mechanical valve	1 year	None	Definite IE	Asymptomatic
8	ASD	Amplatzer device	Amplatzer	Not specified	Salmonella	Definite IE	Continued on IV antibiotics. Poor clinical course requiring intensive care.

P006

Is Cardiac Amyloidosis an Underdiagnosed Disease? Defining Frequency in Colombia

Dr. Monica Vidal[1], Dr. Alejandro Delgado[1], Dr. Juan Luis Londoño[2], Dr. Nilson Lopez[1]
[1]Hospital Pablo Tobón Uribe, Medellín, Colombia, [2]Hospital San Vicente Fundación, Medellín, Colombia

Background/Aims: Transthyretin cardiac amyloidosis (CM-ATTR) is an underrecognized cause of heart failure (HF), and published data from Latin America remain limited. This study aims to determine the frequency and clinical characteristics of CM-ATTR in older patients diagnosed with HF and preserved or mildly reduced left ventricular ejection fraction (LVEF).
Methods: A prospective cross-sectional, multicenter study in Medellín-Colombia, previously approved by the ethics committee, including 107 patients (p), aged ≥60 years with diagnosis of HF, LVEF ≥40%, and left ventricular hypertrophy (LVH; septal wall thickness ≥12mm). Immunoglobulin light-chain amyloidosis was excluded in all participants before performing bone scintigraphy with 99m-Tc-hydroxymethylene-diphosphonate (99mTc-HMDP). CM-ATTR was diagnosed using a Perugini score ≥2 and the heart-to-contralateral lung (H/CL) ratio ≥1.5 and ≥1.3 at 1 and 3 hours, respectively.
Results: The mean age 73±8 years; 54 women (50.5)]. CM-ATTR was diagnosed in 21p (19.6%), 14 were men (66.6%). The cohort exhibited a high burden of comorbidities, most commonly hypertension (80.9%), atrial fibrillation (33.3%), and chronic kidney disease (28.6%). Compared with the overall cohort, CM-ATTR patients more frequently had a history of atrioventricular block (23%) and carpal tunnel syndrome (13%), and more often reported dyspnea (80%) and fatigue (52%) at diagnosis. The mean LVEF was 56% in the overall cohort, and the mean septal thickness was 13 mm. The Perugini score and the H/CL index showed a high diagnostic performance at 3 hours, comparing them with the results at 1 hour, with a sensitivity and specificity of 100% in both evaluations at 3 hours (Table 1).
Conclusions: In this Colombian cohort, 19.6% of patients >59 years with HF, LVH, and preserved or mildly reduced LVEF were diagnosed with CM-ATTR. These findings suggest that this condition may be underdiagnosed and support the inclusion of 99mTc-HMDP scintigraphy in the evaluation of secondary causes of HF in similar high-risk groups.

Conflict of Interest
We don´t have conflict of interest

Table

Table 1. Scintigraphic findings at 1 hour and 3 hours after administration of the radiopharmaceutical.				
		PERUGINI 1H		
		POSITIVE: 2-3 (n)	NEGATIVE: 0-1 (n)	TOTAL (n)
H/CL 1H	POSITIVE (>1.5) (n)	20	0	20
	NEGATIVE (<1.5) (n)	2	85	87
	TOTAL (n)	22	85	107
		PERUGINI 3H		
		POSITIVE: 2-3 (n)	NEGATIVE: 0-1 (n)	TOTAL (n)
H/CL 3H	POSITIVE (>1-3) (n)	21	0	21
	NEGATIVE (<1.3) (n)	0	86	86
	TOTAL (n)	21	86	107

P007

Diagnostic Value of Dual-Time-Point 18F-Fluorocholine PET/CT in Hyperparathyroidism: A Latin American Retrospective Cohort

Dr. Melissa Alvarez[1], Dr. Rosita Nohemy Dorado Castillo[1], Dr. Diana Carolina Quijano Galvis[1], Dr. Luz Maritza Pabon Castilla[1], Jefe de enfermería John Jairo Torres Gallego[1], o Jefe de enfermería Beatriz Elena Guzman Narvaez[1], Técnico Juliana Maria Venegas Sanchez[1], Técnico Jessenia Jimenez Moreno[1], Técnico Javier Andrés Garces Giraldo[1], Técnico Jenner Pulido Pasaje[1]
[1]Fundación Valle Del Lili, Cali, Colombia

Background: 18F-FCH PET/CT is increasingly used to localize hyperfunctioning parathyroid glands when conventional imaging is non-diagnostic[1]. Dual-time-point may improve lesion conspicuity[2], but the optimal timing remains uncertain. 2021 European Association of Nuclear Medicine guideline recommends delayed imaging at ~60 minutes and, when feasible, an early acquisition at ~5 minutes, as some lesions are visible only early[3,4]. This study aimed to determine the optimal scan time by identifying the phase with the highest lesion-to-background contrast in a Latin American cohort.
Methods: Single-center retrospective study of 85 consecutive patients with hyperparathyroidism who underwent dual-time-point 18F-FCH PET/CT. Early images were acquired ~5–10 minutes post-injection and delayed images at 60 minutes, from the nose to the chest. Collected variables included demographics, biochemistry, images and PET/CT outcome. Early and delayed images were compared visually and quantitatively (parathyroid lesion and skeletal muscle background SUVmax) and the lesion-to-muscle ratio.
Results: The cohort included six males, mean age 65±12.5 years(range 20–87). All patients had prior parathyroid scintigraphy that was negative or inconclusive. Comorbidities included chronic kidney disease in 16/85 and osteopenia/osteoporosis in 53/85; five patients had cancer diagnosis. PET/CT was positive in 43/85 (50.6%) and negative in 41/85 (48.2%); one incidental thyroid carcinoma was detected. Compared with negative result group, positives cases showed higher values PTH and calium levels (PTH 285.5±433.6 pg/mL; calcium 10.2±0.8 mg/dL). Visually, delayed-phase predominance occurred in 21/43(48.8%), including three patients visible only on late images; early-phase predominance occurred in 14/43(32.6%) with no cases visible only on early point; and no relevant change occurred in 8/43. 18.6% Ectopic glands were localized and 14% patients presented multigland disease. Lesion and background SUVmax, were numerically higher on delayed images ($p>0.05$), but the lesion-to-muscle background ratio was lower.
Conclusions: Delayed images provided the greatest conspicuity, while roughly one-third were better seen on early images, supporting routine dual-phase acquisition

References
1. Cuderman A, Senica K, Rep S, Hocevar M, Kocjan T, Sever MJ, et al. 18F-Fluorocholine PET/CT in Primary
Hyperparathyroidism: Superior Diagnostic Performance to Conventional Scintigraphic Imaging. J Nucl Med. 2020;61(4):577-83. doi:10.2967/jnumed.119.229914.
2. Broos WAM, Wondergem M, van der Zant FM, Knol RJJ. Dual-Time-Point 18F-Fluorocholine PET/CT in Parathyroid Imaging. J Nucl Med. 2019;60(11):1605-10.
3. Petranović Ovčariček P, Giovanella L, Carrió Gasset I, Hindié E, Huellner MW, Luster M, et al. The EANM practice guidelines for parathyroid imaging. Eur J Nucl Med Mol Imaging. 2021;48(9):2801-22.
4. Rep S, Lezaic L, Kocjan T, Pfeifer M, Sever MJ, Simoncic U, et al. Optimal scan time for evaluation of parathyroid adenoma with [18F]-fluorocholine PET/CT. Radiol Oncol. 2015;49(4):327-33.
Conflict of Interest
The authors declare no conflicts of interest.
This study received no external financial support.
Ethics approval.
The study protocol was approved by the Ethics Committee of Fundación Valle del Lili.

P008

Stimulated Pre-Ablative Thyroglobulin: Can It Be Used as a Parameter to Avoid Ablation?

Dr. Irene Arma[1], Ana Maria Mollerach[1], Isabel Hume[1], Constanza Cianciarelli[1], Maria Jose Chacon[1], Ana Wayngarten[1], Fabiana Russo Picasso[1], Nadia Pabstleben[1], Florencia Zalarrayan[1], Carlos Collaud[1]
[1]Hospital Italiano De Buenos Aires, CABA, Argentina

Background/Aims: Several studies suggested that in patients with differentiated thyroid cancer (DTC), pre-ablative stimulated thyroglobulin (sTg) levels <1ng/mL may serve as a criterion to guide the decision for radioiodine (RAI) therapy. The aim of this study was to assess whether patients with negative sTg differ from those with positive sTg in terms of findings on post-therapy whole-body scintigraphy (WBS), for the detection of functional thyroid remnants.
Methods: A retrospective analysis was conducted on 111 consecutive patients (p) with DTC who underwent total thyroidectomy and were referred for RAI therapy. Pre-treatment sTg levels (with TSH >30µU/mL) and thyroglobulin antibody(TgAb) status were recorded. Sixteen patients with positive TgAb were excluded.
WBS findings were classified as WBS- (negative, no uptake) or WBS+ (positive, any uptake). Patients were stratified into two groups: sTg <1ng/mL and sTg >1ng/mL. Results were categorized as:
Concordant: sTg <1ng/mL with WBS–, or sTg >1ng/mL with WBS+.
Discordant: sTg <1ng/mL with WBS+, or sTg >1ng/mL with WBS–.
Concordance was assessed using Cohen's kappa coefficient, and discordance was analyzed with McNemar's test.
Results: WBS+ 85/95p (89.5%); WBS– 10/95p (10.5%).
sTg <1ng/mL (26p): WBS+ 22/26 (84.6%); WBS– 4/26 (15.4%).
sTg >1ng/mL (69p): WBS+ 63/69 (91.3%), WBS– 6/69 (8.7%).
Concordant results: 67p (70.5%).
The kappa coefficient was 0.083, indicating very low concordance between sTg and WBS.
Discordant results: 28p (29.5%), most frequently in the subgroup with sTg <1 ng/mL and WBS+ (22/26, 84.6%).
Discordance was statistically significant (McNemar's test, p=0.0046).
Conclusion: The majority of patients showed positive WBS findings. An sTg <1ng/mL does not exclude the presence of functioning thyroid remnants. Therefore, sTg should not be used as the only parameter to decide whether to perform RAI therapy in DTC patients.

Conflict of Interest
No Conlict of Interest

Table

Concordant	STg<1 ng/mL WBS -	4 p	67 (70,5%)
	sTg >1 ng/mL WBS+	63 p	
Discordant	sTg >1 ng/mL WBS -	22 p	28 (29,5%)
	sTg<1 ng/mL WBS +	6 p	

Correlation Between Pre-Ablative Thyroglobulin (sTg) and Post-RAI Whole-Body (WBS) Findings

P009

Primary Cultures and FISH analysis in Mesenchymal Cells from Osteomalacia-Inducing Tumors (TIO)

Dra. Patricia Gargallo[1], **Dr. Maria Jose Bastianello**[1], Lic Diego Biscochea[1], Dr Roxana Chirico[1], Grupo Argentino de TIO Grupo Argentino de TIO[2], Tech Brenda Konowalik[1]
[1]CEMIC University Hospital, Buenos Aires, Argentina, [2]Grupo Argentino de TIO, CABA, Argentina

Introduction: Tumor-Induced Osteomalacia (TIO), is a paraneoplastic syndrome characterized by hyperphosphaturia, hypophosphatemia, and reduced vitamin D levels. This disease is caused by tumors that secrete FGF23, particularly phosphaturic mesenchymal tumors (PMTs). Due to their non-specific clinical manifestations and difficulty in locating the tumors, diagnosis and treatment are often delayed. PET/CT with Gallium-68 DOTATATE offers higher sensitivity and specificity for tumor localization. In most cases, the presence of FN1::FGFR1 and FN1::FGF1 fusions, detected by FISH (fluorescent in situ hybridization), can aid in diagnosis and targeted therapies.
Objective: To develop an in vitro model to study mesenchymal cells derived from TIO and analyze FGFR1 gene rearrangements using FISH.
Materials and Methods: Primary monolayer cultures were established from five fresh biopsies with histological diagnosis of PMT. FISH analysis were performed using the FGFR1 break-apart (BA) probe (Live, Lexel).
Results: Stable cell growth was achieved in four cases, with fusiform cell morphology. Once confluence was reached, cells were cryopreserved in liquid nitrogen. In one of the five cases, a positive FGFR1 rearrangement was detected. This patient was a 42-year-old female. PET/CT Ga-68 DOTATATE detected tracer uptake in a soft tissue nodular structure, located beneath the first cuneiform of the right foot, without the bone. Surgical removal of the tumor was complete, and biochemical parameters normalized.
Conclusion: culturing mesenchymal cells derived from TIO provides a suitable in vitro model for genetic studies. The patient with FGFR1 positive rearrangement showed a favorable clinical evolution after removal. In contrast, the three other cases without FGFR1 rearrangements had a more aggressive course, with multiple metastases and infiltration into surrounding tissues without clear boundaries. Although it has been described that complex rearrangements may escape detection by FISH using FGFR1 BA probe (1,2), it cannot be ruled out that these aggressive tumors could present different genetic profiles.

Conflict of Interest
None

P010

Diagnostic utility of 11C-methionine PET/CT in primary hyperparathyroidism: national experience in Uruguay

Dr. Eduardo Lischinsky[1], Dr. Omar Alonso[1,2], Ismael Cordero[1,2], Eduardo Savio[1,2], Javier Giglio[2], Dr. Juan Pablo Gambini[1,2]
[1]CMNIM, Hospital De Clínicas "Dr. Manuel Quintela" - Universidad De La República, Montevideo, Uruguay, [2]Centro Uruguayo de Imagenología Molecular (CUDIM), Montevideo, Uruguay

Background/Objectives: Primary hyperparathyroidism requires precise preoperative localization of hyperfunctioning parathyroid tissue for successful minimally invasive surgery. When conventional imaging including dual-phase 99mTc-sestamibi scintigraphy and neck ultrasonography yield negative or inconclusive results, advanced molecular imaging with aminoacid tracers represents a promising second-line option. This study evaluates the diagnostic utility of 11C-methionine positron emission tomography/computed tomography in patients with primary hyperparathyroidism at a single PET/CT center in Uruguay.
Methods: Retrospective analysis of 46 patients with primary hyperparathyroidism who underwent 11C-methionine PET/CT between 2011-2022. All patients had clinical and biochemical evidence of primary hyperparathyroidism with negative or inconclusive 99mTc-sestamibi scintigraphy. Studies were acquired using dedicated PET/CT scanners 60 minutes post-injection of 370-555 MBq 11C-methionine following standardized protocols. Images were interpreted by experienced nuclear medicine physicians using qualitative visual assessment.
Results: The cohort included 46 patients with primary hyperparathyroidism (mean age 65.1±8.6 years, range 42-77). Overall detection rate was 58.7% (27/46 studies). Studies were conclusive in 95.7% of cases (44/46), with 27 positive, 17 negative, and 2 indeterminate results. Among positive studies, anatomical distribution showed right inferior parathyroids in 25.9% (7/27), left inferior parathyroids in 25.9% (7/27), and right superior parathyroids in 18.5% (5/27). Ectopic locations were identified in 29.6% of positive cases (8/27), comprising retroesophageal (2/27), mediastinal (2/27), retroesternal (1/27), suprasternal (1/27), juxtaisthmic (1/27) and retro-jugular (1/27) sites. The radiotracer demonstrated excellent target-to-background contrast in positive cases, enabling precise anatomical localization for surgical planning.
Conclusions: 11C-methionine PET/CT demonstrates valuable diagnostic utility as second-line molecular imaging in primary hyperparathyroidism, with detection rates within the reported range for primary disease in systematic reviews (60-75%). The technique shows particular value for ectopic parathyroid localization, detecting nearly 30% of positive cases in complex anatomical positions. With over 95% conclusive results, this represents a comprehensive series establishing 11C-methionine PET/CT specifically for primary hyperparathyroidism in Uruguay's nuclear medicine practice.

Conflict of Interest
No conflict of interest

Graphic

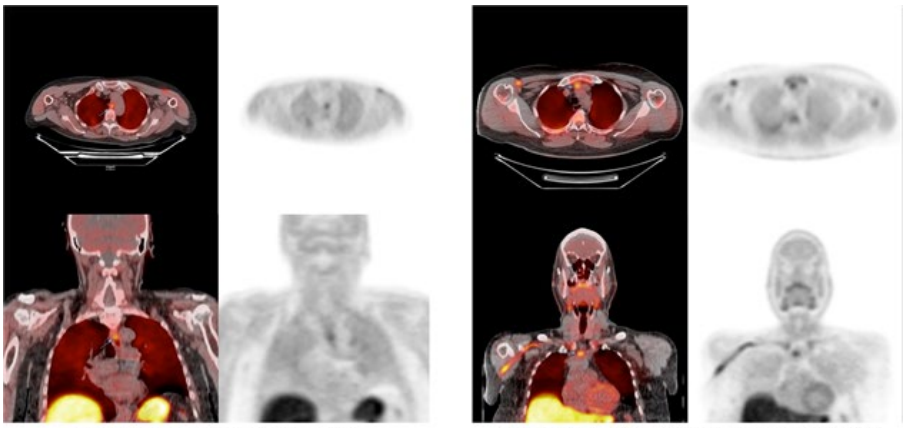

^{11}C-Methionine PET/CT showing ectopic parathyroid adjacent to the aortic arch

^{11}C-Methionine PET/CT showing ectopic parathyroid in the retrosternal region

Figure 1. Ectopic sites detected with 11C-Methionine PET/CT from the sample

Table

Tabla 1. Rendimiento Diagnóstico y Distribución de Localizaciones

Resultado	N° casos	Porcentaje	IC 95%
Positivo	27	58.7%	43.2-73.0%
Negativo	17	37.0%	23.2-52.5%
Indeterminado	2	4.3%	0.5-14.8%
Concluyentes	44	95.7%	85.2-99.5%
TOTAL	46	100.0%	-

Localización	N° casos	Porcentaje
Ectópicas	8	29.6%
Inferior derecha	7	25.9%
Inferior izquierda	7	25.9%
Superior derecha	5	18.5%

P011

Synergistic role of 99mTc-MIBI radioguided surgery and ICG fluorescence in primary and secondary hyperparathyroidism: experience in three cases

Dr. Bettina Martinucci[1], Carolina Furtado[1,2], Mirel Cabrera[2], Ximena Camacho[2], Marcos Tassano[2], Omar Alonso[1], Pablo Duarte[3], Alarico Rodriguez[3], Pablo Cabral[2], Juan Pablo Gambini[2,3]

[1]UA Medicina Nuclear e Imagenología Molecular, Hospital de Clínicas Dr. Manuel Quintela, Facultad de Medicina, UdelaR, Montevideo, Uruguay, [2]Centro de Investigciones Nucleares, Facultad de Ciencias, Universidad de la Republica, Montevideo, Uruguay, [3]Centro Uruguayo de Imagenología Molecular, Montevideo, Uruguay

Introduction: Primary and secondary hyperparathyroidism often require surgical intervention when medical therapy is insufficient. Precise localization and complete resection of hyperfunctioning parathyroid tissue are key to surgical success. 99mTc-sestamibi (MIBI) scintigraphy not only allows preoperative anatomical detection but also enables intraoperative radioguided surgery. Complementarily, indocyanine green (ICG) fluorescence provides real-time intraoperative visualization. The integration of both techniques enhances the precision of parathyroidectomy.

Material and Methods: Three patients undergoing parathyroid surgery, all with prior scintigraphy with Single Photon Emission Computed Tomography and computed tomography (SPECT-CT) for preoperative anatomical localization. Case 1: A 52-year-old woman with primary hyperparathyroidism (PTH 1,240 pg/mL, calcium 11.8 mg/dL). MIBI showed uptake in the right inferior gland. Case 2: A 48-year-old man with secondary hyperparathyroidism on dialysis (PTH 2,428 pg/mL). MIBI localized the left inferior gland. Case 3: A 61-year-old woman with recurrent primary hyperparathyroidism. MIBI revealed ectopic tissue in the mediastinum. In all cases, 4 ml of ICG and 20 mCi of MIBI were administered, facilitating fluorescent visualization with a portable NIR camera for real-time surgical guidance and radioactive confirmation with gamma probe. Resection was verified by intraoperative PTH and pathological examination.

Results: In all three cases, MIBI allowed precise preoperative and intraoperative localization by radioguided surgery, while ICG provided visual identification and intraoperative confirmation. PTH levels decreased significantly (Case 1: 310 pg/mL; Case 2: 1,530 pg/mL; Case 3: 420 pg/mL). No surgical complications were recorded.

Conclusion: The combined use of MIBI and ICG improves surgical precision in primary and secondary hyperparathyroidism. MIBI provides localization and radioguidance, while ICG adds visual confirmation. This synergy optimizes complete resection, shortens surgical times, and improves outcomes.

Keywords: Parathyroidectomy, hyperparathyroidism, 99mTc-MIBI, radioguided surgery, ICG fluorescence.

Conflict of Interest

No

Graphic

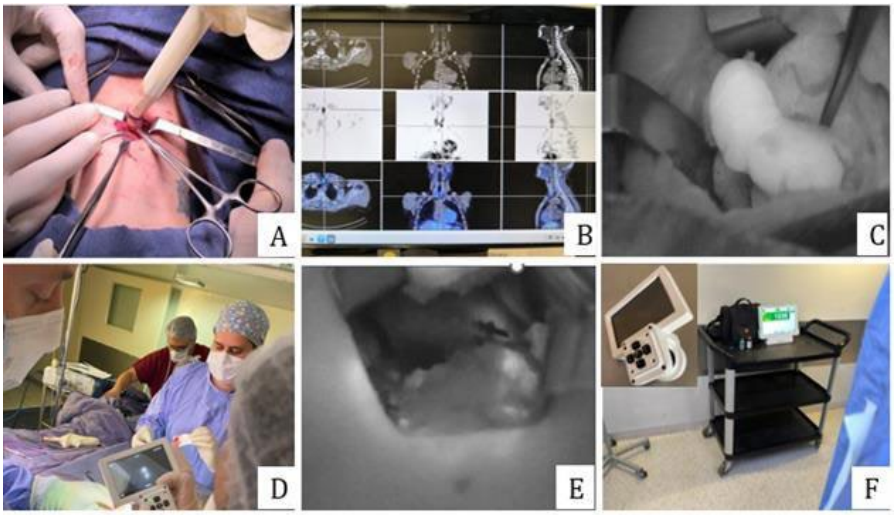

Figure 1. Multimodal guidance in parathyroid surgery using ^99mTc-MIBI and ICG fluorescence.
(A) Intraoperative radioguided dissection with a handheld gamma probe for localization of hyperfunctioning parathyroid tissue.
(B) Preoperative SPECT/CT with ^99mTc-MIBI showing pathological uptake consistent with parathyroid adenoma.
(C) Real-time near-infrared fluorescence imaging after ICG injection, enabling direct visualization of the hyperfunctioning parathyroid gland.
(D) Surgical team using a portable NIR fluorescence camera during parathyroidectomy.
(E) Intraoperative NIR view showing fluorescent uptake within the operative field, confirming parathyroid localization.
(F) Portable near-infrared fluorescence imaging system and gamma probe employed in the operating room.

P012

Beyond the neck: utilizing 18-f-choline pet/ct to uncover the source of primary hyperparathyroidism

Dr. Alejandra Gabriela Salgado[1], Dr Laura Felipe[1], Dr Antonella Kovic[1], Dr Maria del Carmen Alak[1]
[1]Imat, Buenos Aires, Argentina

Background/Aims: In primary hyperparathyroidism (PHPT), localizing the affected parathyroid glands is crucial for planning minimally invasive surgery (MIS). This is traditionally done using SPECT-scintigraphy with MIBI and cervical ultrasound. However, both methods show significant variability in detecting small or ectopic glands. For this reason, 18F-choline PET/CT is increasingly being used to improve localization outcomes and guide surgical planning, often in conjunction with the aforementioned diagnostic methods.
Methods: This was a retrospective observational study conducted from October 2023 to December 2024. Patients with clinical and biochemical suspicion of PHPT and with negative and/or discordant conventional studies (cervical ultrasound/ SPECT (MIBI)) who underwent an 18F-choline PET/CT were included. The following variables were analyzed: parathyroid hormone (PTH) levels, PET/CT positivity or negativity, the location of the findings, and concordance with SPECT (MIBI) and cervical ultrasound in cases where this data was available.
Results: The study included 46 patients, with an average age of 63 years. 90% of the patients were female and 9% male. The average PTH value was 119.97 pg/mL and average SUVmax of the positive findings 3.11.18F-choline PET/CT was positive in 73% of cases and negative in 27%. Negative results were more frequent in patients with minimally elevated PTH levels and negative conventional studies. Regarding the positive findings, 79% were due to intraparathyroid adenomas and/or glandular hyperplasia, 12% were due to ectopic glandular localization in the mediastinum, and 9% were other less common localizations. In 33% of the PET/CT positive cases, there was prior concordant ultrasound data, and in 41% there was concordant SPECT (MIBI) data.
Conclusions: Due to the heterogeneity in patient selection referred to our Nuclear Medicine Department we have a lower sensitivity compared to the literature. Nevertheless, despite this limitation, in our population, 18F-choline PET/CT is a useful method for selecting patients who will benefit from MIS.

Conflict of Interest
No conflict of interest

P013

Role of PET/CT in the follow-up of large vessel vasculitis-an experience in a single center

Dr. Irene Arma[1], Dr Isabel Hume[1], Dr. Ana Mollerach[1], Dr Constanza Cianciarelli[1], Dr. Nadia Pabstleben[1], Dr. Maria Jose Chacon[1], Dr. Ana Wayngarten[1], Dr. Sandra Sunagua[1], University Technologist Mayra Borges[1], Dr Carlos Collaud[1]
[1]Hospital Italiano De Buenos Aires, Caba, Argentina

18F FDG PET/CT has proven useful in the diagnosis of large-vessel vasculitis (LVV), revealing vascular wall inflammation in cases of disease activity. Despite its role in diagnosis, its contribution to monitoring disease activity is less clear
Objective: To evaluate the contribution of 18F FDG PET/CT in patients (p) diagnosed with large vessel vasculitis (LV) for treatment management according to disease activity
Methods: Retrospective study. Eighty PET/CT scans were reviewed in 54 p referred to the PET service with a diagnosis of LVV between January 2010 and June 2023. In 22 of the 54 p, PET was performed for disease monitoring with activity assessment. In 20 of the 22 patients, follow-up was performed at our center. One in 20 p was excluded due to a diagnosis of leukocytoclastic vasculitis
The presence of a homogeneous linear uptake pattern in the vascular wall was considered positive for vasculitis activity, comparing the uptake intensity and SUV value with that of the liver parenchyma. Uptake similar to or greater than that of the liver (score 2 or 3) was considered positive
PET results were compared with clinical diagnostic criteria for LVV, patient evolution and biochemical markers of inflammation
Results:
12/19 PETwith uptake-7/19 PETwithout uptake. 7/12True positive, 5/12false positive, 4/7true negative,3/7false negative (Table 1)
6/12 PET/CT with uptake with corticosteroids (50%)
5/7 PET/CT without uptake with corticosteroids (71%)
8/12 PET with uptake changed management (67%)
5/7 PET without uptake changed management (71%)
PET changed therapeutic management by adding, reducing or discontinuing medication
Conclusion:
Follow-up PET/CT in p with LVV was useful, as it determined a change in therapeutic management in a high percentage of patients, including those who did not present with clinical or laboratory evidence of disease activity
PET/CT provided useful information for treatment even in p who already were receiving corticosteroid therapy

References
Dejaco C, et al. Ann Rheum Dis 2023;0:1–11
Hellmich B, et al. Ann Rheum Dis 2020;79:19–30Arthritis Care & Research Vol. 73, No. 8, August 2021, pp 1071–1087
Conflict of Interest
I have no conflict of interest

Table

	PET WITH UPTAKE	PET WITHOUT UPTAKE	TOTAL
SYMPTOMS AND LABORATORY INFLAMMATION POSITIVE	6 (TP)	2 (FN)	8
NO SYMPTOMS / NO LABORATORY INFLAMMATION	5 (FP)	4 (TN)	9
NO SYMPTOMS / WITH LABORATORY INFLAMMATION POSITIVE	1 (TP)	1 (FN)	2
TOTAL	12	7	19

P014

Diagnostic Value of 18F-FDG PET/CT in Large-Vessel Vasculitis: A Retrospective Study from a Moroccan Cohort

Dr. Yasmine Lasry[1], Dr. Mahdi Ahmed Hassan, Dr. Abir Bakraoui Samlali, Dr. Achraf Msoune, Dr. Ali Benlemlih, Dr. Halima Batani, Dr. Hafsa Bensimimou, Dr. Zakaria Ouassfrar, Pr. Amal Guensi
[1]Ibn Rochd University Hospital, Casablanca, Morocco

Background: 18F-fluorodeoxyglucose (FDG) PET/CT is a metabolic imaging modality that highlights tissues with high glycolytic activity. Primarily used in oncology, it is increasingly applied to detect inflammation, including large-vessel vasculitis (giant cell arteritis and Takayasu arteritis). These rare diseases often present with nonspecific symptoms (e.g., fever, weight loss) and lack specific laboratory markers, making early diagnosis challenging. FDG PET/CT can visualize arterial wall inflammation early and map disease extent, especially in extracranial arteries beyond the reach of a temporal artery biopsy, and it is now recommended by major rheumatology organizations as an essential diagnostic tool for LVV. We aimed to evaluate the contribution of FDG PET/CT in diagnosing and assessing LVV in our patient cohort.
Methods: We conducted a retrospective analysis of all patients with suspected or confirmed LVV (giant cell arteritis or Takayasu arteritis) who underwent 18F-FDG PET/CT at CHU Ibn Rochd, Casablanca, from January 2023 to July 2025. Demographic, clinical, and treatment data were collected. PET/CT scans were reviewed visually; in cases with vascular FDG uptake, inflammation was quantified by the PET Vascular Activity Score (PETVAS), which grades uptake (0–3) in nine arterial territories (max score 27).
Results: Twenty-two patients (mean age 49.8, range 24–78) were included, and 7 (32%) were on corticosteroid therapy. FDG-avid vascular inflammation was observed in 6 patients (27%). Their mean PETVAS was 8.8, reflecting predominantly moderate disease activity, with one high-grade case. PET/CT detected arterial inflammation mainly in extracranial sites (aortic arch, descending thoracic aorta, subclavian arteries) that would have been missed by temporal artery biopsy.
Conclusion: 18F-FDG PET/CT emerges as a pivotal tool for diagnosing and characterizing LVV, enabling both early detection and objective quantification of inflammation. PETVAS is a reliable metric for grading disease activity and may support standardized follow-up strategies.

Conflict of Interest
No conflict of interest.

P015

The value of FDG PET- CT imaging in the management of patients with bone sarcoma and soft tissue sarcoma

Dr. Rawnak Afrin[1], Dr. Shaila Sharmin[1], Dr. Afroza Akhter[1], Dr. Mohana Hossain[1], Prof. Shankar Biswas[1], Dr. Sadia Hossain[1], Dr. Farhana Rahman[1]
[1]Bangladesh Atomic Energy Commission, Dhaka, Bangladesh

Background: Sarcoma comprises a heterogeneous entity of musculoskeletal malignancies arising from a mesenchymal origin. Fluorodeoxyglucose (FDG)-PET/computed tomography (CT) has been increasingly used in bone and soft tissue sarcomas and provides advantages in the initial tumor staging, tumor grading, therapy assessment and recurrence detection.
Aim: To determine the diagnostic & prognostic value of FDG PET/CT in patients with soft tissue or bone sarcoma.
Materials and Method: This prospective study was conducted for 60 months in two well-equipped referral PET-CT center of the capital Dhaka city. Patients presented with histopathology and immunohistochemistry proven soft tissue sarcoma or bone sarcoma were included by purposive sampling. Ethical clearance was taken from Institutional review committee. Whole body FDG PET CT scan was acquired from vertex to mid-thigh in a whole-body PET-CT scanner after administration of 5 to 10 mCi of 18-F FDG.
Results: A total 77 patients, 40 having soft tissue sarcoma and 37 having bone sarcomas were enrolled in this study. 60% of the study population were male and 40% female and maximum 16 patients were in age group in between 10 to 19 years among bone sarcomas. The most common sites ware femur, tibia and around the knee joint. 14 patients had osteosarcoma and 23 had Ewing's sarcoma. The most common metastatic site was lung. 8 patients were responder after treatment among the osteosarcoma variety. 26 patients were male among soft tissue sarcoma group and distant metastasis was common at baseline PET in patients with high grade sarcoma. A high SUVmax before treatment was associated with a poorer prognosis. A high SUVmax after neoadjuvant chemotherapy was linked to a poor histologic response.
Conclusion:
FDG PET/CT can play a pivotal role in refining diagnostic pathways and guiding therapeutic strategies for patients with sarcomas.

Conflict of Interest
Authors have no conflict of interest.

Graphic

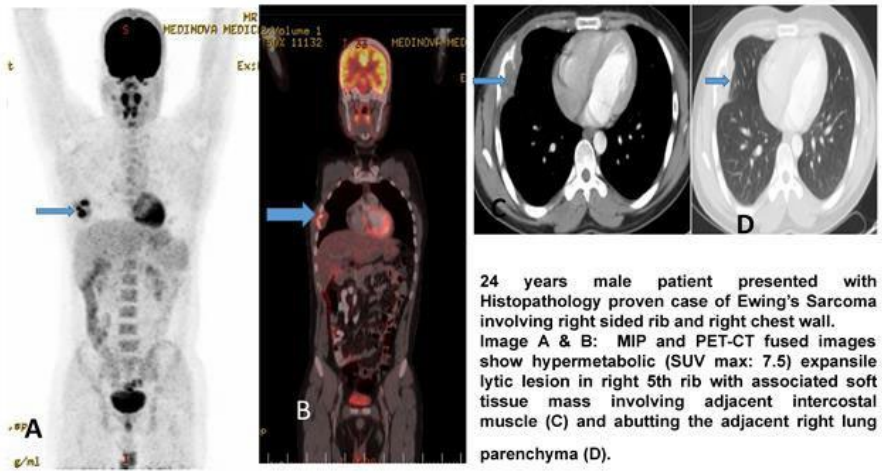

24 years male patient presented with Histopathology proven case of Ewing's Sarcoma involving right sided rib and right chest wall.
Image A & B: MIP and PET-CT fused images show hypermetabolic (SUV max: 7.5) expansile lytic lesion in right 5th rib with associated soft tissue mass involving adjacent intercostal muscle (C) and abutting the adjacent right lung parenchyma (D).

P016

Role of Bone Scintigraphy in Evaluating Painful Knee Arthroplasty: Outcomes from a Single-Centre Cohort

Dr. Jigisha Amin[1], Mr Shreyas Satish[2], Dr Adeel Syed[1], Dr Arman Parsai[1], Dr Nagesh Nagabhusan[1], Dr Tahir Hussain[1], Dr Ewa Nowosinska[1], Dr Manuela Vadrucci[1], Dr Idris Badreddine[1], Dr Mohan Krishnamurthy[1], **Dr. Hosahalli K Mohan**
[1]Department of Nuclear Medicine, Barts Health NHS Trust, London, United Kingdom, [2]Department of Bioengineering, Imperial College London, London, United Kingdom

Background:Persistent pain following knee arthroplasty remains diagnostically challenging. Distinguishing aseptic loosening or infection from non-prosthetic causes is critical for management. This study assessed the clinical utility of bone scintigraphy in guiding management of patients with persistent pain post knee arthroplasty [1-3]
Methods: We retrospectively reviewed 122 bone scans in patients with painful knee arthroplasties (33 male, 89 female; mean age 69 ± 9 years; mean BMI 32 ± 6). The mean interval from implant to symptom onset was 4 years. Bone scan results were correlated with management and, where available, intraoperative findings.
Results: Of 122 bone scans, 54 (44%) were positive and 68 (56%) negative.
20/54 patients with positive scans were referred for surgery; 10 underwent revision, with 8 confirmed pathology (5 loosening, 3 infection), while 2 showed no abnormality (positive predictive value 80%, overall accuracy 84%). One had targeted injection, 21 managed conservatively, and 2 were too early post-implant for intervention. Follow-up data unavailable for 10.
6/68 patients with negative scans were referred for surgery; 3 underwent revision, all showing no loosening or infection, yielding a negative predictive value of 100% in this subset. Four had targeted injection, 53 were reassured and discharged, 1 was too early post-implant, and 1 was referred to spine due to suspected referred pain. Follow-up was missing in 3.
Overall, positive scans led to revision referral (37% vs 9%), while negative scans supported reassurance or conservative management (78% vs 39%).
Interpretation within 12 months post-arthroplasty was unreliable, with 3 false positives from bone remodelling.
Conclusion:
Bone scintigraphy demonstrated high accuracy with an excellent negative predictive value and a high positive predictive value in these patients. Early post-operative scans should be interpreted cautiously. Overall findings support bone scintigraphy as an essential tool available for the clinician in the diagnostic workup of painful knee arthroplasty.

References

[1]. Puijk R, Lubbe P, Sierevelt IN, Kristians AE, Boer J, Nolte PA. The Diagnostic Characteristic and Reproducibility of Bone Scintigraphy Single-Photon Emission Computed Tomography/Computed Tomography for Diagnosing Aseptic Loosening of Uncemented Total Knee Arthroplasty. J Arthroplasty. 2024 Jul;39(7):1707-1713.e1. doi: 10.1016/j.arth.2024.01.005. Epub 2024 Jan 11. PMID: 38218556.

[2]. Boero M, Allocca M, Pisu N, et al. Management of periprosthetic knee joint infections: focus on the role of Nuclear Medicine (v2). Orthopedic Reviews. 2022;14(4). doi:10.52965/001c.39646. PMID:36381502
[3]. Bao, B., Liu, C.S., Masson, E.C.O. et al. Diagnostic accuracy of SPECT/CT arthrography in patients with suspected aseptic joint prostheses loosening. European J Hybrid Imaging 5, 4 (2021). https://doi.org/10.1186/s41824-021-00098-y

Conflict of Interest

None.

P017

Role of Bone Scintigraphy in Evaluating Painful Hip Arthroplasty: Outcomes from a Single-Centre Cohort

Mr Shreyas Satish[1], Dr. Jigisha Amin[2], Dr Adeel Syed[2], Dr Arman Parsai[2], Dr Nagesh Nagabhusan[2], Dr Tahir Hussain[2], Dr Ewa Nowosinska[2], Dr Manuela Vadrucci[2], Dr Idris Badreddine[2], Dr Mohan Krishnamurthy[2], **Dr. Hosahalli K Mohan**
[1]Department of Bioengineering, Imperial College London, London, United Kingdom,
[2]Department of Nuclear Medicine, Barts Health NHS Trust, London, United Kingdom

Background: Persistent pain following hip arthroplasty presents diagnostic uncertainty, with aseptic loosening, infection and non-prosthetic causes being part of the differential diagnosis. This study assessed the clinical utility of bone scintigraphy in guiding management of patients with persistent pain post hip arthroplasty [1-3].
Methods: We retrospectively reviewed 39 bone scans in patients with painful hip arthroplasties (13 male, 26 female; mean age 56 ± 19 years; mean BMI 32 ± 6; 15 with comorbidities). The mean interval from implant to symptom onset was 7 years. Bone scan results were correlated with subsequent management and, where available, intraoperative findings.
Results: Of 39 bone scans, 11 (28%) were positive and 28 (72%) negative.
6 out of 11 patients with positive scans were referred for surgery but all were still awaiting revision at the time of data collection. One patient had biopsy-proven infection and was also awaiting surgery. Two patients were managed conservatively. Follow-up data were missing for 2 patients.
2 out of 28 patients with negative scans underwent revision surgery with no loosening found intraoperatively, giving a negative predictive value of 100% in this subset. 23 patients (82%) were managed conservatively without further intervention. Follow-up data was missing for 3 patients.
Overall, positive scans led to referral for surgical revision, while negative scans guided reassurance or conservative management.
Conclusion: Bone scintigraphy guided the clinical management of patients with painful hip arthroplasties. Positive scans helped clinicians confidently refer patients for surgical revision, while negative scans provided reassurance, supporting conservative management or discharge. By clarifying the presence or absence of loosening or infection, bone scans enhanced clinician confidence in decision-making and reduced uncertainty, even in complex cases. Limitations include small sample size and incomplete surgical outcome data for positive scans awaiting revision. Further follow-up is needed to validate the predictive accuracy of positive results.

References
[1]. Puijk R, Lubbe P, Sierevelt IN, Kristians AE, Boer J, Nolte PA. The Diagnostic Characteristic and Reproducibility of Bone Scintigraphy Single-Photon Emission Computed Tomography/Computed Tomography for Diagnosing Aseptic Loosening of Uncemented Total Knee Arthroplasty. J Arthroplasty. 2024 Jul;39(7):1707-1713.e1. doi: 10.1016/j.arth.2024.01.005. Epub 2024 Jan 11. PMID: 38218556.
[2]. Boero M, Allocca M, Pisu N, et al. Management of periprosthetic knee joint infections: focus on the role of Nuclear Medicine (v2). Orthopedic Reviews. 2022;14(4). doi:10.52965/001c.39646. PMID:36381502
[3]. Bao, B., Liu, C.S., Masson, E.C.O. et al. Diagnostic accuracy of SPECT/CT arthrography in patients with suspected aseptic joint prostheses loosening. European J Hybrid Imaging 5, 4 (2021). https://doi.org/10.1186/s41824-021-00098-y
Conflict of Interest
None.

P018

Comparative Imaging in Painful Joint Arthroplasty: Bone Scintigraphy versus X-ray imaging

Dr. Hosahalli K Mohan, Mr. Shreyas Satish[1], Dr. Jigisha Amin[2], Dr. Adeel Syed[2], Dr Arman Parsai[2], Dr. Nagesh Nagabhusan[2], Dr. Tahir Hussain[2], Dr. Ewa Nowosinska[2], Dr. Manuela Vadrucci[2], Dr. Idris Badreddine[2], Dr. Mohan Krishnamurthy[2]
[1]Department of Bioengineering, Imperial College London, London, United Kingdom, [2]Department of Nuclear Medicine, Barts Health NHS Trust, London, United Kingdom

Background: Persistent pain following hip or knee arthroplasty may indicate aseptic loosening, infection, or non-prosthetic causes. Bone scintigraphy is widely used, but its correlation with conventional imaging (X-ray) and impact on management remains unclear [1-2].
Methods: We retrospectively reviewed 157 patients who were referred for bone scintigraphy with to assess for painful hip or knee arthroplasty. There were 63 positive and 94 negative bone scans with corresponding X-ray imaging. We assessed the concordance between both imaging modalities and correlated with patient outcomes.
Results: Of 63 positive bone scans, 20 were concordantly positive on X-ray, 37 were discordant (X-ray negative), and 6 were unreported.
Among the concordant 20, 14 were referred for surgery; 7 underwent revision, with pathology confirmed in 6 (PPV 86%). Of the 37 discordant cases, 11 were referred for surgery; 3 underwent revision, with pathology confirmed in 2 (PPV 67%). Overall, positive bone scans that proceeded to surgery had a PPV of 80%.
Among 94 negative bone scans, 80 were concordantly negative on X-ray, 9 were discordant (X-ray positive), and 5 were unreported. Of the 80 concordant negatives, 6 were referred for surgery; 4 underwent revision, with loosening confirmed in 2. Of the 9 discordant cases, only 1 was referred for surgery, showing no loosening. Overall, for the negative bone scans resulting in conservative management, the negative predictive value was 97%.
Overall concordance between bone scan and X-ray was 64%.
Conclusion: Bone scintigraphy frequently detected pathology not apparent on plain films, guiding clinicians to confidently refer patients for revision when scans were positive. Positive bone scans were more predictive of surgical pathology than positive X-rays, while negative scans reliably guided conservative management.

References

[1]. Blum A, Gondim-Teixeira P, Gabiache E, Roche O, Sirveaux F, Olivier P, Coudane H; Nancy Association for Prosthesis Exploration (NAPE); Raymond A, Louis M, Grandhaye M, Meyer JB, Mainard D, Molé D. Developments in imaging methods used in hip arthroplasty: A diagnostic algorithm. Diagn Interv Imaging. 2016 Jul-Aug;97(7-8):735-47. doi: 10.1016/j.diii.2016.07.001. Epub 2016 Jul 22. PMID: 27452630.
[2]. An YS, Park DY, Min BH, Lee SJ, Yoon JK. Comparison of bone single-photon emission computed tomography (SPECT)/CT and bone scintigraphy in assessing knee joints. BMC Med Imaging. 2021 Mar 26;21(1):60. doi: 10.1186/s12880-021-00590-8. PMID: 33771130; PMCID: PMC8004469.

Conflict of Interest

None.

P019

Value of dual fluorine-18-L-dopa and fluorine-18-fluorodeoxyglucose positron emission tomography in parkinsonism

Dr. Gerson Castillo[1], Miguel Olarte[1], Ana Piana[1], Juan Chavez[1]
[1]Unidad PET/CT, Facultad de Medicina, Universidad Nacional Autónoma de México, Ciudad de Mexico, Mexico

Background/Aims: Parkinsonism includes idiopathic Parkinson's disease, atypical parkinsonian syndromes, and secondary causes, frequently presenting with overlapping early features that complicate diagnosis. 6-[^{18}F]fluoro-L-dopa (FDOPA) PET/CT evaluates presynaptic dopaminergic integrity, while 2-deoxy-2-[^{18}F]fluoro-D-glucose (FDG) PET/CT identifies cortical–subcortical metabolic patterns that support differential diagnosis. The objective of this study was to determine the diagnostic value of dual-tracer brain PET/CT in patients with presumed parkinsonism.
Methods: A retrospective analysis was conducted on 37 patients referred to the PET/CT Unit of the Universidad Nacional Autónoma de México (UNAM) between 2023 and 2025 for suspected parkinsonism. All patients underwent FDOPA and FDG PET/CT following carbidopa premedication. Visual and semi-quantitative assessments were performed, and abnormalities were classified as presynaptic dopaminergic dysfunction, cortical–subcortical hypometabolism, or both. Concordance between tracers was evaluated using McNemar's exact test.
Results: Presynaptic dopaminergic abnormalities on FDOPA PET/CT were identified in 15 of 37 patients (40.5%; 95% CI, 26.3–56.5). FDG PET/CT revealed cortical or subcortical hypometabolism in 25 of 37 (67.6%; 95% CI, 51.5–80.4). Among 16 patients with both modalities categorizable, discordance was observed in 3 (18.8%), without statistical significance ($p = 1.000$). The integrated diagnostic classification was: Parkinson's disease in 14 patients (37.8%), multiple system atrophy in 6 (16.2%), dementia with Lewy bodies in 6 (16.2%), frontotemporal dementia in 3 (8.1%), progressive supranuclear palsy in 2 (5.4%), corticobasal degeneration in 1 (2.7%), non-parkinsonian cortical dementia in 1 (2.7%), and normal studies in 3 (8.1%).
Conclusions
Dual-tracer PET/CT with FDOPA and FDG provides complementary diagnostic insights in parkinsonism. FDOPA confirms presynaptic nigrostriatal degeneration, while FDG delineates cortical–subcortical metabolic signatures characteristic of atypical parkinsonism and dementia-related syndromes. This combined protocol enhanced diagnostic accuracy and confidence, reinforcing its clinical utility in specialized centers.

Conflict of Interest
The authors declare no conflicts of interest.

P020

PISCOM: Advanced Multimodal Functional Neuroimaging Integration of PET and SPECT for Presurgical Epileptogenic Zone Localization

Dr. Katherine Quintero[1], Arnau Farré-Melero[1], Nerea Gutiérrez[2], Sandra Rama[3], Carles Siscar[4], Erick García-Hernández[1], Aida Niñerola[1,2,5], Andrés Perissinotti[1,5], Xavier Setoain[1,2,5]

[1]Hospital Clinic Barcelona, Barcelona, Spain, [2]Universitat de Barcelona, Barcelona, Spain, [3]Hospital Universitario de Salamanca, Barcelona, Spain, [4]Hospital Universitari Doctor Peset de Valencia, Valencia, Spain, [5]Biomedical Research Networking Center of Bioengineering, Biomaterials and Nanomedicine (CIBER-BBN), ISCIII., Barcelona, Spain

Objective: To compare the performance and diagnostic confidence of PISCOM (PET-FDG interictal-subtracted-ictal-SPECT/coregistered whit MRI) versus SISCOM (SPECT interictal-subtracted-ictal-SPECT/coregistered with MRI) in the presurgical evaluation of patients with drug-resistant epilepsy.
Materials and Methods: This retrospective study included patients with drug-resistant epilepsy admitted to our epilepsy unit in 2022. Clinical records, electrophysiological data, and multimodal neuroimaging studies were systematically reviewed and analyzed.
PISCOM and SISCOM imaging datasets were anonymized and randomly presented to four nuclear medicine physicians, including two experts in neuroimaging.
The readers identified and located the potential epileptogenic zone (EZ) and reported their level of diagnostic confidence, blinded to both the imaging modality (SISCOM vs PISCOM) and the presumed EZ established by the epilepsy unit's multidisciplinary team based on complementary diagnostic tests.
Results: A total of 21 patients were included, with a median age of 39 years (range: 20–66 years) at the time of admission to the epilepsy unit. Of these, 4 underwent surgical intervention.
Nineteen cases were evaluated, generating 152 image readings. No statistically significant difference was observed between SISCOM and PISCOM in terms of concordance with the presumed EZ, with both modalities showing a concordance rate of 47.4%. In 71.1% of evaluations, the EZ identified was concordant across both modalities in the same patient.
Expert readers showed slightly higher concordance with the presumed EZ (52.6%) compared to non-experts (42.1%), but without statistical significance ($p = 0.35$).
PISCOM yielded a higher proportion of readings with high diagnostic confidence (40%) compared to SISCOM (28%). The proportions of readings with low (26% PISCOM vs. 30% SISCOM) and moderate (34% PISCOM vs. 42% SISCOM) diagnostic confidence were similar between both techniques.
Conclusion: PISCOM demonstrated equivalent concordance to SISCOM in the identification of the presumed EZ in patients undergoing presurgical evaluation for epilepsy, while offering a higher overall level of diagnostic confidence.

Conflict of Interest
No conflicts of interest

P021

Artificial intelligence as an assistant in the interpretation of 18F-FDG PET/CT in lymphomas according to the Deauville and Lugano criteria

Dr. Luis Colmenter[1], Lic Juan Lubo[2], Dr. José Calderón[2]
[1]Gamanuclear, Cali, Colombia, [2]Medicina Nuclear SA, Valledupar, Colombia

Background/Objectives: The interpretation of 18F-FDG PET/CT in Hodgkin and non-Hodgkin lymphomas requires standardized criteria such as Deauville and Lugano, which are essential for assessing treatment response. However, interobserver variability remains a major challenge. This study aimed to train and validate an artificial intelligence (AI) model based on GPT-5 as an assistant in applying these criteria, in order to improve diagnostic accuracy and support clinical decision-making in multidisciplinary settings.
Methods: A dataset of 40 previously validated PET/CT studies classified according to the Deauville and Lugano criteria was used. The model was trained using supervised learning with feedback from experienced nuclear medicine physicians, prioritizing the detection of relevant uptake in lymph nodes and extranodal organs. Validation was performed on 10 additional cases, comparing the agreement between the AI model and expert interpretations. Institutional ethical approval was obtained.
Results: The model achieved an accuracy of 95% in treatment response classification, showing high concordance with expert interpretations. Its use in multidisciplinary tumor boards enabled the standardized application of the Deauville and Lugano criteria, reducing interobserver variability and strengthening clinical decision-making.
Conclusions: The implementation of a GPT-5-based AI model as an assistant in the interpretation of 18F-FDG PET/CT in lymphomas proved effective and reliable in consistently applying the Deauville and Lugano criteria. This approach contributes to diagnostic standardization, reduces interobserver variability, and facilitates the integration of AI into clinical practice, with a direct impact on the management of patients with lymphoma.

Conflict of Interest
We declare that we have no conflicts of interest in the presentation of this work.

P022

Experience of the National Cancer Institute of Colombia with Lutetium-177 PSMA Therapy in Patients with Metastatic Castration-Resistant Prostate Cancer

Dr. Viviana Andrea Daza Betancourt[1], Dr. Daniel Felipe Galindo Cortes[1], Dr. Hernándo Andrés Benavides Jiménez[1], Dr. Camila Andrea Potal de Motta[1], Dr. Alejandro Jiménez Baraya[1], Dr. María Alejandra Gómez Marting[1], Dr. Marylin Acuña Hernández[2], Dr. Adriana Quiteria Buitrago Gómez[2]
[1]Fundación Universitaria Sanitas, Bogotá, Colombia, [2]Instituto Nacional de Cáncer, Bogotá, Colombia

Introduction: Metastatic castration-resistant prostate cancer (mCRPC) is associated with poor prognosis and limited overall survival [1]. Clinical trials such as VISION [2] and TheraP [3] have demonstrated that Lutetium-177 PSMA (^{177}Lu-PSMA) improves clinical outcomes with manageable toxicity. However, evidence in Latin American populations remains scarce. This study aimed to describe the safety and clinical outcomes of ^{177}Lu-PSMA therapy in Colombian patients with mCRPC treated at the National Cancer Institute (INC)
Methods: A descriptive, retrospective study was conducted in patients with mCRPC who received ^{177}Lu-PSMA I&T at the INC between 2020 and 2023. Demographic, clinical, and treatment-related data were collected to assess toxicity and survival outcomes
Results: A total of 24 patients were included. The mean number of administered cycles was 3.5 (standard dose: 7.4 GBq/cycle); one patient received 10 cycles as extended therapy. Sixteen patients (66.7%) presented high or very high-risk disease. The most frequent hematologic toxicity was anemia (78% overall), followed by lymphopenia (58.3%) and thrombocytopenia (12.5%). Neutropenia occurred in one patient (4.2%). Non-hematologic adverse events included fatigue (33.3%), nausea (16.7%), and xerostomia (8.3%). Median progression-free survival (PFS) was 5.3 months, and median overall survival (OS) was 12 months
Conclusions: ^{177}Lu-PSMA therapy demonstrated a favorable safety profile and manageable toxicity in Colombian patients with mCRPC. Although efficacy outcomes were slightly lower compared with international trials, the results are clinically relevant and highlight the importance of conducting local studies to better understand treatment effectiveness in populations with specific genetic and environmental characteristics
Keywords: prostate cancer, mCRPC, Lutetium-177, PSMA, Colombia, overall survival, progression-free survival

References

1. Thaiss, W., Zengerling, F., Friedrich, J., Hechler, V., Grunert, M., Bolenz, C., Wiegel, T., Beer, A. J., & Prasad, V. (2023). Personalized [177Lu]Lutetium-PSMA Therapy for Patients with Pre-Treated Castration-Resistant Prostate Cancer: A Single Institution Experience from a Comprehensive Cancer Centre. Cancers, 15(12), 3216. https://doi.org/10.3390/cancers15123216

2. Sartor, O., de Bono, J., Chi, K. N., Fizazi, K., Herrmann, K., Rahbar, K., Tagawa, S. T., Nordquist, L. T., Vaishampayan, N., El-Haddad, G., Park, C. H., Beer, T. M., Armour, A., Pérez-Contreras, W. J., DeSilvio, M., Kpamegan, E., Gericke, G., Messmann, R. A., Morris, M. J., … VISION Investigators. (2021). Lutetium-177-PSMA-617 for metastatic castration-resistant prostate cancer. The New England Journal of Medicine, 385(12), 1091–1103. https://doi.org/10.1056/NEJMoa2107322
3. Hofman, M. S., Emmett, L., Sandhu, S., Iravani, A., Joshua, A. M., Goh, J. C., Pattison, D. A., Tan, T. H., Kirkwood, I. D., Ng, S., Francis, R. J., Gedye, C., Rutherford, N. K., Weickhardt, A., Scott, A. M., Lee, S.-T., Kwan, E. M., Azad, A. A., Ramdave, S., … TheraP Trial Investigators and the Australian and New Zealand Urogenital and Prostate Cancer Trials Group. (2021). [177Lu]Lu-PSMA-617 versus cabazitaxel in patients with metastatic castration-resistant prostate cancer (TheraP): a randomised, open-label, phase 2 trial. Lancet, 397(10276), 797–804. https://doi.org/10.1016/S0140-6736(21)00237-3

Conflict of Interest

We declare that we have no conflict of interest

Table

Type of Adverse Event	Grade 1	Grade 2	Grade 3	Grade 4	Unspecified Grade	Total Affected Patients
Hematological						
Anemia	8 (33.3%)	6 (25.0%)	5 (20.8%)	1 (4.2%)*	-	20 (83.3%)
Lymphopenia	3 (12.5%)	7 (29.2%)	4 (16.7%)	-	-	14 (58.3%)
Thrombocytopenia	1 (4.2%)	-	2 (8.3%)	-	-	3 (12.5%)
Neutropenia	-	-	-	-	1 (4.2%)	1 (4.2%)
Non-Hematological						
Fatigue	-	-	-	-	Yes: 8 (33.3%)	8 (33.3%)
Nausea	-	-	-	-	Yes: 4 (16.7%)	4 (16.7%)
Dry Mouth	-	-	-	-	Yes: 2 (8.3%)	2 (8.3%)

*A patient presented severe anemia 10 months after therapy

P023

Standardization of tumor burden in lymphomas with PET/CT: integration of volumetric metrics Deauville and Lugano criteria to optimize clinical decision-making

Señor. Juan Lubo Marin[1], Dr. Luis Colmenter[2,4,6], Dr. José Calderón[1], Dr. Sinay Arevalo[3,5]
[1]Medicina Nuclear S. A., Valledupar, Colombia, [2]Gamanuclear, Valle del Cauca, Colombia, [3]Medicina Nuclear Los Nogales, Bogotá, Colombia, [4]PETCIMAGENES, Quito, Ecuador, [5]Universidad del Rosario, Bogotá, Colombia, [6]Grupo Conceptualizando, Cali, Colombia

Background/Objectives: The Deauville and Lugano criteria recommend complementing visual assessment of ^18F-FDG PET/CT in lymphomas with quantitative tools to objectively measure tumor burden. Metrics such as MTV (Metabolic Tumor Volume), TLG (Total Lesion Glycolysis), TMTV (Total Metabolic Tumor Volume), and TTLG (Total Tumor Lesion Glycolysis) are considered essential, as they provide standardized, reproducible information directly associated with therapeutic response. The aim of this study was to standardize the use of these metrics in PET/CT reports of lymphomas, ensuring accuracy and reliability in clinical interpretation.
Methods: Fifty PET/CT studies of lymphoma patients previously evaluated with Deauville and Lugano criteria were collected. Tumor burden quantification was performed using certified tools (MIN, Metavol, and Singovia), systematically integrating MTV, TLG, TMTV, and TTLG values. Precise definition of lesion targets was applied to control both individual and total tumor burden. Validation was performed by comparing standardized reports with those produced by experienced nuclear medicine specialists. Institutional ethical approval was obtained.
Results: Standardization demonstrated a significant correlation between volumetric metrics and treatment response classification under the Deauville and Lugano criteria. A concordance rate of 93% with expert evaluations was achieved, confirming the reliability of quantification. Proper technical alignment of the process ensured accurate integration of volumetric metrics into reports. The use of automated and semi-automated processes improved precision, enhanced traceability, and reduced interobserver variability.
Conclusions: Tumor burden quantification in lymphoma PET/CT is indispensable and must be part of standard practice, as recommended by the Deauville and Lugano criteria. Rigorous definition of lesion targets, together with integration of MTV, TLG, TMTV, and TTLG using standardized tools (MIN, Metavol, and Singovia), ensures accuracy, reproducibility, and clinical value. Technical alignment of the process and the implementation of automated or semi-automated systems strengthen PET/CT interpretation and optimize clinical decision-making in the management of lymphoma patients within multidisciplinary settings.

Conflict of Interest
We have no conflicts of interest in the presentation of this work.

P024

Clinical experience in oncologic PET/CT: radiomics-based quantification to complement clinical interpretation and standardize tumor burden assessment

Señor. Juan Lubo Marin[1], Dr. Luis Colmenter[2], Dr. José Calderón[1]
[1]Medicina Nuclear S. A., Valledupar, Colombia, [2]Gamanuclear, Cali, Colombia

Background/Objectives: PET/CT reporting has progressively shifted from descriptive assessments toward quantitative evaluations, improving diagnostic objectivity and reproducibility. Radiomics, through the extraction of histogram, shape, and texture features, enables a detailed characterization of tumor heterogeneity, offering a non-subjective, quantitative perspective that complements traditional clinical practice. The objective of this work was to present a multicenter clinical experience where radiomics was retrospectively applied to PET/CT studies already reported by specialists, assessing its contribution in correlating tumor burden with conventional clinical interpretation.
Methods: Twenty consecutive PET/CT studies (18F-FDG and 18F-PSMA), previously reported by nuclear medicine physicians, were reanalyzed. A standardized workflow including image acquisition, reconstruction, segmentation, and radiomic feature extraction was implemented to quantify MTV, TLG, TMTV, and TTLG, together with shape and texture descriptors. All cases were subsequently reviewed with treating clinicians, comparing original clinical interpretations with radiomic profiles reflecting tumor versus non-tumor heterogeneity. Patients continue to be followed with diagnostic approaches increasingly guided by radiomic metrics. Institutional ethics approval was obtained.
Results: The integration of radiomics and volumetric analysis demonstrated strong concordance with clinical interpretation, particularly in differentiating malignant activity from non-tumoral findings such as inflammation or post-treatment effects. Accurate lesion definition and consistent technical alignment enabled reliable longitudinal monitoring of individual and overall tumor burden, directly influencing therapeutic planning. In most cases, elevated TMTV/TTLG values and higher heterogeneity indices correlated with more aggressive clinical behavior, requiring treatment escalation. Conversely, lower burden and homogeneous radiomic signatures supported conservative approaches or maintenance strategies.
Conclusions: In this multicenter clinical experience, radiomics applied to lymphomas and solid tumors using FDG and PSMA tracers provided reproducible, quantitative support that complemented and occasionally redirected PET/CT interpretation. Standardized methodology, careful lesion selection, and integration of volumetric and radiomic parameters consolidate PET/CT reporting as an objective tool, reducing interobserver variability and strengthening multidisciplinary oncologic decision-making.

Conflict of Interest
We declare that we have no conflicts of interest in the presentation of this work.

P025

Implementation of PET/CT 2.0 Reports: From Descriptive to Quantitative in Personalized Oncologic Practice

Señor. Juan Lubo Marin[1], Dr. Luis Colmenter[2], Dr. José Calderón[1]
[1]Medicina Nuclear S. A., Valledupar, Colombia, [2]Gamanuclear, Cali, Colombia

Background/Objectives: Oncologic PET/CT reporting has evolved from a descriptive approach, focused on visual assessment, to a structured quantitative model integrating metabolic and radiomic parameters. This transformation responds to the need for objective, reproducible, and clinically actionable information. Parameters such as SUV, TMTV (Total Metabolic Tumor Volume), and TLG (Total Lesion Glycolysis), combined with radiomics and artificial intelligence (AI), allow improved characterization of tumor burden, prediction of treatment response, and guidance in personalized decision-making. The objective of this work is to highlight the importance of quantitative PET/CT reports in modern oncologic practice, their prognostic value, and their role as a tool for diagnostic precision.
Methods: A narrative review of the literature indexed in PubMed, Scopus, and EANM guidelines was conducted, focusing on the impact of quantitative metrics such as SUV, TMTV, and TLG in different phases of oncologic management. Studies evaluating PET/CT in baseline, interim, post-treatment, and restaging scenarios were analyzed, along with recent publications addressing the role of radiomics and AI in outcome prediction and reduction of interobserver variability.
Results: Quantitative PET/CT reports demonstrated significant correlation with overall survival and therapeutic response in various cancers. The use of TMTV and TLG enhanced risk stratification and enabled differentiation between true disease progression and inflammatory phenomena. The integration of radiomics and AI supported accurate segmentation, assessment of tumor heterogeneity, and generation of non-invasive functional biomarkers, contributing to the standardization of reporting.
Conclusions: The PET/CT 2.0 quantitative reporting model is consolidating as a standard in contemporary personalized oncology. Its implementation ensures precision, reproducibility, and prognostic value, while reducing diagnostic variability and strengthening the role of nuclear medicine physicians as integrators of metabolic, volumetric, and radiomic data. This approach does not rely exclusively on advanced technologies but on adopting standardized protocols and multidisciplinary collaboration, establishing it as a fundamental tool for precision oncology.

Conflict of Interest
We declare that we have no conflicts of interest in the presentation of this work.

P026

Metabolic activity in primary tumor and metastatic lesions of breast cancer according to molecular subtype: preliminary analysis with pet/ct

Dr. Sofía Velázquez[1], Dra. Yazmín Sánchez[1], Dr. Miguel Olarte[1]
[1]Facultad de Medicina Unam, Coyoacan, Mexico

Introduction: The maximum standardized uptake value (SUVmax) in ^18F-FDG PET/CT reflects tumor metabolic activity. Evaluating SUVmax in both the primary tumor and metastases during initial staging of breast cancer allows assessment of tumor aggressiveness, detection of occult spread, and guidance for therapeutic planning.
Materials and methods: Seventeen patients with metastatic breast cancer identified during initial staging with PET/CT were included. Tumors were classified according to molecular subtype: Luminal B HER2–, Luminal B HER2+, Luminal not otherwise specified, HER2+, triple-negative, and unknown. Data recorded included metastatic sites (bone, lung, other sites: visceral and nodal; non-axillary), primary and metastatic SUVmax, and classification of patients as having single-site metastasis (only one site affected) or multiple-site metastases (≥2 sites). Mean and median SUVmax values were calculated for each subtype.
Results: Luminal subtypes showed low to moderate primary SUVmax values (≈5–11) and predominantly bone metastases with lower metabolic activity. Luminal B HER2– presented only multiple-site metastases (2/2, 100%), while Luminal B HER2+ and Luminal not otherwise specified showed a mixed pattern (1/2, 50% single-site metastases). HER2+ showed multiple-site metastases (1/1, 100%) with high primary SUVmax (13.49). Triple-negative tumors displayed high metabolic activity (16.76) and a predominance of multiple-site metastases (2/3, 67%). Unknown cases demonstrated heterogeneity (4/7, 57% single-site metastases; 3/7, 43% multiple-site). In total, 6 bone, 3 lung, and 24 other metastases were registered; 7 patients (41%) had single-site metastases and 10 (59%) multiple.

Conflict of Interest
The authors declare no conflict of interest

Graphic

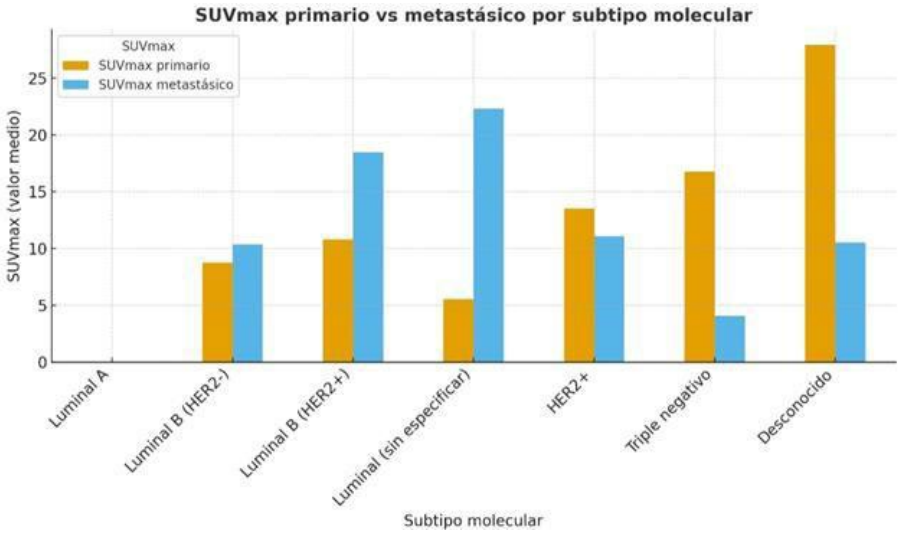

Table

Tabla 1. Distribución de metástasis y SUVmax por subtipo molecular

Subtipo molecular	Total	Hueso	Pulmón	Otros sitio	Media SUVmax	Mediana SUVm	Media SUVmax metastási	Mediana SUVmax metastási	Metástasis únicas	Metástasis múltiple
Luminal	0	0	0	0	–	–	–	–	0 (0%)	0 (0%)
Luminal B	2	1	0	3	8.75	8.75	10.35	10.35	0 (0%)	2 (100%)
Luminal B	2	1	0	3	10.81	10.81	18.45	18.45	1 (50%)	1 (50%)
Luminal (sin	2	1	1	3	5.50	5.50	22.30	22.30	1 (50%)	1 (50%)
HER2+	1	1	0	2	13.49	13.49	11.08	11.08	0 (0%)	1
Triple negativo	3	0	0	4	16.76	16.76	4.08	4.08	1 (33%)	2 (67%)
Desconoci	7	2	3	9	27.90	27.90	10.50	10.50	4 (57%)	3 (43%)
Total	17	6	3	24	14.78	10.81	11.42	10.35	7 (41%)	10

P027

18F-PSMA PET/CT in Prostate Cancer: Initial Experience and Theranostic Roadmap from Bangladesh

Dr. Afroza Akhter[1], Dr. Shaila Sharmin[1], Dr. Rawnak Afrin[1], Dr. Farhana Rahman[1], Dr. Sadia Hossain[1], Prof. Shankar Biswas[1]
[1]Institute of Nuclear Medicine and Allied Sciences, INMAS Dhaka, Bangladesh Atomic Energy Commission, Dhaka, Bangladesh

Background/Aims: Prostate-specific membrane antigen (PSMA) positron emission tomography/computed tomography (PET/CT) has transformed prostate cancer management by improving detection, staging, and restaging, and forms the basis of theranostic approaches such as Lutetium-177 (^{177}Lu)-PSMA therapy. In Bangladesh, imaging has traditionally relied on ultrasound, CT scan, MRI, and ^{99m}Tc-MDP bone scan. The recent introduction of Fluorine-18 (^{18}F)-PSMA-1007 PET/CT at INMAS Dhaka represents a major advance. The forthcoming adoption of Gallium-68 (^{68}Ga)-PSMA PET/CT and ^{177}Lu-PSMA therapy under the approved IAEA Technical Cooperation Project (2026–2027 cycle) will further expand care. We report initial clinical experience and highlight opportunities and challenges of adopting theranostics in a developing-country context.
Methods: Patients with prostate cancer referred for staging, biochemical recurrence, or restaging underwent ^{18}F-PSMA-1007 PET/CT according to international protocols. PSA levels, imaging findings, and therapeutic decisions were documented. A multidisciplinary team (oncologists, nuclear medicine physicians, radiologists, urologists, and surgeons) reviewed cases to guide treatment.
Results: ^{18}F-PSMA PET/CT demonstrated higher sensitivity than conventional imaging for local recurrence, nodal spread, skeletal or distant metastases. Variable PSMA expression was observed, influenced by tumor grade, heterogeneity, and androgen deprivation therapy. Standardized frameworks (PROMISE v2, miTNM) improved reporting by highlighting concordant findings with additive value and excluding discordant findings. Imaging frequently influenced therapeutic strategies.
Conclusion: The introduction of ^{18}F-PSMA PET/CT marks a milestone in prostate cancer care in Bangladesh. However, challenges remain in adopting advanced imaging and theranostics in developing countries, including high cost, limited infrastructure, regulatory hurdles, and the need for awareness and training. Addressing these requires international collaboration, local capacity building, and multidisciplinary teamwork. Bangladesh's early experience provides a model for other low- and middle-income countries. The approved IAEA TC 2026–2027 cycle will support the implementation of ^{68}Ga-PSMA PET/CT and ^{177}Lu-PSMA therapy, establishing a complete theranostic pathway and promoting equitable access to advanced prostate cancer care.

Conflict of Interest

There is no conflict of interest.

Graphic

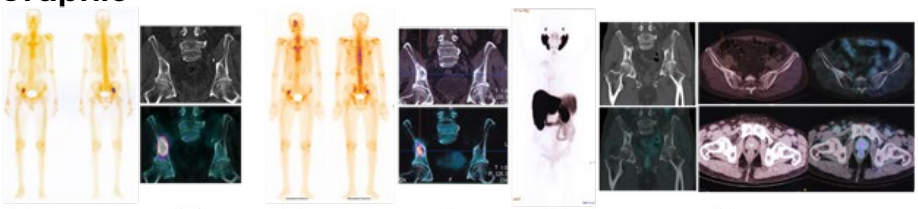

(a) (b) (c) (d) (e) (f)

Figure: A 60-year-old male with prostate adenocarcinoma (Gleason 3+4=7, initial PSA 58.8 ng/mL), history of TURP, and baseline bone scan (24.02.2024) showing osteoblastic metastasis in the right ilium (a, b). The patient received bicalutamide 50 mg daily, goserelin, palliative radiotherapy to bone, and zoledronic acid. Follow-up bone scan (03.06.2025) demonstrated persistent osteoblastic/sclerotic lesion (c, d). However, ^{18}F-PSMA PET/CT (25.06.2025) revealed PSMA-negative ametabolic disease in the right iliac bone with low PSMA expression in residual prostatic tissue (e, f), confirming inactive oligometastasis and leading to stage reclassification.

P028

99mTc-Labeled LHRH Analog versus Trastuzumab: Comparative Targeted Preclinical Imaging of Human Breast Cancer Models via LHRH/HER2 Receptors

Dr. Lucia Alfaya[1], Dr. Ximena Camacho[1], Dr. Mirel Cabrera[1], Dr. María Fernanda García[1], Msc. Ana Laura Reyes[2], TRI Andrea Paolino[2], Dr. Eduardo Savio[2], Dr. Juan Pablo Gambini[2,3], Dr. Pablo Cabral[1]
[1]Departamento de Radiofarmacia, Centro de Investigaciones Nucleares, Facultad de Ciencias, Universidad de la República, Montevideo, Uruguay, [2]Centro Uruguayo de Imagenología Molecular, CUDIM, Montevideo, Uruguay, [3]Centro de Medicina Nuclear e Imagenología Molecular, Hospital de Clínicas, Facultad de Medicina, Universidad de la República, Montevideo, Uruguay

Background/Aims: Triple-Negative Breast Cancer is an aggressive subtype lacking ER/PR/HER2 expression, limiting treatment options mainly to chemotherapy. Luteinizing Hormone-Releasing-Hormone (LHRH) receptors are expressed in some TNBCs, making LHRH-targeted therapies, a promising approach. We previously developed a technetium-99m (^{99m}Tc) radiolabeled LHRH-analog peptide as a potential diagnostic agent (1). This study evaluates its performance in HER2-positive and HER2-negative human breast cancer models alongside radiolabeled trastuzumab to explore LHRH receptor-targeted imaging, especially for HER-2- tumors.
Methods: HYNIC-GSG-LHRH(D-Lys6) was successfully radiolabeled with [^{99m}Tc]Tc and evaluated for cell binding in breast cancer cell lines, including HER2-negative (MDA-MB-231, MCF-7) and HER2-positive (BT-474) models. Trastuzumab was derivatized and radiolabeled with [^{99m}Tc]TcO_{4-}. HER2 expression in these cell lines was confirmed using flow cytometry and binding assays. SPECT/CT imaging was performed in mice bearing MCF-7 and BT-474 tumors, with imaging conducted up to 5 hours post-injection for the peptide and 24 hours post-injection for the antibody.
Results: The [^{99m}Tc]Tc-HYNIC-GSG-LHRH(D-Lys^6)/Tricine/NA complex was radiolabeled with high purity (>98%) and showed specific binding to all tested breast cancer cell lines. SPECT/CT imaging in mice bearing HER2-positive (BT-474) and HER2-negative (MCF-7) tumors confirmed targeted accumulation regardless of HER2 status (Figure 1). In contrast, [^{99m}Tc]Tc-HYNIC-Trastuzumab bound specifically to HER2-positive cells and tumors (Figure 1), with minimal uptake in HER2-negative models, consistent with in vitro results.
Conclusions: [^{99m}Tc]Tc-HYNIC-GSG-LHRH(D-Lys^6) showed high radiochemical purity and specific binding to both HER2-positive and HER2-negative breast tumors, highlighting its potential as a HER2-independent imaging agent. In contrast, [^{99m}Tc]Tc-HYNIC-Trastuzumab was selective for HER2-positive tumors, as expected.Bibliography: 1-Alfaya L, Camacho X, Cabrera M, Tassano M, Savio E, Reyes L, Paolino A, García MF, Fernández M, Gambini JP, Cabral P. Preclinical Evaluation of 99mTc-Labeled LHRH Analog as Cancer Receptor Imaging. Oncology. 2025 Jul 11:1-13.
Acknowledgedments: ANII-Uruguay (POS_NAC2018_1_151180,POS_NAC_2016_1_129986).

Conflict of Interest
No conflict of interest presented

Graphic

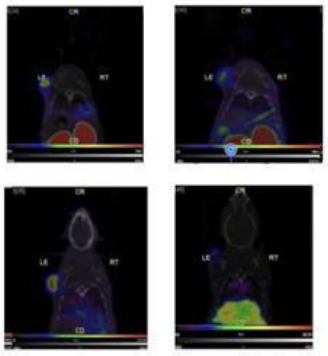

Figure 1 : Transversal SPECT/CT images of [^{99m}Tc]Tc-HYNIC-GSG-LHRH(D-Lys^6)/Tricine/NA complex (top) and [^{99m}Tc]Tc-HYNIC-Trastuzumab (bottom) in female nude mice bearing BT-474 (left) and MCF-7 (right) tumors at 1 or 24 hours p.i.

P029

Staging positron emission tomography in multiple myeloma: extramedullary disease as a predictor of adverse outcomes, cohort 2014–2023

Dr. Melissa Alvarez[1], Dr. Rosita Nohemy Dorado Castillo[1], Dr. Joaquin Donaldo Rosales[1], Dr. Ana María Aguilar González[2], Dr. Juliana Hernández Bolívar[1], Dr. Juan David Marín Escobar[1], Dr. Kevin Bueno Espitia[1], Dr. Diana Carolina Quijano Galvis[1], Dr. Luz Maritza Pabón Castilla[1], Dr. Lina María Góez Mogollón[1]
[1]Fundacion Valle Del Lili, Cali, Colombia, [2]Hospital Universitario Del Valle, Cali, Colombia

Background/Aims: Multiple myeloma is a plasma-cell neoplasm with heterogeneous prognosis. Extramedullary disease, defined as plasma-cell infiltration outside the bone marrow, is associated with high-risk cytogenetic alterations and aggressive clinical behavior. Although international studies have shown that extramedullary disease detected by staging positron emission tomography/computed tomography (PET/CT) is linked to inferior survival, data from Latin American cohorts remain limited. This study aimed to evaluate the prognostic impact of extramedullary disease identified at staging PET/CT in a Colombian cohort of patients with multiple myeloma.
Methods: We performed a retrospective analysis of a cohort including adults diagnosed with multiple myeloma between March 2014 and December 2023 at Fundación Valle del Lili. All patients underwent staging PET/CT at diagnosis. Clinical, laboratory, cytogenetic, treatment, and imaging data were collected. Primary outcomes were overall survival and progression-free survival. Kaplan–Meier curves and Cox proportional-hazards models were applied. Institutional ethics approval was obtained.
Results: A total of 243 medical records with PET/CT performed during the study period were reviewed. Of these, 51 corresponded to patients undergoing staging for multiple myeloma. Thirty cases were excluded as they were extrainstitutional, leaving 21 patients who fulfilled all inclusion criteria. In this final cohort, the presence of extramedullary disease at diagnosis was associated with shorter overall and progression-free survival, in concordance with international reports. Previous studies have reported median overall survival ranging from 14.8 to 63.5 months in patients with extramedullary disease compared with 26.9 to 79.9 months in those without, with an adjusted hazard ratio for mortality close to 1.4 (95% CI 1.16–1.71). [1–3]
Conclusions: In our Latin American cohort, extramedullary disease detected by staging PET/CT was identified as an independent predictor of adverse outcomes. These findings reinforce the prognostic utility of PET/CT at diagnosis and support risk-adapted therapeutic strategies in the region.

References
1. Montefusco V, Gay F, Spada S, De Paoli L, Di Raimondo F, Ribolla R, et al. Outcome of paraosseous extra-medullary disease in newly diagnosed multiple myeloma patients treated with new drugs. Haematologica. 2020;105(1):193-200. doi:10.3324/haematol.2019.219139.
2. Zanwar S, Sidana S, Shune L, Puglianini OC, Pasvolsky O, Gonzalez R, et al. Impact of extramedullary multiple myeloma on outcomes with idecabtagene vicleucel. J Hematol Oncol. 2024;17(1):42. doi:10.1186/s13045-024-01555-4.
3. Ho M, Paruzzo L, Minehart J, Nabar N, Noll JH, Luo T, et al. Extramedullary multiple myeloma: challenges and opportunities. Curr Oncol. 2025;32(3):182. doi:10.3390/curroncol32030182.
Conflict of Interest
The authors declare no conflicts of interest.
The authors have no relevant financial or non-financial interests to disclose.
The study protocol was approved by the Ethics Committee of Fundación Valle del Lili.

P030

Treatment with 177Lu-PSMA radioligand: tumor volume and PSA behavior and their relationship with overall survival

Dr. Matias Cimin[1], Dra. Roxana Chirico[1], Dra. Nathalie Abreu[1], Lic. German Pitarch[1], Lic. Brenda Konowalik[1], Dr. Alejandro Valda[1], **Dr. Maria Jose Bastianello**[1]
[1]CEMIC University Hospital, Buenos Aires, Argentina

Background: Radioligand therapy with 177Lu-PSMA has emerged as a novel therapeutic option in castration-resistant prostate cancer (CRPC), demonstrating overall survival (OS) benefit with favorable tolerability. This study retrospectively evaluated prostate-specific antigen (PSA) kinetics and tumor volume, and their association with OS.
Methods: We analyzed 36 patients with CRPC treated under a compassionate-use protocol with 177Lu-PSMA at CEMIC University Hospital (Buenos Aires, Argentina) between December 2020 and May 2025. Baseline total tumor volume (PSMA-TV) was derived from 18F-PSMA PET-CT segmentations, using hepatic SUVmax as reference. Patients were clinically and biochemically monitored for ≥6 months after the last treatment cycle.
Results: Thirty-six patients received a total of 109 cycles (median: 3; range: 1–6). Median age was 69 years (range: 40–81), median Gleason score was 8 (range: 6–10), and median baseline PSA was 238 ng/mL (range: 0.09–1421). A ≥50% PSA decline (PSA50) after the first cycle occurred in 13 patients (36.1%). PSA flare was observed in 23 patients (63.8%), all after the first cycle, with mean onset at 36.2 days (range: 5–90). Of these, 7 subsequently achieved PSA50 after the second cycle, whereas 16 showed stable or increasing PSA. Median OS was 19.2 months in patients achieving PSA50 versus 9.4 months in those with PSA flare without subsequent decline.
Baseline PSMA-TV averaged 680 mL (range: 13–2770). Patients with PSMA-TV below the mean had longer OS (20 months) compared with those above the mean (9 months).
Conclusions: Low baseline PSMA-TV and early PSA50 response after 177Lu-PSMA therapy were associated with prolonged OS. Conversely, high tumor volume and persistent PSA elevation predicted poorer outcomes.

Conflict of Interest
NONE

P031

Correlation between PSA levels, SUVmax and total tumor volume (TTV) in evaluation response therapy using 18F-PSMA-PET/CT in prostate cancer (PC)

Dr. Indira Eliana Díaz Contreras[1], Dr. Ada Franco Ardila[2], Dr. Iván Vega González[3]
[1]Gamanuclear LTDA, Armenia, Colombia, [2]Universidad Autónoma de Bucaramanga, Bucaramanga, Colombia, [3]Clínica Las Américas AUNA, Medellín, Colombia

PC: prostate cancer;PSA: Prostate-specific antigen;TTV: Tumor metabolic volume;SUVmáx: Standardized Uptake Value;ADT: Androgen Deprivation Therapy;ARSI: Androgen Receptor Signaling Inhibitors

Background: The role of ^{18}F-PSMA-PET/CT in evaluating treatment response in PC remains insufficiently characterized[1,2]. This study assessed correlations among PSA, SUVmáx, and TTV before and after therapy.
Methods: We performed a retrospective analysis of 39 PC patients evaluated at Clínica Las Américas AUNA who underwent two ^{18}F-PSMA-PET/CT scans between January 2022 and May 2025. Clinical, biochemical, and imaging data were collected, and treatment response was categorized. Correlations were analyzed using Spearman's rank test.
Results: The mean age was 70±7.9 years; median iPSA was 43ng/mL (IQR:19.3–100.0). High-risk disease (Gleason 4+4) was common, and 43.6% presented with metastases. Initial therapies included radiotherapy (48.7%), prostatectomy (25.6%), and ADT in most cases. The first PET/CT was performed for staging in 6 patients (17%) and for biochemical recurrence in 33 (89%). The second scan was obtained after a median of 10 months (IQR:6.5–15.5). Treatments included hormonal blockade [ADT, 17.9%; AR inhibitors, 17.9%; ADT+ARSI, 12.8%; ARSI alone, 10.3%] and chemotherapy (17.9%). Responses were classified as progression (51.3%), partial response (30.8%), stable disease (7.7%), and complete response (7.7%). Biochemical and imaging outcomes were heterogeneous. Median PSA increased from 6.1 to 7.7ng/mL post-treatment (+11.56%), whereas SUVmáx decreased from 21.9 to 11.3 (–19.64%), suggesting reduced viable tumor activity. Median TTV remained stable at 33.0cm³, consistent with a greater proportion of non-responders.
Conclusions: PSA, SUVmáx, and TTV were significantly correlated. Post-treatment PSA correlated strongly with TTV ($p=0.844$, $p<0.001$). Baseline TTV was associated with both post-treatment PSA ($p=0.579$, $p<0.001$) and SUVmáx ($p=0.642$, $p<0.001$), suggesting predictive value for incomplete response. The strong correlation between baseline and post-treatment TTV ($p=0.805$, $p<0.001$) supports its reliability. These findings reinforce ^{18}F-PSMA-PET/CT as a tool for treatment response assessment and highlight TTV and SUVmáx as complementary biomarkers to PSA.

References
[1] Beintner-Skawran S, Gafita A, Lorenzini T, Tauber R, Hoberück S, Mattana F, Di Giorgio A, Miederer M, Paller CJ, Djaileb L, Solnes LB, Farolfi A, Ceci F, Eiber M, Voter AF. [68Ga]Ga-PSMA-11 PET tumor volume predicts overall survival of patients with metastatic prostate cancer undergoing taxane-based chemotherapy. J Nucl Med. 2025 Sep; doi:10.2967/jnumed.125.269584.
[2] Albano D, Temponi A, Bertagna F, et al. The prognostic role of staging [^{18}F]PSMA-1007 PET/CT volumetric and dissemination features in prostate cancer. Annals of Nuclear Medicine. 2025;39(3):518-526.
Conflict of Interest
Ninguno

Graphic

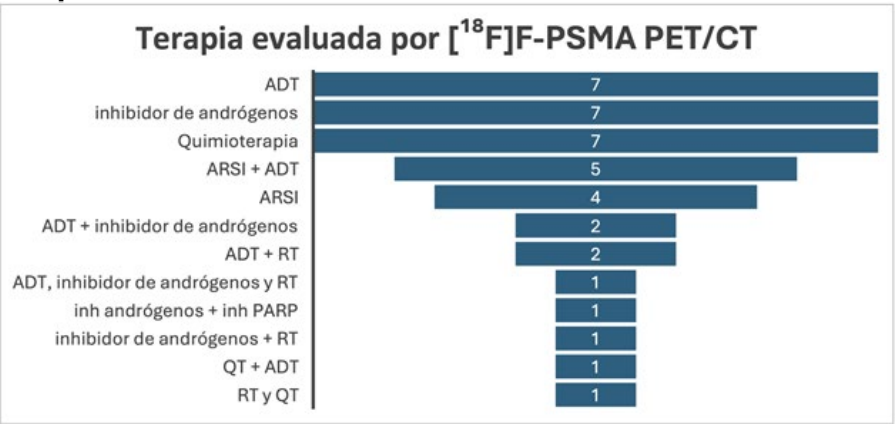

Table

Variable	Spearman Correlation Coefficient	*p-value*
Post-therapy PSA / Post-therapy TTV	0.844	**0.000**
Pre-therapy TTV / Post-therapy TTV	0.805	**0.000**
Pre-therapy TTV / Post-therapy PSA	0.579	**0.000**
Pre-therapy TTV / Post-therapy SUVmax	0.642	**0.000**
Post-therapy TTV / Post-therapy SUVmax	0.558	**0.001**

P032

Long axial field of view (LAFOV) PET-CT scanners in oncology

Prof. Antonia Dimitrakopoulou-Strauss[1], Dr. Leyun Pan[1], Prof. Christos Sachpekidis[1]
[1]German Cancer Research Center, Heidelberg, Germany

Background: Long axial field of view (LAFOV) PET-CT scanners have been recently developed and are already in clinical use in few centers worldwide. Their main characteristic is an increased sensitivity, which results in an increased lesion detectability.
Methods: We performed over 700 dynamic oncological studies with a new Biograph Vision Quadra (Siemens Healthineeers) mostly with [18F]FDG but also with [18F]PSMA-1007, [68Ga]Ga-PSMA-11, [68Ga]Ga-DOTATOC as well as [68Ga]Ga-FAPI-46. The axial FOV is 106 cm. We used a combined scanning protocol consisting of a dynamic series (30-60 min) followed by a whole-body static acquisition. We reduced the administered dose to 2 MBq/kg and used an acquisition time of 10 min for the static acquisition of the body trunk and 5 min for the extremities. We calculated direct and indirect Patlak images for the dynamic series and used different times (30 min and 60 min) for Patlak reconstruction. 2-tissue-compartment-model (2TCM) was also used for comparison.
Results: Although as a general trend the reduction of acquisition time was associated with a decrease of liver signal-to-noise-ratio (SNR) and tumor-to-background-ratio (TBR), we could demonstrate that a 5-min static acquisition of the torso provides comparable diagnostic quality to standard lengths of acquisition. Whole body dynamic and parametric imaging were easily feasible with a good image quality and high temporal and spatial resolution. We could demonstrate, that Patlak Ki images revealed better lesion contrast than SUV images, but did not increase the lesion detection rate. The time window used for Patlak imaging plays a more important role than the direct or indirect Patlak method.
Conclusions: The advent of the novel LAFOV scanners is linked to specific challenges, such as the high purchase price and issues related to logistics and their optimal operation in a nuclear medicine department.

Conflict of Interest
no

Graphic

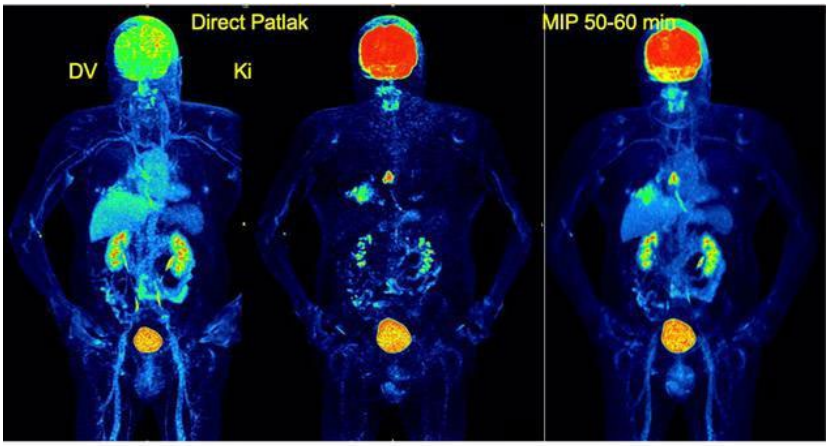

Metastatic lung tumor +
Radiation pneumonitis

P033

Bronchopulmonary neuroendocrine tumors: characterization with [18F]OC and [18F]FDG PET/CT

Dr. Abril Ariadna Flores Perez[1], Dr. Claudia Contreras-Rivera[1], Dr. Ana Lucia Calderón-Ávila[1], Dr. Miguel Ángel Olarte-Casas[1]
[1]Pet/ct Unam, Mexico City, Mexico

Background: Neuroendocrine tumors (NETs) are heterogeneous neoplasms with increasing prevalence; bronchopulmonary NETs represent the second most common site. Well-differentiated tumors include typical carcinoid (TC), classified as Grade 1, with low mitotic count and Ki-67 index, in contrast to atypical carcinoids (AC), classified as Grade 2.[1]
PET/CT evaluates SSTR overexpression through radiolabeled DOTA-peptides. Semiquantitative parameters such as SUVmax are associated with histochemical features and the degree of cellular differentiation. Indications for the study include staging, restaging, therapy selection, and response assessment.[2, 3] [18F]OC provides physical and logistical advantages, offering better lesion-to-background ratio in liver, bone, and lymph nodes. [18F]FDG is useful in AC, and a correlation has been reported between SUVmax values and Ki-67.[4, 5] The aim of the present study was to describe the findings of [18F]OC and [18F]FDG PET/CT in bronchopulmonary neuroendocrine tumors according to their degree of differentiation.
Methods: This was a retrospective study including patients with bronchopulmonary NETs who underwent PET/CT with [18F]OC and/or [18F]FDG at the UNAM PET/CT Unit between January 2022 and April 2025. Clinical, histopathological, and semiquantitative PET/CT data were collected.
Results: Thirteen patients were evaluated, 9 with TC and 4 with AC. In patients with TC, [18F]OC demonstrated high lesion uptake (SUVmax 13.67 [1.90–61.48], SUVmean 2.94 [1.47–10.28]), compared with AC (SUVmax 7.41 [1.59–], SUVmean 2.41 [1.07–]). [18F]FDG uptake in TC vs AC showed SUVmax of 3.18 and 6.26, and SUVmean of 1.66 and 3.29, respectively. Tumor detection rates with [18F]OC in TC were lymph nodes (44.4%), liver (22.2%), and bone (22.2%), whereas with [18F]FDG in AC detection rates were lymph nodes (25%), liver (25%), and bone (25%).
Conclusions: Typical carcinoids showed higher uptake and metastatic detection rates with [18F]OC, while atypical carcinoids demonstrated greater avidity for [18F]FDG, particularly at metastatic sites.

References

1. Nicholson, Andrew G. et al. The 2021 WHO Classification of Lung Tumors. J Thorac Oncol [Internet]. 2022;17. Disponible en: https://www.jto.org/article/S1556-0864(21)03316-5/fulltext
2. Haug AR, Auernhammer CJ, Wängler B, Schmidt GP, Uebleis C, Göke B, Cumming P, Bartenstein P, Tiling R, Hacker M. 68Ga-DOTATATE PET/CT for the early prediction of response to somatostatin receptor-mediated radionuclide therapy in patients with well-differentiated neuroendocrine tumors. J Nucl Med. 2010;51(9):1349-56.

3. Naswa N, Sharma P, Kumar A, Soundararajan R, Kumar R, Malhotra A, Ammini AC, Bal C. 68Ga-DOTANOC PET/CT in patients with carcinoma of unknown primary of neuroendocrine origin. Clin Nucl Med. 2012;37(3):245-51.
4. Pérez, D.J., Ávila-Rodríguez. Methods to radiolabel somatostatin analogs with [18F]fluoride: current status, challenges, and progress in clinical applications. J Radioanal Nucl Chem. 2020;326:1519-42.
5. Rufini V, Lorusso M, Inzani F, Pasciuto T, Triumbari EKA, Grillo LR, Locco F, Margaritora S, Pescarmona E, Rindi G. Correlation of somatostatin receptor PET/CT imaging features and immunohistochemistry in neuroendocrine tumors of the lung: a retrospective observational study. Eur J Nucl Med Mol Imaging. 2022;49(12):4182-93.

Conflict of Interest

The authors have no conflict of interest

P034

Sacral insufficiency fracture after radioteraphy treatment for cervical cancer: detection and characterization by 18F-FDG-PET/CT: 12 years of experience

Dr. Maximiliano Francabandiera[1], Dra. Paola Corona[1], Dra. Florencia Arabolaza[1], Dr. Federico Matorra[1], Dr. Nicolás Bustos[1], Dra. Berenice Fiamingo[1], Dr. Christian González[1], Dra. Sonia Traverso[1], Dr. Gabriel Bruno[1]
[1]Centro Diagnóstico Nuclear, Caba, Argentina

Background/Aims: Sacral insufficiency fractures (SIFs) are stress fractures that, among other causes, can be induced by pelvic radiotherapy (PRT). They may be asymptomatic or cause nonspecific pelvic pain, which can sometimes be intense and mistakenly suggest bone metastasis. Our objective is to demonstrate the utility of 18F-FDG PET/CT in characterizing and diagnosing SIFs in patients with cervical cancer (CC) treated with external beam radiotherapy (EBRT), and to report our 12-year experience.
Methods: A retrospective evaluation was conducted on 18F-FDG PET/CT scans of cervical cancer patients (p) who underwent EBRT between 2011 and 2023. To assess metabolic activity, visual parameters and the maximum Standardized Uptake Value (SUVmax) were considered. For reporting, studies were indexed using an Apache Solr™ search engine (https://solr.apache.org/).
Results: Out of 883 patients evaluated, aged between 24 and 77 years (average: 54.6), 37p (4.1%) showed imaging findings consistent with SIFs involving the sacral alae bilaterally in 24p and unilaterally in 13p. In all cases, PET findings revealed linear FDG uptake (parallel to the sacroiliac joint) with SUVmax values ranging from 1.5 to 5.6 (average: 2.9). Most cases (31p) showed morphological correlation on CT (fracture lines, focal increased bone density, or subtle mixed or sclerotic structural bone changes), while the remaining 6p had no CT findings. Only 4p experienced moderate to severe pelvic pain, while the others were either asymptomatic or had vague, nonspecific symptoms. Post-EBRT SIFs can occur between 2 months and more than 8 years after completion of EBRT, with a median onset between 6 and 20 months. Eight patients underwent follow-up PET/CT, showing decreased metabolic activity and reparative sclerotic bone changes over time.
Conclusions: 18F-FDG PET/CT is a useful tool for characterizing and diagnosing EBRT-induced SIFs in cervical cancer patients, enabling differentiation from metastatic bone involvement and facilitating appropriate therapeutic management.

Conflict of Interest
The authors declare that they have no conflicts of interest.

Graphic

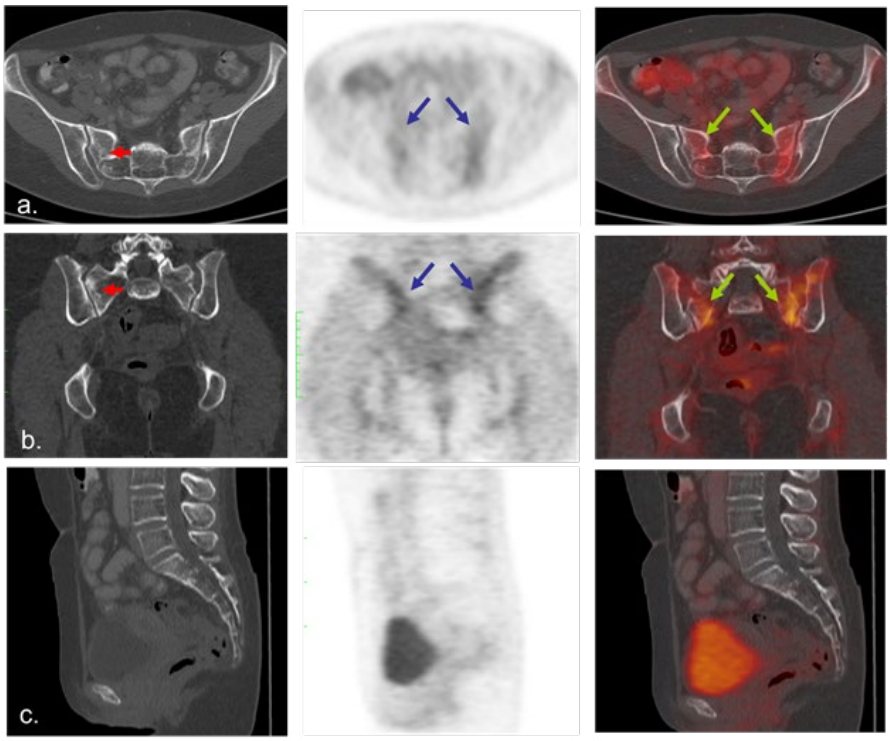

P035

Unspecific mesenteric uptake on 18F-PET/CT in post-treatment lymphoma: a “don’t touch” pitfall

Dr. Maximiliano Francabandiera[1], Dra. Paola Corona[1], Dr. Christian González[1], Dra. Florencia Arabolaza[1], Dr. Nicolás Bustos[1], Dra. Berenice Fiamingo[1], Dra. Sonia Traverso[1], Dr. Gabriel Bruno[1]
[1]Fundacion Centro Diagnostico Nuclear, Caba, Argentina

Background / Aims: 18F-FDG PET/CT is an essential tool in lymphoma assessment. Focal mesenteric fat uptake, although uncommon, can mimic recurrence disease. Our objective is to describe the findings and follow-up the evolution of unspecific mesenteric uptake (UMU) in post-treatment lymphoma (PTL) patients, to facilitate it´s recognition and avoid unnecessary interventions.
Methods: We retrospectively evaluated 18F-FDG PET/CT scans of 10 PTL patients who presented UMUs as a finding and they had at least one follow-up PET-CT scan.
Results: Of the 10 patients (p), 1 had Hodgkin lymphoma and 9 non-Hodgkin lymphoma (8 follicular lymphoma, 1 diffuse large B-cell lymphoma). All p exhibited UMU after treatment, corresponding on CT scan to a focal densification of mesenteric fat (higher density than normal fat but lower than soft tissue) with a “peritoneal margin,” and that morphological feature helps to differentiate from lymphadenopathy. SUVmax ranged from 2.2 to 7. In 5 p, UMU had complete resolution on follow-up PET/CT (6–27 months), while the remaining 5p showed persistence of the finding, with partial resolution in 4. 8p had UMU as the only finding with favorable resolution of other pathological lesions; 2p showed progression disease, however the UMUs improved. Although histopathological confirmation was not available, the clinically asymptomatic course and the findings observed in follow-up PET/CT suggest that when the findings are characteristic, no intervention is necessary. UMU is interpreted as a potential post-treatment inflammatory process, since isolated case reports with similar morphologic characteristics and histological confirmation have described as fat necrosis.
Conclusions: Recognizing UMUs morphological characteristics on CT scan and its evolution on follow-up imaging helps to reduce false positives and optimize clinical decision-making, avoiding unnecessary interventions or therapies. Considering that UMU may correspond to fat necrosis, its suggested to classify them as a “don’t touch” pitfall and recommend its follow-up.

Conflict of Interest
The authors declare that they have no conflicts of interest.

Graphic

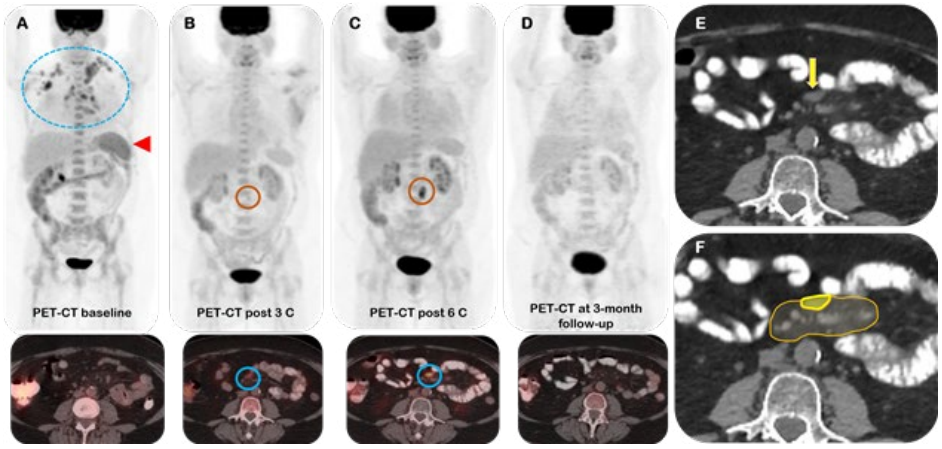
A
B
C
D
E
F
PET-CT baseline
PET-CT post 3 C
PET-CT post 6 C
PET-CT at 3-month follow-up

P036

Clinical Significance of Sentinel Lymph Node Scintigraphy in Breast Cancer Patients Attended by the Brazilian Public Health Service

Mrs. Stephanie Freitas[1], Ms. Ana Julya Fernandes[2], Dr. Sandra Sanches[1,2], Dr. Talita Santos[2], Dr. Priscila Santana[2], Dr Luciene Mota[2]
[1]Hospital das Clinicas da Universidade Federal De Minas Gerais, Belo Horizonte, Brazil, [2]Faculdade de Medicina da Universidade Federal de Minas Gerais, Belo Horizonte, Brazil

Background/Aims: Breast cancer is the most prevalent malignant neoplasm among women and a major cause of cancer-related mortality in Brazil. Accurate staging is essential for prognosis, as lymph node involvement is a critical determinant in guiding therapeutic planning. Sentinel Lymph Node Biopsy (SLNB) guided by scintigraphy is a less invasive technique utilized for the analysis of lymph node status.
This study aims to evaluate the outcomes of scintigraphy-guided SLNB in breast cancer patients treated within a specific Brazilian Public Health Service (University Hospital). The principal objective was to assess the technique's contribution to the preservation of the lymphatic chain in patients who are clinically negative for axillary involvement.
Methods: This investigation was conducted as a retrospective, descriptive study based on the analysis of clinical and histopathological patient data. The study cohort comprised 233 examinations for sentinel lymph node (SLN) localization performed on breast cancer patients at the designated University Hospital between January 2018 and December 2023. Prior to data inclusion, all patients provided written informed consent authorizing the use of their clinical information for research purposes.
Results: Analysis of the total patient cohort (N=233) demonstrated that 73 patients (31.3%) yielded positive SLNB findings, confirming metastatic involvement. Conversely, the majority of patients, 160 (68.7%), presented with negative SLNB results. Regarding histological subtype, Invasive Lobular Carcinoma accounted for the highest rate of lymph node metastasis at 38%, closely followed by Invasive Ductal Carcinoma at 35%.
Conclusions: The present study underscores the critical importance of scintigraphy-guided SLNB for the accurate staging and subsequent therapeutic decision-making in breast cancer patients. The absence of lymph node involvement is pivotal, as it permits the preservation of the lymphatic chain. This preservation, in turn, significantly reduces the physical and psychological morbidity associated with treatment, thus promoting a better quality of life for the patients.

Conflict of Interest
The authors declare that they have no conflict of interest.

P037

Disease-Free Survival in Thyroid Cancer Patients with Extrathyroidal Extension as the Sole Risk Factor

Dr. Helen Johana Mejía Efeer[1], **Dr. María Alejandra Gómez Marting**[1], Dr. Adriana Quiteria Buitrago Gómez[2], Dr. Edward Díaz Rodríguez[2], Dr. Diana Cuéllar[2], Dr. Humberto Varela Ramírez[1], Dr. Viviana Andrea Daza Betancourt[1], Dr. Angie Paola Llanos Cuellar[1], Dr. Ana Milena Guadrón Naranjo[1], Dr. Hernando Andrés Benavides Jiménez[1]
[1]Fundación Universitaria Sanitas, Bogotá, D.C., Colombia, [2]Instituto Nacional de Cancerología, Bogotá, D.C., Colombia

Background: Differentiated thyroid carcinoma is the endocrine neoplasm with the most favorable prognosis. Patients are stratified according to recurrence risk to guide therapy. In the intermediate-risk group, extrathyroidal extension is associated with worse outcomes, and guidelines recommend adjuvant radioactive iodine (RAI). However, no standard activity has been universally established for this indication, resulting in variability across treatment centers.
Objective: To evaluate disease-free survival in patients with well-differentiated papillary thyroid carcinoma and extrathyroidal extension as the sole risk factor, treated with adjuvant RAI at 30 mCi versus 100 mCi in two nuclear medicine centers in Bogotá, Colombia, between 2020 and 2022.
Methods: A retrospective analysis was conducted on patients with papillary thyroid carcinoma and extrathyroidal extension as the only recurrence risk factor. All received adjuvant RAI with 30 or 100 mCi of 131-I orally, depending on the center. Clinical follow-up continued until August 2025. The effect of administered activity on disease-free survival was assessed.
Results: According to preliminary findings, a total of 1,238 medical records were reviewed (238 from INC and 1,000 from Medicina Nuclear Palermo). Seven patients with infiltrative follicular variant papillary thyroid carcinoma and extrathyroidal extension were identified, all female. One patient (14.3%) received 100 mCi and six (85.7%) 30 mCi. The mean age was 56.3 years. The mean follow-up was 59.7 months, with no recurrences documented by imaging or histopathology.
Conclusions: No patient experienced recurrence during five years of follow-up, with 100% disease-free survival in both treatment groups. No differences were observed between 30 and 100 mCi of 131-I, supporting our hypothesis. These findings are consistent with reports in the literature (>90%). Nevertheless, the small sample size and the limited number of patients treated with 100 mCi preclude definitive conclusions, underscoring the need for prospective studies with larger cohorts.

Conflict of Interest
The authors declare no conflicts of interest.

P038

Local experience with post-surgical hepatic remnant assessment using hepatobiliary SPECT scintigraphy

Dr. Alejandro Rojas[1], **Dr. Francisco Gomez**[1], Dr. Carlos Mandiola[1], Dr. Jaime Castillo[1], Dr. Juan Dupouy[1], Dr. Jose Tomas Donoso[1], Dr. Rocio Hidalgo[1], Dr. Byron Riedel[1], Dr. Francisco Tortorolo[1], Ms. Catalina Serrano[1], Dr. Teresa Massardo[1]
[1]Hospital Clinico Universidad De Chile, Santiago, Chile

Introduction: It is difficult to certainly assure that the future liver remnant is able to maintain an adequate function post-partial hepatectomy due to different conditions. Hepatobiliary scintigraphy mainly with 99mTc-mebrofenin has been advocated as a promising tool for this topic due to its high liver extraction fraction. Morphological imaging with volumetric calculation does not provide enough security as a risk prognostic method.
Aim: To evaluate our initial experience with mebrofenin prior to liver hepatic procedures. We studied 13 patients (age: 28-82 years;7/13 males) submitted to Associating Liver Partition and Portal vein ligation for Staged hepatectomy (ALPPS), left or right hepatectomy.
Method: The technique was based on 2023 Joint EANM /SNMMI/IHPBA guidelines [1]. Priorly, 3 control cases studied with DISIDA due to duodenogastric reflux were performed. Acquisition: After IV mebrofenin, 6 min abdominal dynamic frames, 8 min SPECT and later dynamic excretion until 30 min. The index was normalized to body surface area.
Results: Twelve cases due to malignancies (liver metastasis, mostly colon, cholangial or hepatocarcinoma) and another case to a reparative procedure post-cholecystectomy. The liver remnant region of interest was drawn with the surgeon and ranged between 29 and 52% with a Mebrofenin Uptake Rate (MUR) between 6,6 and 11,8 (%/min/m2) being the safe cutoff>2,7. No patients were excluded from surgery due to our test results and none deceased in the early postoperative period. Global functional hepatic scores are shown in the Table. There was not acute liver failure with a median survival of 1020 days; 5 dead for cancer progression with lung/liver chronic insufficiency. A fusion image case pre and post-surgery is presented.
Conclusion: This experience has been very positive ameliorating patient's safety in a multidisciplinary team. We are currently merging CT and SPECT images to improve surgical approaches. It will be applied to liver donors in the future.

References

[1]Arntz PJW, et al. Joint EANM/SNMMI/IHPBA procedure guideline for [99mTc]Tc-mebrofenin hepatobiliary scintigraphy SPECT/CT in the quantitative assessment of the future liver remnant function. HPB (Oxford). 2023 Oct;25(10):1131-1144. doi: 10.1016/j.hpb.2023.06.001.

Conflict of Interest

None

Graphic

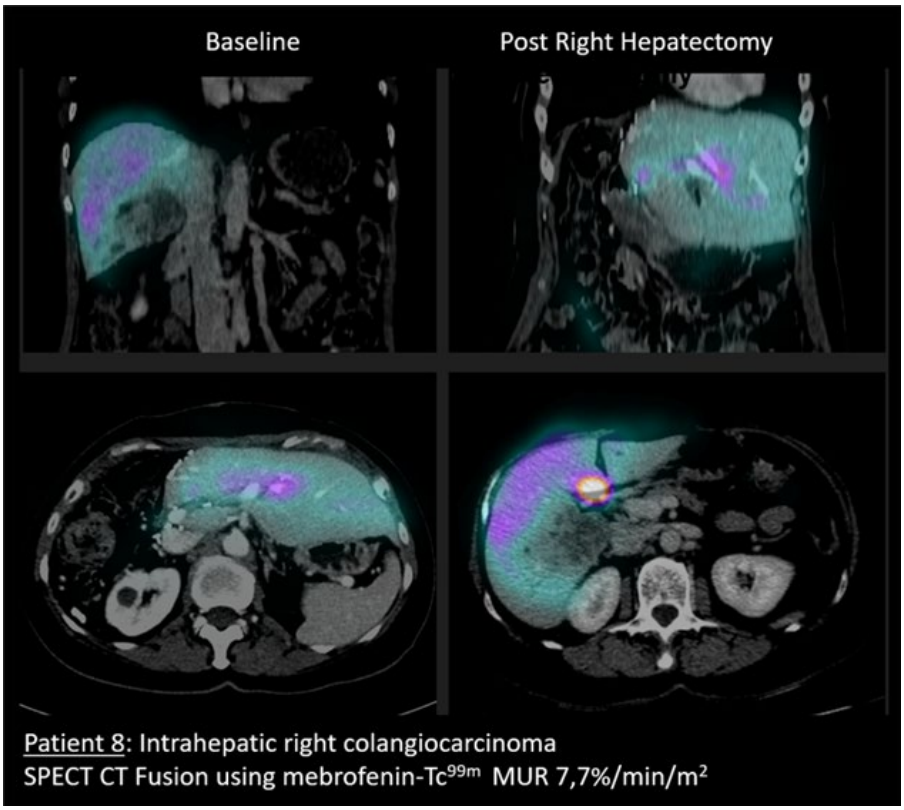

Table

Liver function variables 13 cases , 14 exams	N (%) Median (range)
Cirrhosis	1/10 (10%)
Prior hepatic surgery	4/10 (40%)
Median Albumin-Bilirrubin (**ALBI**) score	-2,93 (-3,09 to -1,9)
ALBI Grade 1 2 3	 5/7 (71,4%) 2/7 (23,6%) 0/7 (0%)
Basal Seric Bilirrubin >2 INR >1,5 Albumin <3,5	 0/9 (0%) 1/9 (11,1%) 2/8 (25%)
Post-surgery Bilirrubin INR	 0,93 (0,33-3,01) 1,24 (1,08-2,61)
International Study Group of Liver Surgery (**ISGLS**) criteria for post hepatectomy liver failure None A B C	 8/9 (88,9%) 1/9 (11,1%) 0/9 (0%) 0/9 (0%)

P039

Intraoperative ICG Fluorescence for Perfusion Assessment in Digestive Tract Surgery

Dr. Bettina Martinucci[1], Carolina Furtado[1,2], Mirel Cabrera[2], Ximena Camacho[2], Marcos Tassano[2], Omar Alonso[1], Gustavo Burroso[3], Pablo Duarte[3], Pablo Cabral[2], Juan Pablo Gambini[2,3]
[1]UA Medicina Nuclear e Imagenología Molecular, Hospital de Clínicas Dr. Manuel Quintela, Facultad de Medicina, UdelaR, Montevideo, Uruguay, [2]Centeo de Investigaciones Nucleares, UdelaR, Montevideo, Uruguay, [3]Centro Uruguayo de Imagenología Molecular, Montevideo, Uruguay

Background: Tissue perfusion integrity is a critical determinant of anastomotic safety. Vascular disruption is strongly associated with leakage, stenosis, and fistula formation, leading to major postoperative complications. Indocyanine green (ICG) fluorescence enables real-time, objective intraoperative assessment of microcirculation, providing surgeons with an additional tool to optimize decision-making in reconstructive gastrointestinal procedures.
Methods: Perfusion was evaluated in four patients with oncologic and non-oncologic digestive tract conditions. Case 1: a 54-year-old woman undergoing esophagectomy for grade IV achalasia with megaesophagus; Case 2: a 49-year-old man undergoing esophagectomy for squamous cell carcinoma; Case 3: a 59-year-old man undergoing partial left colectomy for colon adenocarcinoma with primary anastomosis; Case 4: a 67-year-old man undergoing Hartmann's reversal. In all procedures, intravenous ICG (0.5 mg/kg) was administered at two intraoperative time points: early, for stump evaluation, and after anastomosis. Perfusion was assessed using both laparoscopic infrared filters and a portable near-infrared camera. Parameters analyzed included perfusion visualization at proximal and distal stumps and at the completed anastomosis.
Results: Fluorescence imaging provided clear delineation of perfused margins and guided the selection of anastomotic sites. In areas showing reduced signal intensity, ICG fluorescence enabled intraoperative adjustment of resection lines. Concordance between direct surgical inspection and fluorescence findings was high, and in all cases, the technique reinforced the safety of intraoperative decisions. No adverse events were associated with ICG administration. Importantly, none of the patients developed postoperative complications related to anastomotic failure.
Conclusions: ICG-based perfusion assessment proved to be a reliable, reproducible, and effective intraoperative strategy for optimizing anastomotic planning in gastrointestinal surgery. Its routine use may significantly reduce ischemia-related complications and represent a valuable technological advance with direct impact on modern surgical practice.

Conflict of Interest
no

Graphic

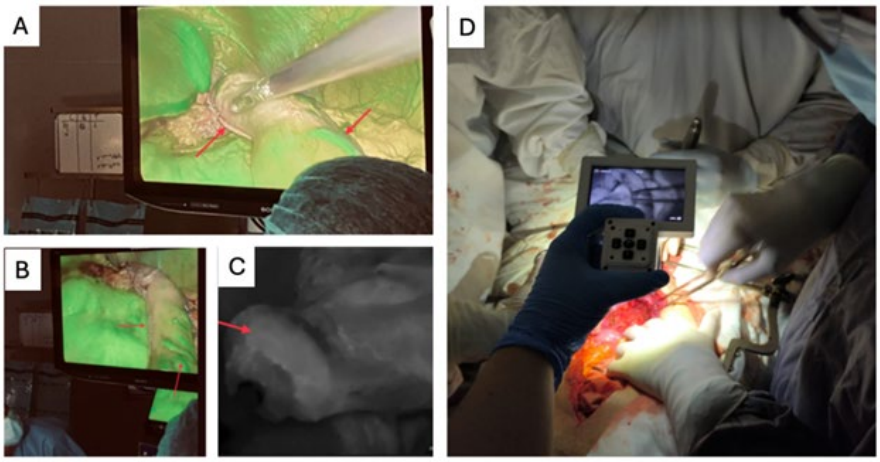

Figure 1. *Intraoperative assessment of tissue perfusion using indocyanine green (ICG) fluorescence. Sequential images illustrate clear visualization of proximal and distal stumps as well as completed anastomosis, enabling precise surgical decision-making.*

P040

Utility of 18F-FDG PET/CT in the characterization of solitary pulmonary nodule

Dr. Rosita Aracely Mendoza Santa Cruz[1], Dr. Daniel Santos Orihuela[1], Dr. Benjamin Gamarra Mujica[1]
[1]Guillermo Almenara Irigoyen National Hospital, LIMA, Perú

Background / Aims: Positron emission tomography/computed tomography (PET/CT) with fluorine-18–labeled fluorodeoxyglucose (18F-FDG) is indicated for the characterization of solitary pulmonary nodule (SPN). It helps to estimate the probability of malignancy, with high sensitivity (90–97%) and moderate specificity (70–85%). However, 18F-FDG PET/CT may yield false-positive results (10–25%) in infectious diseases or inflammation. In addition, carcinoid, bronchoalveolar, and mucinous tumors may produce false-negative results with normal or moderate FDG uptake. The aim of this study was to determine the diagnostic efficacy of 18F-FDG PET/CT in patients with SPN, for the detection of primary pulmonary neoplasia.
Methods: A retrospective analysis was performed on 94 patients with SPN evaluated using a Philips PET/CT scanner with 18F-FDG, with injected activity adjusted according to patient weight. Clinical variables (age, sex), nodule characteristics (size, location, type, histology), and metabolic parameters such as maximum standardized uptake values (SUVmax) were recorded according to standardized protocols.
Results: Among the 94 patients evaluated, 20 cases had a histological diagnosis positive for primary pulmonary neoplasia; of these, 19 were positive on 18F-FDG PET/CT, and one was negative despite malignant histology. The remaining 74 patients were PET/CT negative with benign pathologies, predominantly infectious such as tuberculosis, fibrosis, and others. The 20 patients with malignancy had a mean age of 65.85 years (range 37–83); 65% were women. Most nodules were located in the left upper lobe (35%) and were solid in type (85%). The average size was 23.7 mm. The predominant histology was adenocarcinoma with lepidic pattern (40%) (Table 1). The mean SUVmax was 5.63 (range 0–15.1) (Figure 1). Specificity was 100%, sensitivity 95%, positive predictive value 100%, and negative predictive value 98.7%.
Conclusions: 18F-FDG PET/CT is a highly accurate and reliable tool for the detection of primary pulmonary neoplasms.

Conflict of Interest
The authors declare no conflicts of interest

Graphic

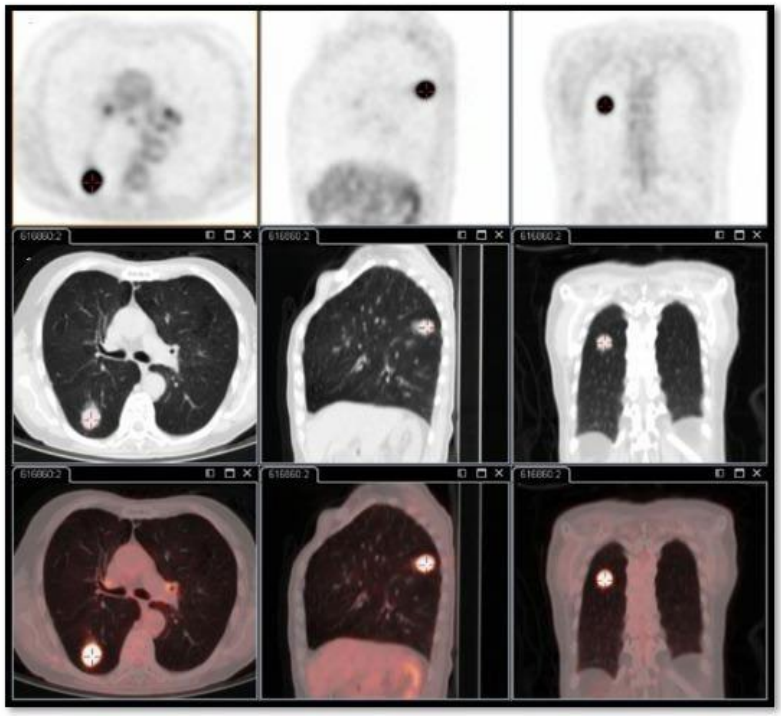

Figure 1. *Seventy-four-year-old male patient with a history of smoking. 18F-FDG PET/CT showing a solid SPN in the superior segment of the right lower lobe, measuring 29 mm with SUVmax 15.1, and histology of poorly differentiated non-mucinous invasive adenocarcinoma. a. PET b. CT c. PET/CT, each in axial, sagittal, and coronal views.*

Table

Histological Type	Number of Patients	Percentage (%)
Adenocarcinoma	19	95
• Adenocarcinoma with lepidic pattern	8	40
• Invasive adenocarcinoma with acinar pattern	3	15
• Mucinous adenocarcinoma	4	20
• Adenocarcinoma with papillary pattern	2	10
• Poorly differentiated non-mucinous invasive adenocarcinoma	2	10
Squamous cell carcinoma	1	5
Total	**20**	**100**

Table 1. *Histological types of patients with malignant SPN*

P041

Preliminary analysis of clinical and radiomic correlations in castration-resistant prostate cancer using consecutive [18F] PSMA-PET

Dr. Claudia Paola Pedraza García[1], Dr. Miguel Ángel Olarte Casas[1], Dra. Ana Karina Miranda Playas[1], Dra. Oliva Granados Rangel[1], Dr. Gustavo Rafael Govea Torres[2], Dr. Arturo Avendaño Estrada[3,4]

[1]Unidad PET/CT, Facultad de Medicina, Universidad Nacional Autónoma de México (UNAM), , Ciudad De México, México, [2]Departamento de Fisiología, Universidad Autónoma de Nuevo León, Monterrey, México, [3]Unidad Radiofarmacia-Ciclotrón, División de Investigación, Facultad de Medicina, Universidad Nacional Autónoma de México, Ciudad De México, México, [4]Centro de Investigación sobre el Envejecimiento, Centro de Investigación y de Estudios Avanzados Sede Sur, México., Ciudad de México, México

Background: Castration-resistant prostate cancer (CRPC) is biologically heterogeneous, making treatment response assessment challenging. Prostate-specific membrane antigen (PSMA) PET has proven highly sensitive for staging, but its role in longitudinal monitoring is less defined [4,5]. Radiomics applied to [18F]PSMA PET allows extraction of quantitative biomarkers that may complement SUVmax, PSMA tumor volume (PSMA-TV), and total lesion burden (PSMA-TL) [1–3]. This study analyzed correlations between clinical data and radiomic features from sequential [18F]PSMA-1007 PET scans in CRPC.

Methods: Fifteen patients from an ongoing cohort underwent two consecutive PSMA PET/CT scans at UNAM (2022–2025). Mean injected activity was 444.9 MBq, uptake 62–65 min. Whole-body PSMA-TV and PSMA-TL were calculated with syngovia. Radiomic features (texture, morphology, intensity) were extracted from prostate, lymph nodes, and bone metastases using LIFEx (≥64 voxels). Clinical variables included age, PSA, Gleason score, ISUP grade, metastases, and treatments. All variables were normalized and analyzed with Spearman correlations (ρ=0.70–0.80, $p<0.05$) and clustered. The protocol was approved by the Ethics Committee of the Faculty of Medicine, UNAM, and all patients provided informed consent.

Results: A total of 3,370 significant correlations were identified and grouped into six clusters. Strong associations were observed between tumor burden (PSMA-TV, PSMA-TL) and prostate texture features (ρ=0.72–0.79). Lymph nodes showed consistent but slightly weaker correlations ($\rho\approx$0.71–0.73). Bone metastases displayed higher variability, with some features up to ρ=0.79. SUVmax correlated consistently with prostate radiomics, but less robustly in bone lesions.

Conclusions: Radiomic features from [18F]PSMA PET, especially texture descriptors and tumor burden metrics, provide complementary information in CRPC. Associations were strongest in prostate and lymph nodes, while bone metastases reflected greater heterogeneity. SUVmax remained reliable for primary tumor activity but limited in metastatic disease. These findings support incorporating radiomics into predictive models to enhance monitoring of progression and treatment response in CRPC.

References
1. Molin K, Barry N, Gill S, et al. Evaluating the prognostic value of radiomics and clinical features in metastatic prostate cancer using [68Ga]Ga-PSMA-11 PET/CT. Phys Eng Sci Med. 2025;48(1):329-41. doi:10.1007/s13246-024-01516-8.
2. Kleiburg F, de Geus-Oei LF, Spijkerman R, et al. Baseline PSMA PET/CT parameters predict overall survival and treatment response in patients with metastatic castration-resistant prostate cancer. Eur Radiol. 2025;35:4223-32. doi:10.1007/s00330-025-11360-3.
3. Gutsche R, et al. Radiomic analysis of [68Ga]Ga-PSMA PET/CT to monitor response to [177Lu]Lu-PSMA-617 therapy. Cancers (Basel). 2023;15:1422.
4. Mew A, Chau E, Bera K, Ramaiya N, Tirumani SH. Recommendations from imaging, oncology, and radiology organizations to guide management in prostate cancer: summary of current recommendations. Radiol Imaging Cancer. 2025;7(1):e240091.
5. Küper AT, Kersting D, Telli T, Herrmann K, Rominger A, Afshar-Oromieh A, et al. PSMA-PET follow-up to assess response in patients not receiving PSMA therapy: is there value beyond localization of disease? Theranostics. 2024;14(9):3623-33.

Conflict of Interest

The authors declare no conflicts of interest.

Graphic

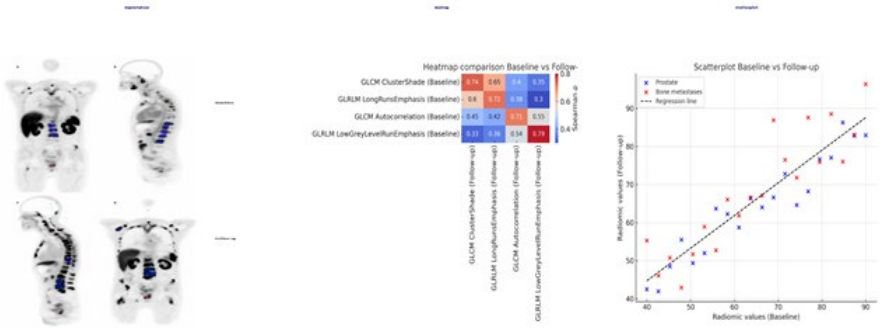

Figure 1. Comparative analysis of radiomic features from baseline and follow-up [18F]PSMA-PET.
Left panel: representative baseline (A–B) and follow-up (C–D) images in a patient with castration-resistant prostate cancer (CRPC), illustrating the segmentation process and demonstrating disease progression.
Central panel: heatmap comparison of radiomic features shows moderate-to-strong correlations (ρ = 0.70–0.79) between baseline and follow-up acquisitions, supporting temporal reproducibility.
Right panel: scatterplot of prostate and bone lesion features reveals overall consistency across time points, highlighting the heterogeneity that characterizes disease evolution.

Table

Module	Variables included	Examples of key correlations	Clinical interpretation	Potential usefulness
Texture	GLCM (ClusterShade, Autocorrelation), GLRLM (LongRuns, LowGreyLevelRunEmphasis), GLSZM	ρ=0.74, p=0.01 between GLCM ClusterShade (Baseline vs Follow-up); ρ=0.79, p=0.008 in bone with GLRLM	Reflects intratumoral heterogeneity and microstructural changes	Biomarkers of aggressiveness and treatment response
Morphology	Sphericity, compactness, tumor volume	ρ=0.72, p=0.02 between prostate volume and PSMA-TL	Structural changes and lesion size	Monitoring tumor volume and treatment control
Intensity	SUV histograms (mean, deviation, percentiles)	ρ=0.70, p=0.03 between SUVmean and radiomic histogram features	Tracer metabolism and uptake	Assessment of residual metabolic activity
Tumor burden	TL-PSMA, MTV-PSMA	ρ=0.73, p=0.01 correlation with total radiomic tumor volume	Global disease extension	Prognostic and progression marker
Metastatic spread	Bone and lymph node metastases	ρ=0.71, p=0.02 between bone count and GLRLM textures	Represents systemic disease biology	Estimation of total metastatic burden
Treatments	Lines of hormonal therapy, chemotherapy or radiotherapy	Significant association (p<0.05) with radiomic changes between Baseline and Follow-up	Therapeutic impact on tumor phenotype	Response monitoring and personalization

Table 1. Radiomic and clinical correlation modules (ρ=0.70–0.80, p<0.05). Variables included and examples of significant correlations with ρ and p values, clinical interpretation, and potential use as biomarkers in metastatic castration-resistant prostate cancer.

P042

Prognostic value of baseline 18F-FDG PET/CT metabolic parameters in breast cancer and their association with histologic features and disease-free survival

Dr. Bethsabel Rodriguez Encinas[1], MD Eva Lorena Valadez Montero[1], MD Irma Soldevilla Gallardo[1]
[1]The American British Cowdray Medical Center, Mexico City, Mexico.

Aims: Metabolic parameters from 18F-FDG PET/CT may reflect tumor aggressiveness and serve as prognostic biomarkers [1,2]. This study aimed to evaluate the predictive value of baseline metabolic parameters—SUVmax, MTV, and TLG—and their relationship with histologic subtype, molecular subtype, Ki-67 index, and disease-free survival (DFS) in patients with non-metastatic breast cancer.
Methods: A retrospective observational study was conducted on 14 patients with invasive breast carcinoma (stages I–III) who underwent a baseline PET/CT at The American British Cowdray Medical Center between 2018 and 2024. Inclusion criteria were a complete histopathologic report and a minimum follow-up of 12 months. Metabolic parameters were obtained from the primary lesion using a 41% SUVmax threshold. DFS was analyzed with the Kaplan-Meier method, while comparisons and correlations were performed with the Kruskal-Wallis and Spearman tests, respectively [3].
Results: The median age was 55 years. Molecular subtypes were Luminal B (50%), Luminal A (28.6%), and Triple-Negative (21.4%). Median (IQR) values were: SUVmax 6.3 (3.5–9.6), MTV 9.2 mL (4.5–17.7), and TLG 62.5 (22.7–115.8). No significant differences in metabolic parameters were found between subtypes ($p>0.15$). SUVmax showed a moderate but non-significant positive correlation with Ki-67 ($\rho=0.34$, $p=0.23$). Kaplan-Meier curves revealed a non-significant trend toward shorter DFS in patients with high SUVmax and TLG [4,5].
Conclusions: Baseline PET/CT metabolic parameters did not differ significantly between molecular subtypes but showed a positive trend with proliferative activity (Ki-67). Higher SUVmax and TLG were associated with a non-significant trend toward poorer DFS. This ongoing work suggests that PET/CT metabolic markers could serve as accessible prognostic indicators in this population.

References

1. Koo HR, Park JS, Kang KW, Cho N, Chang JM, Bae MS, et al. 18F-FDG uptake in breast cancer correlates with immunohistochemically defined subtypes. Eur Radiol. 2014;24(3):610–618.
2. Lee MI, Jung YJ, Kim D Il, Lee S, Jung CS, Kang SK, et al. Prognostic value of SUVmax in breast cancer and comparative analyses of molecular subtypes: a systematic review and meta-analysis. Medicine (Baltimore). 2021;100:e26745.
3. Groheux D, Sanna A, Majdoub M, De Cremoux P, Giacchetti S, Teixeira L, et al. Baseline tumor 18F-FDG uptake and modifications after neoadjuvant chemotherapy are prognostic of outcome in ER+/HER2+ breast cancer. J Nucl Med. 2015;56(6):824–831.

4. Topuz ÖV, Arslan E, Usul G. Relation between primary tumor SUVmax value, Ki-67 proliferation index and axillary metastasis in patients with triple-negative breast cancer. Bagcilar Med Bull. 2025.
5. Aogi K, Kadoya T, Sugawara Y, Kiyoto S, Shigematsu H, Masumoto N, et al. Utility of 18F-FDG PET/CT for predicting prognosis of luminal-type breast cancer. Breast Cancer Res Treat. 2015;150(2):209–217.

Conflict of Interest

The authors declare no conflicts of interest.

Graphic

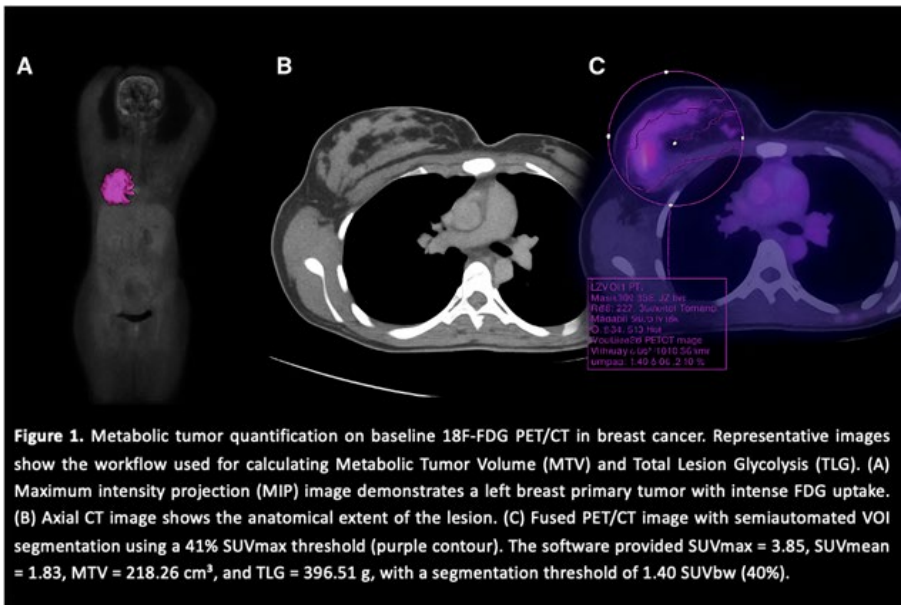

Figure 1. Metabolic tumor quantification on baseline 18F-FDG PET/CT in breast cancer. Representative images show the workflow used for calculating Metabolic Tumor Volume (MTV) and Total Lesion Glycolysis (TLG). (A) Maximum intensity projection (MIP) image demonstrates a left breast primary tumor with intense FDG uptake. (B) Axial CT image shows the anatomical extent of the lesion. (C) Fused PET/CT image with semiautomated VOI segmentation using a 41% SUVmax threshold (purple contour). The software provided SUVmax = 3.85, SUVmean = 1.83, MTV = 218.26 cm^3, and TLG = 396.51 g, with a segmentation threshold of 1.40 SUVbw (40%).

Table

Table 1. Metabolic parameters by molecular subtype (median, IQR)

Parameter	Luminal A-like	Luminal B-like	Triple-negative	p-value*
SUVmax (primary)	5.9 (3.4–9.4)	6.6 (3.8–9.9)	8.5 (5.4–10.2)	0.151
MTV	8.3 (4.2–12.7)	9.7 (5.6–20.5)	10.8 (6.3–21.5)	0.625
TLG	48.9 (18.0–87.5)	65.4 (25.7–132.4)	74.2 (30.5–144.1)	0.592

*Kruskal–Wallis test for intergroup comparison.

P043

Diagnostic Value of Quantitative Parameters of Intraprostatic Uptake of F18-PSMA-1007 in the Risk Classification of Prostate Cancer

Profe. Juan Carlos Rojas Montenegro[1], Dr. Sebástian Ayala Zapata[2], Prof. Miguel Angel Olarte Casas[3]
[1]Universidad Del Valle - Facultad de Salud - Medicina Nuclear, Cali, Colombia, [2]Hospital Universitario del Valle - Facultad de Salud - Medicina Interna, Cali, Colombia, [3]Universidad Autónoma de Mexico - Facultad de Medicina - Unidad de PET/CT, Ciudad de Mexico, Mexico

Background and Objectives: The aim of the study was to evaluate the effect of the quantitative parameters of PET/CT with 18F PSMA-1007 (PSMA) in patients with newly diagnose of prostate cancer (PCa) without treatment, exploring its predictive value with the D'Amico risk criteria. [1], [2], [3].
Methods: Of 276 patients with prostate cancer referred to the PET/CT Unit of the Autonomous University of Mexico from January 1 to September 15, 2025, for a PET-CT study with PSMA; Of 64 patients referred for staging, 34 patients with newly diagnosed and histologically confirmed PCa, without previous treatment, were selected.
A PET/CT scan with PSMA was performed for primary staging and the risk group was assigned according to the D'Amico criteria, exploring each of the quantitative parameters of PSMA. (SUVmax, SUVmean, tumor burden volumes, including prostate/psoas ratio (P/M ratio)).
Results: Of 34 patients who met the inclusion criteria, finding no significant differences between the average values of the quantitative parameters of PSMA and the D'Amico risk groups, except for PSA levels, which were statistically significant among the 3 risk groups. When the P/M ratio (Prostate/Psoas ratio) discriminating capacity was evaluated, a cut-off value of 9.5 in the AUC of 0.75 was found to differentiate between a High and a Low risk.
Conclusion: No significant differences were found between the mean values of the quantitative parameters of the 18F PSMA-1007 and the D'Amico risk groups, except for PSA values, and a cut-off value of 9.5 for the P/M variable had a good capacity for discrimination between high- and low-risk patients. The results suggest that the P/M ratio could play an important role in the classification of risk groups in PCa, but studies with greater statistical power are required to establish this.

References

1.Hofman MS, Lawrentschuk N, Francis RJ, et al. Prostate-specific membrane antigen PET-CT in patients with high-risk prostate cancer before curative-intent surgery or radiotherapy (propsma): a prospective, randomised, multicentre study. Lancet 2020;395:1208-1216.
2. Shuoming Zhou, et al. Diagnosed 18F-DCFPyL PET/CT in Newly Diagnosed Prostate Cancer: Diagnostic Value of Intraprostatic PSMA Uptake in Risk Classi cation of Prostate Cancer. Front. Oncol. 12:800904.doi: 10.3389/fonc.2022.800904.

3. Schmuck S, von Klot CA, Henkenberens C, Sohns JM, Christiansen H, Wester HJ, et al. Initial Experience With Volumetric (68)Ga-PSMA I&T PET/CT for Assessment of Whole-Body Tumor Burden as a Quantitative Imaging PSMA PET/CT in Risk Classi cation Biomarker in Patients With Prostate Cancer. J Nucl Med (2017) 58 (12):1962–8. doi: 10.2967/jnumed.117.193581.

Conflict of Interest

NN

Graphic

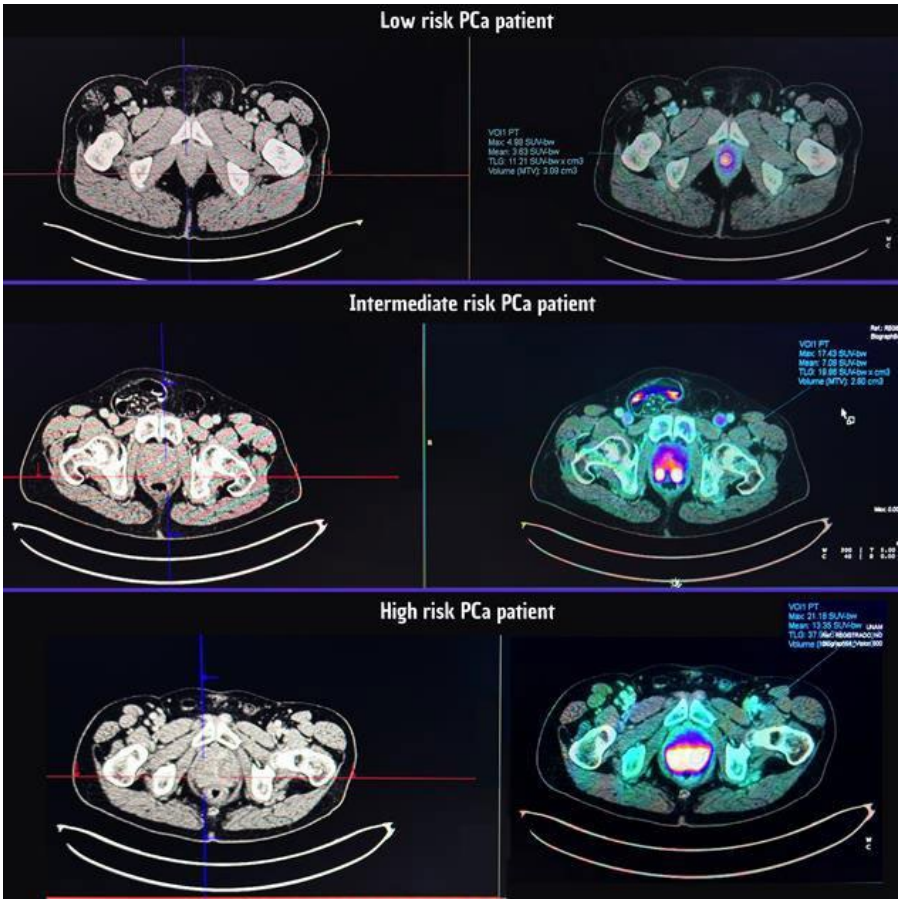

Table

Grupo (Estadio clínico)	N	PSA mediana [Q1–Q3]	SUVmax mediana [Q1–Q3]	SUVmean mediana [Q1–Q3]	PSMA-TV mediana [Q1–Q3]	TL-PSMA mediana [Q1–Q3]	P/M mediana [Q1–Q3]
Alto	22	14.41 [9.53–46.45]	8.20 [4.94–11.22]	5.24 [3.16–7.07]	3.58 [2.89–4.91]	16.83 [10.68–30.70]	12.93 [7.73–18.85]
Intermedio	10	9.55 [6.72–11.65]	4.15 [3.52–5.33]	3.25 [2.65–4.29]	2.88 [2.25–5.42]	11.89 [9.10–14.84]	6.91 [5.54–9.68]
Bajo	2	4.83 [4.67–5.00]	4.72 [4.09–5.34]	3.69 [3.08–4.29]	5.56 [3.26–7.85]	14.93 [9.83–20.02]	7.48 [6.41–8.56]

P044

Clinical impact of somatostatin analogue PET/CT on therapeutic decision-making in neuroendocrine tumors

Dr. Florencia Savio[1], Dr. Ivan Lyra, Dra Dahiana Amarillo, Dr. Diego Ferreira, Dra. Florencia Gentini, Dr Mathías Jeldrés, Dra. Cecilia Castillo, Dr. Gabriel Krygier, Ing. Rafael Alonso, Dra Marisa Fazzino, Dr Eduardo Savio, Dr Alarico Rodríguez, Dr Gustavo Burroso, Dr Nicolás Niell, Dr Juan Pablo Gambini
[1]Unidad Académica de Medicina Nuclear e Imagenología Molecular, Hospital de Clínicas "Dr. Manuel Quintela", Facultad de Medicina Udelar, MONTEVIDEO, Uruguay, [2]Unidad Académica de Oncología Clínica, Hospital de Clínicas "Dr. Manuel Quintela", Facultad de Medicina Udelar, Montevideo, Uruguay, [3]Servicio de Oncología Clínica, Asistencial Médica Maldonado, Maldonado, Uruguay, [4]Servicio de Oncología Clínica, Médica Uruguaya, Montevideo, Uruguay, [5]Servicio de Oncología Clínica, Hospital Británico, Montevideo, Uruguay, [6]Unidad Académica de Métodos Cuantitativos, Facultad de Medicina Udelar, Montevideo, Uruguay, [7]Centro Uruguayo de Imagenología Molecular, Montevideo, Uruguay

Background/Aims: Neuroendocrine tumors (NETs) represent a heterogeneous group of malignancies in which nuclear medicine plays a fundamental role. PET/CT with radiolabeled somatostatin analogues (Ga-DOTA peptides) has become the gold standard for staging, restaging, and therapy selection. This modality not only provides superior diagnostic accuracy but also facilitates theranostic approaches by selecting patients for peptide receptor radionuclide therapy (PRRT) with 117Lu-DOTATATE.
Methods: A retrospective, multicentric, observational study with an analytical component of 151 patients with histologically confirmed NETs diagnosed between 2012 and 2023 was conducted. Clinical, histopathological, imaging, and therapeutic data were collected. Descriptive statistics were applied, and changes in management before and after PET/CT were assessed using the Bowker symmetry test. This study was approved by CUDIM ethics committee and by the ethics committee of each participant healthcare institution.
Results: The median age at diagnosis was 57 years (range: 18–80 years); 54% were men. The most common primary sites were the small intestine (27%) and pancreas (20%), with the liver and lymph nodes as the main metastatic sites. PET/CT was indicated for restaging in 56% of cases, initial staging in 35%, detection of unknown primary tumor in 7%, and eligibility for PRRT in 1%. Notably, PET/CT results led to therapeutic modifications in 59% of cases, most frequently modifying surgical indications or redirecting treatment to systemic therapy or follow-up.
Conclusions: Somatostatin analogue PET/CT is a cornerstone of NET management, directly influencing therapeutic strategies in more than half of patients. Its integration exemplifies the power of nuclear medicine to deliver precision oncology through the theranostic paradigm, particularly by guiding 177Lu-DOTATATE PRRT and optimizing surgical and systemic interventions.

Conflict of Interest
The authors have no conflicts of interest to declare

P045

Clinical impact of 99mTc-hynic-toc spect/ct in neuroendocrine tumors: experience from an oncology hospital in Ecuador

Dr. Christian Toalongo Moreno[1,2], Dra. Karina Zurita Vivero[2], Dr. Paul Villalba Meneses[2]
[1]SOLCA Oncology Hospital, Guayaquil, Ecuador, [2]Indoamérica Technological University, Quito, Ecuador

Background / Aims: Neuroendocrine tumors are a heterogeneous group of neoplasms with variable biological behavior. Detection of somatostatin receptors by molecular imaging is essential for diagnosis and follow-up. Positron emission tomography/computed tomography (PET/CT) with 68Ga-DOTATATE is the gold standard, but its availability in Latin America is limited. Single photon emission computed tomography/computed tomography (SPECT/CT) with 99mTc-HYNIC-TOC (octreotide) has emerged as an accessible and cost-effective alternative. The aim of this study was to describe the initial experience at an oncology hospital in Guayaquil, Ecuador, regarding diagnostic performance and clinical impact of SPECT/CT with 99mTc-HYNIC-TOC in patients with suspected or confirmed neuroendocrine tumors.
Methods: A retrospective observational study was conducted at SOLCA Oncology Hospital in Guayaquil, Ecuador, including patients who underwent SPECT/CT with 99mTc-HYNIC-TOC between 2023 and 2025. Clinical data, tumor location, imaging findings, and correlation with histology or complementary imaging were analyzed. Proportions with 95% confidence intervals (CI) and odds ratios (OR) were calculated to assess the relationship between scan positivity and therapeutic changes.
Results: A total of 136 patients were included (60 men and 76 women), aged 23–85 years (mean: 61). Gastroenteropancreatic tumors were most frequent (72.8%), followed by bronchopulmonary tumors (16.2%). The overall detection rate was 87.5% (119/136; 95% CI: 81.2–92.1). Hepatic metastases were observed in 28.7% and lymph node involvement in 31.6%. In 67.6% of patients (92/136), findings led to therapeutic modifications. The positive predictive value for management change was 77.3%, with a strong association between scan positivity and clinical impact (OR: 117.7; 95% CI: 6.9–2021.5).
Conclusions: SPECT/CT with 99mTc-HYNIC-TOC is a practical and effective diagnostic tool for evaluating neuroendocrine tumors in Ecuador. Conducted at an oncology hospital in Guayaquil, this study shows that the technique provides clinically relevant information, addresses limited PET/CT with 68Ga-DOTATATE availability, and decisively contributes to therapeutic decision-making, influencing more than two-thirds of patients.

Conflict of Interest
None declared

Graphic

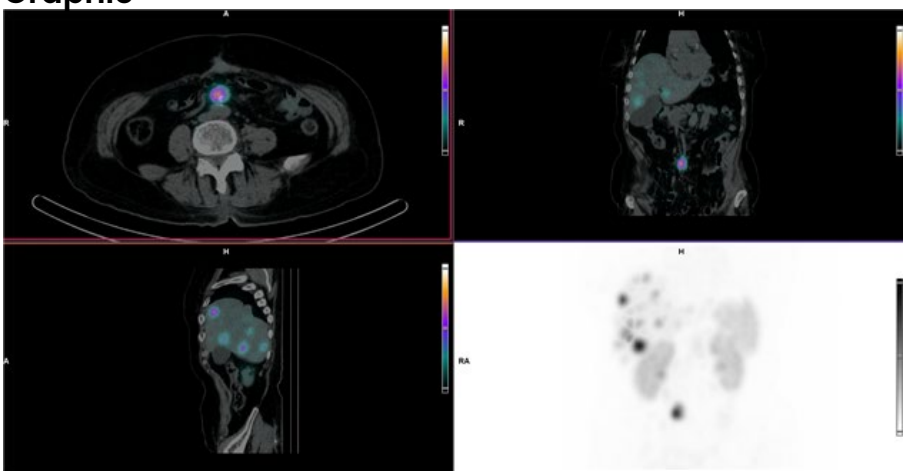

Table

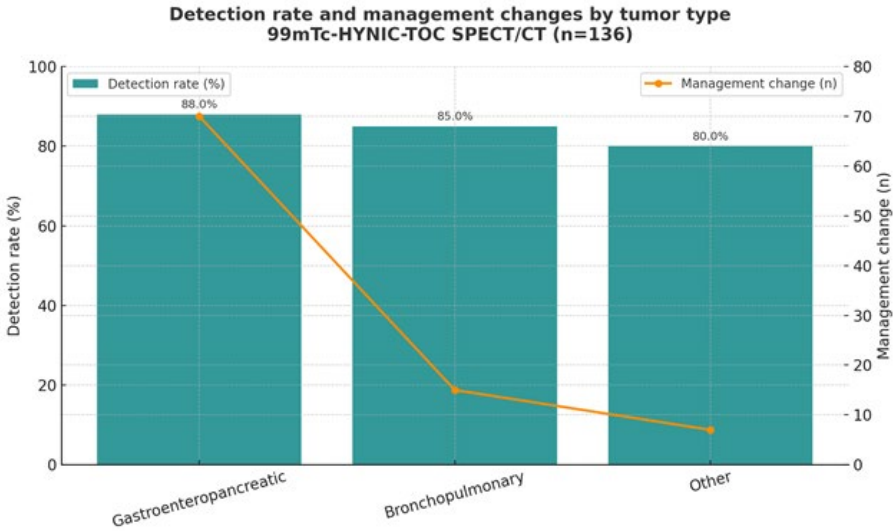

P046

Male Breast Cancer and F-18 FDG PET/CT, Preliminary Results

Prof. Funda Üstün[1], Mrs Büşra Özdemir Günay[2], Mr Aygün Aslan[3]
[1]Trakya University Medical Faculty, Edirne, Turkey, [2]Giresun Training and Research Hospital, Giresun, Turkey, [3]Rize Training and Research Hospital, Rize, Turkey

Aims: Breast carcinoma in men is an uncommon disease. F-18 FDG PET/CT is the most important hybrid imaging used in the diagnostic, staging, follow-up, and treatment evaluation response in cancer patients. The aim of this study was to analyse the performance of F-18 FDG PET/CT systemic staging, restaging in male breast cancer patients.
Methods:
In this Institutional Review Board–approved retrospective study, our database was screened for male patients who had proven breast cancer by histopathological and underwent F-18 FDG PET/CT between January 2014 December 2024.
Results: A retrospective analysis of F-18 FDG PET/CT findings was performed on 25 male breast cancer patients (mean age: 63 years; range: 42-82 years) who underwent primary staging and restaging. Histopathological examination revealed that 19 cases (76%) were diagnosed with invasive ductal carcinoma. Sixteen of the patients were referred for initial staging, and nine for restaging. Eleven of the 16 patients referred for initial staging were present preoperatively. Preoperative SUVmax values of these patients with primary masses ranged from 1.8 to 13.5. In the entire patient group, metastases were found in 11 patients on PET/CT, and 7 of these 11 patients were in the axilla. When the presence of concurrent malignancy was evaluated (12%), one patient had lung cancer and two patients had prostate cancer. Additionally, areas suspicious for synchronous malignancy (lung, rectum, and prostate) were detected in 3 patients on PET/CT.
Conclusions: F-18 FDG PET/CT has a significant impact on initial staging and restaging treatment planning in male breast cancer patients. Because F-18 FDG PET/CT provides information about regional nodal, and distant metastases and other occult primary cancers. In male breast cancer patients, the important contribution of F-18 FDG PET/CT in disease diagnosis and management cannot be ignored.

Conflict of Interest
No

P047

Combined predictive value of quantitative PET/CT and multiparametric MRI parameters for risk stratification in prostate cancer: a preliminary analysis

MD Eva Lorena Valadez Montero[1], MD Bethsabel Rodriguez Encinas[1]
[1]Centro Medico ABC, Mexico City, Mexico

Background/Aims: Accurate risk stratification is crucial for managing prostate cancer. While multiparametric MRI (mpMRI) is standard, combining it with ^{18}F-PSMA PET/CT could improve non-invasive assessment. This study aims to evaluate the combined predictive value of quantitative parameters from both imaging modalities for risk stratification in patients with prostate cancer.
Methodology: This preliminary analysis from the ABC Medical Center includes the first 12 treatment-naïve patients with a diagnosis of prostate cancer who underwent both ^{18}F-PSMA PET/CT and prostate mpMRI. This study received prior ethics approval from the institutional authorities. Quantitative parameters were extracted from both modalities, including the maximum Standardized Uptake Value (SUVmax), Total Lesion Glycolysis (TLG), and PSMA-Tumor Volume (PSMA-TV) from PET/CT, as well as the Apparent Diffusion Coefficient (ADC) and PI-RADS v2.1 score from mpMRI. The correlation between imaging parameters was assessed using Pearson's coefficient. Furthermore, SUVmax and ADC values were compared among the D'Amico risk classification groups (Low, Intermediate, and High).
Preliminary Results: A moderate positive correlation was found between SUVmax and the PI-RADS score (r=0.54), and a moderate negative correlation was observed between SUVmax and ADC (r=-0.42), indicating that lesions with higher metabolic activity tend to have higher suspicion on mpMRI and greater diffusion restriction. The analysis by risk groups demonstrated a statistically significant upward trend in SUVmax values as the D'Amico risk group increased. Similarly, ADC values showed a tendency to decrease in higher-risk groups.
Conclusion: Our preliminary findings suggest a significant correlation between quantitative parameters from PSMA PET/CT and mpMRI, which capture complementary biological aspects of the tumor. SUVmax, in particular, shows strong potential for differentiating between clinical risk groups. The integration of these metrics could improve non-invasive risk stratification in prostate cancer, although validation of these results in a larger patient cohort is required.

Conflict of Interest
The authors declare that the research was conducted in the absence of any commercial or financial relationships that could be construed as a potential conflict of interest.

Graphic

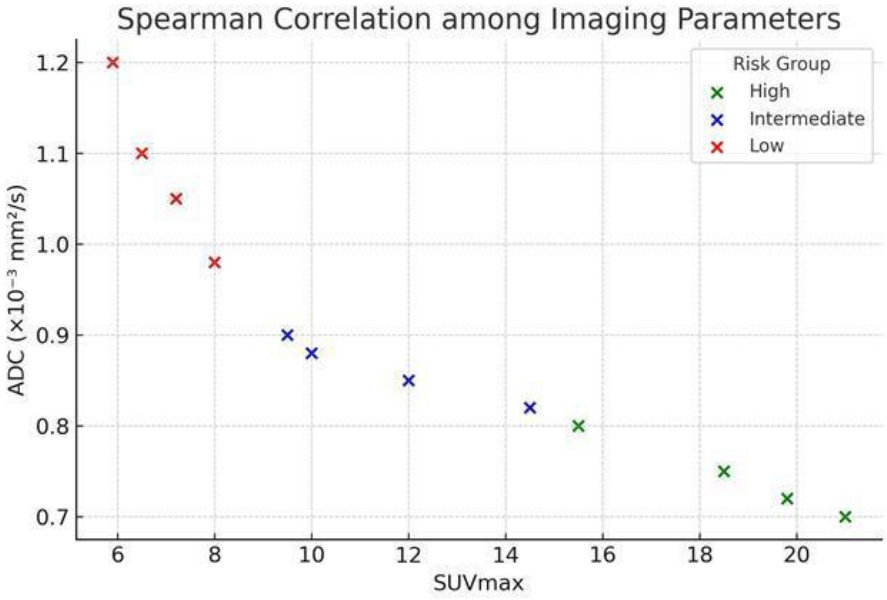

Table

Variable	Median	Mean	SD	Min	Max
Age	68.5	66.83	9.42	52.0	77.0
PSA	8.45	11.54	9.23	3.0	27.79
Gleason	7.0	7.36	1.03	6.0	9.0
PIRADS	4.5	4.3	0.82	3.0	5.0
ADC	0.61	0.61	0.12	0.41	0.77
APE	0.12	0.29	0.32	0.03	0.94
SUVmax	7.6	11.03	7.72	3.6	26.5
MTV	33.99	30.95	18.41	5.61	71.37
TLG	99.44	170.25	239.28	26.58	918.53

P048

Role of Meckel's Scan for Gastrointestinal Bleeding and/or Anemia: Experience in Nuclear Medicine, Hospital San Juan de Dios, Chile

Dr. Sebastián León[1], Dra. Gilda Donoso[1,2], Dra. Gabriela Mundaca[2]
[1]Universidad De Chile, Santiago, Chile, [2]Hospital San Juan de Dios, Santiago, Chile

Background/Objectives: Meckel's Diverticulum (MD), one of the most common congenital malformations of the gastrointestinal tract, is an important cause of gastrointestinal bleeding in pediatrics [1]. In approximately 2% of the population, is located close to the ileocecal valve, and typically presents clinically <2 years old [2]. Given the clinical suspicion, pertechnetate scintigraphy is the study of choice for its high sensitivity (85-95%). Our goal was to evaluate the results obtained in our service and conduct a follow-up of these patients.
Methods: Approved by local ethics comitee. Studies for MD performed between 2021-2025 were reviewed. Technique: Premedication with omeprazole 0.5 mg/kg IV . Sixty minutes later, pertechnetate: 50-100 µCi/kg. Dynamic images (1frame/minute) were acquired for 30 minutes over the abdominopelvic region, anterior view. Posteriorly the acquisition of 1-minute static antero-posterior and lateral post-void images in a 128x128 matrix. Tomographic acquisition (SPECT) was performed with 32 views, 20 seconds per view, 64x64 matrix, 360°.
Results: A total of 19 studies: 18 patients(2 adults, 5 females, and 13 males). Age:2months-36years. Principal referral diagnosis was gastrointestinal bleeding (16 cases), 1-case anemia, and 1-case gastric ulcer. Three positive cases: 2 in periumbilical area and 1 in hypogastrium (Image 1)—all were surgically confirmed. All patients were clinically followed up. Negative results: there was only 1 false negative (Table 1).
Conclusions: The sensitivity of 75% and specificity of 100% in our study, as well as the observed locations of the MDs, are consistent with international literature [3]. The study defined the surgical management for all 3 positive patients. It`s noteworthy an adult female with a positive scan. The only false negative case underwent surgery based on clinical presentation. There were no false positives. Our report confirms the important role of this simple, accessible, and minimally invasive study in suspected MD and gastrointestinal bleeding, mainly in children.

References

[1]: Aboughalia HA, Cheeney SHE, Elojeimy S, Blacklock LC, Parisi MT. Meckel diverticulum scintigraphy: technique, findings and diagnostic pitfalls. Pediatr Radiol. 2023 Mar;53(3):493-508. doi: 10.1007/s00247-022-05527-z. Epub 2022 Nov 3. PMID: 36323958.
[2] Titley-Diaz WH, Aziz M. Meckel Scan. 2023 Jul 25. In: StatPearls [Internet]. Treasure Island (FL): StatPearls Publishing; 2025 Jan–. PMID: 32809335.
Li B, Gao J, Ding X, Li X, Yu Y, Long Y, Wang X, Wu X, Gao Y. [3]Diagnostics accuracy of [99mTc]pertechnetate scintigraphy in pediatric patients with suspected Meckel's diverticulum: a 12-year, monocentric, retrospective experience. Front Med (Lausanne). 2025 May 21;12:1585313. doi: 10.3389/fmed.2025.1585313. PMID: 40470036; PMCID: PMC12133809.

Conflict of Interest

No conflicts of interests

Graphic

Date	Age (years)	Referral Diagnosis	Result	Location	Confirmed Diagnosis
5/09/2025	10	LGIB	POSITIVE	PERIUMBILICAL	MECKEL'S DIVERTICULUM
19/05/2025	10	LGIB/THALASSEMIA	NEGATIVE		THALASSEMIA/IRON DEFICIENCY ANEMIA
4/04/2025	1	UGIB/HEMANGIOMA	NEGATIVE		MECKEL'S DIVERTICULUM/HEMANGIOMA
28/03/2025	1	UGIB/HEMANGIOMA	NEGATIVE		MECKEL'S DIVERTICULUM/HEMANGIOMA
23/08/2024	34	UGIB	POSITIVE	UMBILICAL	MECKEL'S DIVERTICULUM
12/06/2024	14	GIB	POSITIVE	HYPOGASTRIC	MECKEL'S DIVERTICULUM
11/04/2024	36	GIB	NEGATIVE		HEMORRHOIDAL PATHOLOGY
4/01/2024	4	MECKEL'S DIV.	NEGATIVE		ABDOMINAL VENOLYMPHATIC MALFORMATION
23/11/2023	1	UGIB OBS MECKEL	NEGATIVE		INTRAHEPATIC CHOLESTASIS
11/10/2023	1	UGIB ANEMIA	NEGATIVE		GASTRIC ULCER
29/05/2023	6	GIB VATER SYNDROME	NEGATIVE		PORTAL VEIN CAVERNOMATOSIS
13/03/2023	10	GASTRIC ULCER	NEGATIVE		DUODENAL ULCER
25/01/2023	2	GIB	NEGATIVE		MYELODYSPLASIA REFRACTORY ANEMIA
19/05/2022	9	LGIB	NEGATIVE		ANAL PATHOLOGY
16/05/2022	0Y 2M	ANEMIA	NEGATIVE		CONGENITAL ERYTHROBLASTOPENIA
13/12/2021	14	LGIB/ANEMIA	NEGATIVE		IRON METABOLISM DISORDER
5/11/2021	5	LGIB	NEGATIVE		HYPERPLASTIC RECTAL POLYP
20/09/2021	2	GIB	NEGATIVE		IRIDA SYNDROME GENETIC STUDY
7/07/2021	4	MECKEL'S DIV.	NEGATIVE		HYPERPLASTIC RECTAL POLYP

Table 1: Register of cases with requested study for Meckel's diverticulum. Lower Gastrointestinal Bleeding (LGIB), Upper Gastrointestinal Bleeding (UGIB), and Gastrointestinal Bleeding (GIB) were the main referral diagnoses. One patient underwent the examination twice, both with a negative result.

Table

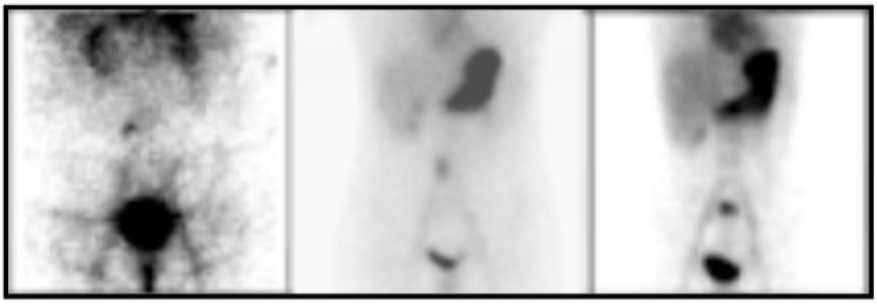

Image 1: Series of images of the 3 positive cases of the study, the first two located in the umbilical projection area and the third in the hypogastrium.

P049

Reproducibility of Volumetric Parameters in [18F]-PSMA-1007 PET/CT: A Comparison Between Two Analysis Platforms

Mrs. Nathaly Barbosa[1], Dr Daniel Felipe Galindo Cortés[2], MSc Adriana Carolina Aya-Porto[1], Dr Clarena Zuluaga[1], Dr Carlos Granados[1]
[1]Centro De Tratamiento E Investigación Sobre Cáncer, Bogota, Colombia,
[2]Fundación Universitaria Sanitas, Bogota, Colombia

Background / Objectives: Volumetric quantification in positron emission tomography/computed tomography (PET/CT) with prostate-specific membrane antigen (PSMA) ligands has emerged as a promising imaging biomarker for prognosis and therapeutic response assessment in patients with prostate cancer. However, for clinical translation, reproducibility across different analysis platforms must be ensured. This study aimed to compare the metabolic tumor volume (MTV) and total lesion glycolysis (TLG) derived from two independent software platforms and assess their concordance and operational feasibility.
Methods: We retrospectively analyzed 50 patients with prostate cancer who underwent [^{18}F]-PSMA-1007 PET/CT between. Lesions were segmented using a standardized threshold of SUVmax >4.0, followed by the manual exclusion of physiological uptake. Data are expressed as median and interquartile range (IQR). The Wilcoxon signed-rank or sign test (for tied data) was applied. Associations were assessed using Spearman's correlation coefficients. Agreement was evaluated using Bland–Altman plots, the percentage of observations within the limits of agreement (LoA), and Lin's concordance correlation coefficient (CCC).
Results: The median MTV was 39.9 mL on the first platform and 43.9 mL on the second platform ($p < 0.001$). The median TLG values were 259.2 and 281.5, respectively ($p < 0.001$). MTV and TLG showed very strong rank correlation ($r \geq 0.99$). Bland–Altman analysis indicated small biases with narrow 95% limits of agreement for both metrics, and the ratio Bland–Altman (percent difference) results were consistent, supporting interchangeability. Lin's CCC was excellent (≥0.98) for MTV and TLG.
Conclusions: Volumetric parameters from [^{18}F]-PSMA-1007 PET/CT demonstrated excellent reproducibility across two independent platforms. These findings support the interchangeable use of these software in clinical research and routine practice, advancing the standardization of quantitative PET biomarkers for prostate cancer.

Conflict of Interest
The authors report no conflicts of interest. MIM Software was used under a research agreement.

P050

Baseline [^{18}F]PSMA-1007 PET Uptake Predicts Lesion Absorbed Dose During ^{177}Lu-PSMA-I&T Therapy

Mrs. Nathaly Barbosa[1], Dr Clarena Zuluaga[1], Dr Carlos Granados[1]
[1]Centro De Tratamiento e Investigación Sobre Cáncer, Bogota, Colombia

Background / Aims: Baseline PET uptake may serve as a predictor of absorbed dose in radionuclide therapy. Most available evidence derives from studies using [^{68}Ga]PSMA and ^{177}Lu-PSMA-617. We aimed to evaluate whether SUVmean and SUVmax from baseline [^{18}F]PSMA-1007 PET/CT predict lesion absorbed dose during [^{177}Lu]Lu-PSMA-I&T therapy in patients with metastatic castration-resistant prostate cancer (mCRPC).
Methods: We retrospectively analyzed 10 patients with mCRPC who underwent baseline [^{18}F]PSMA-1007 PET/CT and were treated with [^{177}Lu]PSMA-I&T, receiving a mean administered activity of 7.1 GBq per cycle. Lesions were segmented on the baseline PET/CT using a 50% SUVmax threshold and mapped to post-therapy images for dosimetric evaluation. Correlation and linear regression analyses were performed to assess the predictive value of SUVmean for Dmean and SUVmax for Dmax.
Results: A total of 47 lesions were analyzed. Higher baseline uptake was strongly associated with higher absorbed dose per unit of administered activity. SUVmean correlated with Dmean ($r = 0.83$, $R^2 = 0.69$), with the regression model: Dmean [Gy/GBq] = −0.59 + 0.15·SUVmean. SUVmax correlated with Dmax ($r = 0.89$, $R^2 = 0.79$), with the model: Dmax [Gy/GBq] = −1.06 + 0.16·SUVmax.
Conclusions
Baseline [^{18}F]PSMA-1007 PET metrics are strongly correlated with lesion absorbed dose during [^{177}Lu]PSMA-I&T therapy. SUVmean predicts mean dose and SUVmax predicts maximum dose, supporting their value as predictors for personalized dosimetry in mCRPC. These results should be validated in a prospective and independent patient cohort.

Conflict of Interest
The authors report no conflicts of interest. MIM Software was used under a research agreement.

Graphic

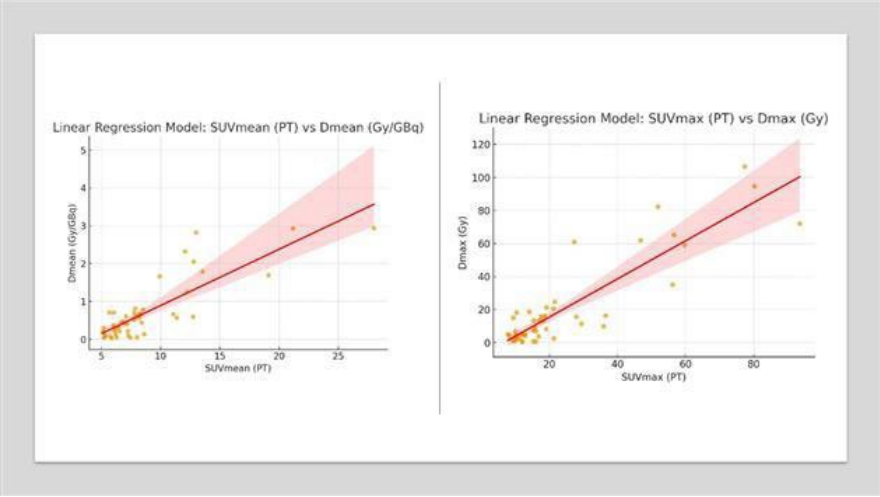

P051

Protocol optimization for myocardial perfusion studies, based on image quality parameters

Señora. Juana Cárdenas Rojas[1], Señora. Andrea Abril Fajardo[1], Señor. Agustín Daza Moreno[2], Señora. Sara Rámirez Aguirre[2], Señora. Claudia Gutierrez Villamil[3]
[1]Universidad Nacional De Colombia, Bogotá, Colombia, [2]Fundación Santa Fe, Bogotá, Colombia, [3]Fundación Cardioinfantil, Bogotá, Colombia

Background/Aims: Anthropomorphic phantom images are analyzed through quality image metrics, obtaining the main parameters for a new acquisition protocol for myocardial studies. The protocol reduces the activity provided to patients, considering the evaluation results, where the contrast and spatial resolution metrics are well-defined, and the lowering of activity does not result in a quality reduction. This work shows the implementation in clinical practice at Fundación Santa Fe de Bogotá.
Methods: The image acquisition was performed using the Pro.Specta Q3 system with the SMARTZOOM collimator. The evaluation of cardiac image quality was carried out through a physical analysis, employing an anthropomorphic heart phantom at first. Image quality assessment was conducted at acquisition levels of 100%, 75%, and 50% activity with different reconstruction parameters. A statistical evaluation determines the best results to be applied to the cardiac images clinical protocol, encompassing both quantitative and qualitative assessments.
Results: In the evaluation of images using the physical simulator, the percentage of contrast and the SNR were analyzed. It was demonstrated that, with lower activity, optimal diagnostic image quality can still be maintained using the simulator. The images obtained with the physical simulator and the SMARTZOOM collimator were also clinically evaluated. Based on these results, an activity of 10 mCi is proposed for myocardial perfusion studies. For this purpose, cardiac image acquisition was performed in patients, where the nuclear physician carried out the corresponding qualitative assessment of the diagnostic image quality.
Conclusions: The study of cardiac images using the SMARTZOOM collimator makes it possible to evaluate the amount of activity administered to a patient, without reducing or compromising image quality, while maintaining contrast percentages and SNR within optimal quantitative parameters.

Conflict of Interest
Does not apply

P052

Real-Time Computational Framework for Standardizing Bed Speed Acquisition in PET/CT Imaging Using NECR-Based Predictive Metrics

Lic. Yesenia Saldierna Martinez[1], Dra. Rocio Hernandez Alvarez[1], MSc Cristhoper Camacho Herrera[1,2]
[1]Hospital Angeles Centro Sur, Queretaro, Mexico, [2]Nuclear Medicine World, Ciudad de Mexico, Mexico

Introduction: Standardization of PET/CT acquisition protocols remains a critical challenge for ensuring reproducible image quality and quantitative accuracy across patient populations and scanners. Variability in bed speed selection by nuclear medicine technologist can compromise diagnostic confidence and inter-study comparability. Real-time assessment of image quality metrics during acquisition is therefore essential.
Methods: We developed a computational code that estimates the Noise Equivalent Count Rate (NECR) using the model:
NECR=A×sensitivity×dwell time
where A represents administered activity, sensitivity accounts for scanner-specific performance, and dwell time corresponds to effective bed duration. The algorithm integrates corrections for patient body mass index (BMI) and incorporates reconstruction algorithm–dependent gain factors to reflect site-specific protocols. Estimated NECR values are subsequently used to predict liver signal-to-noise ratio (SNR) and coefficient of variation (COV) as immediate surrogates of image quality. Post-acquisition validation was performed by comparing estimated liver SNR and COV with measured values obtained in clinical datasets, including liver SNR and thoracic aorta SNR as reference metrics.
Results: Analysis demonstrated strong correlations between estimated and measured image quality parameters, with Pearson correlation coefficients exceeding 0.85 for liver SNR and more conservative results for thoracic aorta SNR across the evaluated cohort. Predicted COV values closely approximated measured liver noise levels with relative differences <5%, confirming robustness of the computational framework. The method consistently reproduced observed site-specific differences arising from reconstruction settings, underscoring the importance of gain factor correction.
Conclusion: This NECR-based computational method provides accurate real-time predictions of PET/CT image quality, enabling standardized bed speed selection tailored to patient habitus and scanner characteristics. By offering immediate quantitative feedback, the approach facilitates protocol optimization, reduces inter-patient variability, and supports harmonization of PET/CT acquisitions. Its implementation has potential to enhance diagnostic confidence and establish a reproducible framework for multicenter clinical trials and clinical practice.
No external funding; support solely from contributing authors.

References
1. Queiroz MA, Delso G, Wollenweber SD, et al. *Clinical image quality perception and its relation to NECR in PET.* EJNMMI Physics. 2019;6(1):22. doi:10.1186/s40658-019-0264-0
2. Carlier T, Ferrer L, Cividini S, et al. *Clinical NECR in 18F-FDG PET scans: optimization of administered activity and time per bed position.* EJNMMI Research. 2021;11(1):25. doi:10.1186/s13550-021-00769-8
3. Akamatsu G, Ishikawa K, Mitsumoto K, et al. *Improvement in PET/CT image quality with a combination of point-spread function and time-of-flight reconstruction.* Annals of Nuclear Medicine. 2012;26(9):636–644. doi:10.1007/s12149-012-0620-z

Conflict of Interest
No conflict of interest reported for this work

P053

Analysis of the diversity and volume of PET CT procedures in prostate cancer patients performed at CUDIM Montevideo-Uruguay: statistical survey

Dr. Gerardo Dos Santos[1,2], Dra. Agustina Banchero[1], Dr. César Ferreira[2], Dr. Eduardo Lischinsky[2], Technologist Ismael Cordero[1], Dr. Omar Alonso[1,2]
[1]Uruguayan Center of Molecular Imaging (CUDIM), Montevideo, Uruguay, [2]Nuclear Medicine and Molecular Imaging Center, Clinical Hospital "Dr. Manuel Quintela", University of Uruguay, Montevideo, Uruguay

Aim/Introduction: To describe the different PET tracers used in our Centre for the imaging evaluation of prostate cancer (PCa) patients.
Materials and Methods:Anonymized statistical information was sought in the database of all users who underwent a diagnostic/therapeutic prostate PET/CT procedure.
Results: From 2010-to-2024 a total of 5074 PET/CT with different prostate tracers were performed:
68Ga-DOTATATE (n=68;1.3%) uptake in lesions expressing somatostatin receptors, would make it a possible diagnostic and theragnostic agent (Lu-177-DOTATATE). (1)
Choline based PET/CT (n=556;10.9%) was widely used due to choline Kinase increased activity, but numerous studies reported a low sensitivity at low PSA levels. (2)
Due to prostate-specific membrane antigen (PSMA) overexpression in PCa, 68Ga-PSMA (Glu-NH-CO-NH-Lys-(Ahx)-[68Ga(HBED-CC]) (n=2045; 40.3%) has been developed as a novel PSMA-ligand, even in patients with low PSA levels. (3)
Several 18F-labelled analogues were introduced into clinical PET imaging in recent years with many advantages over gallium (cyclotron; lower positron energy; higher image quality; delayed imaging).
A novel agent: 18F-AlF-PSMA-11 (n=1555;30.6%), was produced at our center with suitable radiochemical purity in a commercial platform and appropriate for clinical purposes. (4)
The newly introduced 18F-PSMA-1007 (n=810;15.9%) had demonstrated interesting properties: high labeling yields, outstanding tumor uptake and minimal urinary excretion. (5)
New tracers as 11C-S-adenosyl-methionine (SAM;n=3; 0.06%) and 11C-Harmine (CHAR;n=37; 0.7%), would be incorporated into PCa assessment.
Between 2017-2025, 85 patients (mean age 66.8 years;median PSA level 100 ng/ml) with metastatic castration-resistant PCa underwent 177Lu-PSMA therapy (theragnosis), receiving from 1-5 cycles (mean activity 7.0 GBq/cycle) every 6 weeks.

Conclusion: Our center stands out as a pioneer in nuclear medicine imaging prostate cancer, positioning itself as one of the most advanced imaging centers in the region and acts as a regional and international benchmark in diagnosis, therapy and research.

References
(1) Dos Santos G, García Fontes M, Engler H, Alonso O. Intraindividual comparison of 68Ga-DOTATATE PET / CT vs 11C-Choline PET / CT in patients with prostate cancer in biochemical relapse: in vivo evaluation of the expression of somatostatin receptors. Rev Esp Med Nucl Imagen Mol (Engl Ed). 2019 Jan-Feb;38(1):29-37.
(2) Dos Santos G, Alonso O, García Fontes M, Balter H, Engler H. 68Ga-PSMA and 11C-Choline comparison using a tri-modality PET/CT-MRI (3.0 T) system with a dedicated shuttle. Eur J Hybrid Imaging. 2018;2(1):9.
(3) Dos Santos G, Duarte P, Gambini JP, Alonso O. Comparative Evaluation of (18F) AlF-PSMA-HBED-CC and 68Ga-PSMA-HBED-CC in Staging Intermediate-/High-Risk Prostate Cancer: A Prospective Study. Publicado en World J Nuclear Medicine. DOI https://doi.org/ 10.1055/s-0045-1801842. ISSN 1450-1147.
(4) Gerardo Gabriel dos Santos Loureiro, Pablo Duarte Couto, Juan Pablo Gambini Gonzalez, MD, Omar Alonso Nuñez, MD. 18F-AlF-PSMA-HBED-CC as a novel tracer for the evaluation of prostate cancer patients with biochemical relapse: Intraindividual comparison with 68Ga-PSMA-HBED-CC. World Journal Of Urology. EN IMPRENTA.
(5) Gerardo Gabriel dos Santos Loureiro, Pablo Duarte Couto, Juan Pablo Gambini Gonzalez and Omar Alonso Nuñez. Intraindividual Comparison of novel 18F-PSMA-1007 and 18F-AlF-PSMA-HBED-CC PET/CT in the Prospective Evaluation of Prostate Cancer Patients with Biochemical Relapse. International Journal of Clinical Studies & Medical Case Reports. ISSN 2692-5877. DOI: 10.46998/IJCMCR.2025.53.001311. EN IMPRENTA.

Conflict of Interest
No conflict of interest

Graphic

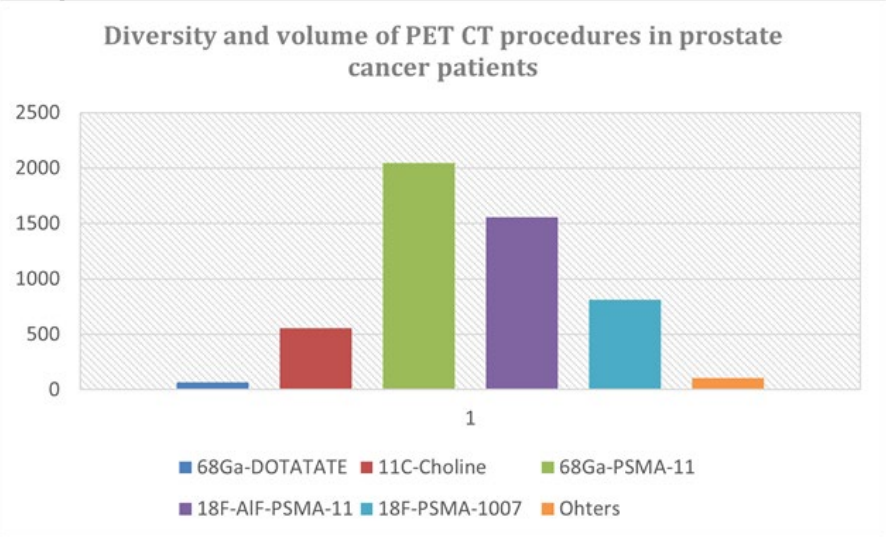

Table

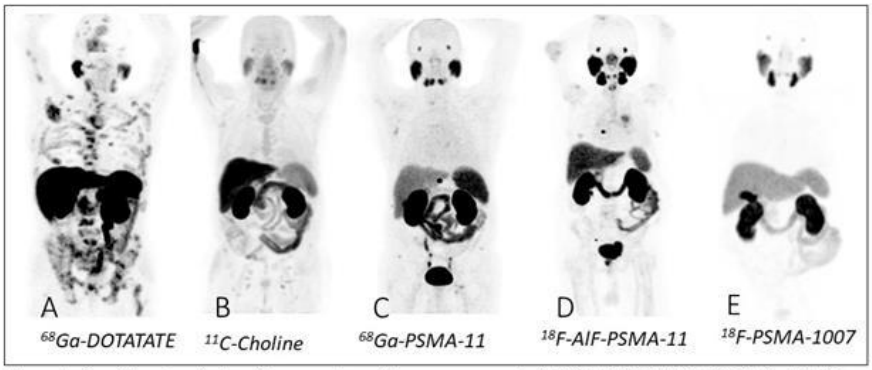

Figure 1. Five different patients with recurrent prostate cancer scanned with ^{68}Ga-DOTATATE (A), ^{11}C-Choline (B), ^{68}Ga-PSMA-11 (C), ^{18}F-AlF-PSMA-11 (D) and ^{18}F-PSMA-1007 (E) PET/CT, showing subtle differences between them. While Choline is dependent on PSA, ^{68}Ga labelled compounds like ^{68}Ga-PSMA-HBED-CC are produced with generators providing limited activity per synthesis. Images of different PSMA tracers were of high visual quality and the normal organ biodistribution has proven highly similar between them. ^{18}F-AlF-PSMA-11 has proven to be cheaper, while ^{18}F-PSMA-1007 had hepatobiliary clearance and low urinary excretion that present clear advantage for pelvic interpretation.

P054

"Redefining the Nursing Role in Nuclear Medicine: Furosemide-Assisted Preparation to Optimize Pelvic Imaging in Genitourinary Cancer"

Lic. Yesenia Saldierna Martinez[1], Dra. Rocio Hernandez Alvarez[1], MSc Cristhoper Camacho Herrera[1,2]
[1]Hospital Angeles Centro Sur, Queretaro, Mexico, [2]Nuclear Medicine World, Ciudad de Mexico, Mexico

Introduction: Tracer accumulation in the urinary bladder during PET/CT can hinder pelvic lesion detection in genitourinary and prostate cancer. Elevated bladder SUV and variable physiologic bowel activity—particularly with ^{18}F-PSMA-1007, which has predominantly hepatobiliary clearance and minimal renal excretion—may interfere with diagnostic interpretation. Intravenous furosemide has been proposed as a strategy to decrease bladder tracer concentration and improve pelvic image quality.
Objective: To evaluate the effect of intravenous furosemide administration on bladder activity reduction and improved pelvic lesion visualization in PET/CT studies with ^{18}F-FDG and ^{18}F-PSMA-1007, as well as to assess the safety of the procedure in patients with comorbidities.
Methods: A prospective study was conducted in 68 patients (42 with prostate cancer and 26 with other genitourinary malignancies) who underwent PET/CT with ^{18}F-FDG or ^{18}F-PSMA-1007. All received 20 mg of furosemide diluted in 250 mL of 0.9% saline, administered intravenously over 30 minutes, starting 30 minutes after tracer injection. Vital signs were recorded before, during, and after infusion, with close monitoring in patients with cardiovascular or metabolic comorbidities.
Results: In ^{18}F-FDG studies, mean bladder SUV decreased by 62% (from 12.4 to 4.7), improving pelvic lesion conspicuity. In the ^{18}F-PSMA-1007 group, a marked reduction in bladder excretion was observed, with SUV values consistently below vascular background SUVmax, allowing more accurate interpretation of the prostatic and nodal regions. No clinically significant adverse events were reported.
Conclusion: Furosemide administration significantly enhances pelvic image quality by reducing bladder SUV and favorably modifying tracer biodistribution. The protocol is safe, reproducible, and suitable for routine PET/CT practice with ^{18}F-PSMA and ^{18}F-FDG, particularly in biochemical recurrence staging of prostate cancer with PSA levels < 1 ng/mL.
No financial support was received apart from the authors themselves.

References

[1] Castaneda P et al. Reducing SUV of the bladder in 18F-FDG PET/CT imaging. Clin Nucl Med. 2015;40(10):790–793.
[2] Evaluation of furosemide-enhanced 18F-FDG PET/CT imaging for urothelial carcinoma. J Nucl Med. 2020;61(Suppl 1):1234.
[3] d'Amico A et al. Effect of furosemide administration before F-18 PET. Nucl Med Commun. 2014;35(12):1238–1243.
[4] Cahenzli MA et al. Furosemide reduces radionuclide activity in the bladder in 18F-PSMA-1007 PET/CT. Eur J Nucl Med Mol Imaging. 2025;52(3):567–575.

[5] Fendler WP et al. EANM/SNMMI joint procedure guideline for PSMA PET/CT in prostate cancer. Eur J Nucl Med Mol Imaging. 2023;50(10):2825–2839

Conflict of Interest: None to be reported

P055

Retreatment with 177Lu-DOTATATE in Patients with Neuroendocrine Tumors: Experience at an Oncology Center

Dr. Hernando Andres Benavides Jimenez[1], Dr Edward Andres Diaz Rodriguez[2], Dra Viviana Andrea Daza Betancourt[1]
[1]Fundacion Universitaria Sanitas, Bogotá, Colombia, [2]Instituto Nacional de Cancerología, Bogota, Colombia

Progressive neuroendocrine tumors (NETs) are malignant neoplasms with poor prognosis. The NETTER-1 and NETTER-2 studies have shown clinical improvement with four-cycle protocols. Retreatment using 2 to 4 cycles has been described in patients with tumor progression, though evidence in Colombia is limited. This study aims to assess the safety and clinical outcomes of retreatment with 177Lu-DOTATATE in patients treated at the National Cancer Institute (INC).
Methods A retrospective review of medical records from 2009 to 2019 was conducted. Patients with NETs who received an initial four-cycle treatment with 177Lu-DOTATATE and were subsequently retreated with at least four additional cycles at the same center were included. Demographic, clinical, toxicity, and outcome data were analyzed for 10 patients.
Results: Of the retreated patients, 90% were women. All received eight total cycles (four initial and four retreatment), with a mean administered activity of 59.2 GBq. After initial treatment, 30% showed partial response and 70% had stable disease. Following retreatment, 20% had partial response and 45% stable disease. The liver was the most common site of progression. Median progression-free survival (PFS) was 37.01 months after initial treatment and 18.6 months post-retreatment. Hematologic parameters declined in both phases, with mild toxicity in one patient during initial treatment and two during retreatment. No grade 3 or 4 nephrotoxicity or hepatotoxicity was observed.
Conclusion: Retreatment with 177Lu-DOTATATE in progressive NETs after initial therapy is safe, well tolerated, and effective. Tumor control and PFS outcomes are comparable to international reports, even with reduced two-cycle protocols.

Conflict of Interest
The authors declare no conflicts of interest.

P056

Transarterial radioembolization with Y-90 and Ho-166 in patients with portal vein thrombosis

Dr. Sandor Czibor[1,2], Boglarka Toth[3,4], Dr. Domonkos Nadasdy-Horvath[1], Dr. David Korda[4], Gabriella Taba[5], Dr. Andras Bibok[4], Dr. Denes Horvathy[4]
[1]Department of Nuclear Medicine, Medical Imaging Centre, Semmelweis University, Budapest, Hungary, [2]Pozitron Medical Diagnostics Ltd., Budapest, Hungary, [3]Faculty of Medicine, Semmelweis University, Budapest, Hungary, [4]Department of Interventional Radiology, Semmelweis University, Budapest, Hungary, [5]Radiation Protection Service, Semmelweis University, Budapest, Hungary

Background: Portal vein thrombosis (PVT) may be present at diagnosis in up to one third of hepatocellular carcinoma (HCC) cases and it not only worsens patient prognosis but also limits the available treatment strategies. Transarterial radioembolization (TARE) emerged as a locoregional treatment that can be used to treat liver tumors, even in the presence of proven PVT. We intend to demonstrate the impact of TARE on tumor response in HCC patients with confirmed PVT.
Methods: We report a single center, retrospective study approved by the institutional ethics committee. 15 HCC patients with PVT were identified out of the 105 patients who underwent TARE with either Y-90 (n=5) or Ho-166 (n=10) isotope since August 2022. The efficacy of the interventions was determined by tumor response on imaging. During follow-up, laboratory and clinical adverse events were classified according to the Common Terminology of Clinical Adverse Events (CTCAE) criteria.
Results: Median (range) injected activity was 6 GBq (1.3-10 GBq) for Ho-166 and 3.5 GBq (1.9-11 GBq) for Y-90 isotopes, respectively. Median (range) tumor absorbed dose was 176 Gy (87-399 Gy) for Ho-166 and 223 Gy (126-468 Gy) for Y-90 products, respectively. 6/15 patients showed progression but 2 of them only after 10 months. The rest (9/15) of the patients achieved durable tumor control with the longest progression-free follow-up period standing at 22.5 months currently. Tumor and normal liver absorbed doses were similar in the cohorts with and without progression. Median patient age was higher among the patients showing progression (70 vs. 61 years). Only 2 patients (13.3%) showed CTCAE Grade 3 clinical complications (severe abdominal pain and transient liver decompensation) and no complications more severe than Grade 3 were observed.
Conclusions: Our results suggest that TARE is a safe and a promisingly efficacious locoregional treatment option for HCC associated with PVT.

Conflict of Interest
Sándor Czibor, Andras Bibok, and Denes Horvathy are proctors for Boston Scientific International B.V. and for Vascular Ventures Ltd.

P057

Correlation between PSA kinetic parameters and progression-free and overall survival in a cohort of patients treated with 177LuPSMA in Colombia

Dr. Daniel Felipe Galindo-Cortes[1], Dr. Viviana Andrea Daza-Betancourt[1], Dr. Sofia Albornoz-Gutiérrez[1], Dr Valeria Andrea Villanueva Bueno[1], Dr Marylin Acuña-Hernández[2], Dr Adriana Quiteria Buitrago-Gómez[2]
[1]Fundación Universitaria Sanitas, Bogotá, Colombia, [2]Instituto Nacional de Cancerología, Bogotá, Colombia

Background: 177LuPSMA therapy is a key treatment for metastatic castration-resistant prostate cancer, with proven impact on progression-free survival (PFS). Early identification of predictive clinical parameters could support decisions about treatment continuation or discontinuation. This study evaluated PSA kinetics after two cycles of treatment with 177LuPSMA and their correlation with outcomes.
Methods: A retrospective analysis was performed in patients treated with 177LuPSMA I&T at the Instituto Nacional de Cancerología (Bogotá, Colombia) from 2020 to 2023. Eligible patients had PSA levels at baseline and after the first and second cycles, with any PSA decline after the second cycle. PSA deltas (baseline vs. post-cycle 1 and baseline vs. post-cycle 2), PSA halving-time, and PSA decline velocity were calculated. Correlation with PFS and overall survival (OS) was assessed using Pearson's coefficient.
Results: Eight of 24 patients met inclusion criteria. Median baseline PSA was 344.5 ng/mL (IQR: 723,8). Mean PFS was 14.25 months (SD: 10,81), and mean OS was 23.56 months (SD: 10,81). After cycle 1, mean PSA delta was −6% (SD: 34), without correlation to outcomes. After cycle 2, mean PSA delta was −62% (SD: 29,9), showing moderate correlation with PFS (r=0.5) and weaker with OS (r=0.29). Five patients (62.5%) achieved ≥50% PSA decline after cycle 2, correlating moderately with PFS and OS (r=0.43 and 0.41). Mean PSA halving-time was 5.85 months (1–27.9) and PSA decline velocity 194.43 ng/mL/month (SD: 325,65), neither associated with outcomes. One patient had a 29% PSA rise after cycle 1 followed by a 94% decline after cycle 2, with no progression at 37 months.
Conclusions: In this cohort, PSA decline after the second cycle, particularly ≥50%, correlated moderately with improved PFS and OS. In contrast, PSA changes after the first cycle, PSA halving-time, and PSA decline velocity showed no association. Larger prospective studies are needed to confirm these findings.

Conflict of Interest
We have no disclosures

Graphic

ROC curves for PSA delta after cycle #2 and mean PFS

ROC curves for PSA delta after cycle #2 and mean OS

Table

Table 1

Metric	Value
Average Age at Therapy Start	74.88 (61-89)
Initial PSA at Therapy (Mean)	963.00 (29.82-5000.00)
Percentage of PSA Decrease (Mean)	62.30 (12.10-94.40)
PSA50% after cycle 2 (% Yes)	62.50%
Progression free survival (Mean)	14.25 (3-37)
Overall survival (Mean)	23.57 (7.53-38.43)
# of 177Lu-PSMA I&T cycles (Mean)	6 (4-10)

P058

Discordant biochemical and radiological responses to Lu177-PSMA therapy in real-world mCRPC patients

Dr. Oscar Herrera Fomperosa[1], Dra. Irma Soldevilla Gallardo[1]
[1]Centro Medico Abc, Álvaro Obregon, Mexico

Background / Objectives: Metastatic castration-resistant prostate cancer (mCRPC) has a poor prognosis [1]. While Lutetium-177 PSMA (Lu177-PSMA) therapy is effective in clinical trials [2, 3], real-world responses are heterogeneous and require modern assessment metrics. This study evaluates the efficacy of Lu177-PSMA in a real-world mCRPC cohort, using both Prostate-Specific Antigen (PSA) decline and modern radiological criteria to measure response.
Methods: We conducted a retrospective study at Centro Médico ABC on ten mCRPC patients treated with a median of 4 cycles of Lu177-PSMA. The study received institutional ethics committee approval. Primary endpoints were biochemical response (PSA reduction ≥50% or PSA50) and radiological response per Prostate Cancer Molecular Imaging Standardized Evaluation (PROMISE v2) criteria [4]. Subgroups based on prior systemic therapy (chemotherapy vs. antiandrogens) were compared using Fisher's exact test and the Mann-Whitney U test.
Results: A PSA50 response was achieved in 60.0% of patients (6/10), with no significant difference between subgroups (Table 1). Of seven patients with radiological assessment, 57.1% (4/7) achieved disease control (Partial Response or Stable Disease), as shown in Figure 1. We observed a notable discordance: 40% of patients with a PSA50 response showed radiological disease progression. The overall correlation between biochemical and radiological responses was not statistically significant (p=0.143).
Conclusions: In this real-world cohort, Lu177-PSMA therapy was effective, showing significant biochemical and radiological disease control. However, the lack of correlation between PSA changes and imaging findings, driven by discordant responses, highlights the critical need for dual monitoring. Radiological evaluation with criteria like PROMISE is essential to accurately assess treatment efficacy, particularly as Lu177-PSMA is used in earlier lines of treatment [5].

References

[1] Kirby M, Hirst C, Crawford ED. Characterising the castration-resistant prostate cancer population: a systematic review. Int J Clin Pract. 2011;65(11):1180-92.
[2] Sartor O, de Bono J, Chi KN, et al. Lutetium-177–PSMA-617 for Metastatic Castration-Resistant Prostate Cancer. N Engl J Med. 2011;385(12):1091-1103.
[3] Hofman MS, Emmett L, Sandhu S, et al. [177Lu]Lu-PSMA-617 versus cabazitaxel in patients with metastatic castration-resistant prostate cancer (TheraP): a randomised, open-label, phase 2 trial. Lancet. 2021;397(10276):797-804.
[4] Seifert R, Emmett L, Rowe SP, et al. Second version of the prostate cancer molecular imaging standardized evaluation framework including response evaluation for clinical trials (PROMISE V2). Eur Urol. 2023;83(5):405-12.

[5] Morris MJ, Castellano D, Herrmann K, et al. 177Lu-PSMA-617 versus a change of androgen receptor pathway inhibitor therapy for taxane-naive patients with progressive metastatic castration-resistant prostate cancer (PSMAfore): a phase 3, randomised, controlled trial. Lancet. 2024;404(10459):1227-39.

Conflict of Interest

The authors declare that they have no conflicts of interest.

Graphic

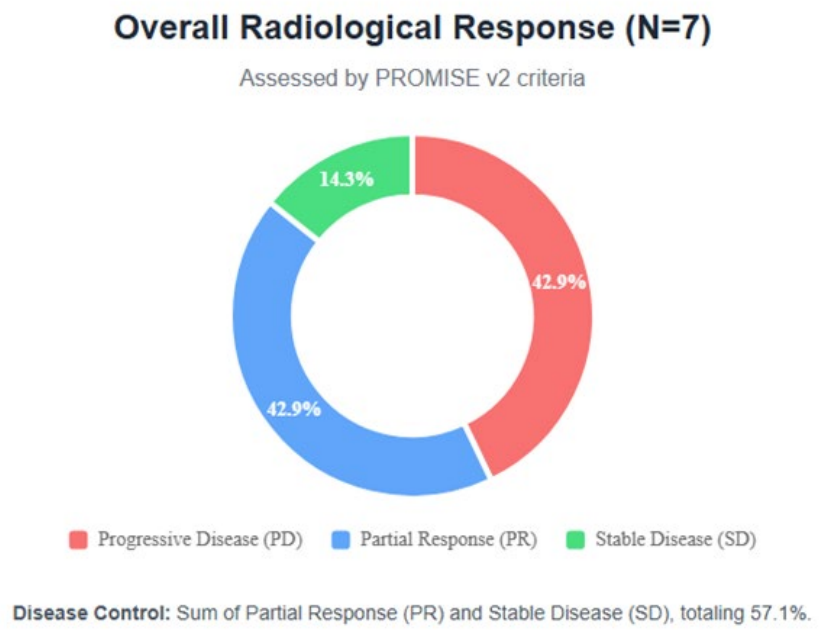

Table

Baseline Characteristics and Biochemical Response

Comparison between treatment subgroups

CHARACTERISTIC	TOTAL COHORT (N=10)	CHEMOTHERAPY (N=5)	ANTIANDROGEN (N=5)	P-VALUE
Age (Median, years)	74.0	76.0	71.0	0.346
Baseline PSA (Median, ng/mL)	11.75	12.4	11.1	1.000
Cycles of Lu177-PSMA (Median [range])	4 [3-6]	4 [4-6]	5 [3-6]	0.175
Biochemical Response (PSA50), n (%)	6 (60.0%)	3 (60.0%)	3 (60.0%)	1.000

P059

Impact of pharmacogenomics on the management of patients with metastatic castrate-resistant prostate cancer requiring radionuclide therapy

Dr. Nihaad Jacobs[1], Ms Nosipho Mabizela[1], Dr Raisa Wessels[1,2], Prof Collet Dandara[1], Dr Khanyisile Hlongwa[1], Dr Stuart More[1]
[1]University of Cape Town, Cape Town, South Africa, [2]National Health Laboratory Service, Cape Town, South Africa

Background: There are limited treatment options for patients with metastatic castrate-resistant prostate cancer (mCRPC). [177Lu]Lu-PSMA radionuclide therapy has shown significant benefit. Multiple factors, including pharmacogenomics, may play a role in treatment outcomes.
Aim: To investigate the impact of pharmacogenomics and germline mutations on treatment response prediction.
Methods: Retrospective study of mCRPC patients treated with [177Lu]Lu-PSMA between January 2018 and December 2022. The DNA of ten archival tissue samples from six patients were extracted and selectively genotyped for CHEK2 and BRCA2 gene mutations, with the intention of correlating mutational data with various response parameters.
This study was approved by the University of Cape Town Faculty of Health Sciences Human Research Ethics Committee; Ref: 665/2024.
Results: Mutational data for all ten samples showed poor DNA integrity. TaqMan assay genotyping for BRCA2 and CHEK2 mutations of all samples demonstrated no DNA amplification.
Post therapy, there was an increase of 82.6% in PSA and 119.6% in the ratio of target lesion counts relative to liver on imaging, with no change in clinical function.
A correlation between mutational data and response parameters could not be derived due to the small sample size and lack of DNA amplification.
Conclusion: The DNA quality from archival tissue was too poor to assess for mutations. Due to the lack of DNA amplification and detection of genomic mutations, a correlation could not be drawn between mutations, scintigraphic and biochemical data in this cohort.
A larger sample size, use of blood samples or fresh tissue and alternative DNA amplification methods may yield results which could assist in determining the use of genomic profiling to facilitate radionuclide therapy.
Potential future research includes DNA analysis with Sanger sequencing to determine if this alternative method of DNA analysis yields mutational data. This method is currently in process using samples analysed in this study.

Conflict of Interest
There are no competing interests.

P060

Implementation of comprehensive geriatric assessment in older adults with differentiated thyroid cancer who require in-hospital radioiodine therapy

Dr. M. Josefina Jofre Manieu[1], Dr. Rocio Quilodrán[1]
[1]Fundacion Arturo Lopez Perez, Santiago, Chile

Background: Patients with differentiated thyroid cancer (DTC) who undergo surgery and present an intermediate-to-high risk of recurrence are candidates for I-131 therapy, with dosing guided by histopathological features. Hospitalization for radioiodine treatment depends on several factors, including the prescribed I-131 activity, patient autonomy, socioeconomic conditions, and the ability to tolerate radioactive isolation with minimal nursing support. Older adults often pose additional challenges due to frequent comorbidities and functional limitations. This study aimed to assess the feasibility and outcomes of implementing a comprehensive geriatric assessment (CGA) in patients over 60 years with resected DTC and indication for inpatient radioiodine therapy.
Method: We retrospectively evaluated 32 older adults referred for CGA between April 2023 and May 2025. The mean age was 74 years (range 63–89), and 63% were women. Nearly all patients (31/32) had comorbidities, most commonly hypertension, diabetes, and renal impairment. Papillary DTC was the predominant subtype (84%). Metastatic disease to lung and/or bone was observed in 57%, and 59% were receiving their first I-131 treatment. A high radioiodine activity (≥100 mCi) was indicated in 88%. The CGA included mental health, geriatric syndromes (frailty, falls, polypharmacy, sensory deficits, continence, and delirium risk), nutrition, and functional status.
Results: Of the cohort, 6 patients (18.8%) presented risk factors that could limit hospitalization, while the remaining were eligible for treatment. More than half (54%) required specific geriatric interventions, with 4 needing further studies and reassessment prior to therapy. Medication optimization was required in 41%. Ultimately, 24 patients received radioiodine; two did not (one administrative, one death from a cardiac event despite prior clearance). Importantly, no complications occurred among treated patients during hospitalization.
Conclusion: These findings support the integration of CGA in older DTC patients requiring radioiodine therapy. Tailored geriatric evaluation and intervention enabled safe hospitalization and favorable short-term outcomes

Conflict of Interest
No conflict of interest.

Table

COMPREHENSIVE GERIATRIC ASSESSMENT *		
ABVD – Barthel Index	n	%
100/100: Independent	20	65
95-60/100: Mild dependence	11	35
55-40/100: Moderate dependence	0	0
35-20/100: Severe dependence	0	0
<20/100: Total dependence	0	0
AIVD – Lawton Scale	n	%
8/8	17	54
7/8	5	16
6/8	3	10
5/8	2	6
4/8	0	0
3/8	1	3
2/8	0	0
1/8	1	3
0/8	1	3
Not included	1	3
Memory	n	%
Preserved	18	58
Benign complaints	10	32
Severe complaints / dangerous forgetfulnes	2	6
Mild cognitive impairment	1	3
Mood	n	%
Preserved	19	61
Decreased	12	39
Sleep	n	%
Preserved	19	61
Controlled with medication	5	16
Decreased	7	22
Frailty	n	%
Robust	18	58
Pre-frail	10	32
Frail	3	10
Appetite	n	%
Preserved	28	90
Altered	3	10
Weight Loss	n	%
Yes	8	25
No	23	75
Falls	n	%
Yes	8	25
No	23	75
Assistive Devices	n	%
Yes	27	87
No	4	13
Urinary Continence	n	%
Without incontinence	20	65
With incontinence	11	35
Bowel Habits	n	%
Without constipation	22	71
With constipation	9	29

Visual impairment	n	%
Yes	23	74
No	8	26
Hearing impairment	n	%
Yes	6	19
No	25	81
Dental Prosthesis	n	%
Yes	16	52
No	15	48
Polypharmacy	n	%
Yes	21	68
No	10	32
Inappropriate Prescription	n	%
Yes	10	32
No	21	68
Delirium Risk	n	%
Low	22	71
Moderate	6	19
High	3	10
BMI	n	%
Normal weight (18.5-24.9)	9	29
Overweight (25-29.9)	11	36
Moderate obesity (30-34.9	8	26
Severe obesity (35-39.9)	1	3
Not included	2	6
MNA-SF		
Normal	15	48
At risk of malnutrition	2	6
Malnutrition	1	3
Not included	13	42

* 31 patients (1patient with mood disorder doesn't complete CGA)

P061

Predictive factors of progression in neuroendocrine tumors and paragangliomas treated with lutetium-177-DOTATATE therapy

Dr. Oscar Lucio[1], Dr. Miguel Corza[1]
[1]Instituto Nacional De Ciencias Médicas Y Nutrición Salvador Zubirán, Mexico City, Mexico

Background/Aims: Neuroendocrine tumors and paragangliomas are a heterogeneous group of malignancies that benefit from targeted radionuclide therapy. Lutetium-177-DOTATATE is an established treatment for progressive neuroendocrine tumors. However, the factors influencing disease progression under Lu-177-DOTATATE therapy remain only partially understood. This study aimed to evaluate clinical, pathological, and treatment-related variables associated with progression following Lu-177-DOTATATE therapy.
Methods: We retrospectively analyzed patients with neuroendocrine tumors treated with Lu-177-DOTATATE at our institution. Variables assessed included age, sex, histological grade, primary site, prior treatments (surgery, radiotherapy, somatostatin analogues, chemotherapy), and adherence to treatment. Correct dosing intervals were defined as a maximum of 6–8 weeks between successive administrations. Progression was determined based on clinical and imaging criteria. Logistic regression and survival analyses were performed.
Results: A total of 31 patients were included. The mean age was 56 years (14.7± SD); 65% were male. Histological grades 1, 2, and 3 were represented. Progression occurred in 34% of the cohort. The mean progression-free survival was 20.1 months. In multivariate analysis, older age (OR = 1.09), lack of prior radiotherapy (OR = 1.77, p = 0.02), and higher histological grade (p = 0.01) were associated with an increased risk of progression. Interval compliance showed no significant association. Survival analysis supported these findings.
Conclusions: Older age, absence of prior radiotherapy, and higher histological grade were independently associated with an increased risk of progression in patients receiving Lu-177-DOTATATE for neuroendocrine tumors. Correct dosing intervals did not significantly influence outcomes. These findings highlight the need for further studies on synergic therapies and may help refine patient selection and follow-up strategies.

Conflict of Interest
The corresponding authors declare no conflict of interest.

Graphic

Figure 2. Kaplan-Meier progression free months

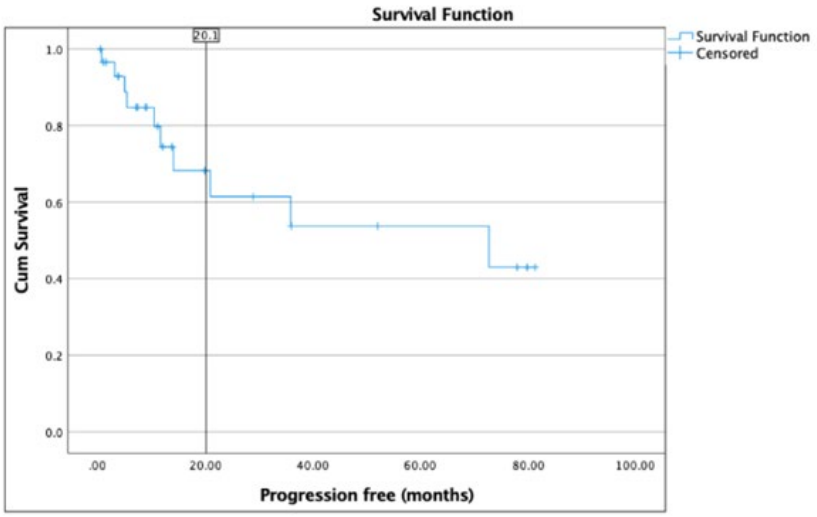

Table

Table 1. Comparison of clinical characteristics between patients with and without progression

Variable	With progression	Without progression	p-value
Age (years)	68 ± 11	61 ± 10	0.03
Male sex (%)	58	49	0.12
Grade 3 (%)	40	18	0.01
Previous radiotherapy (%)	20	46	0.02
Correct intervals (%)	65	68	0.79

P062

The role of SPECT/CT imaging after radionuclide therapy in metastatic castration-resistant prostate cancer

Mrs. Lisa MacFarlane[1,2]
[1]Peter MacCallum Cancer Centre, Melbourne, Australia, [2]Sir Peter MacCallum Department of Oncology, The University of Melbourne, Melbourne, Australia

Introduction: Imaging with Single Photon Emission Computed Tomography (SPECT/CT) after radionuclide therapy (RNT) is becoming increasingly important in the management of metastatic castration-resistant prostate cancer (mCRPC). Its purpose extends beyond simple response monitoring; it provides insights into therapy efficacy, disease progression, and patient management strategies. Evidence demonstrates that post-RNT SPECT/CT can predict overall survival and influence management decisions in nearly half of treated patients. This positions post-RNT SPECT/CT imaging as a cornerstone in advancing precision medicine.
Method: A review of the published literature was conducted, focusing on post-RNT SPECT/CT imaging following PSMA-targeted RNT, with particular emphasis on imaging timing, dosimetry, findings and efficacy.
Results: Comparative studies of 4-hour versus 24-hour SPECT/CT scans[1] suggest that early imaging is a practical, cost-effective option for regional patients, while multi-timepoint acquisitions are required for accurate dosimetry[2]. Dosimetry allows calculation of absorbed doses for both tumours and organs-at-risk, providing individualised treatment guidance. The Precision Dosimetry Biomarker Project seeks to harmonise calibration and workflow across centres to improve consistency. Case studies highlight clinical responses, including PSA reductions and tumour volume shrinkage, emphasising the therapeutic impact of 177Lu-PSMA when guided by imaging and dosimetry. Post-RNT SPECT/CT performed in the Violet trial has highlighted the efficacy of 161Tb-PSMA RNT[3]. Using different radionuclides such as 177Lu-Lutetium and 161Tb-Terbium underscore how decay properties and imaging characteristics can influence both dosimetry and clinical outcomes.
Conclusion: Post-RNT imaging provides prognostic information, guides adaptive treatment strategies, and supports safe dose personalisation. Whilst 177Lu-PSMA imaging is performed in many centres, new RNT treatments using 161Tb-PSMA ligands will also guide treatment decision, and the protocols for imaging with 161Tb will be validated with further research. Ultimately, post-RNT SPECT/CT imaging represents a key tool in advancing precision oncology and improving outcomes for patients with mCRPC.

References

1. Swiha M et al, JNM. 2024;65(12):1939-1944
2. Jackson P et al, Semin Nucl Med. 2022;52(2):243-254
3. Buteau, JP et al. Lancet Oncol. 2025;26(8):1009-1017

Conflict of Interest

no conflict of interest identified

P063

Exponential growth of lutetium-177 therapies at a leading cancer center in Latin America

Lic. Mariano Portillo[1], Dr. Martina Musumeci[1], Lic. Marcos Mussio[1], Tec. Luis Genovese[1], Tec. Delfina Eugeni[1], Tec. Ariel Arispe[1], Dr. Luciana Arburua[1], Dr. Silvina Racioppi[1]
[1]Servicio de Medicina Nuclear, Instituto Alexander Fleming, Buenos Aires, Argentina

Background and Objectives: Access to therapies with radiolabeled peptides and ligands using lutetium-177 shows significant heterogeneity worldwide and regionally. In Latin America, implementation remains limited. The objective was to perform a descriptive analysis of the use of these therapies in our center.
Materials and Methods: We retrospectively analyzed the Nuclear Medicine Department databases related to therapeutic procedures with lutetium-177, including somatostatin analogs and PSMA-targeted ligands.
Results: Between June 2019 and August 2025, 62 patients with inoperable metastatic neuroendocrine tumors were treated (28 women (45.2%), 34 men (53.8%); age range 29–83 years). The largest group was between 50–59 years (32.2%). Primary tumor sites were small intestine (45.2%) and pancreas (38.7%). A total of 211 doses of 177Lu-DOTATATE were administered, with a progressive increase: from 3.8% in 2019 to 32.2% in 2024.
Between October 2021 and August 2025, 30 patients with metastatic prostate cancer and PSMA overexpression were treated (age range 55–85 years). Of these, 35% presented de novo metastases, 53% had nodal involvement, and 77.8% had a PSMA Score of 3. Treatment distribution showed steady growth, reaching 48.7% in 2024. Projections for 2025 indicate further increases for both therapies.
Regarding economic access, for 177Lu-DOTATATE, 66% of treatments were covered by private insurance and 23% by self-payment; for 177Lu-PSMA, 55% were self-paid and 31% covered by private insurance.
Conclusion: The exponential growth of radiometabolic therapy in our center is evident despite barriers in access and availability. Strengthening technical and medical training, along with institutional coordination, is essential to meet current and projected demand.

Conflict of Interest
The authors declare that they have no conflict of interest.

P064

Low Risk, Lasting Vigilance: Recurrence Patterns in Papillary Thyroid Microcarcinoma

Dr. Shaila Sharmin[1], Dr. Afroza Akhter[1], Dr. Mohana Hossain[1], Dr. Rahima Perveen[1], Dr. Rawnak Afrin[1], Dr. Tanima Biswas[1], Dr. Sadia Hossain[1], Dr. Sabrina Islam[1], Dr. Farhana Rahman[1], Dr. Tanvirul Hasan[1], Dr. Shankar Biswas[1]
[1]Institute Of Nuclear Medicine & Allied Sciences, INMAS, Dhaka, Bangladesh, Atomic energy commission, Dhaka, Bangladesh

Background: Papillary thyroid microcarcinoma (PTMC), defined as tumors ≤1 cm, is increasingly diagnosed due to widespread use of high-resolution imaging and fine-needle aspiration cytology. Although PTMC generally carries an excellent prognosis, recurrence remains a clinical concern that can influence surveillance and management.
Methods: We retrospectively analyzed 103 patients with PTMC treated between 2022 to 2024. Radioiodine therapy (RAIT) was administered according to American Thyroid Association (ATA) guidelines. Patients with incomplete records or follow-up <12 months were excluded. Demographic data, tumor characteristics, surgical interventions, RAIT, biochemical markers, comorbidities, and recurrence patterns were reviewed.
Results: Among the 103 patients, 91 were female (88.4%) and 12 male (11.6%), with a female-to-male ratio of 7.5:1 and mean age 38 ± 1 years (range 17–69). All underwent total thyroidectomy. 15 patients (14.5%) had PMTC with lymph node metastasis at diagnosis. Radioiodine (RAIT) was administered according to American Thyroid Association (ATA) guidelines, doses ranging from 50 to 150 mCi. During follow-up, 7 patients (6.7%) demonstrated recurrence: 6 patients (5.8%) were positive in large dose scan after one year, and 1 presented again with lymph node metastasis on follow up neck ultrasound proven by cytology. No deaths occurred during the study period.
Conclusion: Papillary thyroid microcarcinoma is generally considered as a low-risk thyroid malignancy; however, recurrence can occur. Our analysis emphasizes that “low risk” does not mean “no risk,” and lifelong surveillance remains essential in the management of papillary thyroid microcarcinoma.

Conflict of Interest
There is No conflict of interest

P065

Cost-utility analysis of [177Lu]PSMA therapy compared to Cabazitaxel in patients with mCRPC from the perspective of the Colombian Health System

Dr. Marylin Acuña Hernandez[1], Dr Sebastián Camilo Venegas Osorio[2], Magister Aurelio Mejía Mejía[2]
[1]Instituto Nacional De Cancerología - Universidad De Antioquia, Bogota, Colombia, [2]Universidad De Antioquia, Medellin, Colombia

Introduction: Metastatic castration-resistant prostate cancer (mCRPC) poses a significant clinical and economic burden on the Colombian healthcare system. In patients who progress following taxane-based chemotherapy, novel therapies such as [177Lu]PSMA have demonstrated clinical efficacy; however, their adoption requires context-specific economic evaluation.
Objective: To assess the cost-utility of [177Lu]PSMA compared to Cabazitaxel in patients with mCRPC, from the perspective of the Colombian General Health Social Security System.
Methods: A partitioned survival model was developed using a 24-month time horizon, monthly cycles, and a 5% annual discount rate. Overall survival (OS) and progression-free survival (PFS) curves were fitted using Weibull distributions. Cost data were obtained from SISPRO (CUPS), SISMED, the national price thermometer, and supplier records. Utility values were sourced from international literature. Both deterministic and probabilistic sensitivity analyses were conducted.
Results: [177Lu]PSMA yielded 0.717 QALYs compared to 0.649 with Cabazitaxel. The incremental cost was COP $11,237,696, resulting in an incremental cost-effectiveness ratio (ICER) of COP $167,002,673 per QALY—exceeding the national willingness-to-pay threshold of COP $87 million. In the probabilistic analysis, [177Lu]PSMA was dominant in 100% of simulations.
Conclusions: Although not cost-effective under average deterministic assumptions, [177Lu]PSMA
demonstrated greater clinical benefit and efficiency in real-world scenarios. Policy recommendations include exploring price negotiation strategies, promoting domestic radiopharmaceutical production, and strengthening Colombia's regulatory framework for nuclear medicine.

Conflict of Interest
We do not have

Graphic

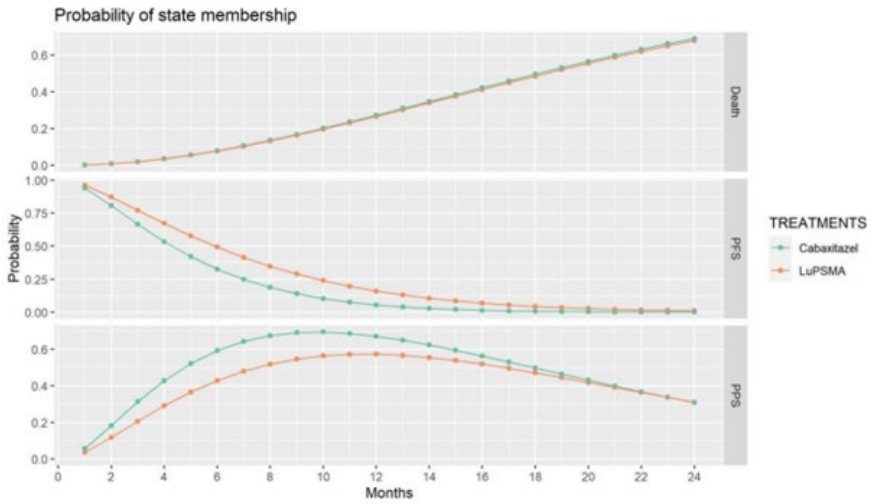

Fuente: obtenido del Software web INES con datos producto de la investigación de los autores

Table

Tabla 7. Resultados caso tipo

Tecnología	Costo total (COP)	Desenlace (AVAC)	Costo incremental (COP)	Efectividad incremental (AVAC)	RICE (COP/AVAC)
[^{177}Lu]PSMA	$128,552,821	0,717	$11,237,696	0,06729	$167,002,673
Cabazitaxel	$117,315,124	0,649			

Fuente: elaboración propia

P066

Cost-utility of therapy with 177Lu-DOTAPEPTIDE: Systematic review of the literature

Dr. Marylin Acuña Hernandez[1], Dr. Paula Alejandra Mendez Mercado[2], Dr. Olga Liset Sanchez Orduz[3]
[1]Instituto Nacional De Cancerología - Universidad De Antioquia, Bogota, Colombia, [2]Los Cobos Medical Center, Bogota, Colombia, [3]SPECT Medicina Nuclear SAS, Bucaramanga, Colombia

Introduction: In recent years, an increasing use of radionuclide therapies has been observed in different pathologies. In the case of neuroendocrine tumors, the clinical trials NETTER-1 and NETTER-2 demonstrated clinical effectiveness, positioning this type of therapy among the first-line management options for these conditions. Consequently, it is necessary to establish the cost-utility.
Objective: Conduct a systematic review of the literature on cost-utility studies of therapy with 177Lu-DOTAPEPTIDE compared with other treatment options such as Everolimus, Sunitinib, and Somatostatin Analogs for the management of patients diagnosed with unresectable, locally advanced, or metastatic neuroendocrine tumors who present progression to treatment, and for whom functional and molecular studies document the expression of somatostatin receptors.
Methodology: A literature search was performed using MeSH, DeCS, and free terms combined with Boolean operators in the following databases: PUBMED, Embase, Cochrane, INAHTA, Lilacs, OpenGrey, and Google Scholar. A total of 200 articles were retrieved; after removing duplicates and studies without full text, 7 articles remained, to which the CHEERS criteria were applied to assess methodological quality.
Results: The literature reported 6 complete economic evaluations and 1 incomplete, conducted in countries such as France, Norway, Sweden, Scotland, the Netherlands, the United Kingdom, Italy, and the United States. In all scenarios, the dominant alternative from the third-party payer perspective (healthcare system) for patients diagnosed with unresectable, locally advanced, or metastatic neuroendocrine tumors with disease progression was 177Lu-DOTAPEPTIDE, showing higher gains in QALYs and better ICER per QALY gained.
Conclusion: In all scenarios, from the perspective of the third-party payer in the countries analyzed, the dominant alternative for patients diagnosed with unresectable, locally advanced, or metastatic neuroendocrine tumors who present progression to treatment is 177Lu-DOTAPEPTIDE.

Conflict of Interest
No conflicts of interest declared

P067

Cost-utility of therapy with 177Lu-PSMA: Systematic review of the literature

Dr. Marylin Acuña Hernandez[1], Dr. Paula Alejandra Mendez Mercado[2], Dr. Olga Liset Sanchez Orduz[3]
[1]Instituto Nacional De Cancerología - Universidad De Antioquia, Bogota, Colombia, [2]Los Cobos Medical Center, Bogota, Colombia, [3]SPECT Medicina Nuclear SAS, Bucaramanga, Colombia

Introduction: In recent years, due to the increasing incidence of prostate carcinoma among young and middle-aged populations and the diagnosis at more advanced stages, several authors have reported rising costs in therapy.
Objective: Conduct a systematic review of the literature on cost-utility studies of 177Lu-PSMA therapy compared with taxane-based management and standard therapy in patients diagnosed with metastatic castration-resistant prostate cancer (mCRPC).
Methodology: A literature search was conducted using MeSH, DeCS, and free terms combined with Boolean operators in the following databases: PUBMED, Embase, Cochrane, INAHTA, Lilacs, OpenGrey, Renata, and Google Scholar. A total of 470 articles were retrieved; after removing duplicates and studies without full text, 6 articles remained, to which the CHEERS criteria were applied to evaluate methodological quality.
Results: The literature reported 5 complete economic evaluations and 1 incomplete regarding the costs of 177Lu-PSMA therapy in patients diagnosed with castration-resistant prostate carcinoma, comparing it with standard management or taxanes. Four of the studies found the former alternative to be more costly in countries such as Norway, Canada, the Netherlands, and Colombia, but not in the United States and Germany. Notably, some full economic evaluations published in countries such as Canada did not include data required for health economic assessments within their reports, thereby limiting interpretation. However, in all scenarios, 177Lu-PSMA therapy was associated with higher QALY gains.

Conflict of Interest
No conflicts of interest declared

P068

Current situation and challenges of nuclear medicine in Perú

Dr. Shirley Alarcon[1]
[1]Clinica Ricardo Palma, Lima, Perú

Background: Nuclear medicine in Peru has experienced progressive growth over the last decade; however, limitations remain of infrastructure, availability of radiopharmaceuticals, and geographical distribution. The objective of this study is to describe the current situation of nuclear medicine centers, human resources, and equipment in the country and compare it with Latin America.
Methods: A review was conducted of the official records of licenses issued by accredited centers and available equipment from the Peruvian Institute of Nuclear Energy (IPEN)(1) and the number of active nuclear physicians Medical Association of Peru (CMP)(2) and national population data for 2025.
Results: There are currently 43 nuclear medicine centers in Peru: 37 conventional centers (31 gamma cameras and 6 SPECT/CT) and 6 PET/CT centers, all of which are located in Lima. The current licenses correspond to 37 centers with Tc-99m, 32 with I-131, 15 with Sm-153, 6 with F-18, 4 with Lu-177, and only 2 with cyclotrons for local production of radioisotopes. There are 93 nuclear physicians active registered with the CMP, but only 48 practice in the specialty. In relation to the national population (34 million), there is 1 gamma camera/SPECT for every 918,000 inhabitants and 1 PET/CT for every 5.6 million, with a marked concentration in Lima. In comparison, the Latin American average for PET/CT is 1 per 3.3 million inhabitants, which places Peru below the regional average(3).
Conclusions: Nuclear medicine in Peru shows progress in human resources and the opening of centers, although with limited availability of PET/CT and emerging radioisotopes, as well as a strong centralization in Lima. Compared to other Latin American countries, Peru lags behind in terms of equipment density per capita(4). These findings highlight the need for policies that promote decentralization, equitable access, and investment in radiopharmacy and specialized training to achieve regional standards.

References

1. Peruvian Institute of Nuclear Energy (IPEN). (2025). Registry of licenses for nuclear medicine practices in Peru. Lima: IPEN
2. Medical Association of Peru (CMP). (2025). National registry of medical specialists in nuclear medicine. Lima: CMP.
3. Di Carli, M. F., Dorbala, S., Curillova, Z., & Carrio, I. (2015). Positron emission tomography/computed tomography in developing countries: A report of the International Atomic Energy Agency. Journal of Nuclear Medicine, 56(10), 1629–1634. https://doi.org/10.2967/jnumed.115.160044
4. Pérez, J., et al. (2022). Nuclear medicine in Latin America: Current status and perspectives. Revista Española de Medicina Nuclear e Imagen Molecular, 41(4), 205–212. https://doi.org/10.1016/j.remnie.2022.02.003

Conflict of Interest

No disclosures

Graphic

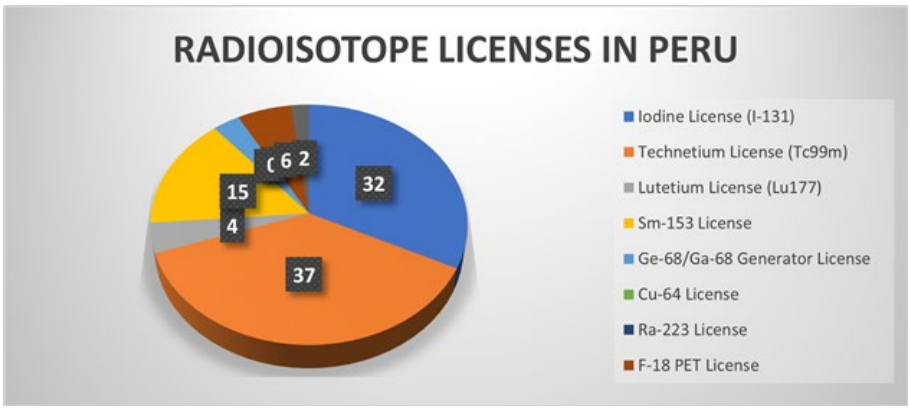
RADIOISOTOPE LICENSES IN PERU
32
37
4
15
6
2
Iodine License (I-131)
Technetium License (Tc99m)
Lutetium License (Lu177)
Sm-153 License
Ge-68/Ga-68 Generator License
Cu-64 License
Ra-223 License
F-18 PET License

P069

Public/public-private synergy in the creation of the Nuclear Medicine Service in Uruguay

Lic. Andreína Blanco[2], Dr. Alarico Rodriguez[1], Dr. Gustavo Burroso[1], Dr. Pablo Duarte[1], Dr. Carlos Heugerot[2], Dr. Pablo Cabral[2], Prof. Juan Gambini[1]
[1]Cudim, Montevideo, Uruguay, [2]DNSFFAA, Uruguay

Equitable access to functional imaging technologies remains a challenge for public health systems. In Uruguay, the Dirección Nacional de Sanidad de las Fuerzas Armadas (DNSFFAA) serves over 140,000 users, demanding innovative solutions to secure comprehensive diagnostics. In partnership with the Centro Uruguayo de Imagenología Molecular (CUDIM), a cooperative model was established to create a Nuclear Medicine Service at the Military Hospital. This work describes the development of the service, highlighting inter-institutional synergy and its impact on diagnostic capacity in the public sector.
Methods: collaborative project between the DNSFFAA and CUDIM integrated financial resources, hospital infrastructure, radiopharmacy expertise, SPECT/CT imaging, and professional training. This descriptive, retrospective study assessed the incorporation of the service into the Military Hospital Health Network, its contribution to diagnostic capacity, technetium-99m (^99mTc) radiopharmaceutical availability, and the adoption of standardized protocols. Ethical approval was obtained from institutional review boards.
Results: The Nuclear Medicine Service strengthened the comprehensive imaging portfolio of the Military Hospital, complementing radiology, CT, and ultrasound. It increased diagnostic autonomy within the DNSFFAA, reduced dependence on external providers, and improved timeliness of access to complex studies. Reliable supply of ^99mTc radiopharmaceuticals and protocol standardization enhanced diagnostic quality. The Military Hospital is now positioned as a referral center for advanced functional imaging in the public sector.
Conclusions: The creation of the DNSFFAA Nuclear Medicine Service through cooperation with CUDIM represents a successful public/public-private model, expanding imaging capacity and providing a strategic diagnostic reserve for the country. This initiative benefits more than 140,000 users and offers a blueprint for other systems aiming to broaden access to advanced functional imaging.

Conflict of Interest
NONE

P070

The current state of the PET Imaging Site Qualification Program for amyloid PET scans conducted in Japan

Dr. Hirofumi Fujii[1,2], Dr. Yasuhiko Ikari[3], Dr. Keisuke Tsuda[4], Mr. Kazuaki Mori[5], Dr. Ukihide Tateishi[6], Dr. Kenji Hirata[7], Dr. Hiromitsu Daisaki[8], Dr. Makoto Hosono[9], Dr. Hiroshi Ito[10], Dr. Michio Senda[3]

[1]Japan Radioisotope Association, Tokyo, Japan, [2]National Cancer Center, Kashiwa, Japan, [3]Kobe City Medical Center General Hospital, Kobe, Japan, [4]Juntendo University, Tokyo, Japan, [5]Toranomon Hospital, Tokyo, Japan, [6]Institute of Science Tokyo, Tokyo, Japan, [7]Hokkaido University, Sappro, Japan, [8]Gunma Prefectural College of Health Sciences, Maebashi, Japan, [9]Kindai University, Osakasayama, Japan, [10]Fukushima Medical University, Fukushima, Japan

Background/Aims: The Japanese Society of Nuclear Medicine initiated the PET Imaging Site Qualification Program (J-PEQi) in 2013 to standardize the quality of PET scans in clinical studies. The program was updated to apply to clinical practice in 2019. This study reviewed the current state of the updated program for amyloid PET scans in Japan.
Methods: In the J-PEQi for amyloid PET scans, scanning protocols and image quality are examined every three years using Hoffman 3D brain phantoms and cylindrical phantoms, considering contrast, noise, uniformity, artifacts, technical errors (such as bubbles inside phantoms), and spatial resolution. Longitudinal changes in the numbers of facilities with qualifications were assessed, and the reasons for failure to qualify were investigated. Ethics committee review of the study was not required because it did not involve any human or animal tests.
Results: The number of J-PEQi-qualified facilities increased rapidly in 2024, primarily due to qualification becoming mandatory for performing amyloid PET scans under coverage by public health insurance. As at August 2025, 391 scanners from 336 facilities were qualified by J-PEQi. Since 2019, image data have been submitted from a total of 532 scanners, of which 473 (89%) passed the examination and 59 (11%) failed. The causes of failure were poor contrast (18 cases), significant noise (17 cases), non-uniformity (12 cases), artifacts (9 cases), technical errors (6 cases), and inadequate spatial resolution (2 cases). Through repeated trials, all facilities were eventually qualified, unless they chose to discontinue.
Conclusions: After the introduction of the updated J-PEQi, over 80% of PET facilities in Japan obtained qualification, thereby enabling them to deliver high-quality amyloid PET imaging. J-PEQi has contributed to quality control of amyloid PET scans in clinical practice as well as in clinical studies in Japan.

Conflict of Interest
Nothing to declare

Graphic

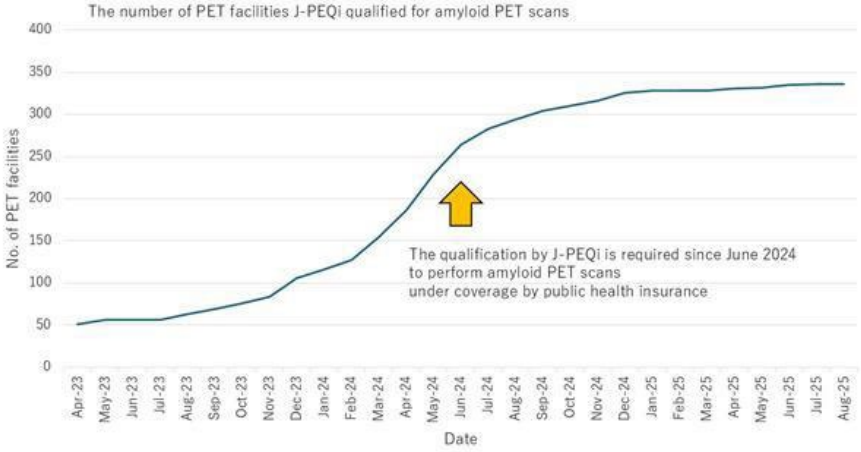
The number of PET facilities J-PEQi qualified for amyloid PET scans
No. of PET facilities
400
350
300
250
200
150
100
50
0
Apr-23
May-23
Jun-23
Jul-23
Aug-23
Sep-23
Oct-23
Nov-23
Dec-23
Jan-24
Feb-24
Mar-24
Apr-24
May-24
Jun-24
Jul-24
Aug-24
Sep-24
Oct-24
Nov-24
Dec-24
Jan-25
Feb-25
Mar-25
Apr-25
May-25
Jun-25
Jul-25
Aug-25
Date
The qualification by J-PEQi is required since June 2024
to perform amyloid PET scans
under coverage by public health insurance

P071

Implementation of the IAEA QUANUM Program to Achieve GMP Certification at CUDIM Radiopharmacy

Dr. Javier Giglio[1], Dra. Ingrid Kreimerman[1], Chemistry Maia Zeni[1], Dra. Ana Rey[2], Dr. Alarico Rodríguez[1], Dr. Gustavo Burroso[1], Dr. Eduardo Savio[1]
[1]Departamento de Radiofarmacia, Centro Uruguayo de Imagenología Molecular (Cudim), Montevideo, Uruguay, [2]Área de Radioquimica, Facultad de Química, UdelaR, Montevideo, Uruguay

Background and Objective: Since its establishment in 2010, the Radiopharmacy Department of the Uruguayan Center for Molecular Imaging (CUDIM) has developed its quality system within a hospital radiopharmacy framework. In 2018, the department adopted the IAEA Quality Management Audits in Nuclear Medicine (QUANUM) program, a specialized audit framework for nuclear medicine services. Members of the Quality Assurance Committee received IAEA training, and QUANUM checklists were integrated into internal audits.[1]
In 2024, CUDIM aimed to transition from a hospital radiopharmacy to a pharmaceutical laboratory to obtain market authorization for radiopharmaceuticals. The radiopharmacy was licensed by the Ministry of Public Health of Uruguay (MSP) as a Pharmaceutical Laboratory and initiated the registration process for radiopharmaceuticals under WHO Good Manufacturing Practices (GMP).[2]
Methodology: Since 2019, internal QUANUM-based audits have been conducted, followed by corrective action plans to address non-conformities and improve quality standards in production and quality control. In 2022, an external IAEA audit was performed, and subsequent efforts focused on resolving identified findings.
Results: The 2019 internal audit revealed 76.9% compliance (88.3% -Radiopharmacy), with 61 non-conformities (9 critical, 38 major, 14 minor), prompting corrective actions. By 2022, internal compliance reached 88.8% (91.6% - Radiopharmacy), and the external IAEA audit reported 89.8%. The 2023 internal audit, conducted prior to the MSP inspection, showed 89.9% compliance with 24 non-conformities (3 critical, 17 major, 4 minor) (table 1). In 2025, the MSP inspection, based on WHO checklists, identified 16 non-conformities (2 critical, 8 major, 6 minor), all of which were addressed through a corrective action plan.
Conclusions: The IAEA QUANUM program provided an effective framework for establishing, auditing, and maintaining a high-quality management system in a nuclear medicine facility. Its structured approach enabled CUDIM to meet WHO GMP standards, culminating in GMP certification of the Radiopharmacy Department by the MSP in June 2025 (figure 1).

References
[1] - INTERNATIONAL ATOMIC ENERGY AGENCY, QUANUM 3.0: An Updated Tool for Nuclear Medicine Audits , IAEA, Vienna (2021)
[2] - Good manufacturing practices for pharmaceutical products: main principles. In: WHO Expert Committee on Specifications for Pharmaceutical Preparations: thirty-second report. Geneva: World Health Organization; 2014: Annex 2.

Conflict of Interest
No competing interests to declare

Graphic

REPÚBLICA ORIENTAL DEL URUGUAY
MINISTERIO DE SALUD PUBLICA

MSP

Serie A 366257
DIRECCIÓN GENERAL DE FISCALIZACIÓN
DIVISIÓN FISCALIZACIÓN

CERTIFICADO EN BUENAS PRÁCTICAS DE FABRICACIÓN

Se certifica que la Empresa:

RAZÓN SOCIAL: CENTRO URUGUAYO DE IMAGENOLOGÍA MOLECULAR (CUDIM)
RUT: 216137350014
PROPIETARIO/APODERADO: DR. PABLO DUARTE
DOMICILIO: AV. RICALDONI Nº 2010 - MONTEVIDEO, REPÚBLICA ORIENTAL DEL URUGUAY
TELÉFONO: 24803238
DIRECTOR TÉCNICO: Q.F. EDUARDO SAVIO

Se encuentra sometida a inspecciones periódicas en las que se verifican las Buenas Prácticas de Fabricación de acuerdo a lo establecido en el Decreto Nº 440/2016, adopción de la Resolución GMC Nº15/09, Informe Nº 37, Serie Nº 908, de la Organización Mundial de la Salud (OMS), Anexo 4 "Buenas Prácticas de Fabricación para Productos Farmacéuticos, principios fundamentales" y en los Reportes Técnicos de la OMS Serie Nº 961, Informe Nº 45, Anexo 6 "Buenas Prácticas de Fabricación para Productos Farmacéuticos Estériles" y Serie Nº 1025, Informe Nº 54, Anexo 2 "Guía en Buenas Prácticas de Fabricación para Productos Radiofarmacéuticos de la Agencia Internacional de Energía Atómica y de la Organización Mundial de la Salud".

Cumple las Buenas Prácticas para la Fabricación de especialidades farmacéuticas (radiofármacos)- soluciones estériles en viales por llenado aséptico.

Cumple las Buenas Prácticas de Laboratorio para análisis fisicoquímico y microbiológico de radiofármacos.

Se extiende el presente certificado en la Ciudad de Montevideo, República Oriental del Uruguay, a los 24 días del mes de setiembre de 2025, caducando el mismo en caso de incorporación o modificación de procesos, de condiciones o tipos de productos en la actividad de la empresa o si se constata incumplimiento de la normativa mencionada.

Certificado vigente hasta el 4/06/2026
Ref. 5493/2024
SB/rs

Ing. Quím. Silvia Belvisi Crossa
Directora Gral. de Fiscalización
DIGEFI -M.S.P.

"LA LECHE MATERNA ES LA MEJOR PARA EL RECIEN NACIDO Y EL LACTANTE". LEY Nº 17.803

Table

General Checklist	1. Strategies	2. Radiat Reg	3. Patient R.Prot	4. QA System	5. Equip. QA/QC	6. IT Syst	7. Clin Serv	8. Spec. Diag.P	9. Ther Serv	10. Spec. Ther.P	11. RP Lev 1	12. RP Lev 2	13. RP Lev 3	TOTAL
2019														
% Scoring	81.6	85.9	75	51.7	59.4	36.4	59.8	88.3	-	-	88.6	93.8	82.4	**76.9**
N. of NC	5	5	3	10	4	10	15	10	-	-	2	0	2	**66**
2023														
% Scoring	86.8	90.2	95.8	71.7	71.4	75	88	99.1	82.1	95.4	88.5	93.8	92.6	**89.9**
N. of NC	2	2	0	6	2	3	2	0	5	1	2	0	0	**25**

P072

Ejection fraction obtained manually during the rotary internship at the Institute of Nuclear Medicine of the San Francisco Xavier University

Lic. Elizabeth Huanca[1], Lic. Marcelo Torrez, Doctora Lidya Quevedo, Lic. Mery Orosco, Lic. Katherine Romero
[1]Universidad San Francisco Xavier De Chuquisaca, Sucre, Bolivia

Ventriculography is a study in Nuclear Medicine used to obtain images where ventricular function can be quantified, the technique consists of taking images of the cardiac cycle after marking red blood cells; the processing of the images and the obtaining of the ejection fraction of the left ventricle is done automatically or manually. A retrospective study was carried out of a total of 371 balanced ventriculography studies, 20 studies were randomly selected, corresponding to 11 women between the ages of 32 and 69 years and 9 men between the ages of 39 and 76 years, respectively; The studies were obtained by marking red blood cells in vivo, saturating at 6 megacounts, being the representation of the cardiac cycle of 24 images. The studies were processed manually to obtain the ejection fraction of the left ventricle by an instructor (A) and two students (B and C) of the rotating internship in Nuclear Medicine of the Bioimaging Career of the Faculty of Technological Sciences of Health, carrying out a total of 60 processes. The results indicate that the left ventricular ejection fraction LVEF obtained by A was 53%, by B 59%, by C 57% in female patients, while in males the LVEF obtained by A was 48%, for B 54% and for C 50%, respectively. The standard deviation of the data obtained by AB was 5.01, by AC 3.98 and by BC 2.95 in females in relation to the standard deviation of data obtained in males by AB is 6.20, by AC 3.69 and by BC of 4.24. Concluding that obtaining the ejection fraction is operator dependent, observing that the data obtained by B and C are overestimated in relation to the data obtained by A. The processing protocols developed by the students were very useful for subsequent rotations

Conflict of Interest
There is no conflict of interest

P073

Research work practice program of radiopharmacy with an integrative approach to the 5th level of the career pharmacy at USFX

Lic. Elizabeth Huanca[1], Licenciada Rita Vasquez
[1]Universidad San Francisco Xavier De Chuquisaca, Sucre, Bolivia

Bolivia currently has three Nuclear Medicine and Radiotherapy mega centers that were implemented
with cutting-edge technology during the last three years, at the Universidad San Francisco Xavier, the Study Plan of the last two decades of the Pharmaceutical Chemistry Career does not contemplate the subject of Radiopharmacy.
The objective of this work was to design an Investigative Work Practice program for the subject of Radiopharmacy, with an integrative and systematizing concept of the knowledge and skills of the Pharmaceutical Chemist, through the development of Good Radiopharmaceutical Practices, with an integrative approach to the subjects of the cycle of the exercise of the profession, which will justify the relevance of reincorporation of this subject into the study plan of the Career.
Regarding the methodology, an interview was carried out with 30 professionals who graduated from the Faculty of Pharmacy and Biochemistry and some one teachers.
The results indicate that 56.6% did not take the subjects of Radiopharmacy, 20% They indicated that the study of the Radiopharmacy subject was helpful in acquiring certain skills such as seriousness, honesty, agility of thought due to the fact of dealing with a special material that requires concentration and careful work, in accordance with radiological protection standards. When teachers were asked why the subject of Radiopharmacy was eliminated from the curriculum, the answers were: a lot of workload for the student, in addition to the fact that it was a subject with no future, not very applicable in our environment, and that it was dangerous due to radiation.
In conclusion, the ignorance of scientific and technological advances in the field of Nuclear Medicine - Radiopharmacy, and its projections for the Pharmaceutical Chemist professional, harms the comprehensive training of the future professional. The reincorporation of study of Radiopharmacy will respond to the needs of society.

Conflict of Interest
There is no conflict of interest

P074

Project Management Applied to the Implementation of a Nuclear Medicine Service in Bogotá, Colombia: Experience and Proposal for Standardization

Dr. Maria Martinez[1], Ingenieria Lenys Roncancio, Fisica medica Lorena Sandoval
[1]Clinica Del Country, Bogota, Colombia

Background / Objectives: Nuclear Medicine has assumed a central role in the comprehensive management of cancer, becoming an essential tool for early diagnosis, staging, therapeutic response assessment, and monitoring of organ damage caused by various treatments. In Colombia, the cancer burden continues to rise and remains one of the leading causes of morbidity and mortality. The availability of nuclear medicine services in the country is still limited, creating barriers to access and delays in diagnosis, which negatively affect the timeliness and effectiveness of treatments.
Methods: We propose a structured model for the implementation of nuclear medicine projects using standardized methodologies from the Project Management Institute (PMI), applicable to projects with long implementation timelines and focused on minimizing time and cost risks.
Results: Implementation and commissioning of the Nuclear Medicine Service at Clínica del Country in Bogotá, Colombia.
Conclusions: Ensuring the viability and cost-effectiveness of the service produces a positive impact both on clinical practice and on the healthcare system as a whole. The implementation of a nuclear medicine service is often perceived as a high-cost investment, which discourages healthcare providers (IPS). However, detailed analysis shows that such projects generate significant benefits by optimizing patient diagnostic pathways, reducing healthcare costs, strengthening the healthcare network, and contributing to the financial sustainability of institutions.

References

1. 2018 ACC/HRS/NASCI/SCAI/SCCT Expert Consensus Document on Optimal Use of Ionizing Radiation In Cardiovascular Imaging: Best Practices for Safety and Effectiveness: A Report of the American College of Cardiology Task Force on Expert Consensus Decision Pathways. Hirshfeld JW, Ferrari VA, Bengel FM, et al. Journal of the American College of Cardiology. 2018;71(24):e283-e351. doi:10.1016/j.jacc.2018.02.016.
2. 2018 ACC/HRS/NASCI/SCAI/SCCT Expert Consensus Document on Optimal Use of Ionizing Radiation in Cardiovascular Imaging: Best Practices for Safety and Effectiveness. Hirshfeld JW, Ferrari VA, Bengel FM, et al. Catheterization and Cardiovascular Interventions : Official Journal of the Society for Cardiac Angiography & Interventions. 2018;92(2):E35-E97. doi:10.1002/ccd.27659.
3. Joint EANM, SNMMI, and IAEA Enabling Guide: How to Set Up a Theranostics Center. Herrmann K, Giovanella L, Santos A, et al. Journal of Nuclear Medicine : Official Publication, Society of Nuclear Medicine. 2022;63(12):1836-1843. doi:10.2967/jnumed.122.264321.
4. Structure and Activities of Nuclear Medicine in Kuwait. Elgazzar AH, Owunwanne A, Alenezi S. Seminars in Nuclear Medicine. 2016;46(4):359-67. doi:10.1053/j.semnuclmed.2016.01.007.

5. A Method for Validating PET and SPECT Cameras for Quantitative Clinical Imaging Trials Using Novel Radionuclides. Bailey DL, Willowson KP, O'Keefe G, et al. Journal of Nuclear Medicine : Official Publication, Society of Nuclear Medicine. 2025;66(2):315-322. doi:10.2967/jnumed.124.268578.
6. Nuclear Medicine Training and Practice in the Czech Republic. Kamínek M, Koranda P. European Journal of Nuclear Medicine and Molecular Imaging. 2014;41(8):1646-7. doi:10.1007/s00259-014-2806-7.

Conflict of Interest
There is not a Conflict of Interest

P075

Radiological Safety: Estimating Radiation Exposure for Non-Occupationally Exposed Healthcare Personnel in Nuclear Medicine Procedures

Mrs. Lorena Sandoval Castillo[1], Mrs. Sandra Barrera[1], Mrs. Nidya Zambrano[1], Mr. Carlos Quiroga[1], Mr. Gerardo Cortés[1]
[1]Clínica del Country, Bogotá, Colombia

Background/Aims: In diagnostic nuclear medicine, some procedures require the participation of non-occupationally exposed healthcare personnel, such as radioguided surgery or examinations that require sedation or anesthesia. This study aims to measure and estimate the radiation exposure of this personnel, using Tc-99m Sestamibi, Tc-99m nanocolloid, and F-18 FDG, to provide quantitative data that confirms the safety of these procedures by applying recommended radiological protection practices.
Methods: During the first semester of 2025, dose rates and exposure times were measured and recorded using a Geiger-Müller detector for 19 patients who underwent radioguided surgery. A digital dosimeter was also provided to the staff in the operating rooms. For PET/CT examinations, measurements were taken for 5 patients who required sedation or anesthesia. The final data analysis focused on estimating the received effective dose, using the median and 75th percentile as evaluation metrics.
Results: For conventional nuclear medicine procedures, the estimated effective doses for healthcare personnel were: stretcher bearer, 0.7 ± 0.05 µSv; caregiver or family member, 16.8 ± 1.12 µSv; and the maximum estimated dose for healthcare personnel in operating rooms, 24.79 µSv. In the case of PET/CT examinations, maximum doses of 68.0 ± 9.88 µSv were recorded.
Conclusions: The estimated dose values demonstrate that radiation exposure in radioguided surgery and PET/CT procedures is significantly low and remains well below the annual regulatory limits. While these procedures are inherently safe, the results underscore the importance of a radiological safety culture founded on proper radiological protection practices, including maintaining a safe distance, minimizing the number of personnel required, and seeking support from nuclear medicine staff when necessary.

Conflict of Interest
The authors, [Lorena Sandoval, Sandra Barrera, Nidya Zambrano, Carlos Quiroga y Gerardo Cortés], declare that there are no conflicts of interest—whether personal, financial, commercial, academic, or of any other nature—that could have affected the impartiality of the results and analysis presented in this work. The research has been conducted independently and without receiving sponsorship or support from any public or private entity with interests in the topic

P076

Reducing Extremity Radiation Exposure in Dynamic PET/CT Studies in Clinica del Country

Mrs. Lorena Sandoval Castillo[1], Mrs. Viviana Andrade[1], Mrs. Claudia Piñeros[1], Mr. Carlos Quiroga[1], Mr. Gerardo Cortés[1]
[1]Clínica Del Country, Bogotá, Colombia

Background/Aims: Dynamic PET/CT studies using radiopharmaceuticals like F-18 choline and F-18 FET present a challenge in radiation protection. The handling and administration of these radiopharmaceuticals have led to significant exposure to the hands of occupationally exposed personnel (OEP). The objective of our study was to evaluate and optimize protocols to reduce this exposure without affecting the quality of the procedures.
Methods: For dose rate measurements, we used a Geiger-Müller detector, and we measured distances and times during the procedures. Additionally, we reviewed and analyzed the extremity dosimetry reports of the technologists who performed these procedures. Based on the initial measurements, we adjusted and optimized the procedures for handling, administration, and patient positioning for image acquisition.
Results: Personal ring dosimetry reports showed variations of up to eight times their reference level. Dose rate measurements at 30 cm recorded a value of 120.27 ± 37.48 uSv/h, which confirmed the need to review and standardize the technique. Following the optimization of the administration process and the implementation of new safety measures, dose rates at 30 cm were recorded at 2.59 ± 2.62 uSv/h, demonstrating a significant reduction in extremity exposure for OEP.
Conclusions: This study demonstrates that, through systematic evaluation and optimization of procedures, it is possible to effectively reduce radiation exposure for personnel involved in the administration of radiopharmaceuticals for dynamic studies.

Conflict of Interest
The authors, [Lorena Sandoval, Viviana Andrade, Carlos Quiroga, Gerardo Cortés], declare that there are no conflicts of interest—whether personal, financial, commercial, academic, or of any other nature—that could have affected the impartiality of the results and analysis presented in this work. The research has been conducted independently and without receiving sponsorship or support from any public or private entity with interests in the topic.

P077

Role of PET/MRI in localizing the epileptogenic focus in drug-resistant epilepsy

Dr. Genesis Rodriguez Ugalde[1], Dra. Lady Sanchez Gomez, Dr. Andres Bello Murguia., Dr. Jose Antonio Serna Macias, Dr. Jorge Schalch de León.
[1]Hospital Privado, Ciudad de Mexico, Mexico

Antecedent: Drug-resistant epilepsy affects up to 30% of patients with epilepsy and represents a diagnostic and therapeutic challenge. Surgery can offer seizure control by precisely locating the epileptogenic focus. Magnetic resonance imaging (MRI) is the first-line technique; however, up to 40% of studies may be negative or inconclusive [1]. 18F-FDG PET combined with MRI allows anatomical and metabolic information to be combined in a single acquisition [2]. The objective of this study is to review the clinical utility of PET/MRI in drug-resistant epilepsy, highlighting common scenarios in practice.
Objective: To review the clinical utility of PET/MRI in refractory epilepsy.
Methodology: A literature review was conducted, focusing on the diagnostic performance of 18F-FDG PET and PET/MRI in refractory epilepsy [3,4]. The information was integrated to identify relevant clinical data and assess their impact on surgical planning.
Result: Three scenarios emphasize the greatest utility of PET/MRI. First, when MRI shows a structural lesion, the presence of concordant hypometabolism on PET reinforces the localization of the focus and predicts better postoperative outcomes. Second, in patients with negative MRI, PET can identify focal hypometabolism. Third, in malformations of cortical development, PET often shows more extensive hypermetabolism than the structural alteration, facilitating a more precise functional delineation of the epileptogenic zone. These scenarios integrate metabolic and structural findings, favoring multidisciplinary decision-making.
Conclusions: PET/MRI benefits include confirming lesions detected by MRI, identifying foci in patients with negative MRI, and delineating functional extension in cortical malformations. Integrating this technique into a multidisciplinary approach improves surgical planning and provides a more favorable prognosis [5].

References

Courtney MR, et al. Association of localizing 18F-FDG PET hypometabolism with favorable outcome after epilepsy surgery. Neurology. 2024.
Flaus A, et al. 18F-FDG PET/MR in focal epilepsy: a new step for presurgical evaluation. Eur J Radiol. 2021.
Czarnetzki C, et al. Yield of non-invasive imaging in MRI-negative focal epilepsy. J Neurol. 2024.
Wang X, et al. Hypometabolic patterns of focal cortical dysplasia in PET. Front Neurosci. 2023.
Wang F, et al. 18F-FDG PET/CT for localizing the epileptogenic focus: a review. Neuropsychiatr Dis Treat. 2024.

Conflict of Interest

No tenemos conflitos de interes.

Graphic

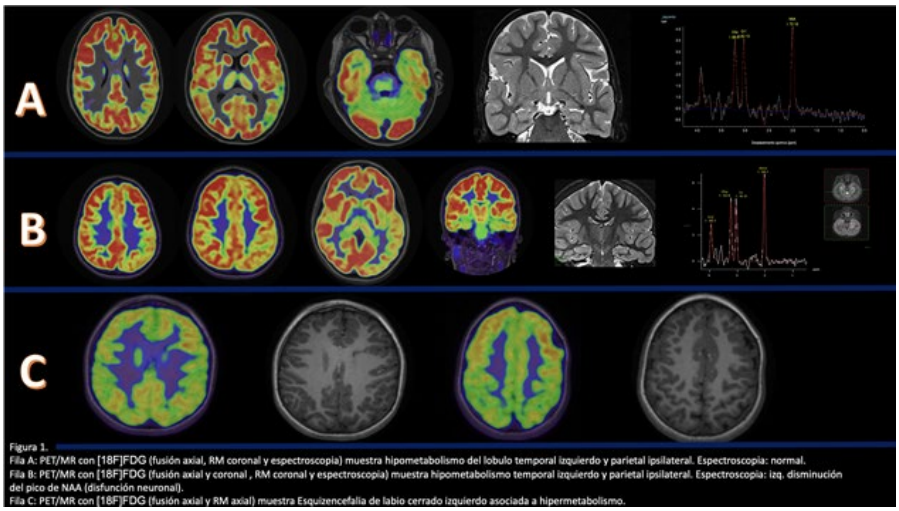

Figura 1.
Fila A: PET/MR con [18F]FDG (fusión axial, RM coronal y espectroscopia) muestra hipometabolismo del lobulo temporal izquierdo y parietal ipsilateral. Espectroscopia: normal.
Fila B: PET/MR con [18F]FDG (fusión axial y coronal , RM coronal y espectroscopia) muestra hipometabolismo temporal izquierdo y parietal ipsilateral. Espectroscopia: izq. disminución del pico de NAA (disfunción neuronal).
Fila C: PET/MR con [18F]FDG (fusión axial y RM axial) muestra Esquizencefalia de labio cerrado izquierdo asociada a hipermetabolismo.

Author Index

A

B

Burroso, Gustavo	O49, O50, O74, O79, P039, P044, P069, P071
Bustos, Nicolás	O25, P005, P034, P035

C

Caballero Calabuig, Elisa Veronica	O55
Cabello, Jorge	O22, O33
Cabral, Pablo	O46, O49, O50, O65, P011, P028, P039, P069
Cabrera, Mirel	O46, O49, O65, P011, P028, P039
Cabrera Galeana, Paula Anel	O81
Cabrera Rojas, Angie	P002
Caetano Albino da Silva, Eduardo	O78
Calderón, José	P021, P023, P024, P025
Calderón, Stephany	O23
Calderón Ávila, Ana L.	O62, P033
Camacho, Ximena	O46, O49, O65, P011, P028, P039
Camacho Herrera, Cristhoper	O30, P052, P054
Campisi, Roxana	P005
Cantillo, Eliecer	O09
Cárdenas Rojas, Juana	P051
Cardozo, Eduardo	O53
Carrillo, Eliana	O71, O73
Carrillo Vázquez, Daniel	O36
Carter, Lukas	O14
Casares, Antonio	O44
Casas Calabuig, Laura	O55
Castillo, Cecilia	P044
Castillo, Gerson	P019
Castillo, Jaime	P038
Castillo Arias, Carolina	O56
Cavagna Matti, Franco Jose	O55
Cazzamalli, Samuele	O06, O66
Ceballos, Jose	O18
Cely, Erika Xiomara	O23
Chacon, Maria Jose	O89, P008, P013
Charalambous, Panos	O32

D

E

F

Farré-Melero, Arnau	P020
Fazzino, Marisa	P044
Fazzo Barbin, Flávia	O78
Felipe, Laura	P012
Feng, Yutian	O15
Fernandes, Ana Julya	P036
Fernandez, Rene	O31
Ferrando, Federico	O41, O43
Ferrando, Rodolfo	O10, O12, O41, O43
Ferreira, César	O70, P053
Ferreira, Diego	P044
Ferro Flores, Guillermina	O81
Fiamingo, Berenice	P034, P035
Flores Perez, Abril Ariadna	P033
Foro, Palmira	O71, O72, O73
Francabandiera, Maximiliano	P034, P035
Franco, Eliana	O23
Franco-ardila, Ada Katerine	O82, P031
Freitas, Stephanie	P036
Fujii, Hirofumi	P070
Funes, Francisco	O25
Furtado Prieto, Carolina	O49, O50, P011, P039

G

Galindo Cortes, Daniel Felipe	P022, P049, P057
Gallazzi, Fabio	O48
Gallegos, Wendy	O77
Galvez, Kenny	O86
Gama, Manlio Gerardo	O04
Gamarra Mujica, Benjamin	P040
Gambini, Juan Pablo	O46, O49, O50, O65, O74, O79, P010,P028, P039, P044, P069
Gamboa, Andres	O77
Garces Giraldo, Javier Andrés	P007
Garces Albir, Marina	O56
Garcia, Camilo	O29, O57, O58
García, César	O77

H

M

S

T

Zheng, Yifan	O26, O33
Zhu, Hua	O83
Zuluaga, Clarena	P049, P050
Zurita Vivero, Karina	P045

Organized by

WORLD FEDERATION OF NUCLEAR MEDICINE AND BIOLOGY

ACMNIM
ASOCIACIÓN COLOMBIANA DE MEDICINA NUCLEAR E IMÁGENES MOLECULARES

alasbimn
Asociación Latinoamericana de Sociedades de Biología y Medicina Nuclear

In cooperation with

IAEA

Organizing Agency

Bco Congresos
Barceló GRUPO

Pl. Europa, 17-19 1ª planta
08908 L'Hospitalet de Llobregat, Barcelona (España)
+34 93 882 38 78 · wfnmb2026@bcocongresos.com